Isomer production in fragmentation reactions

Zsolt Podolyák

UNIVERSITY OF SURREY

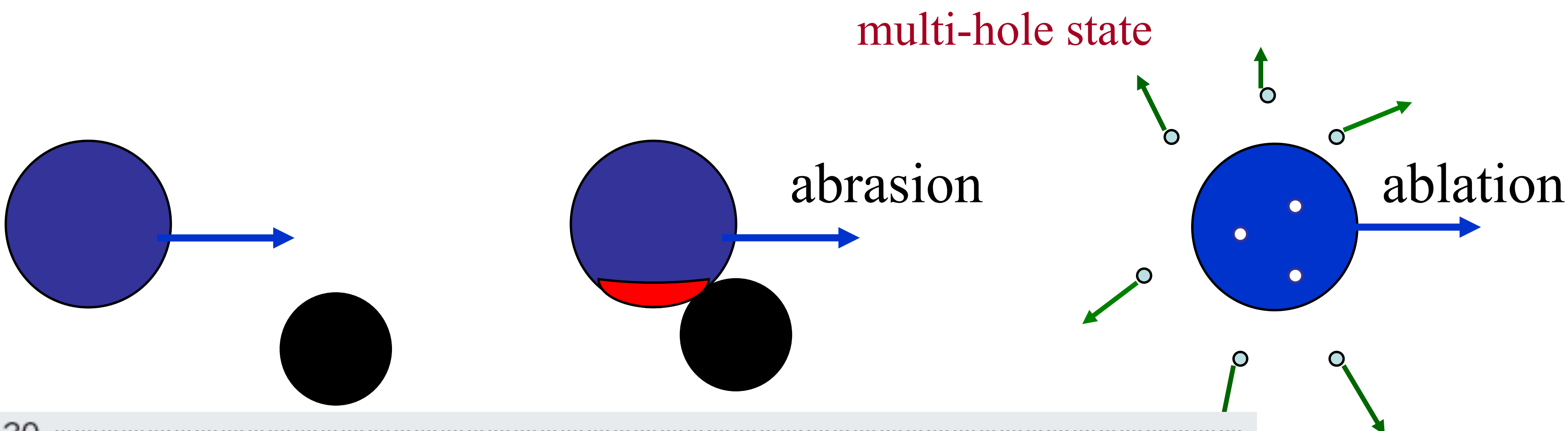

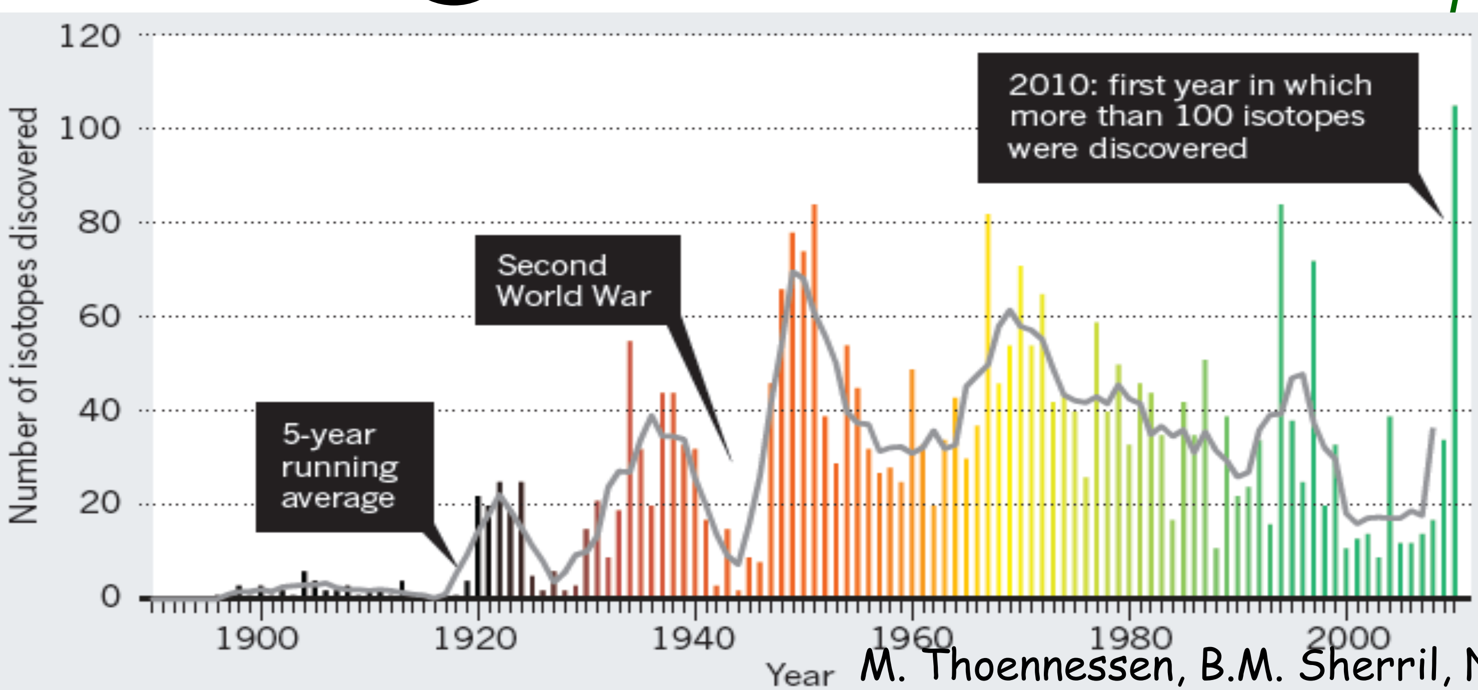

M. Thoennessen, B.M. Sherril, Nature 473 (2011) 25

Fragmentation

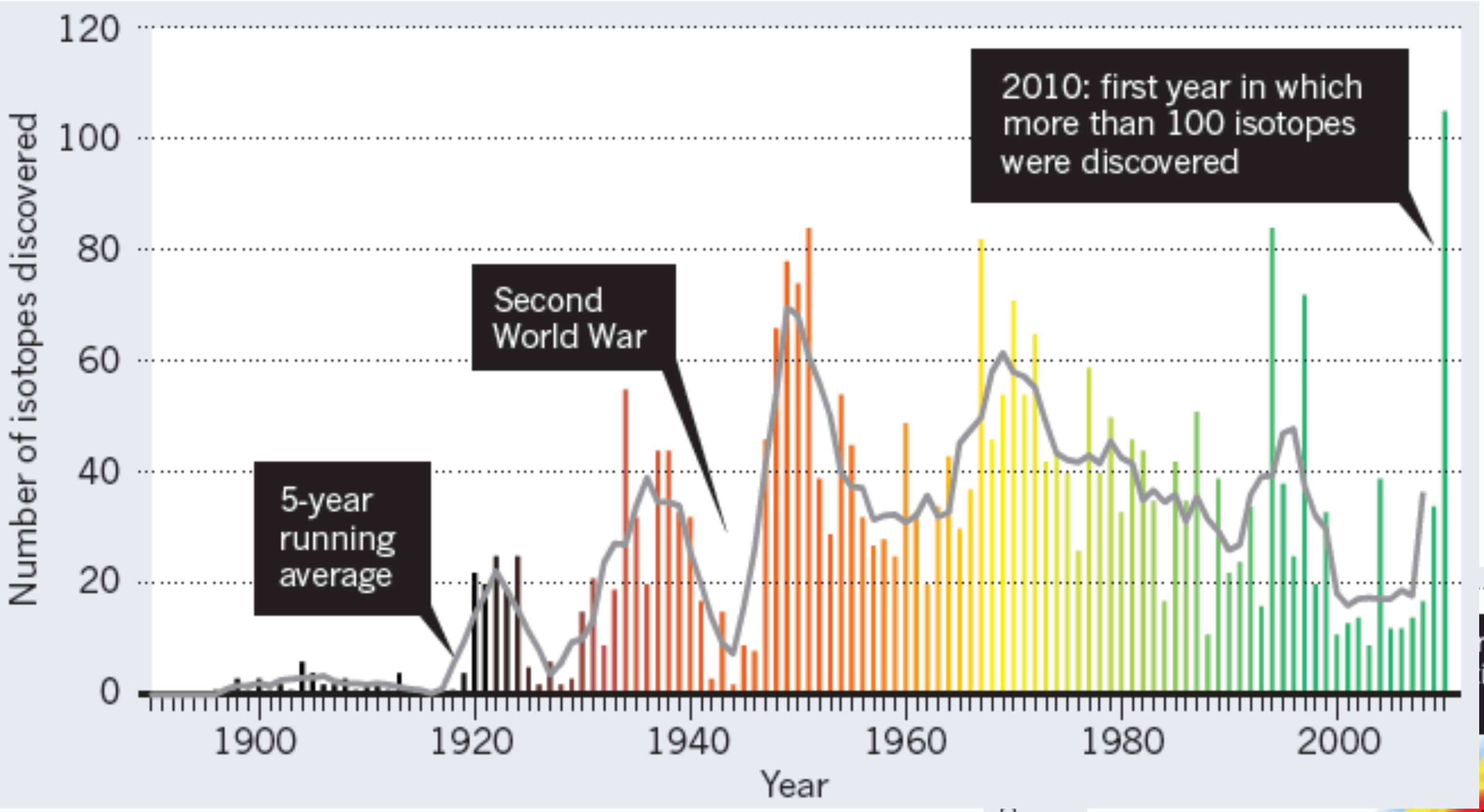

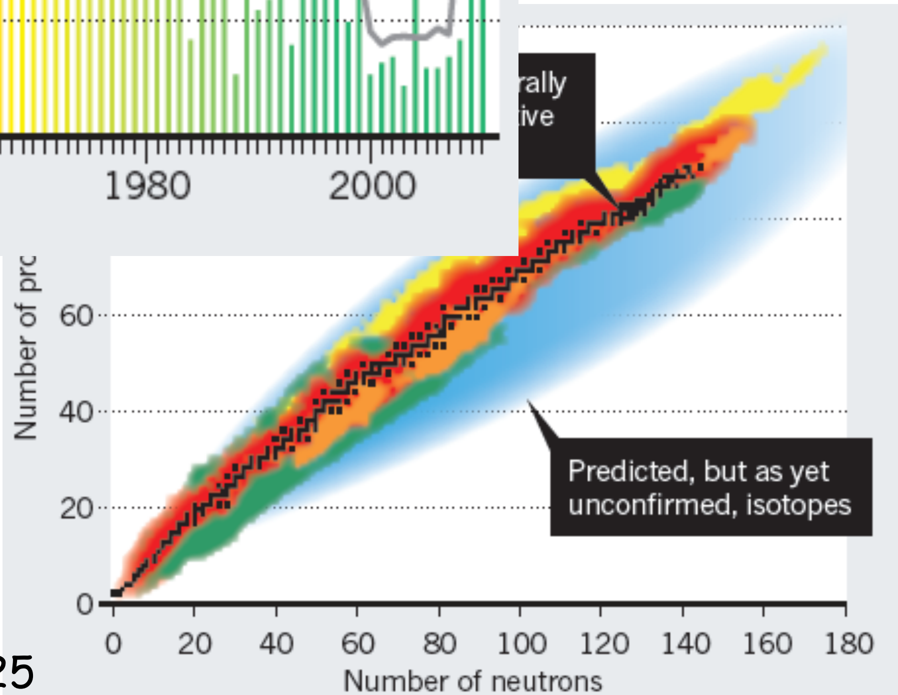

M. Thoennessen, B.M. Sherril, Nature 473 (2011) 25

Isomer production in fragmentation reaction

Zsolt Podolyák
University of Surrey

UNIVERSITY OF SURREY

In flight fragmentation (and fission): separation and identification

Fragment Separator (GSI, Darmstadt, Germany)

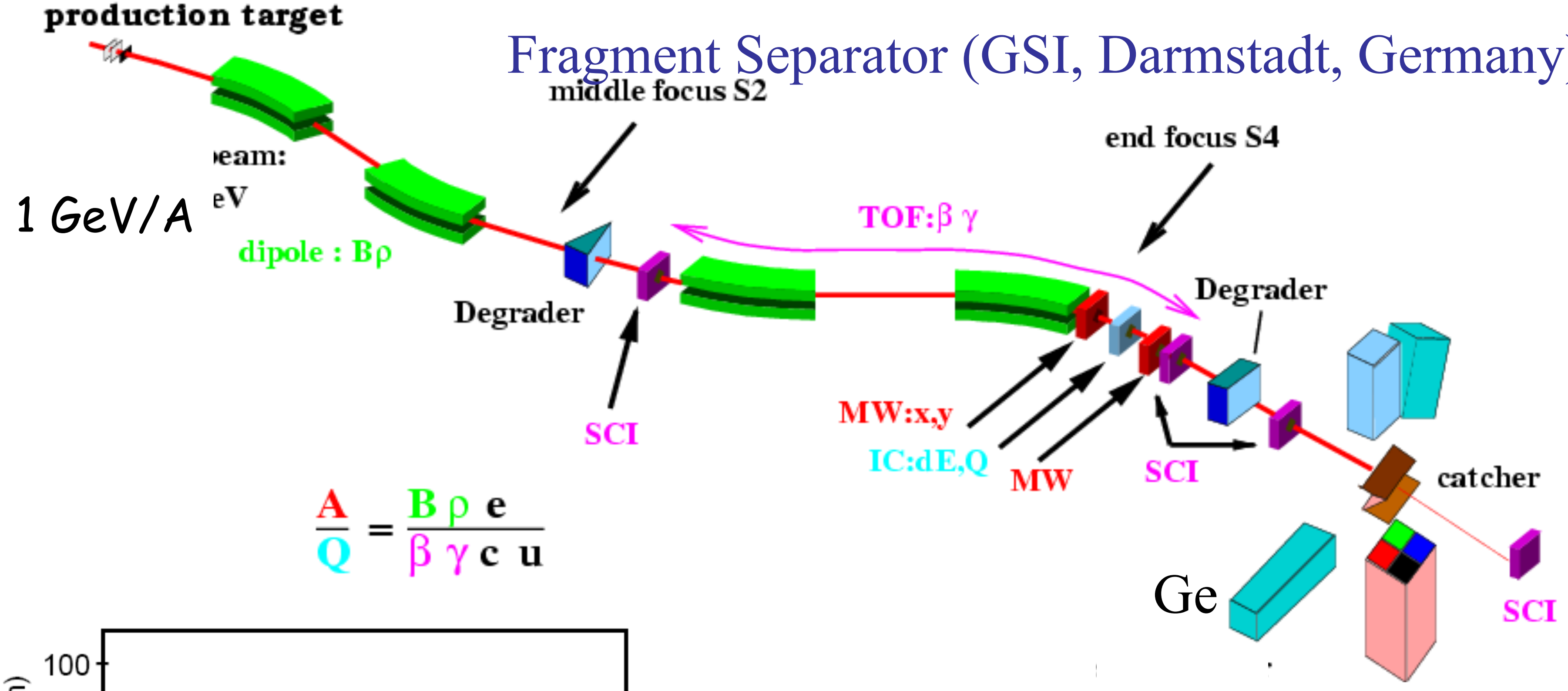

$$\frac{A}{Q} = \frac{B\rho\ e}{\beta\ \gamma\ c\ u}$$

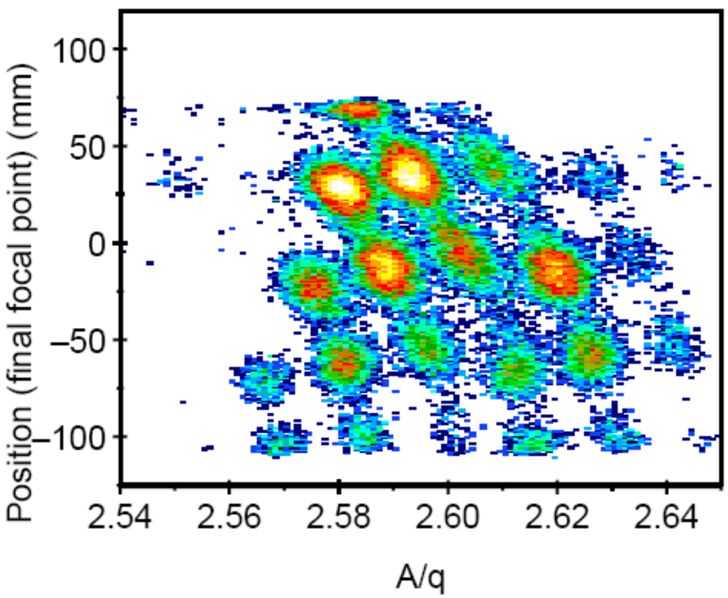

Isomers:

-Very sensitive (decays): info about exotic nuclei

-Isomeric beams (in storage rings, in reactions)

In flight fragmentation (and fission): separation and identification

Fragment Separator (GSI, Darmstadt, Germany)

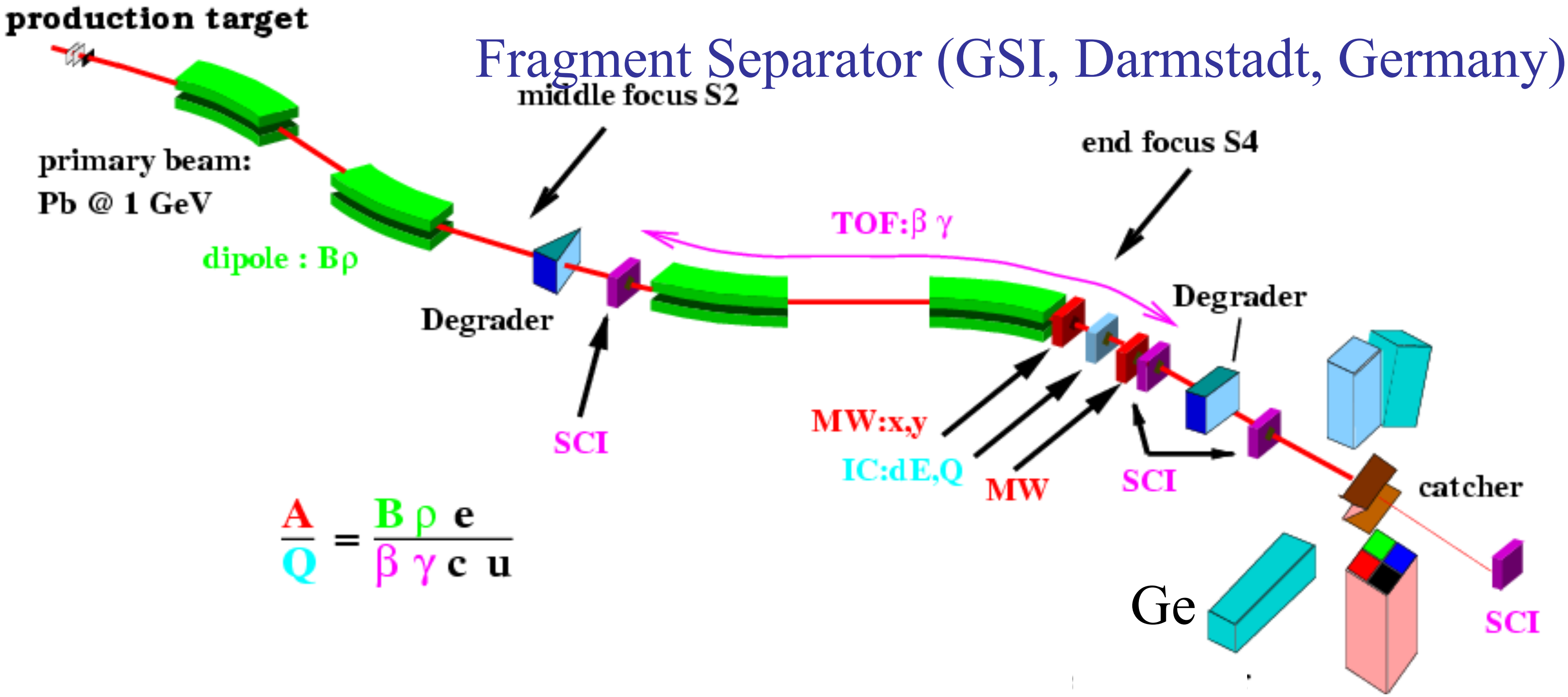

Relativistic energy fragmentation: => heavy ions

Isomeric decay spectroscopy:

- decay correlated with the fragment
- ***very sensitive***

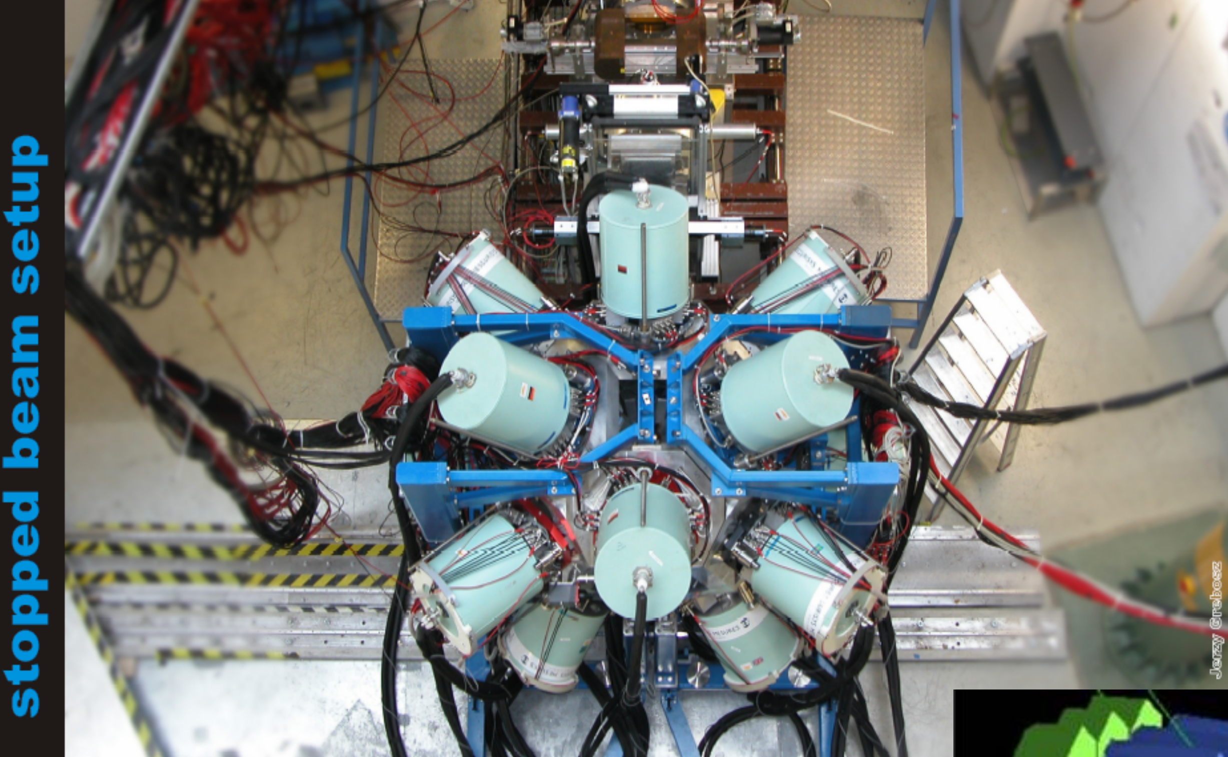

Past: RISING

Future: DESPEC
(DEGAS array)

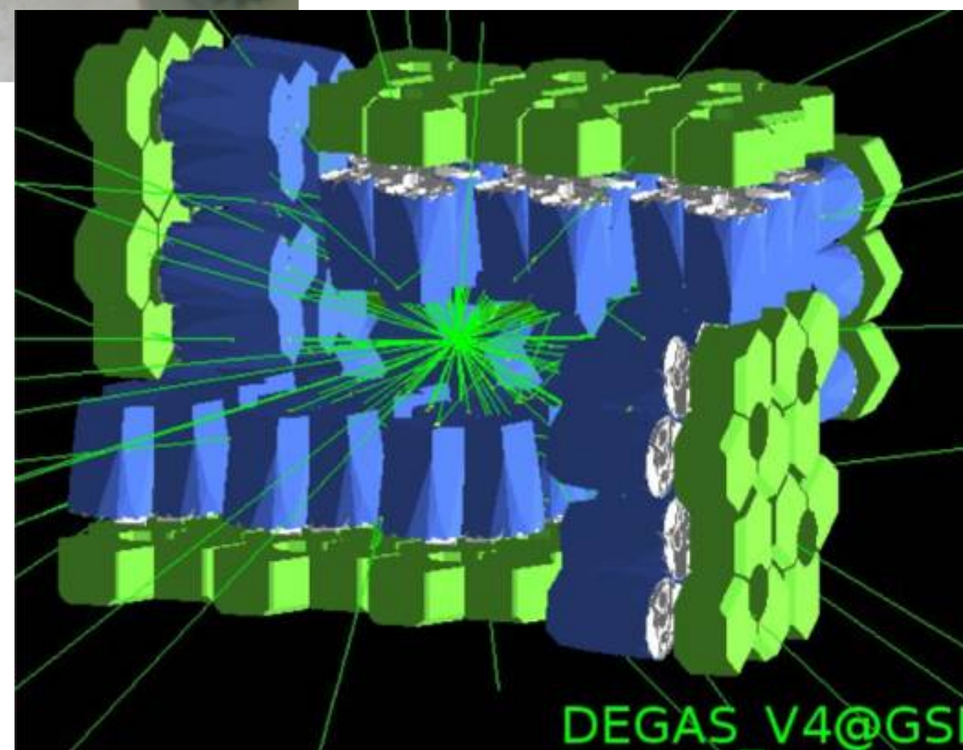

Isomers are special

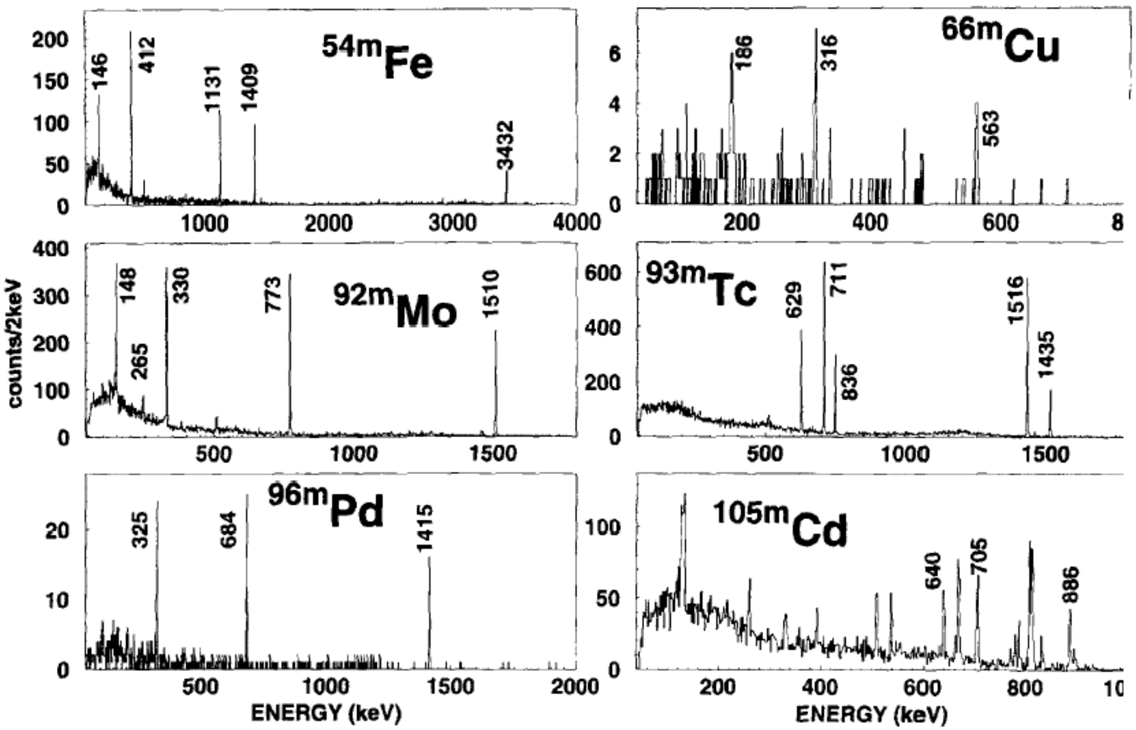

R. Grzywacz et al., Phys. Lett. B 355 (1995) 439.

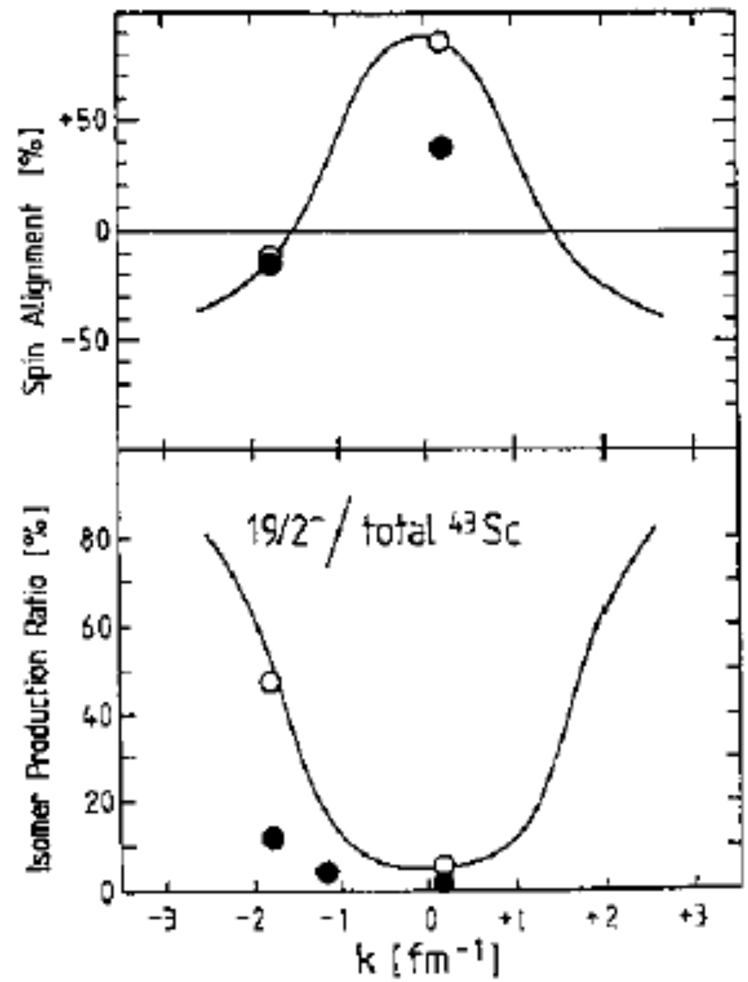

W.-D. Schmidt-Ott et al., Z. Phys. A 350 (1994) 215.

Highest spin from fragmentation: I=(55/2) isomer in ^{213}Rn

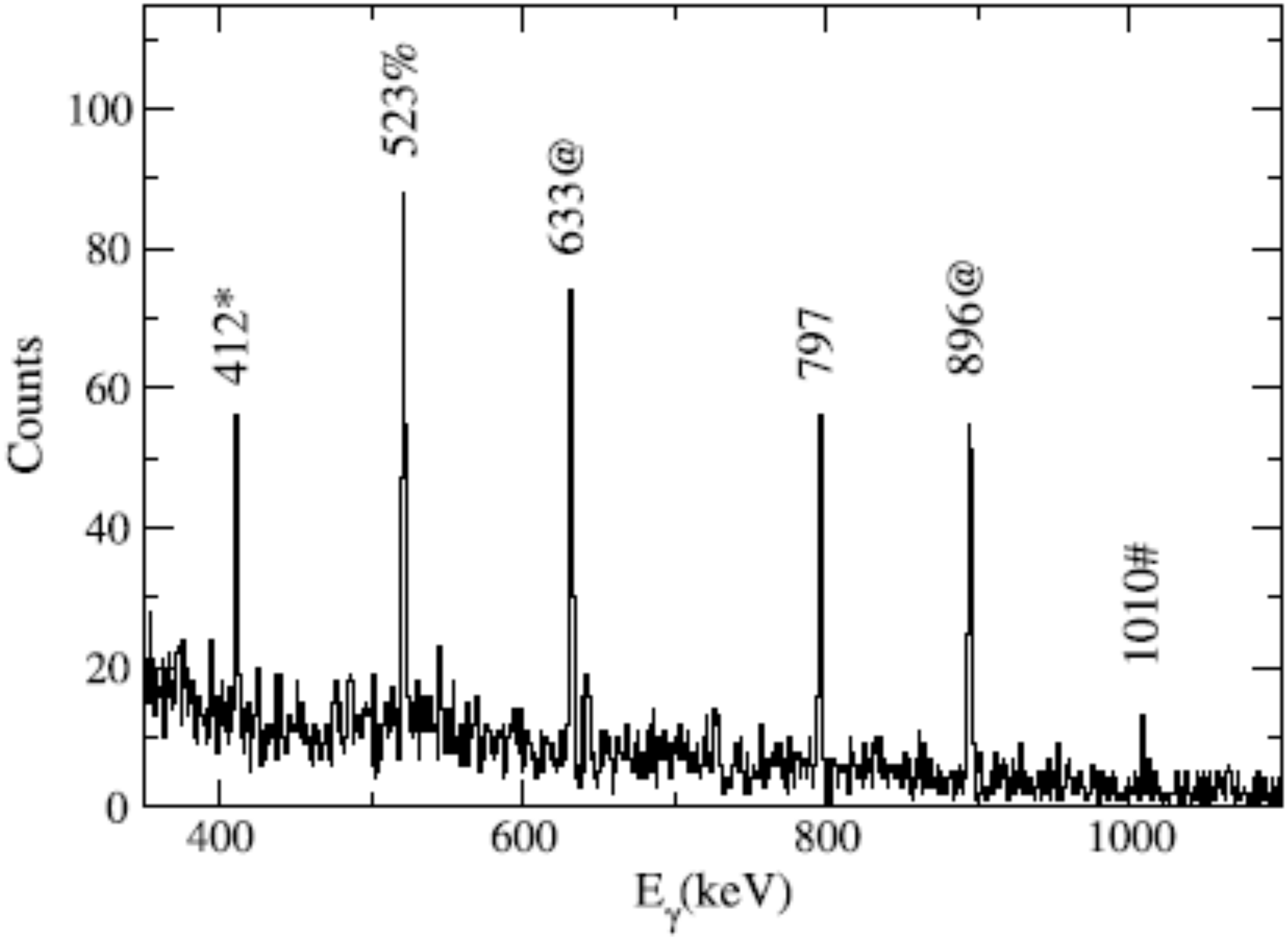

Fig. 1. Gamma-ray energy spectrum obtained in coincidence with ^{213}Rn ions using a time gate of width 1.4 μs starting ~50 ns after the prompt flash. The transitions used to obtain the isomeric ratios for the $(55/2)^+$, $43/2^-$, $31/2^-$ and $25/2^+$ levels are denoted # * % and @ respectively.

A.M. Denis Bacelar et al., Phys. Lett. B 723, 302 (2012)

Isomeric ratios from ^{208}Pb and ^{238}U fragmentation

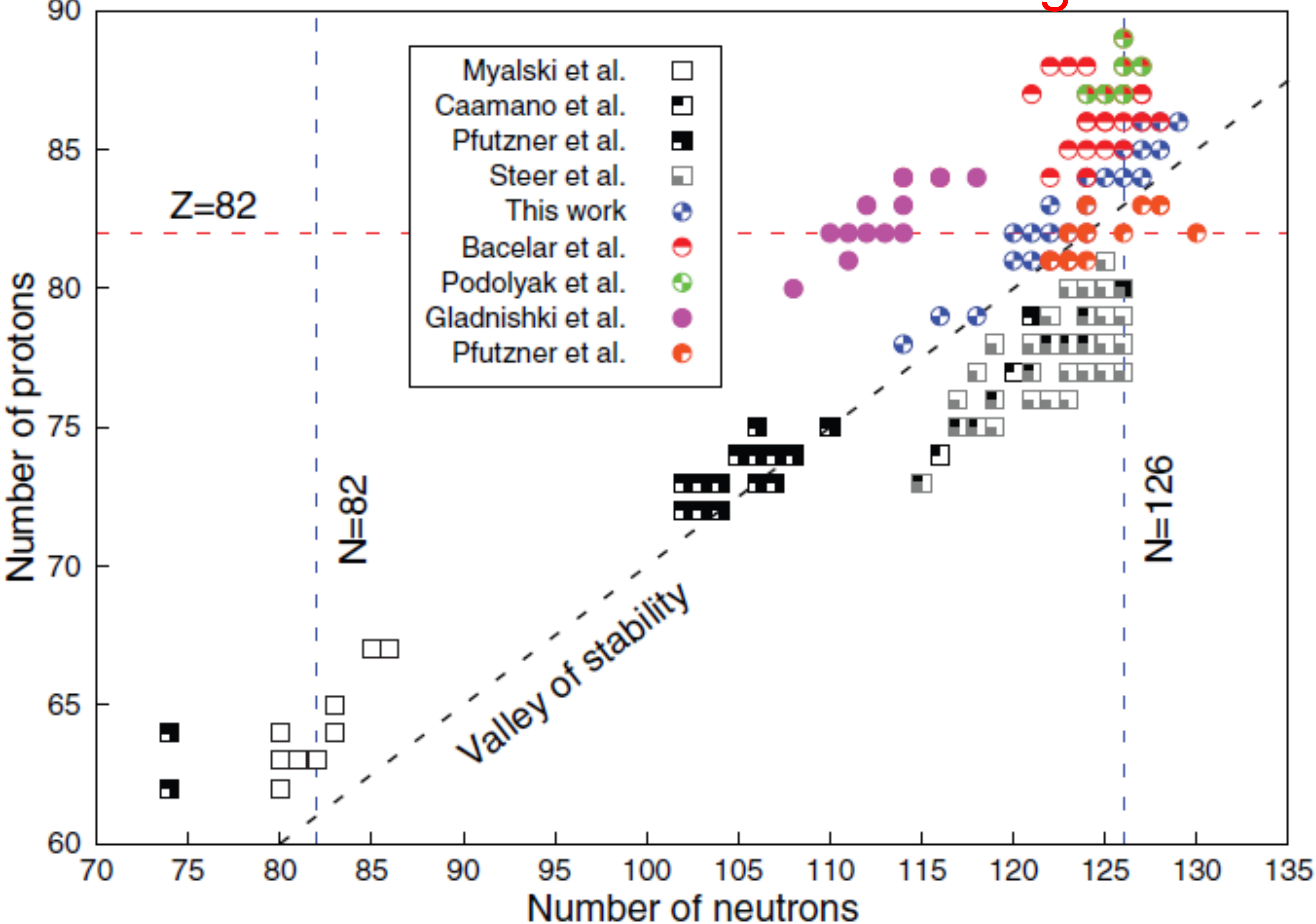

M. Bowry et al., Phys. Rev. C 88, 024611 (2013)

Isomeric ratio vs spin

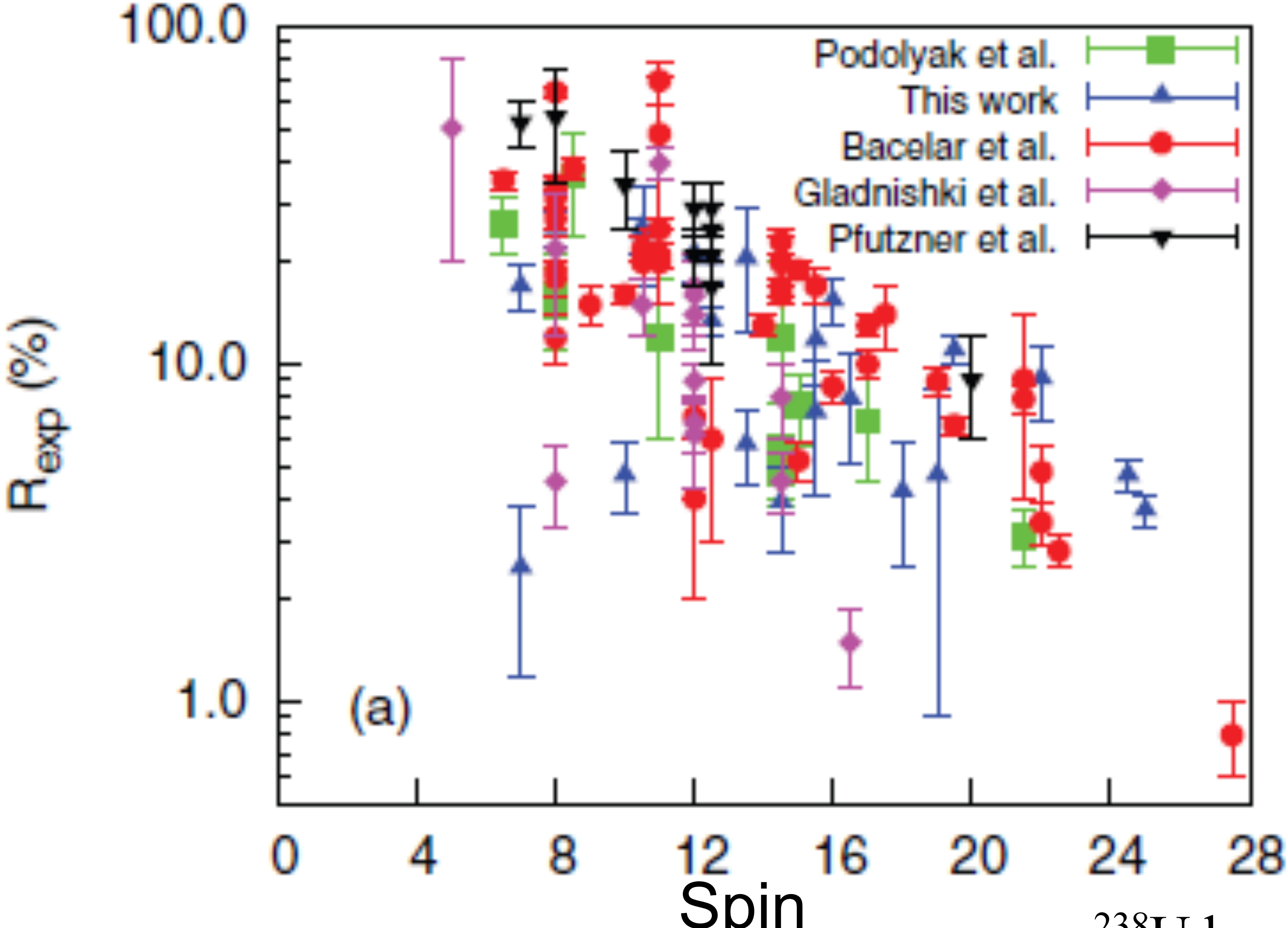

M. Bowry et al., Phys. Rev. C 88, 024611 (2013)

^{238}U beam

if $A_{projectile}-A_{fragment}$~large

Statistical abrasion-ablasion model (ABRABLA code)

Excitation energy

~27 MeV/abrated nucleon=

=2 x single particle (holes) energy

Angular momentum

from single particle states only

Is this good enough?

Ablated nuclei/abraded nuclei ~2

Good cross sections

M. De Jong, A.V. Ignatyuk and K.-H. Schmidt, Nucl. Phys. A 613 (1997) 435

Isomeric ratio

$$R_{\exp} = \frac{N_{isomer}}{N_{total}}$$

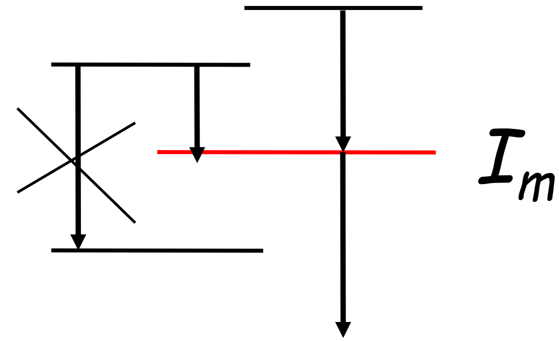

$$P(I) = \frac{2I+1}{2\sigma_f^2} \exp\left(-\frac{I(I+1)}{2\sigma_f^2} \right)$$

Spin-cutoff parameter:

$$\sigma_f^2 = 0.16 A_p^{2/3} \frac{(A_p - A_f)(\nu A_p + A_f)}{(\nu+1)^2 (A_p - 1)}$$

$\langle j_z^2 \rangle$

$$\rho_{theo} = \int_{I_m}^{\infty} P(I)\, dI$$

(sharp cut-off approx.)

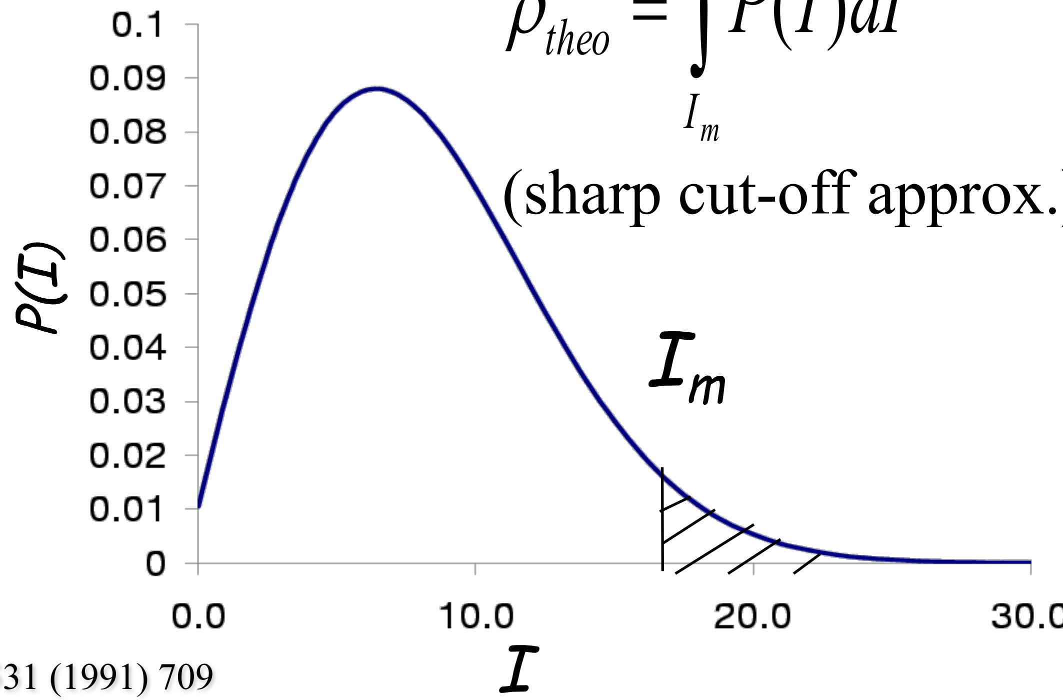

J.-J. Gaimard and K.-H. Schmidt, Nucl. Phys. A 531 (1991) 709

M. De Jong, A.V. Ignatyuk and K.-H. Schmidt, Nucl. Phys. A 613 (1997) 435

Comparison with theory

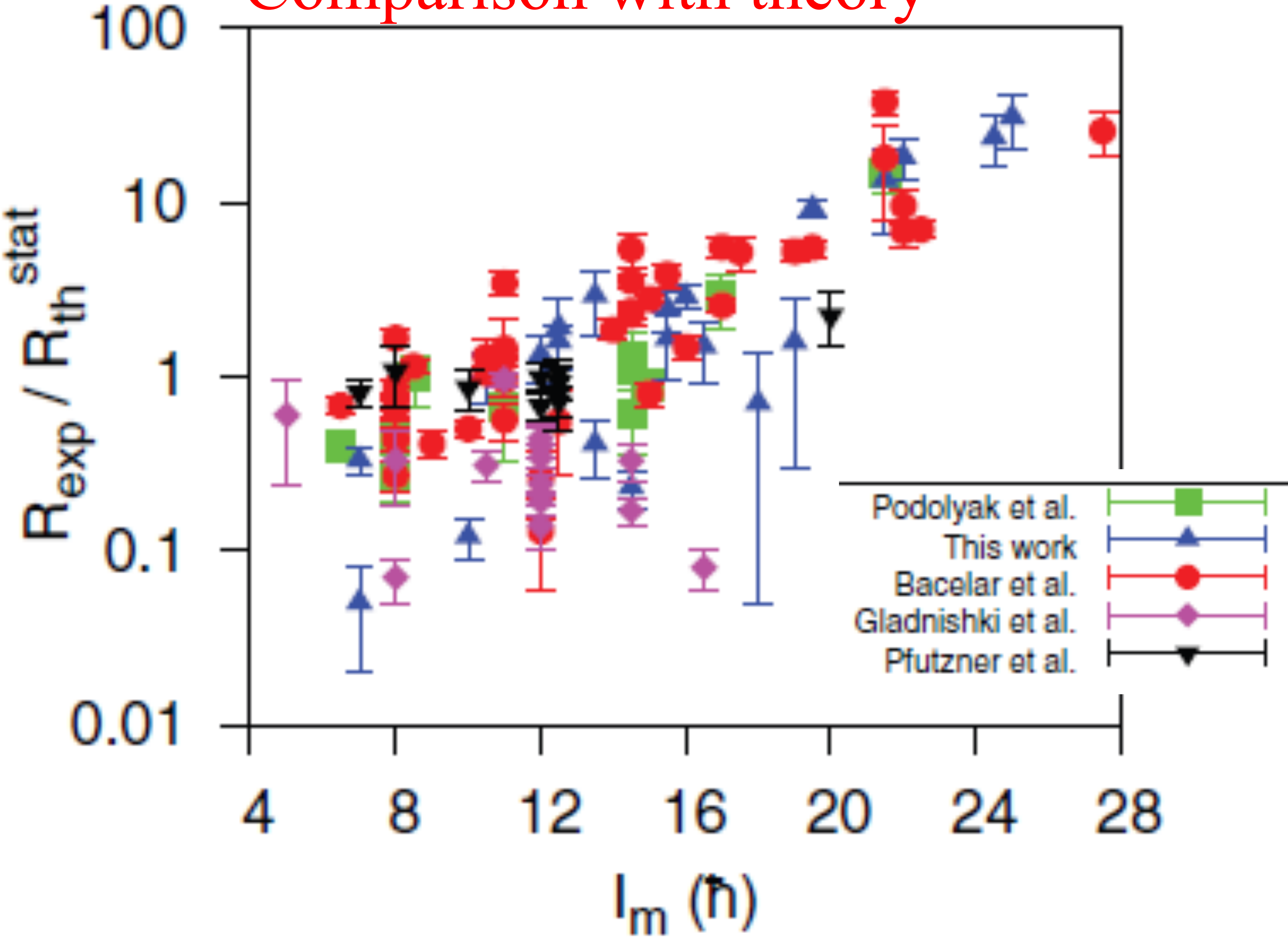

M. Bowry et al., Phys. Rev. C 88, 024611 (2013)

Nuclear structure has to be considered

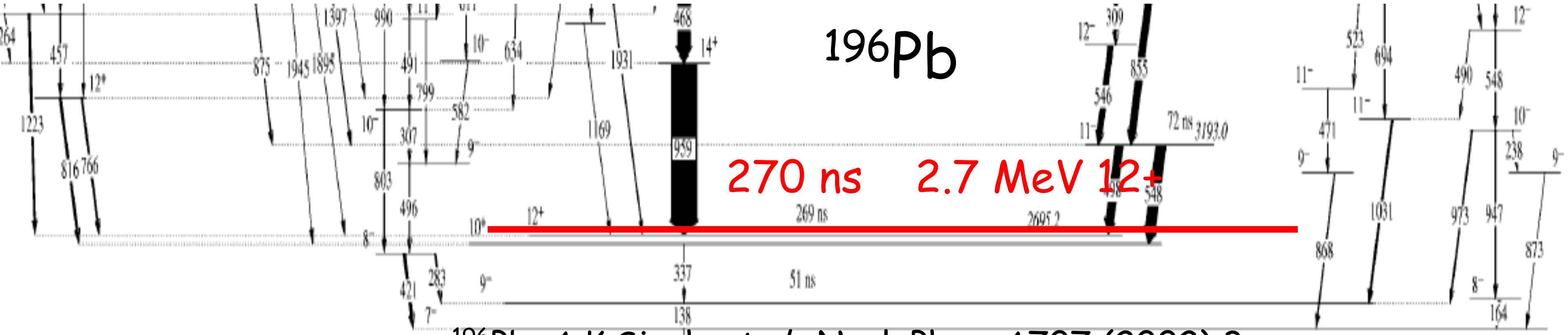

^{196}Pb: A.K.Singh *et al.*, Nucl. Phys. A707 (2002) 3

$^{186}W(^{16}O,6n)$ at 110 MeV; $^{170}Er(^{30}Si,4n)$ at 144 MeV

fusion-evaporation reaction!

$$\varphi = I_{isomer}/(I_{parallel}+I_{isomer}) = I_{isomer} / I_{total}$$

$$\rho_{exp}=R_{exp}/\varphi$$

ρ_{exp} - the probability of populating states with higher spin than the isomer – can be compared with theory!

Without structure considerations

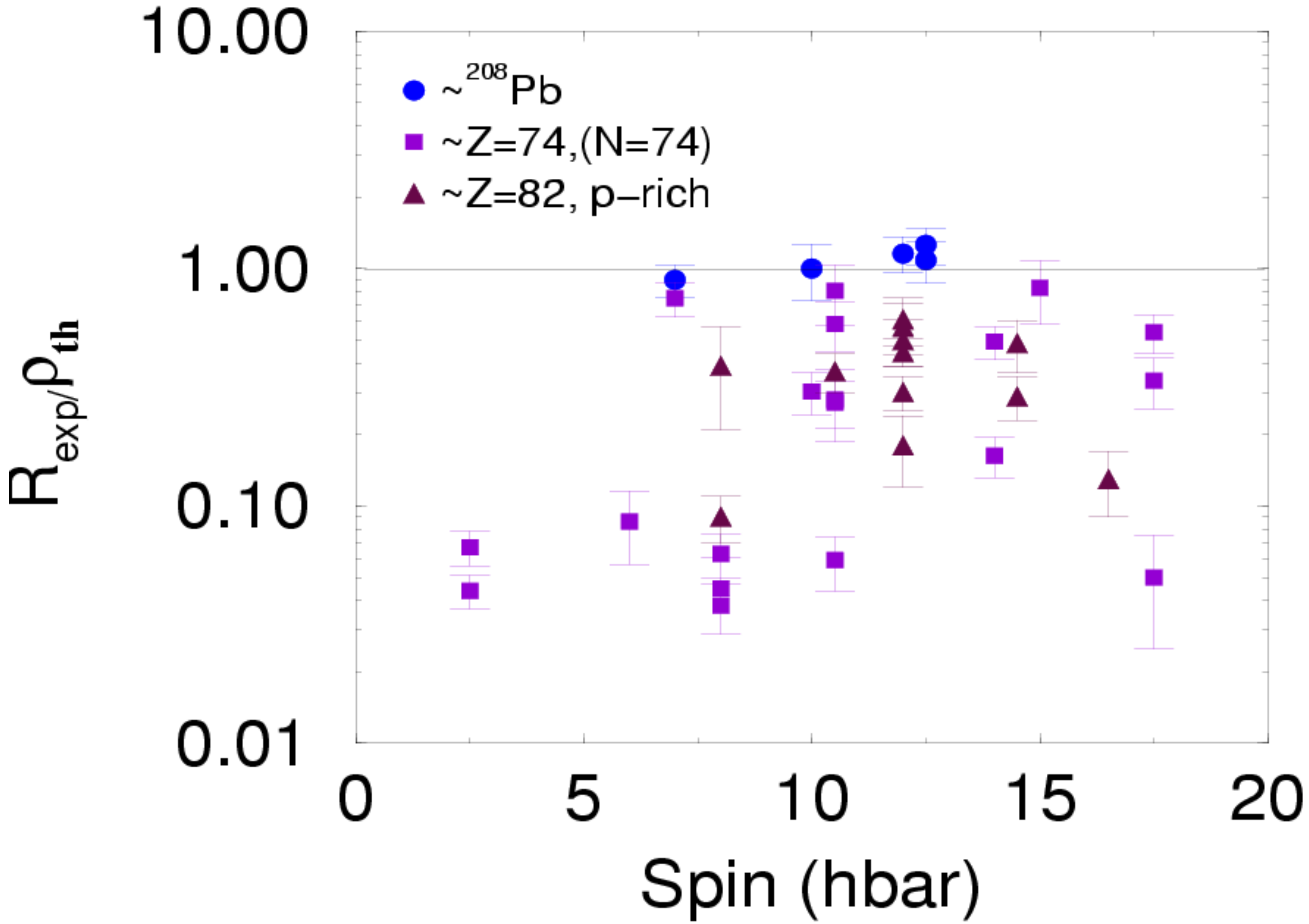

With structure considerations

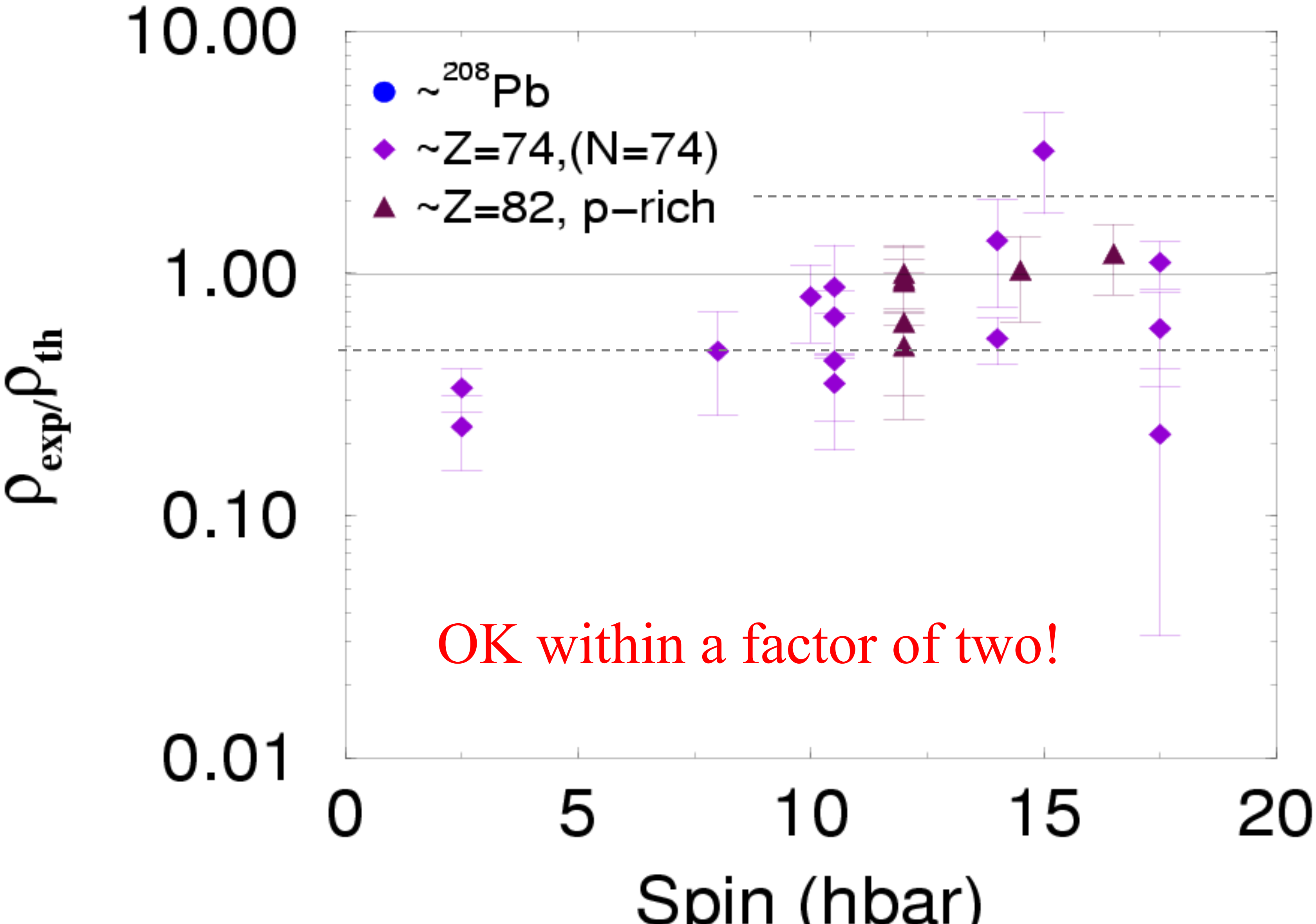

Zs. P. , Acta Phys. Pol. B36 (2005) 1269

Comparison with theory

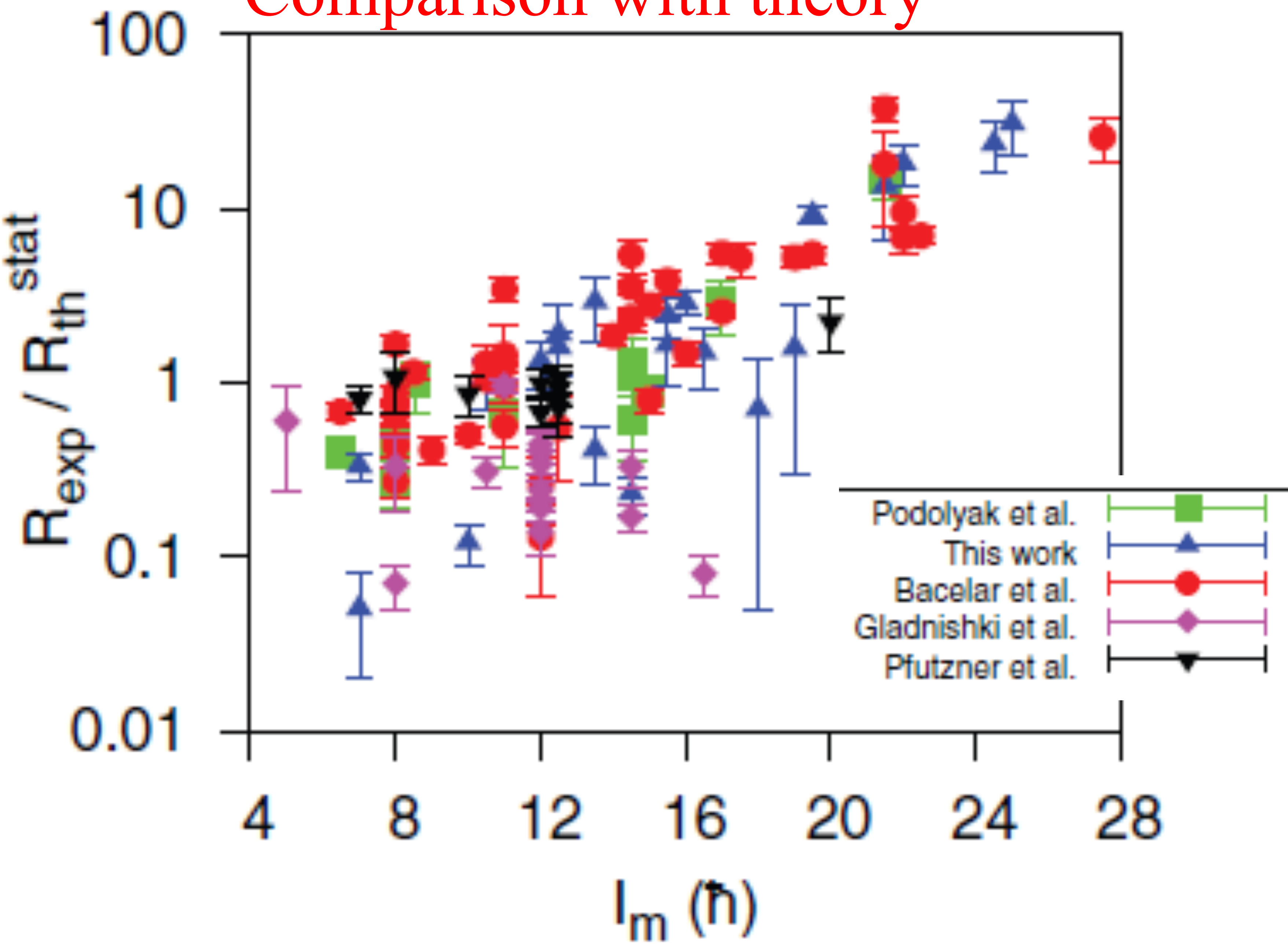

M. Bowry et al., Phys. Rev. C 88, 024611 (2013)

Isomeric ratios following fragmentation

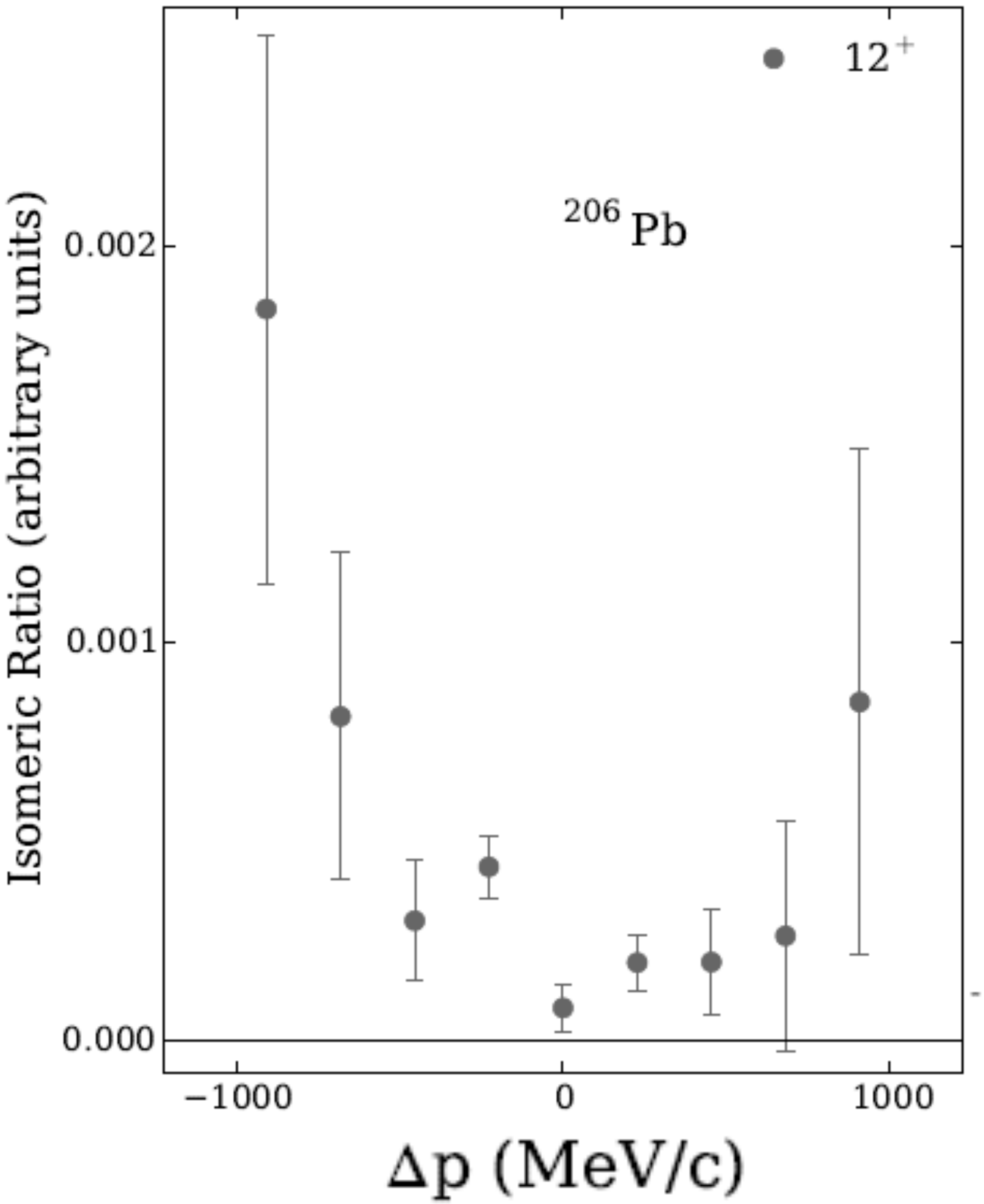

N. Lalović et al., to be published

^{208}Pb → ^{206}Pb
at E/A=1 GeV

Fragments are slower than projectile: momentum shift (friction)

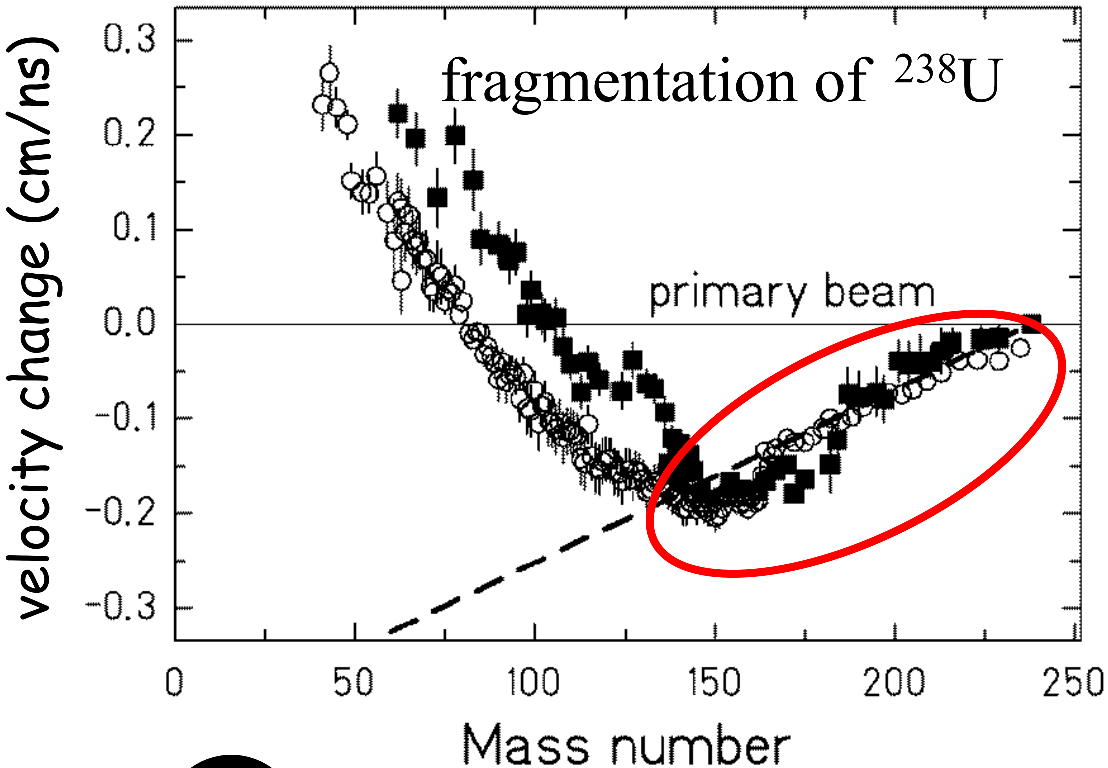

M.V. Ricciardi et al., PRL 90 (2003) 212302

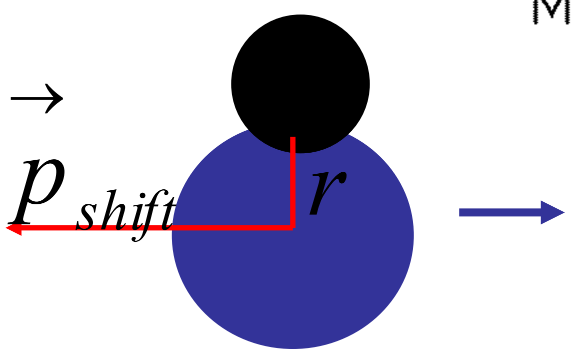

$$\vec{I} = \vec{r} \times \vec{p}_{shift}$$

⇨ angular momentum produced

(collective)

I perpendicular to the beam

We need to couple: single particle holes *I* (any direction in 3D)
collective *I* (2D)

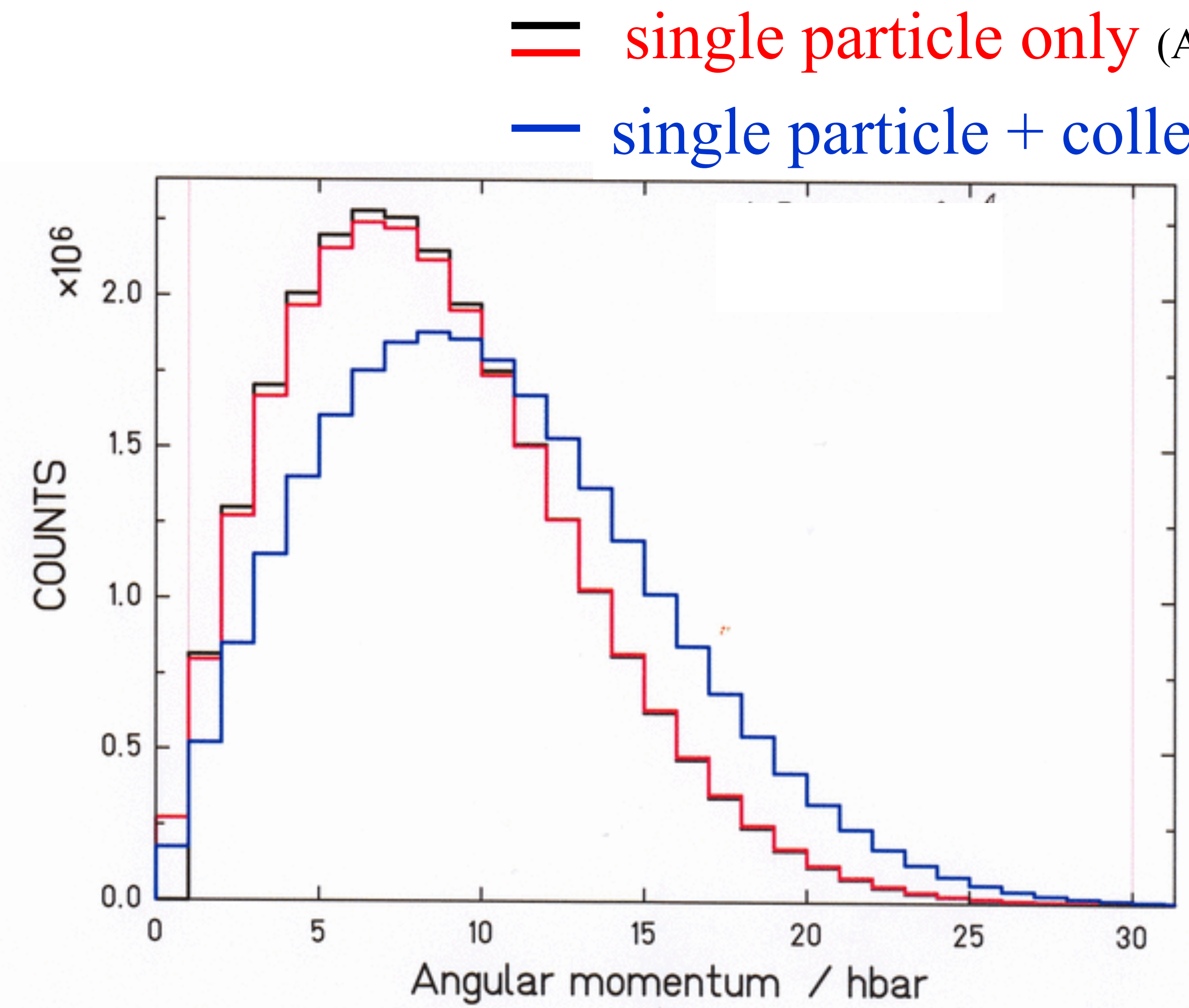

increased high-spin population due to **collective *I***

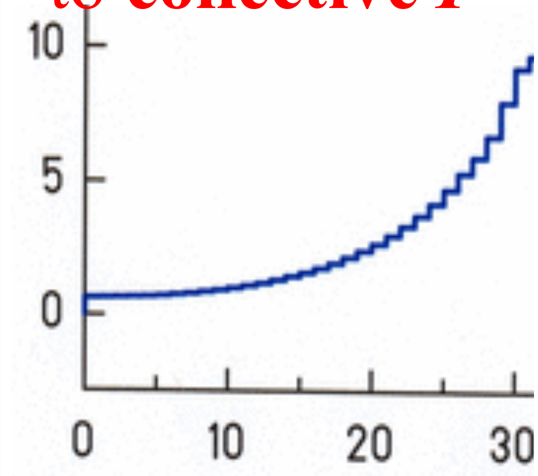

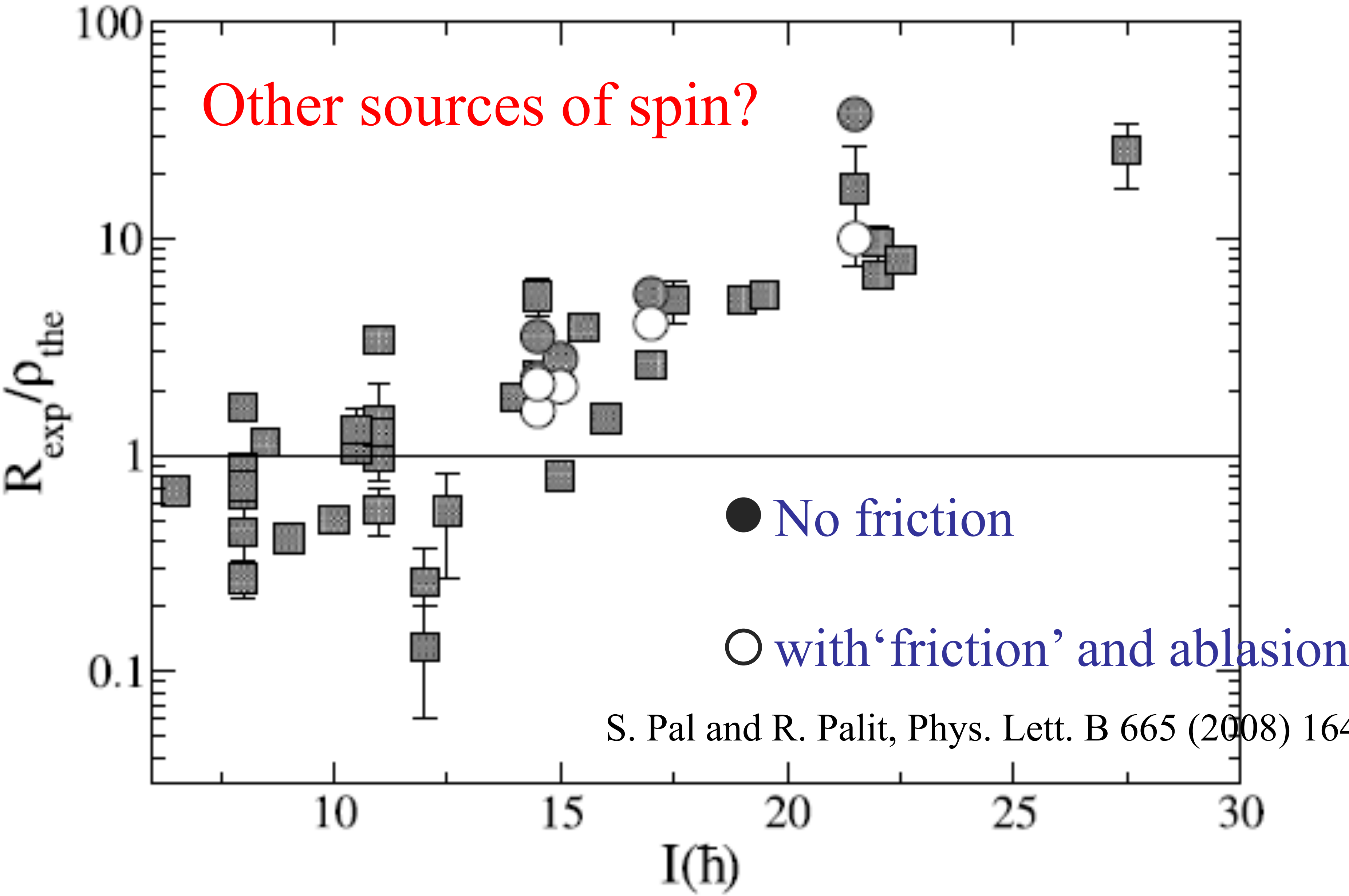

A.M. Denis Bacelar et al., Phys. Lett. B 723, 302 (2012)

Comparison with theory (sharp cut-off approx.)

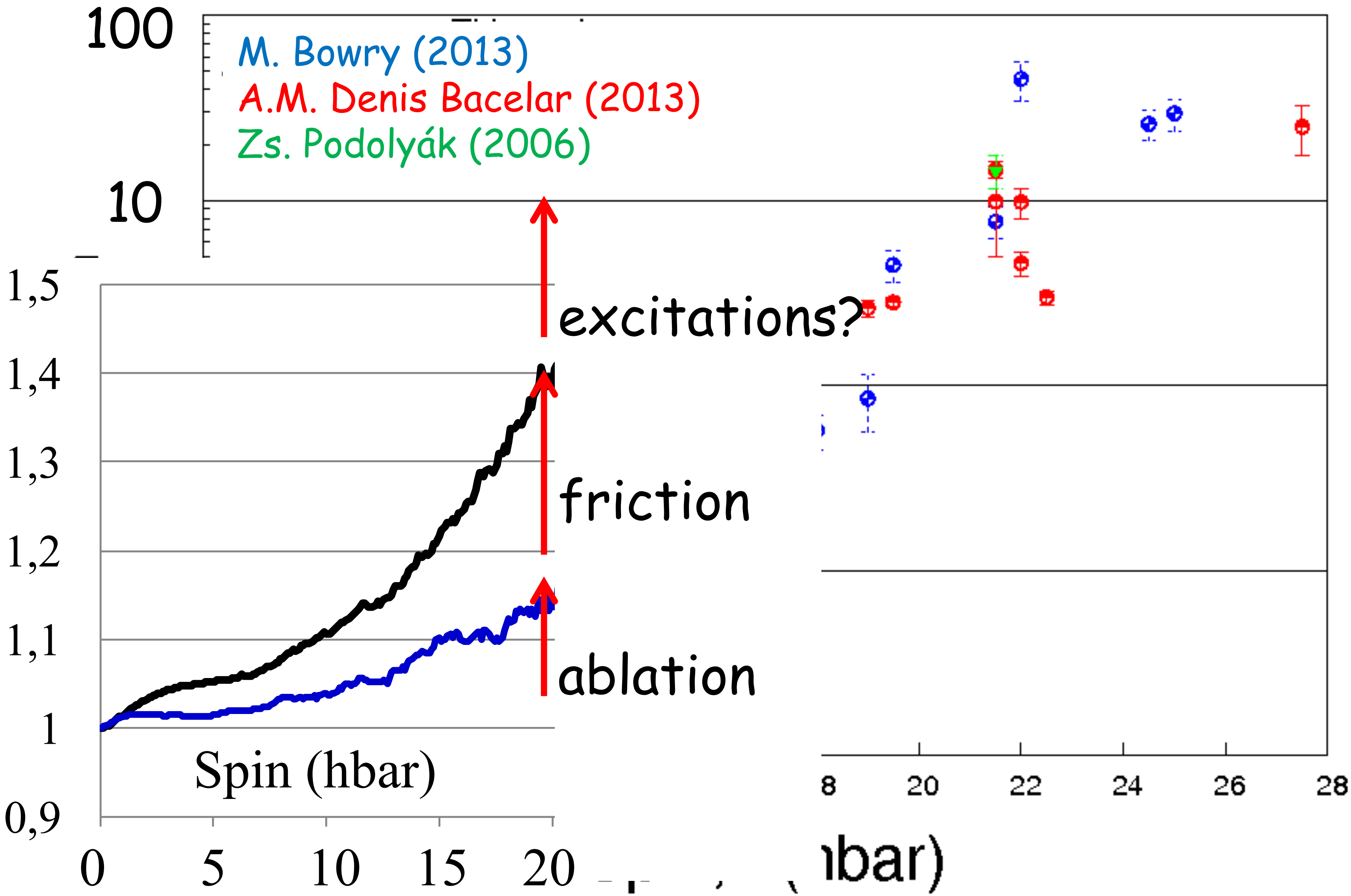

Simplified theory (analytical formula)

$$P(I) = \frac{2I+1}{2\sigma_f^2} \exp\left(-\frac{I(I+1)}{2\sigma_f^2}\right) \quad \Rightarrow \quad \rho_{theo} = \int_{I_m}^{\infty} P(I)\,dI$$

(sharp cut-off approx.)

Spin-cutoff parameter:

$$\sigma_f^2 = 0.16 A_p^{2/3} \frac{(A_p - A_f)(\nu A_p + A_f)}{(\nu+1)^2 (A_p - 1)}$$

$\langle j_z^2 \rangle$

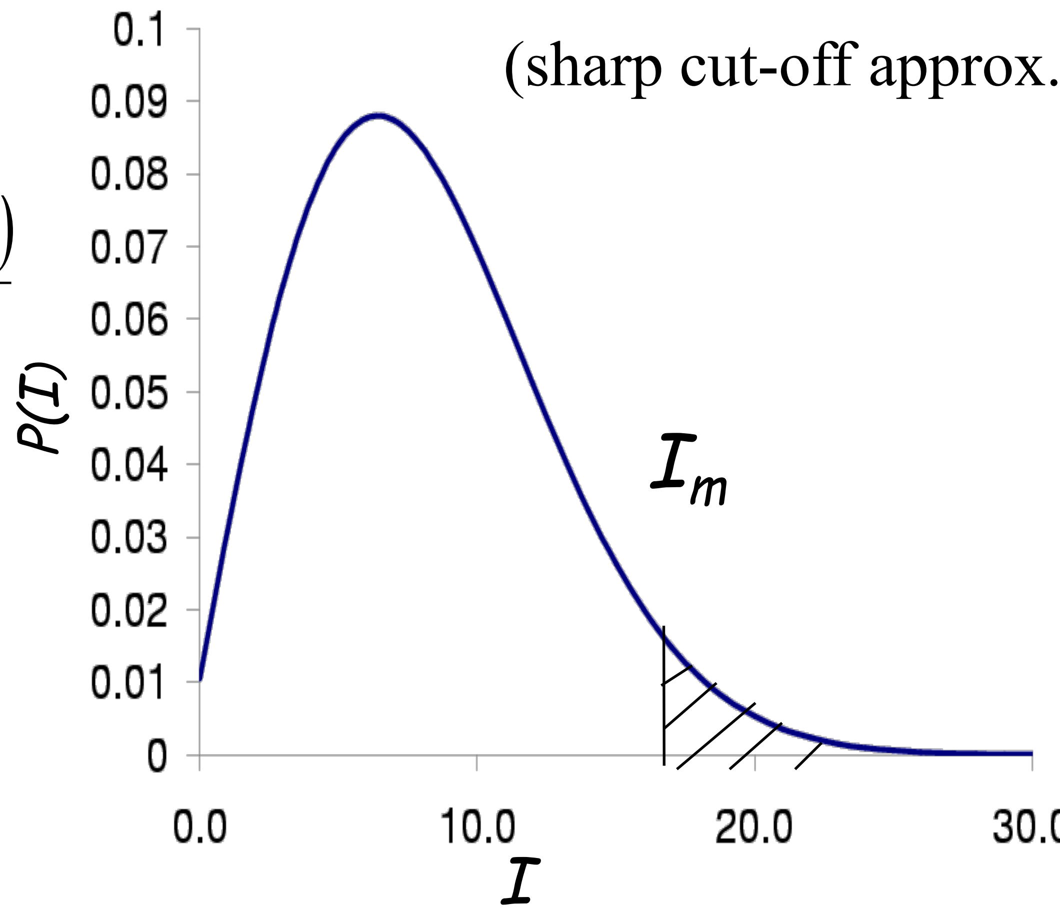

J.-J. Gaimard and K.-H. Schmidt, Nucl. Phys. A 531 (1991) 709

M. De Jong, A.V. Ignatyuk and K.-H. Schmidt, Nucl. Phys. A 613 (1997) 435

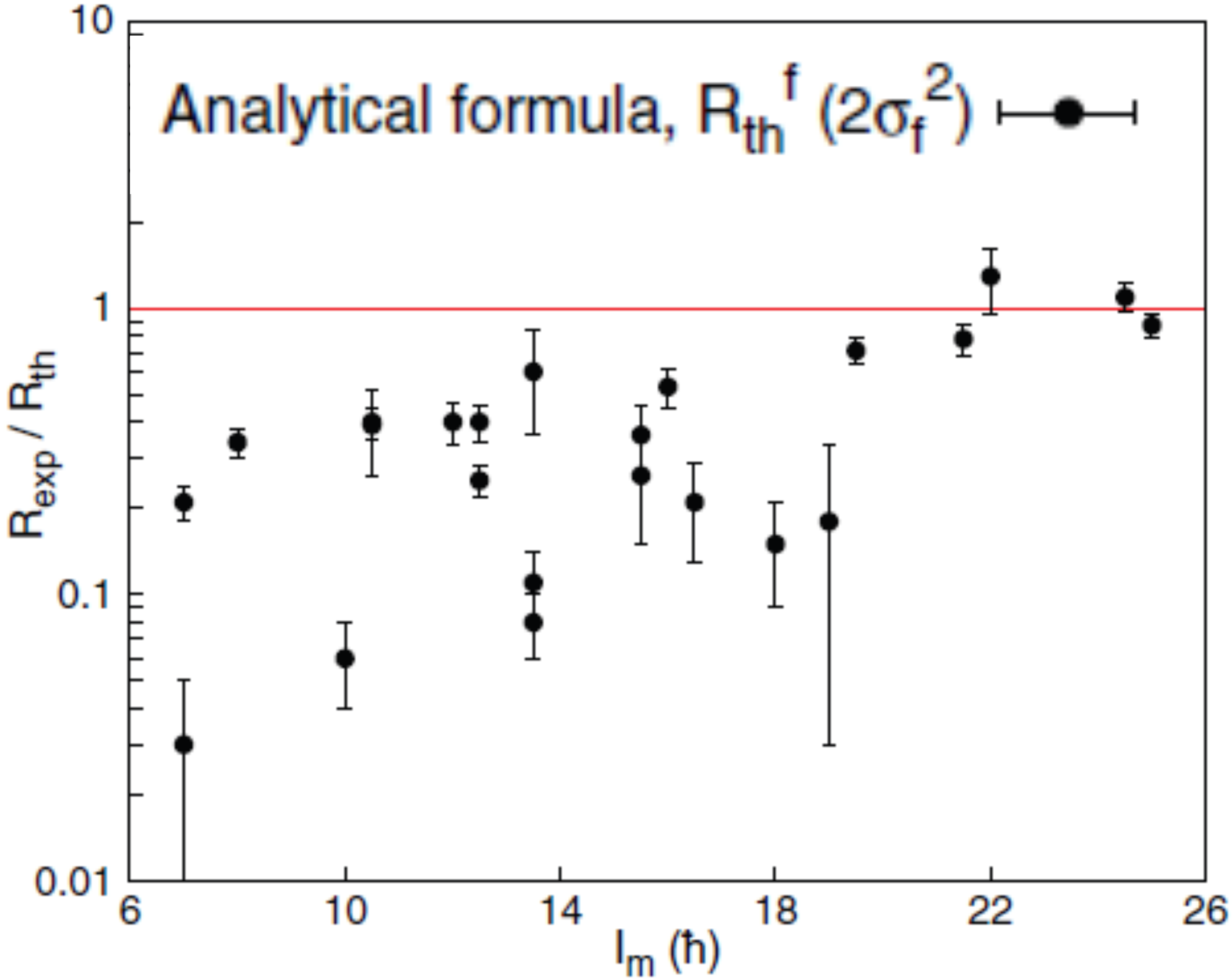

FIG. 8. (Color online) Isomeric ratios determined in the current study (see Table I) compared with the theoretical population predicted by the analytical formula only [Eq. (3)] plotted as a function of angular momentum of the isomeric state. The spin-cutoff parameter in Eq. (3) was multiplied by a factor of 2.

M. Bowry et al., Phys. Rev. C 88, 024611 (2013)

Population of isomers by ***two-proton knockout*** reaction in ^{206}Hg

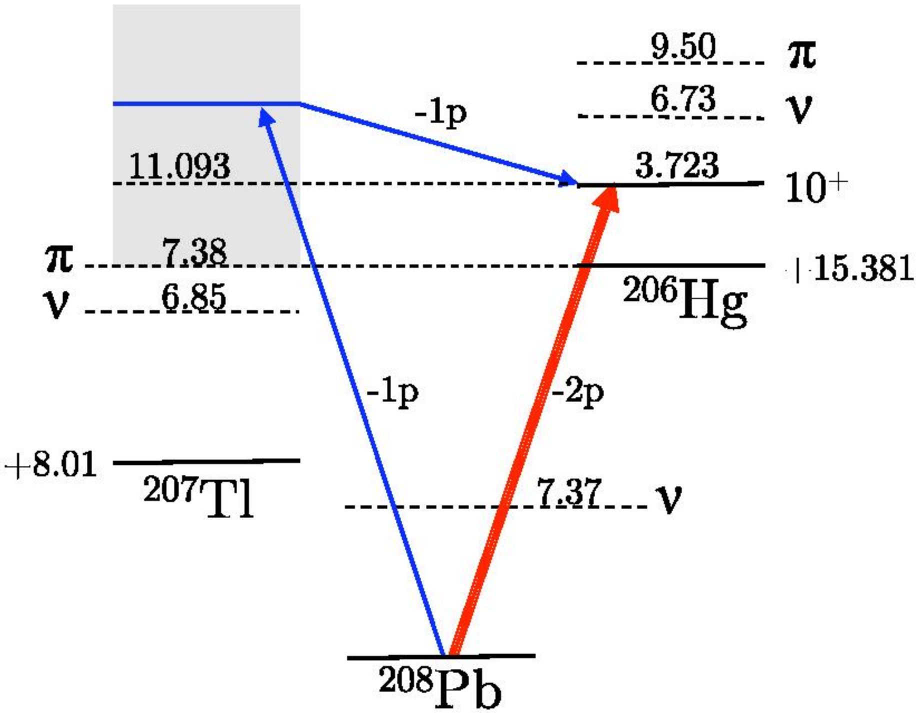

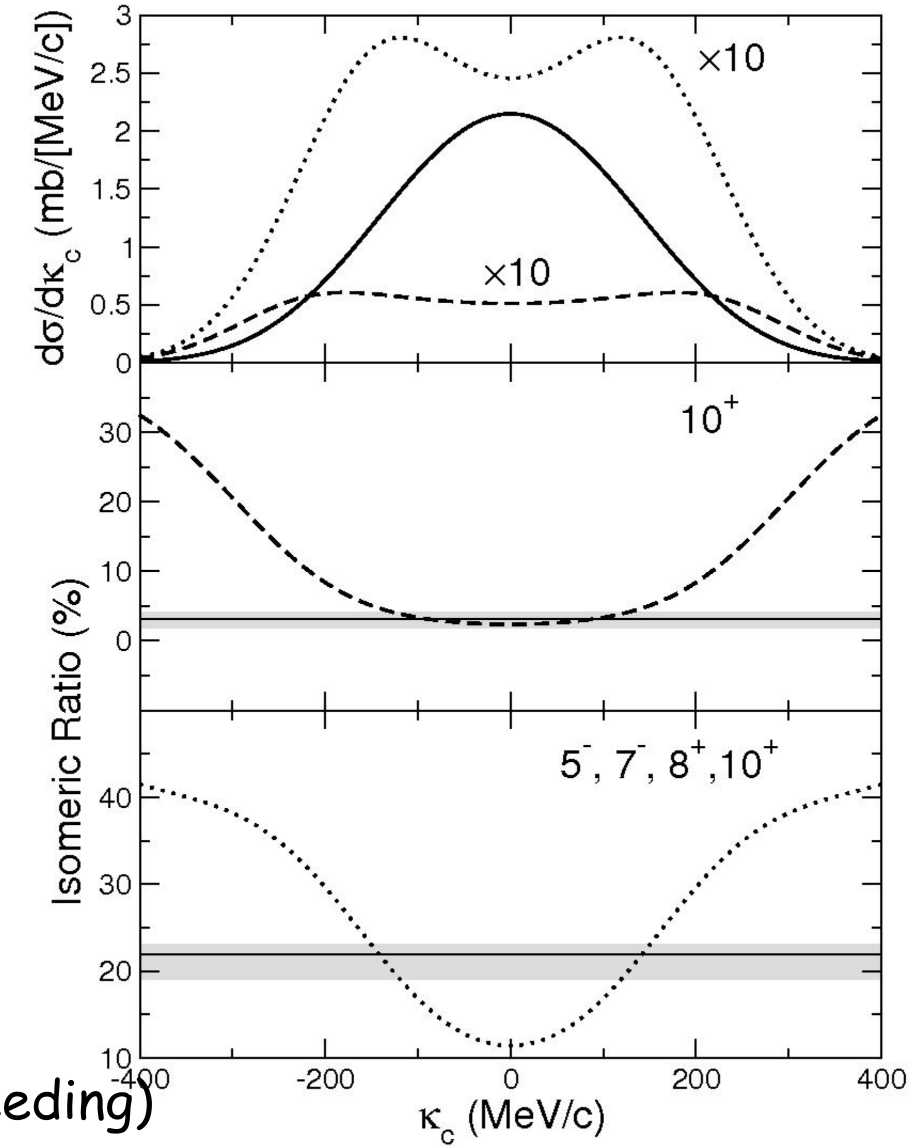

Isomeric ratios		fig.
Exp.	Theory	——— Total
3(1)%	4.7	- - - - 10+
22(+1-2)%	18.8	.... 5- (with feeding)

E.Simpson *et al.*, Phys. Rev. C 80 (2009) 064608.

Isomeric ratio as function of longitudinal momentum

5- isomer

— Theory
-- Theory + 3.1%

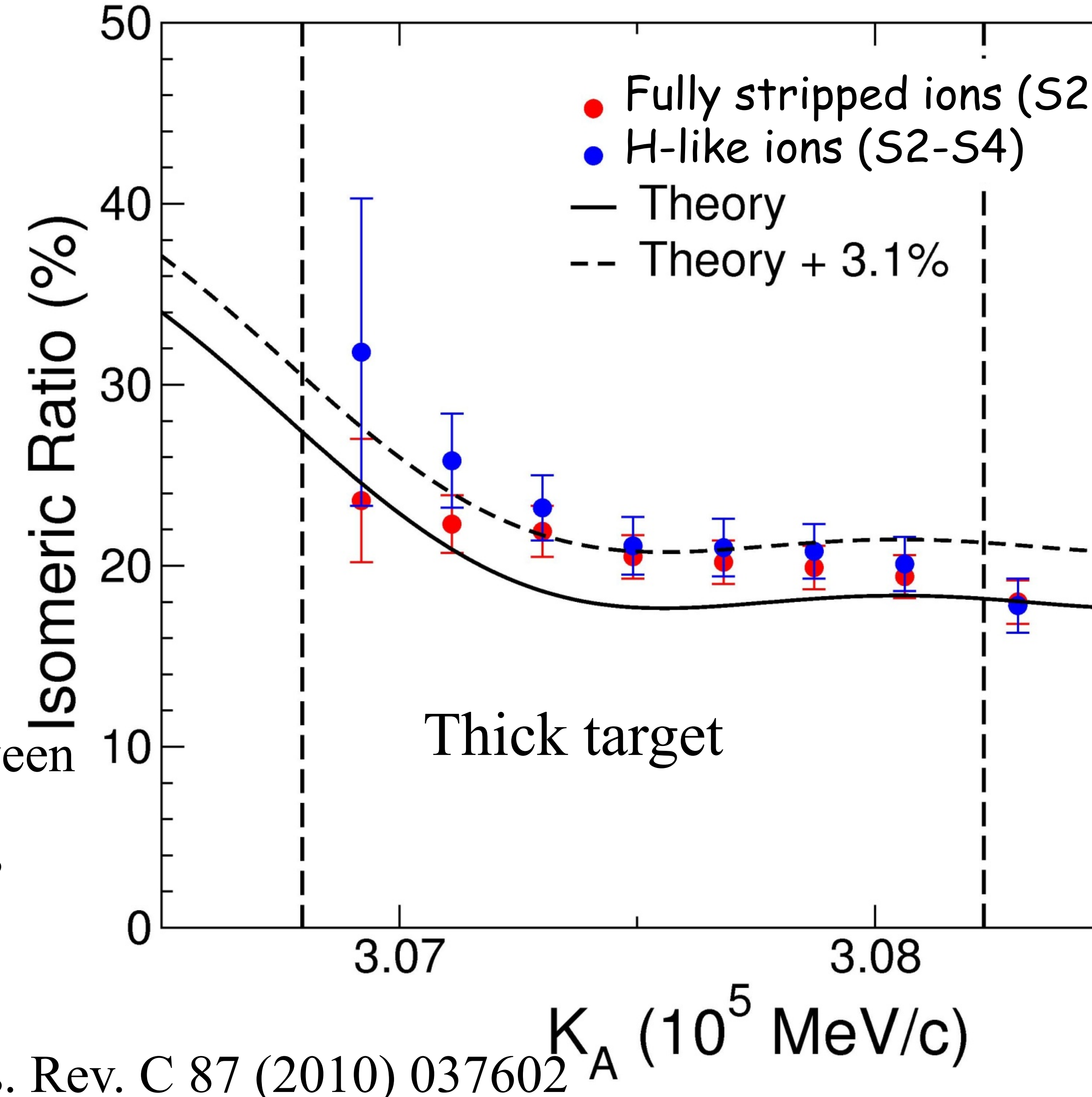

(3.1%=difference between experiment and theory; additional feeding?)

E. Simpson et al., Phys. Rev. C 87 (2010) 037602

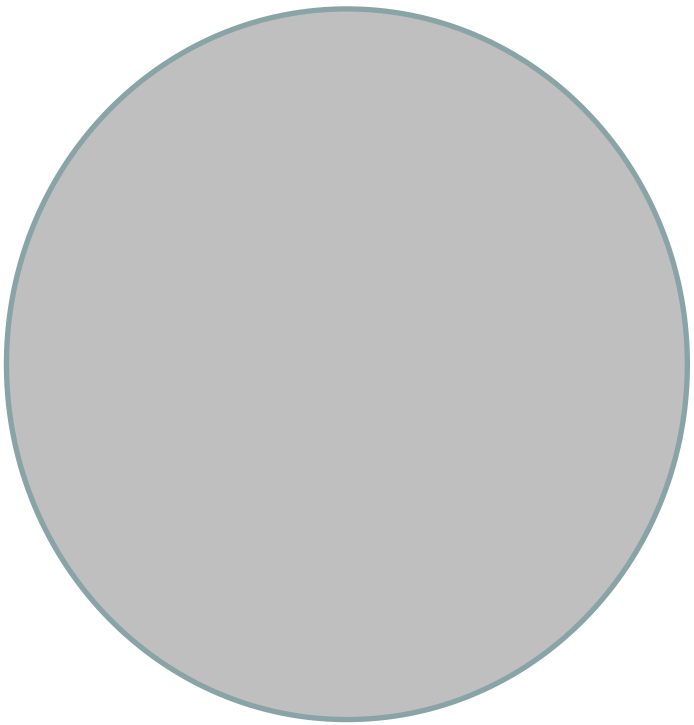

OR

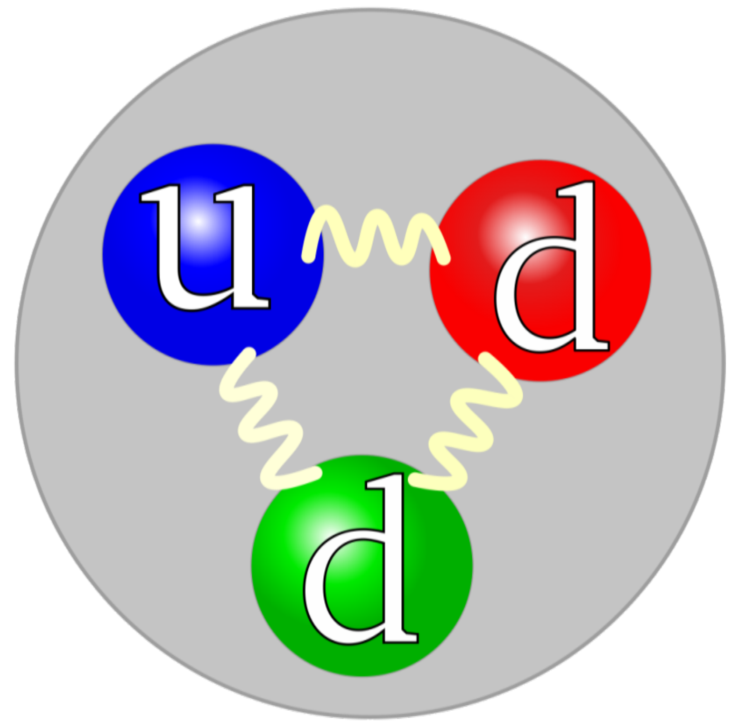

?

FIRST OBSERVATION OF THE Δ RESONANCE IN RELATIVISTIC HEAVY-ION CHARGE-EXCHANGE REACTIONS

D. Bachelier et al., Phys. Lett. 172, 23 (1986)

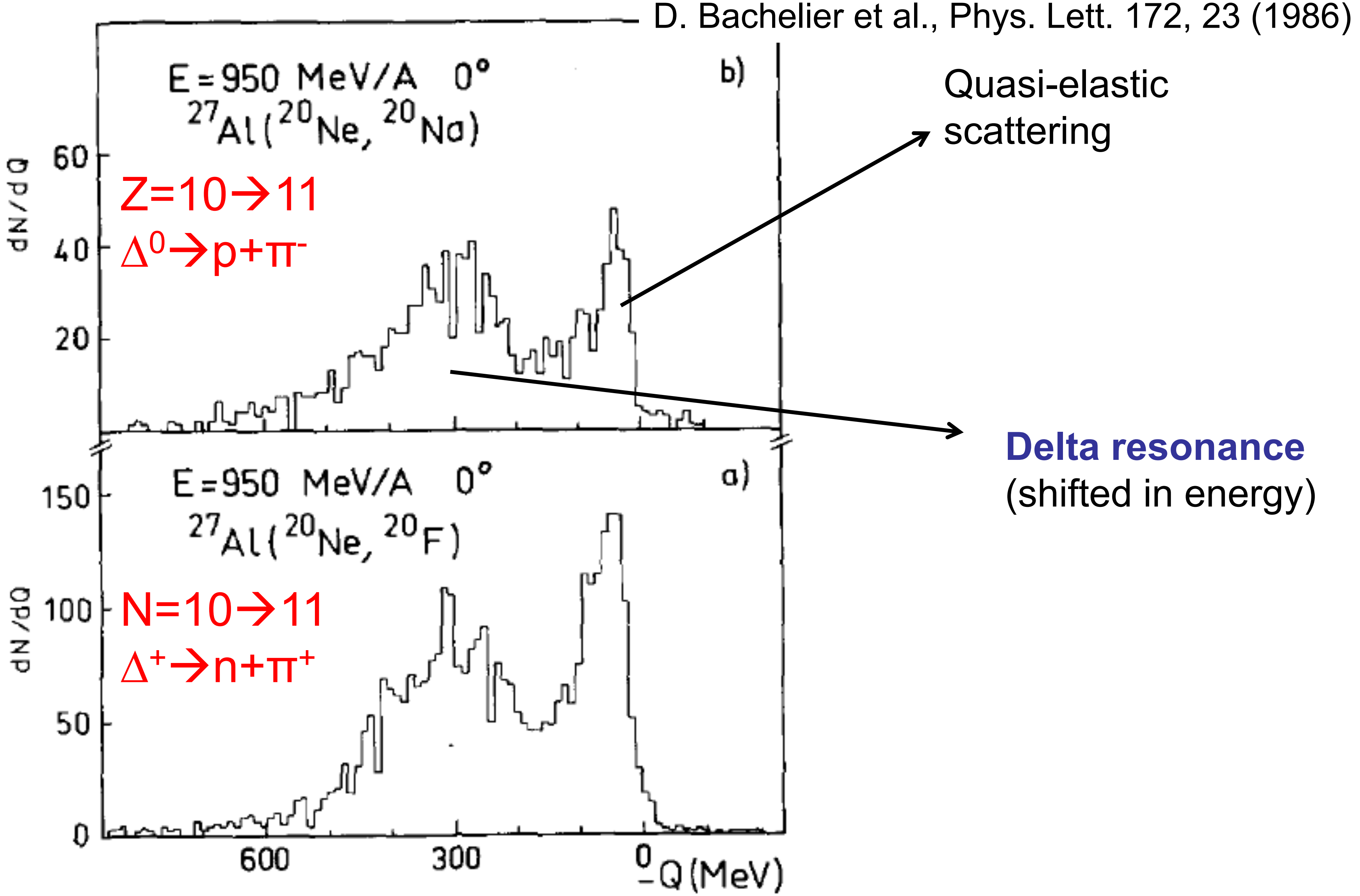

Role of nucleonic resonances in reactions

(but not for individual excited states)

experiment

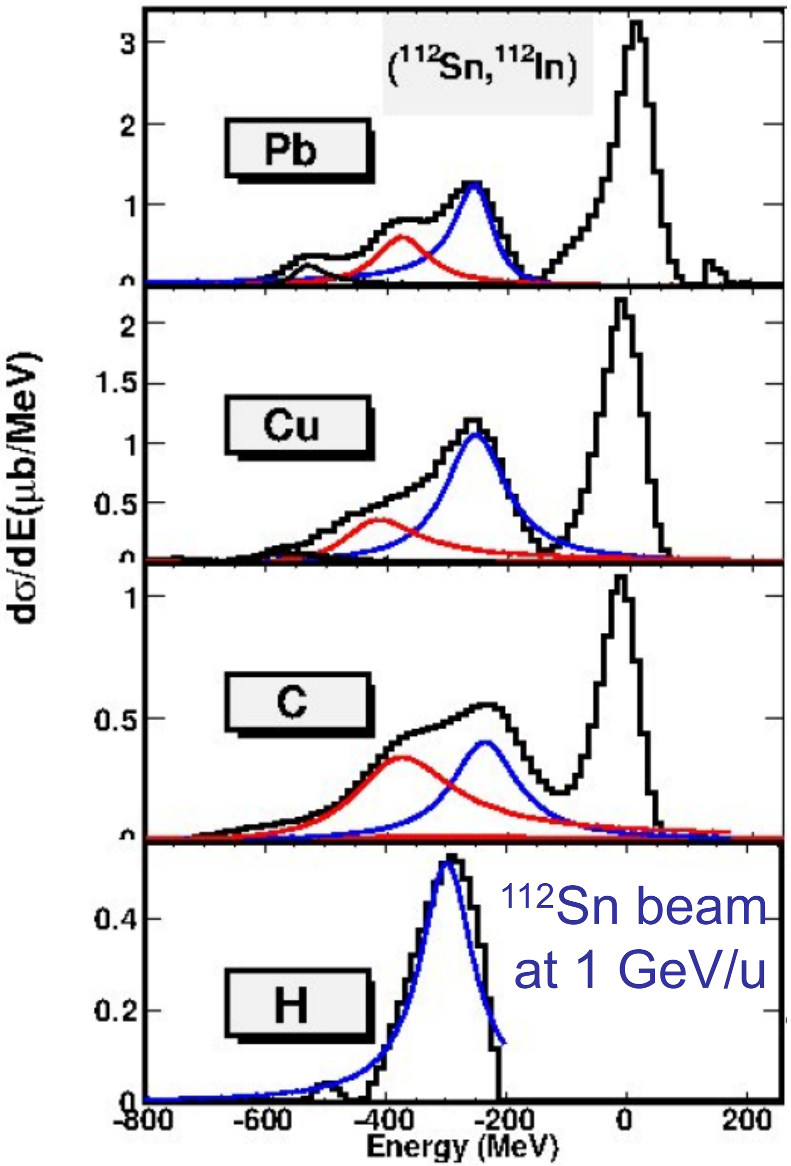

J. Benlliure et al., JPS Conf. Proc. 6, 020039 (2015)

theory

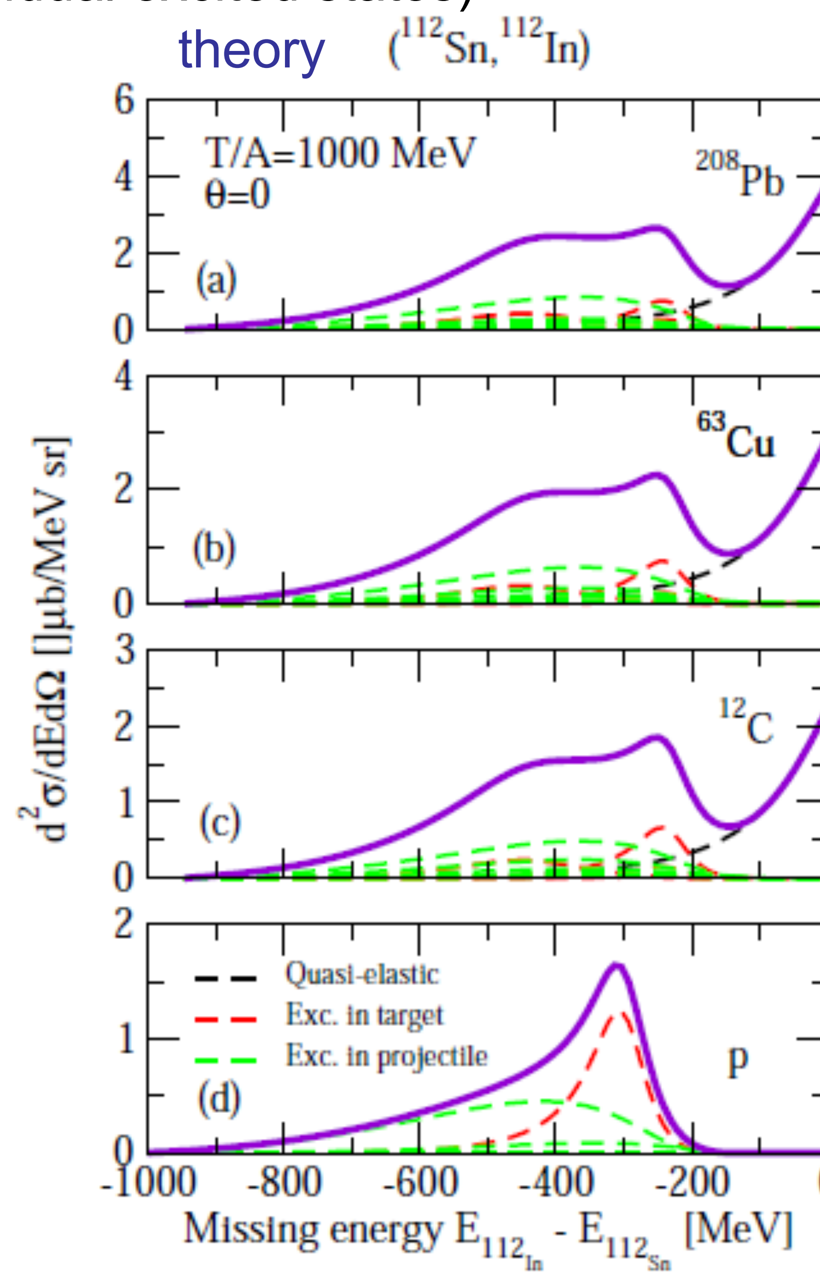

I. Vidana et al., EPJ Web of Conferences 107, 10003 (2016)

Z →Z+1 processes

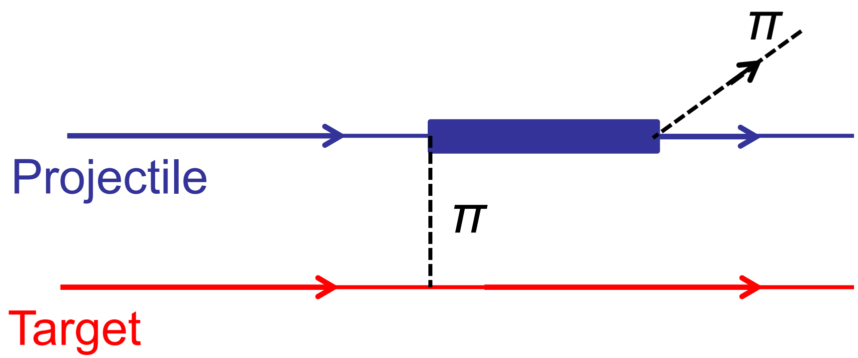

$$p(n,\Delta^0)p = p(n,p\pi^-)p$$
$$p(n,\Delta^+)n = p(n,p\pi^0)n$$
$$n(n,\Delta^0)n = n(n,p\pi^-)n$$

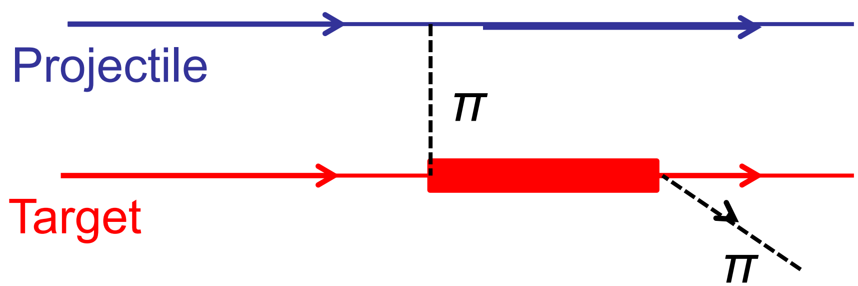

$$p(n,p)\Delta^0 = p(n,p)n\pi^0$$
$$p(n,p)\Delta^0 = p(n,p)p\pi^-$$
$$n(n,p)\Delta^- = n(n,p)n\pi^-$$

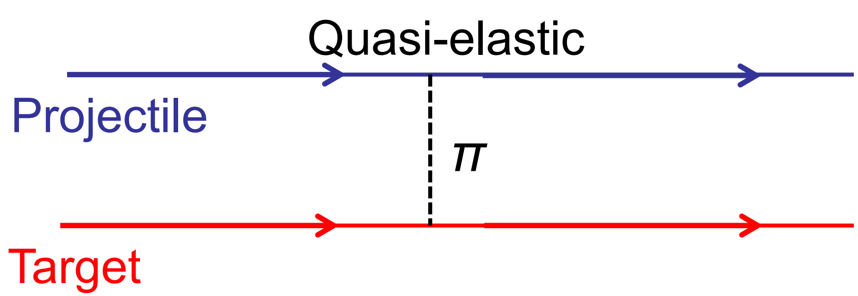

p(n,p)n

Only the Δ resonance shown

$^{56}Fe_{30} \rightarrow {}^{54}Fe_{28} + 2n$

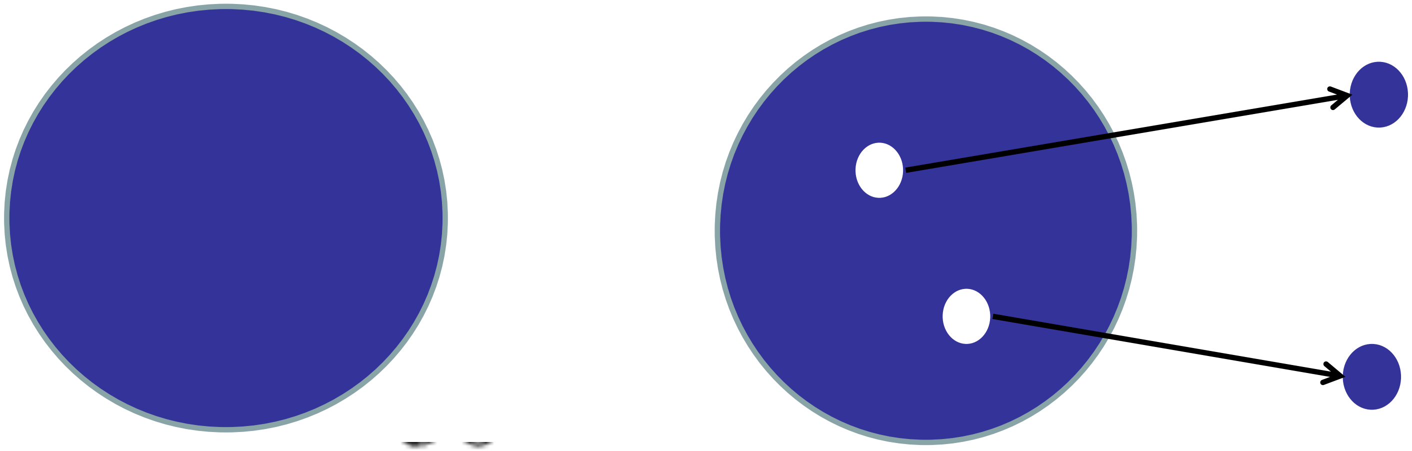

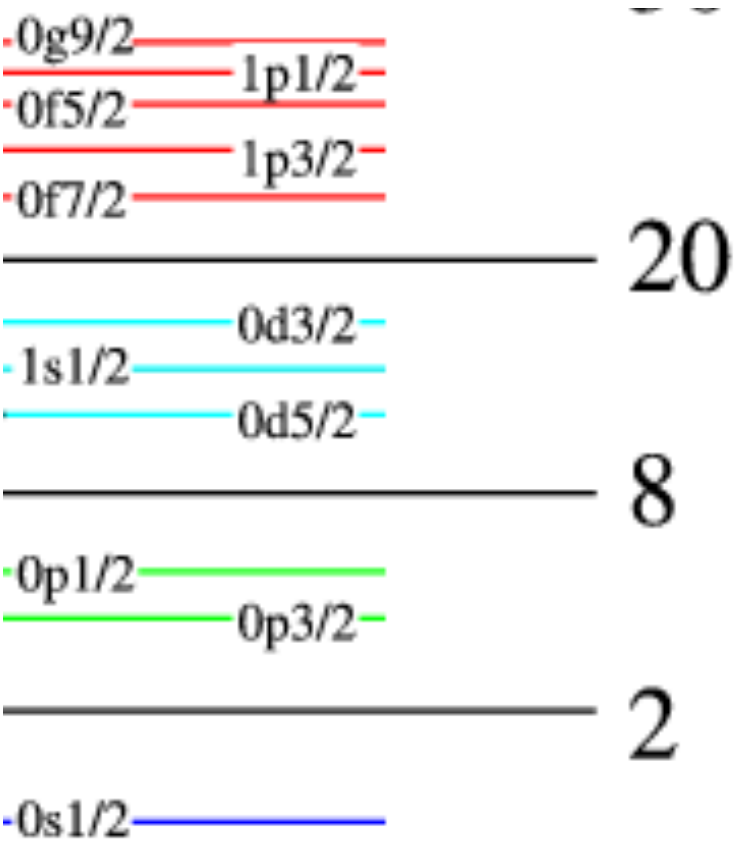

2 neutron states populated

Max spin is 6

10^{+} isomer in ^{54}Fe

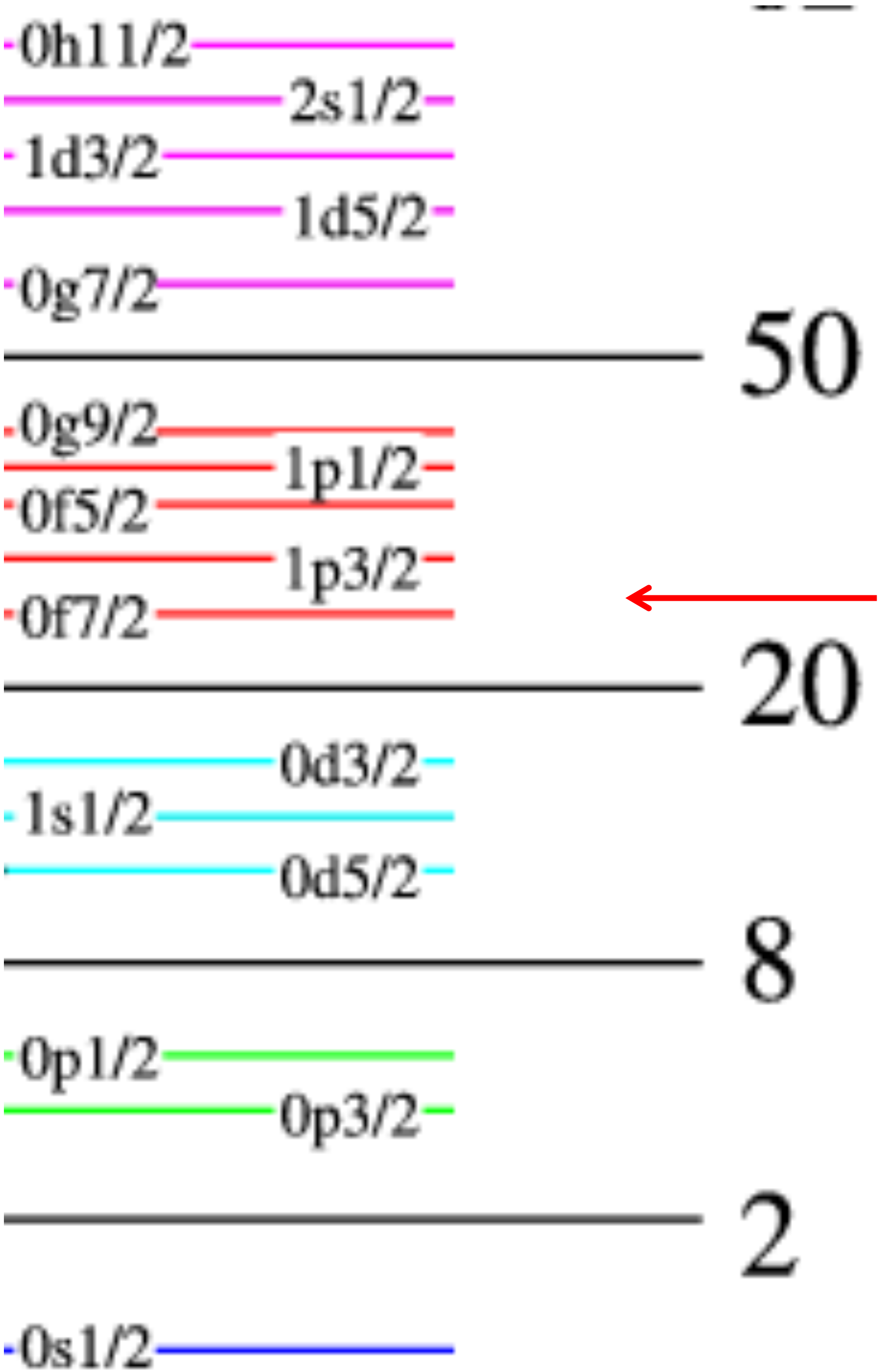

Predominantly $\pi f^{-2}_{7/2}\ \nu f^{-1}_{7/2} p_{3/2}$

$T_{1/2}$=364(7) ns

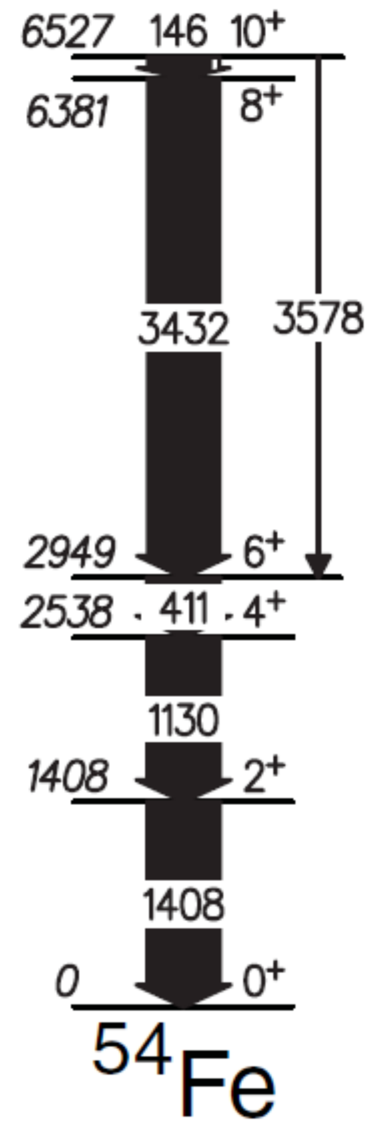

Decay of the $I^{\pi}=10^{+}$ metastable state in ^{54}Fe

Δp = -750, -247 MeV/c

Δp= -247, +247 MeV/c

Δp= +247, +750 MeV/c

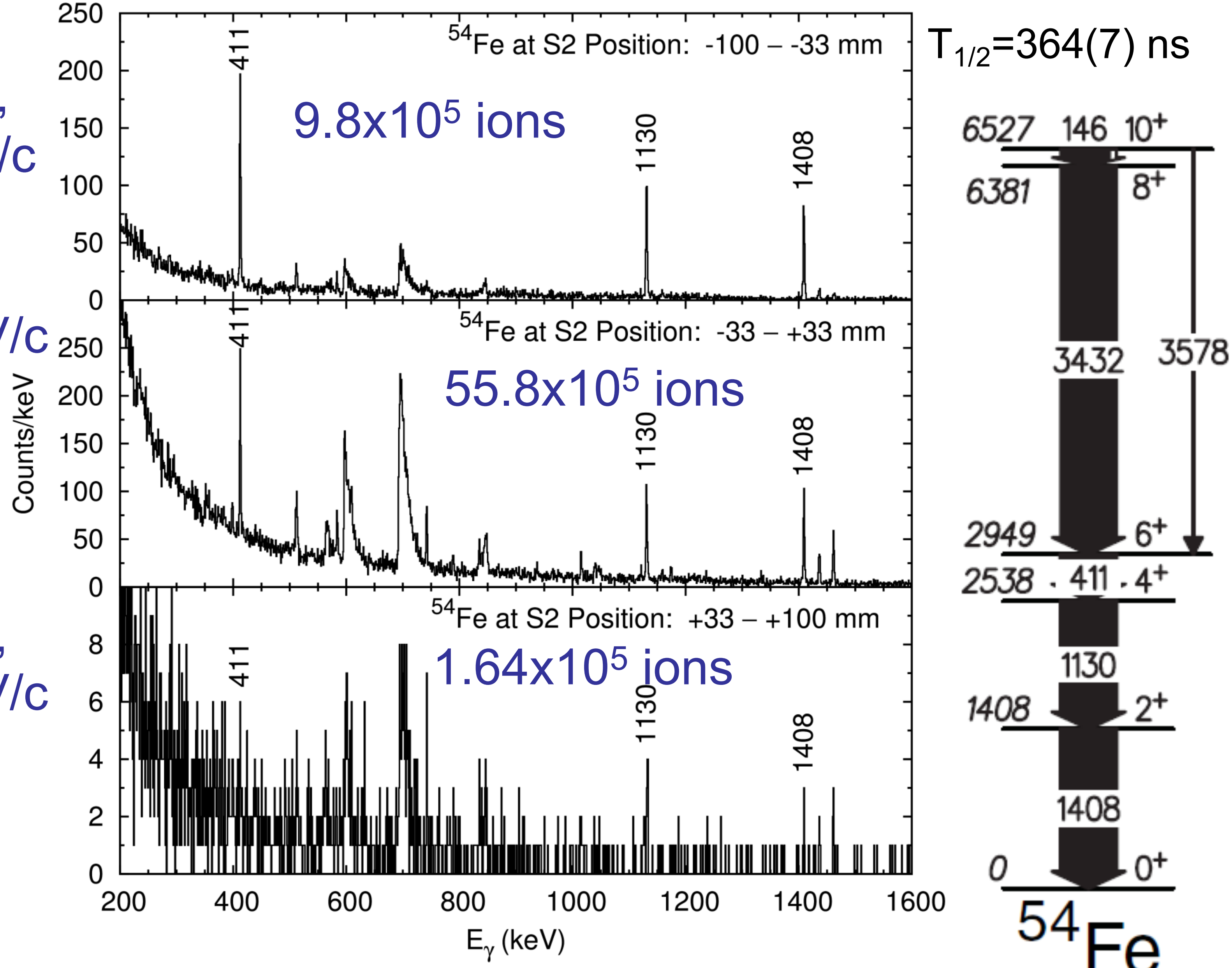

Zs. Podolyák et al., PRL 117, 222302 (2016)

Momentum distribution of ^{54}Fe nuclei

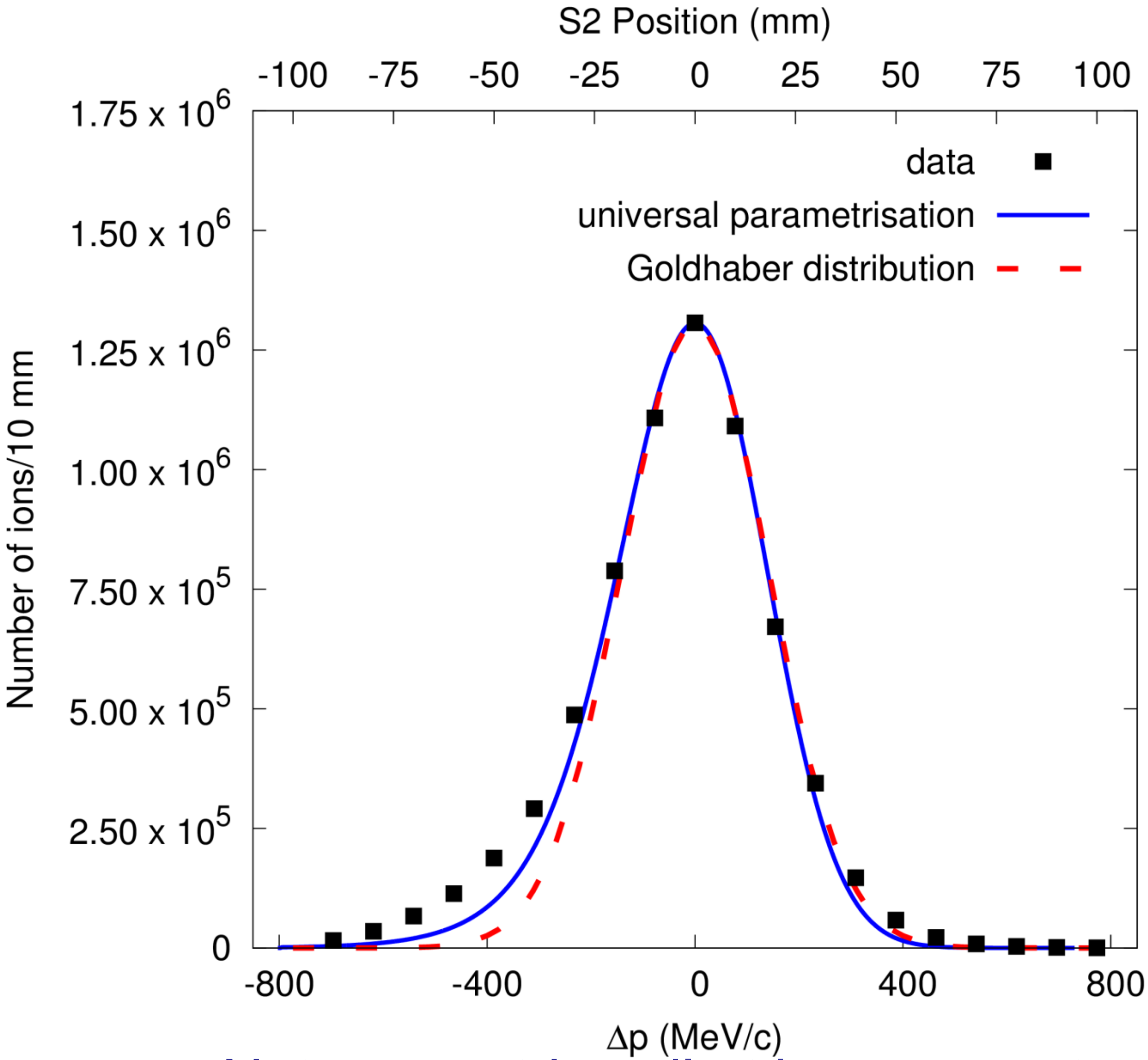

Not symmetric: tail at low momentum

Universal parametrisation: O. Tarasov, NPA 734 (2000) 536

Isomeric ratio of the 10^+ isomer

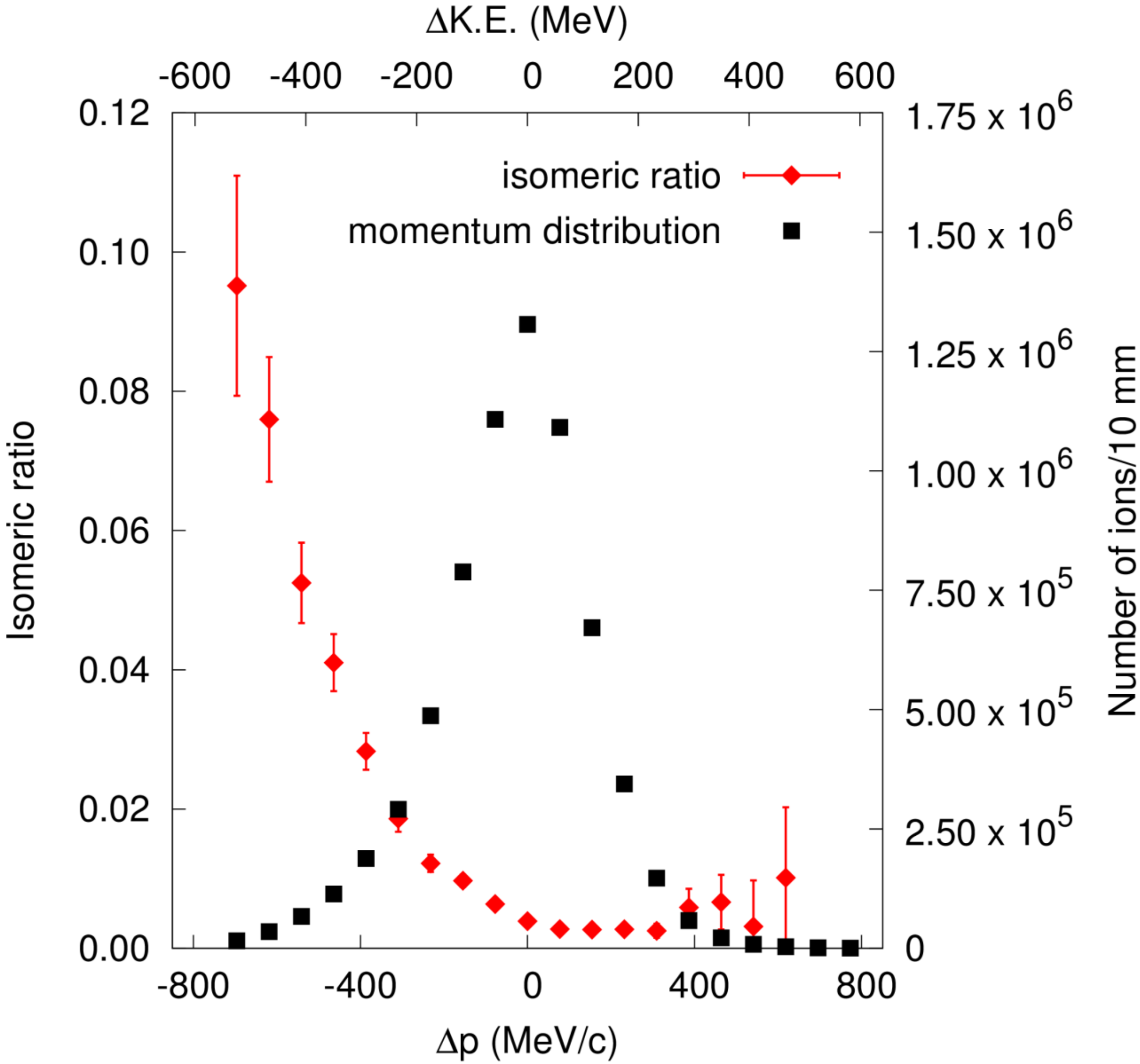

=> the isomer is produced in the low momentum tail

Isomeric ratios following fragmentation

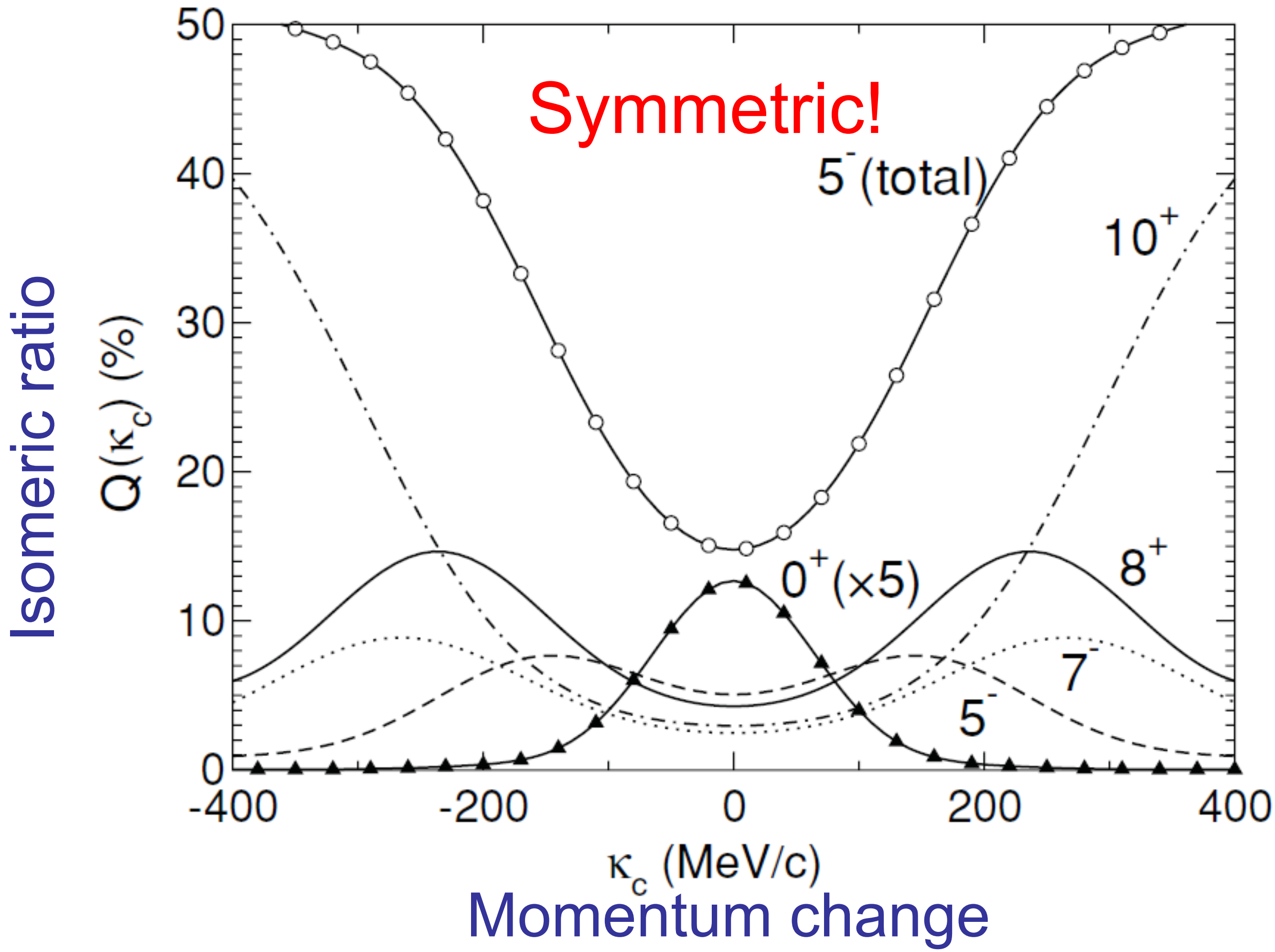

FIG. 2. Calculated isomeric ratios, as a function of residue momentum, in the projectile rest frame in the absence of broadening

E.C. Simpson et al., Phys. Rev. C 82, 037602 (2010)

$^{208}Pb \rightarrow {}^{206}Hg$

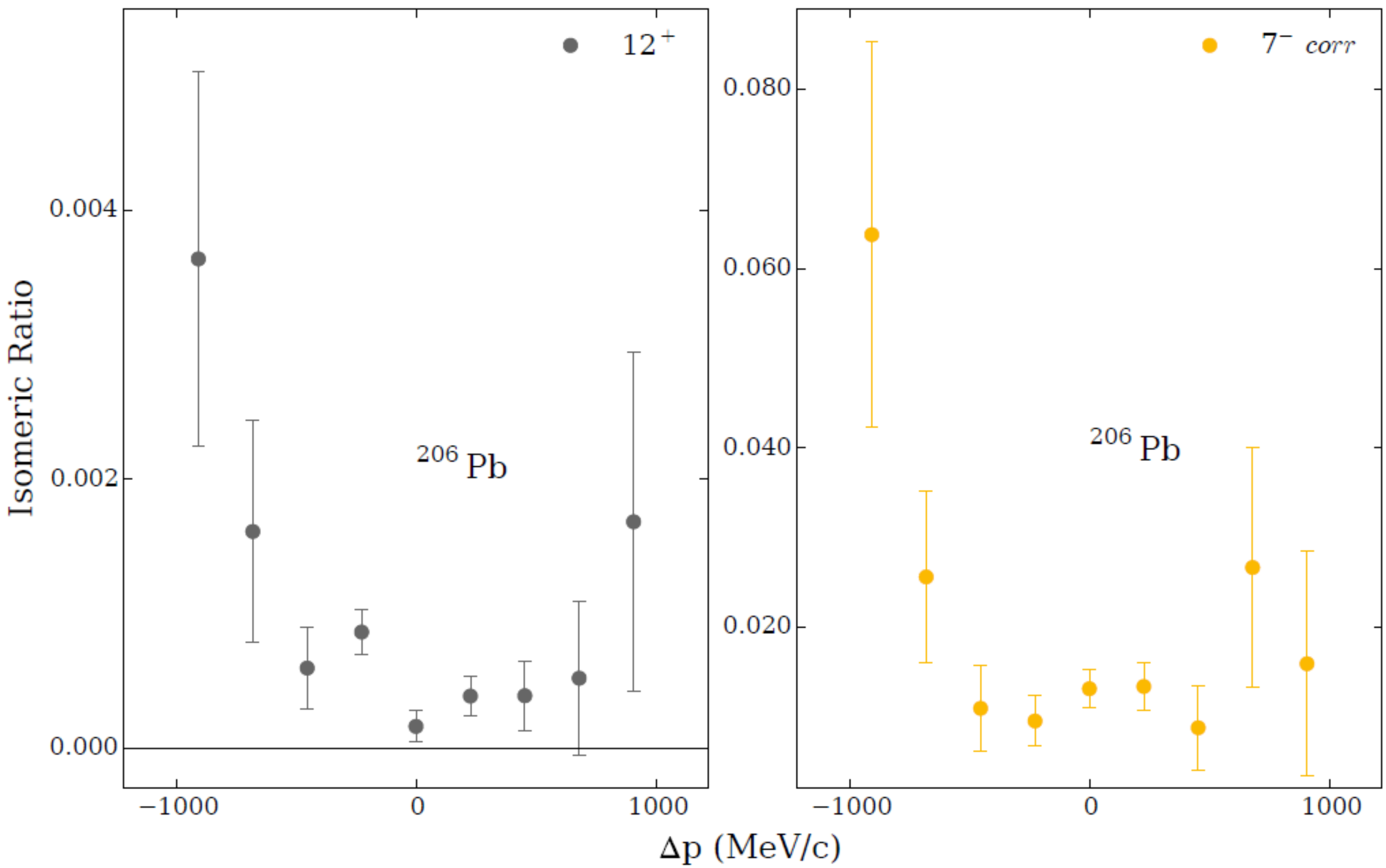

N. Lalovic et al, to be published

Population via nucleonic resonances

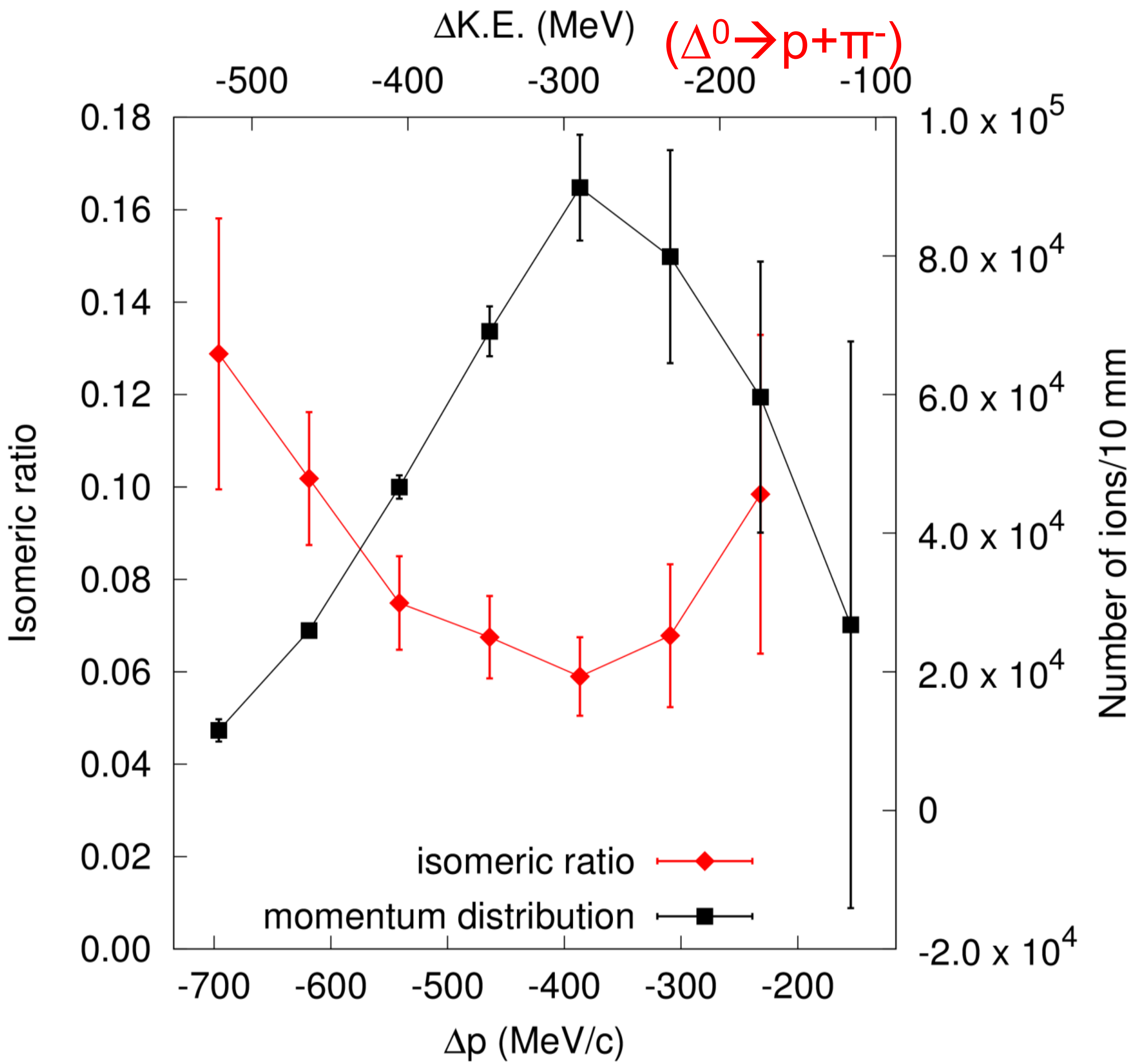

$^{56}Fe \rightarrow {}^{54}Fe$

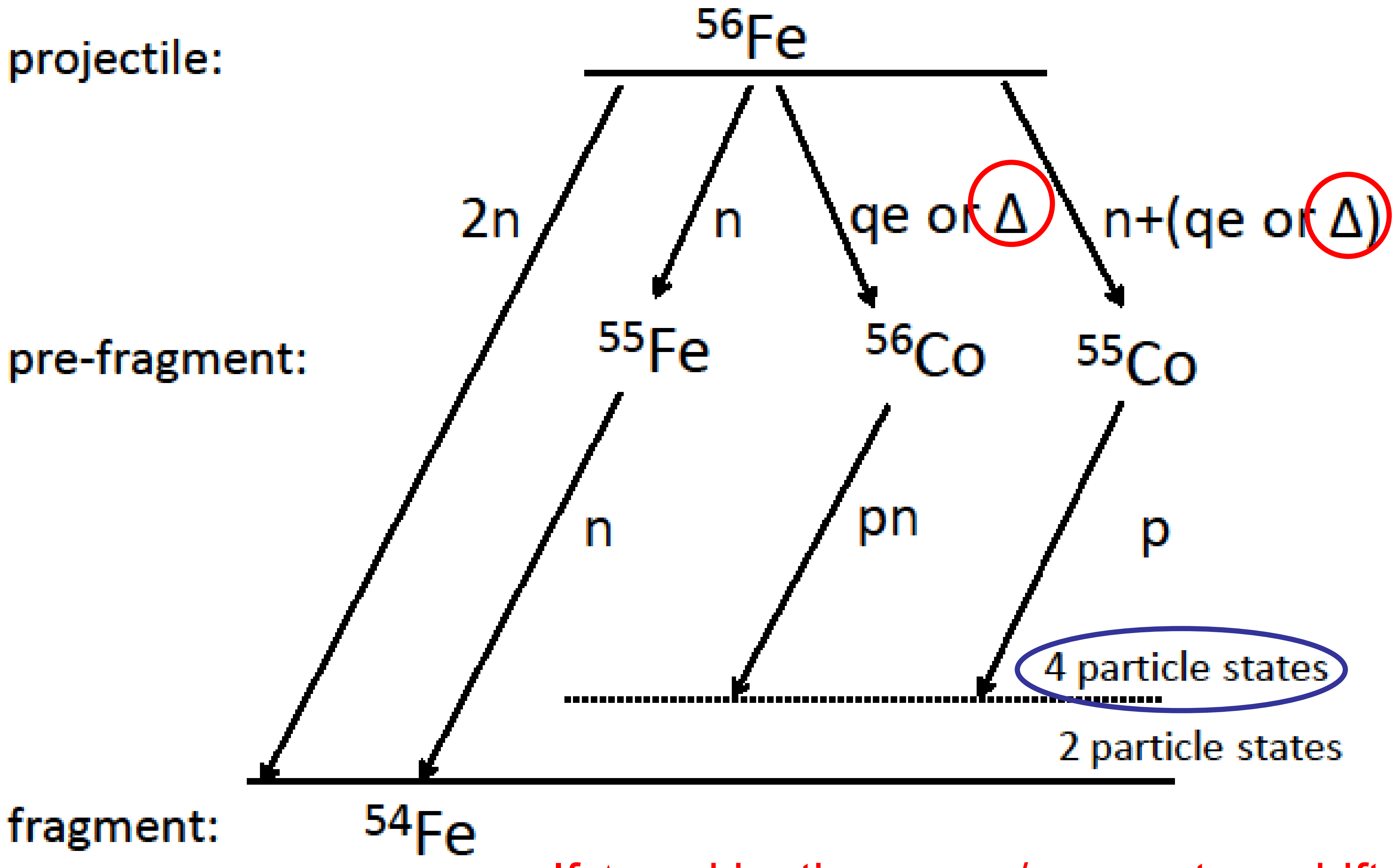

If Δ => kinetic energy/momentum shift

qe=quasi-elastic

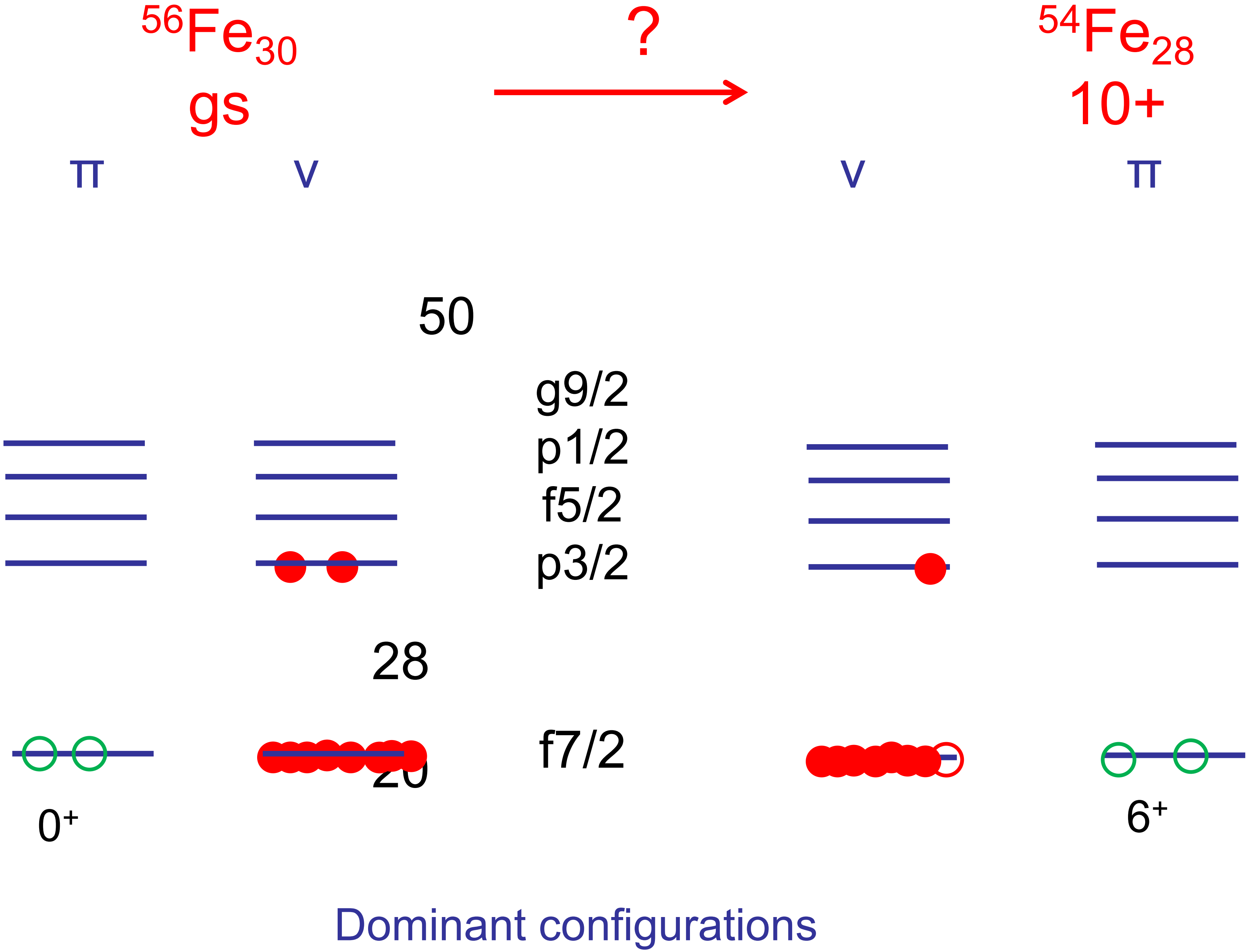
$^{56}Fe_{30}$
gs
?
$^{54}Fe_{28}$
10+
π
ν
ν
π
50
g9/2
p1/2
f5/2
p3/2
28
f7/2
20
0^+
6^+
Dominant configurations

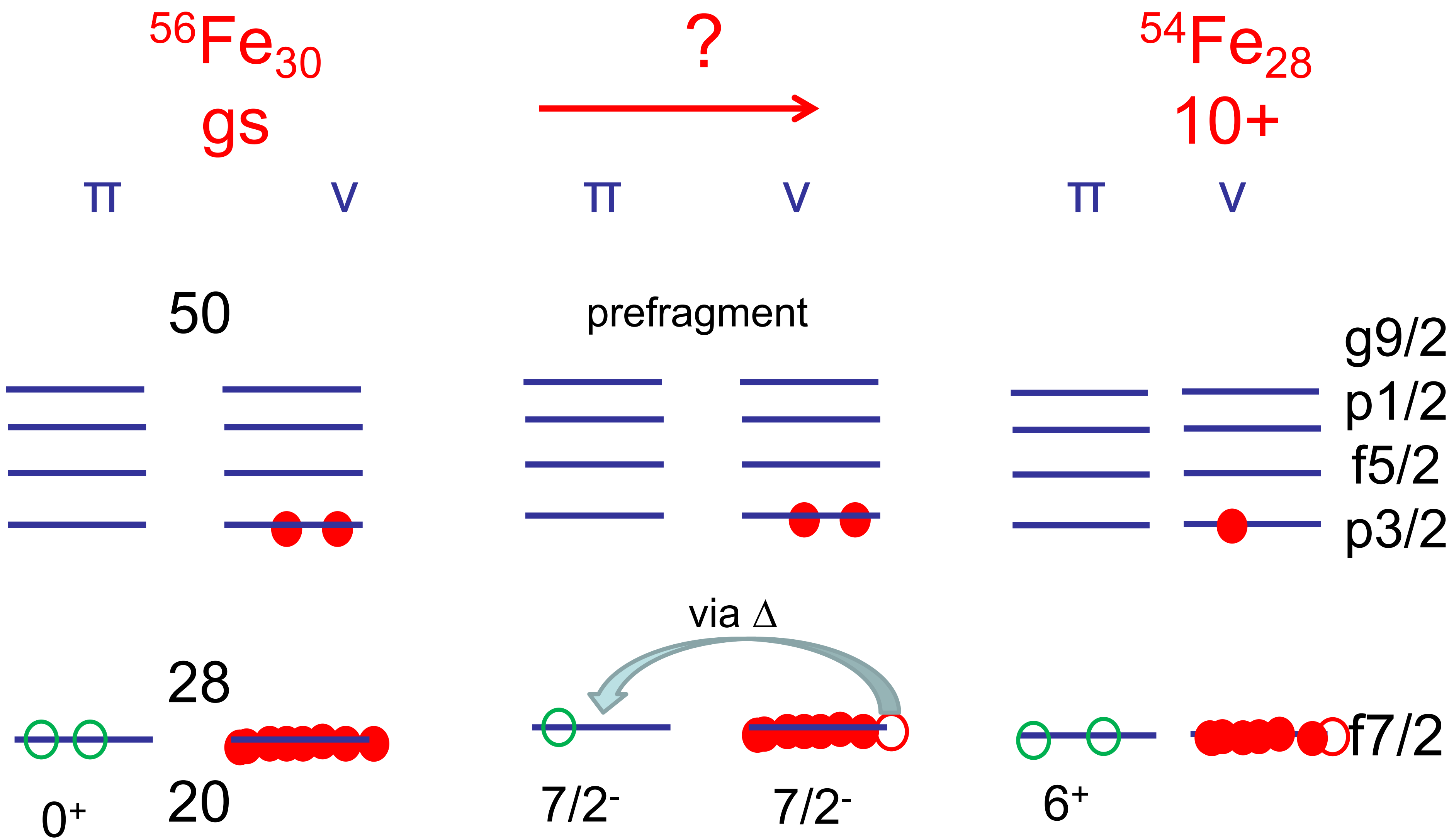

Dominant configurations

Summary

Neutron-rich N~126 and south-east of ^{208}Pb

Shell-model has high predictive power
(structure calculations)

First-forbidden – allowed β-decay competition?

First-forbidden β-decay calculations?

10^{+} populated in ^{54}Fe from ^{56}Fe at E/A=500 MeV

Which states are populated in
high-energy charge-exchange (Δ) reactions?

Conclusions

Production of ^{238}U fragments hindered by fission

Fission probability described considering the level density

At high-spins the angular momentum from abraded nuclei are not enough: contributions from evaporation, friction, excitations

High-spin states are produced with higher probability

than expected (isomeric beams)

Can this be related to:

the spin distribution of level density?

level density through spin dependence of fission?

Thanks!

Conclusions

Reasonable predictability for isomer production

-factor of two *if* structure is known (I<15hbar)

High-spin states are produced with higher probability

than expected (isomeric beams)

At high-spins the angular momentum from abraded nuclei are not enough: contributions from evaporation, friction, excitations

Isomeric ratios from (one or) two-particle removal understood

Importance of nucleonic excitation (^{54}Fe 10^{+} isomer)

Thanks!

Collaborators

PHYSICAL REVIEW C **88**, 024611 (2013)

Population of high-spin isomeric states following fragmentation of ^{238}U

M. Bowry,[1] Zs. Podolyák,[1] S. Pietri,[2] J. Kurcewicz,[2] M. Bunce,[1] P. H. Regan,[1] F. Farinon,[2] H. Geissel,[2,3] C. Nociforo,[2] A. Prochazka,[2] H. Weick,[2] N. Al-Dahan,[1] N. Alkhomashi,[1] P. R. P. Allegro,[4] J. Benlliure,[5] G. Benzoni,[6] P. Boutachkov,[2] A. M. Bruce,[7] A. M. Denis Bacelar,[7] G. F. Farrelly,[1] J. Gerl,[2] M. Górska,[2] A. Gottardo,[8] J. Grębosz,[9] N. Gregor,[2] R. Janik,[10] R. Knöbel,[2] I. Kojouharov,[2] T. Kubo,[11] N. Kurz,[2] Yu. A. Litvinov,[2] E. Merchan,[2] I. Mukha,[2] F. Naqvi,[12] B. Pfeiffer,[2,3] M. Pfützner,[13] W. Plaß,[3] M. Pomorski,[13] B. Riese,[2] M. V. Ricciardi,[2] K.-H. Schmidt,[2] H. Schaffner,[2] C. Scheidenberger,[2,3] E. C. Simpson,[1] B. Sitar,[10] P. Spiller,[2] J. Stadlmann,[2] P. Strmen,[10] B. Sun,[2,14] I. Tanihata,[15] S. Terashima,[14] J. J. Valiente Dobón,[8] J. S. Winfield,[2] H.-J. Wollersheim,[2] and P. J. Woods[16]

[1]*Department of Physics, University of Surrey, Guildford GU2 7XH, United Kingdom*
[2]*GSI, Planckstrasse 1, D-64291 Darmstadt, Germany*
[3]*IInd Physical Institute, Justus-Liebig University Giessen, D-35392 Giessen, Germany*
[4]*University of São Paulo, São Paulo 05508-900, Brazil*
[5]*University Santiago de Compostela, 15706 Santiago de Compostela, Spain*
[6]*INFN Sezione di Milano, Dipartimento di Fisica, Via Celoria 16, 20133 Milano, Italy*
[7]*School of Computing Engineering and Mathematics, University of Brighton, Brighton BN2 4GJ, United Kingdom*
[8]*INFN, Laboratori Nazionali di Legnaro, Legnaro (Padova), Italy*
[9]*The Henryk Niewodniczański Institute of Nuclear Physics, PL-31-342 Kraków, Poland*
[10]*Department of Nuclear Physics and Biophysics, Comenius University, Mlynská dolina, 842 48 Bratislava, Slovakia*
[11]*RIKEN Nishina Center, 2-1 Hirosawa, Wako, Saitama 351-0198, Japan*
[12]*Department of Physics, University of Yale, New Haven, Connecticut 06511-8499, USA*
[13]*Faculty of Physics, University of Warsaw, PL-00-681 Warsaw, Poland*
[14]*School of Physics and Nuclear Energy Engineering, Beihang University, Beijing 100191, China*
[15]*Research Center for Nuclear Physics, 10-1 Mihogaoka, Ibaraki, Osaka 567-0047, Japan*
[16]*School of Physics and Astronomy, University of Edinburgh, Edinburgh EH9 3JZ, United Kingdom*

(Received 2 June 2013; published 16 August 2013)

Thanks!

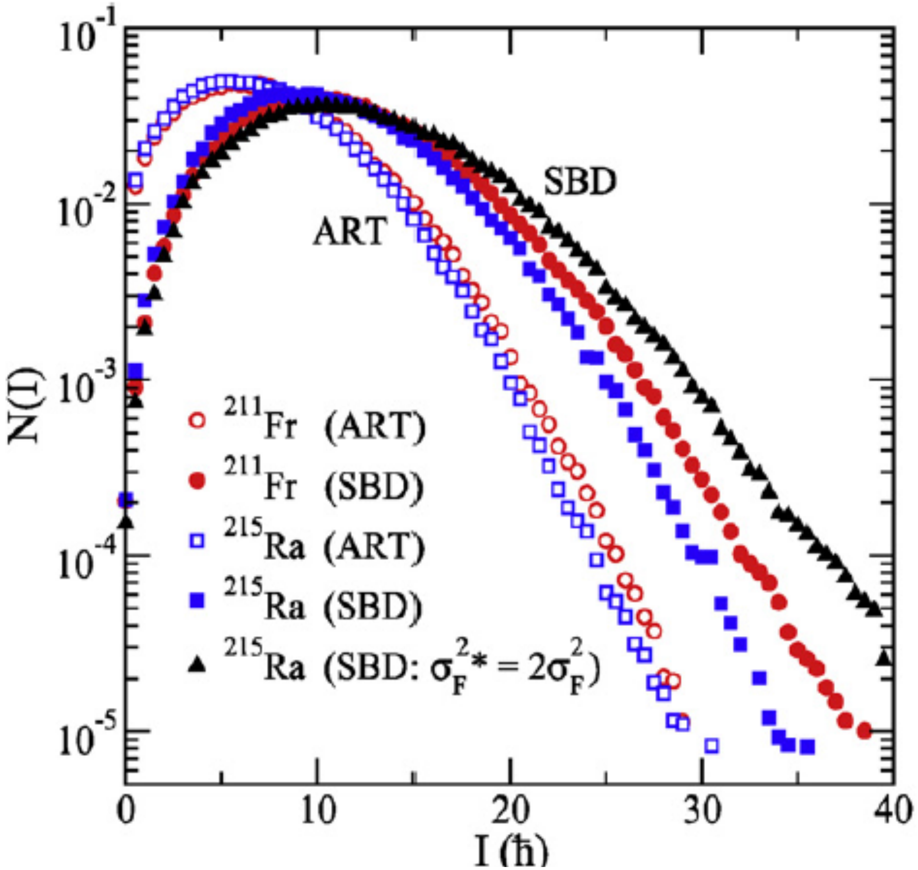

Abrasion (incl. friction)
(relativistic transport model)

Abrasion+ablation
(+sequential binary decay)

Ion	I^π	E (keV)	R_{exp} [%]	R_{the}^{ART} [%]	R_{the}^{SBD} [%]
^{211}Fr	$29/2^+$	2423	5.7(19)	2.59	10.03
^{212}Fr	15^-	2492	7.5(18)	2.24	9.15
^{213}Fr	$29/2^+$	2538	12(8)	2.65	10.82
^{214}Ra	17^-	4147	6.8(23)	0.58	3.20
^{215}Ra	$43/2^-$	$3757 + \Delta$	3.1(6)	0.07	0.82

Better agreement

S. Pal and R. Palit, Phys. Lett. B 665 (2008) 164.

Fragmentation (spallation) reactions at relativistic energies:

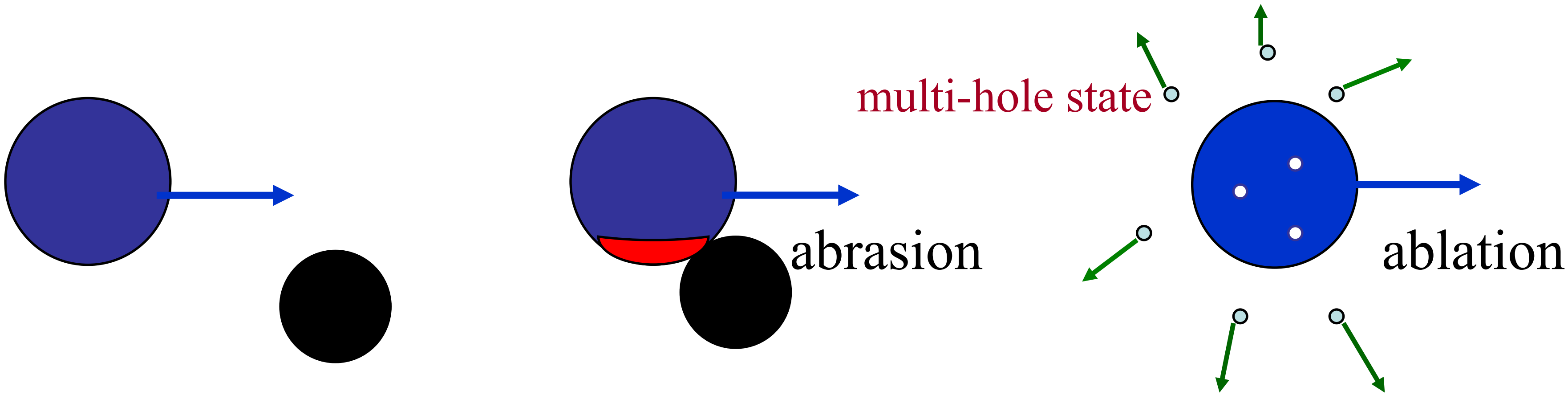

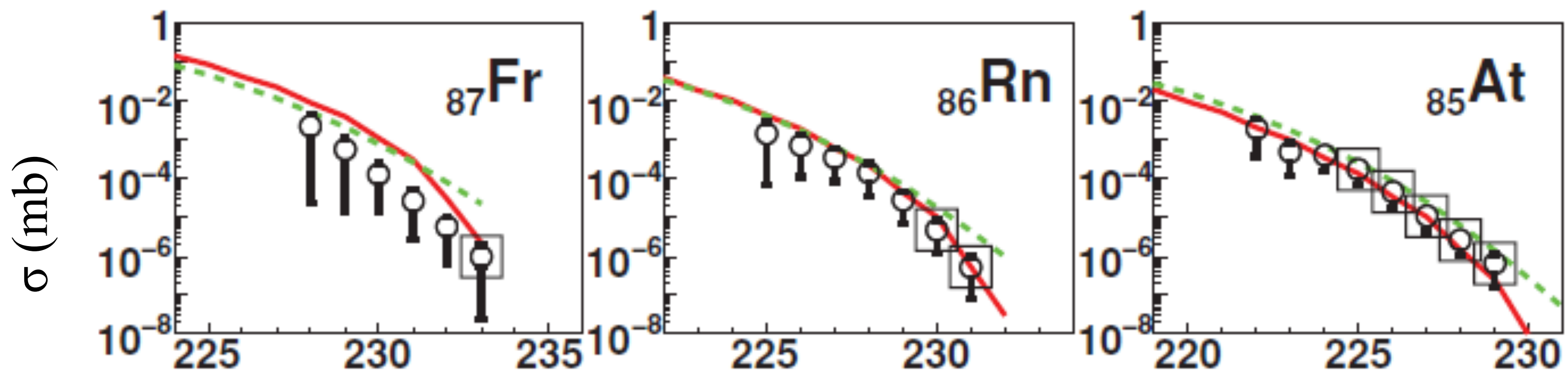

H. Alvarez-Pol et al., Phys. Rev. C 82, 041602(R) (2110)

To be discussed: Cross section: measures the end product

Spin: info mainly about abrasion

Fragmentation (spallation) reactions at relativistic energies:

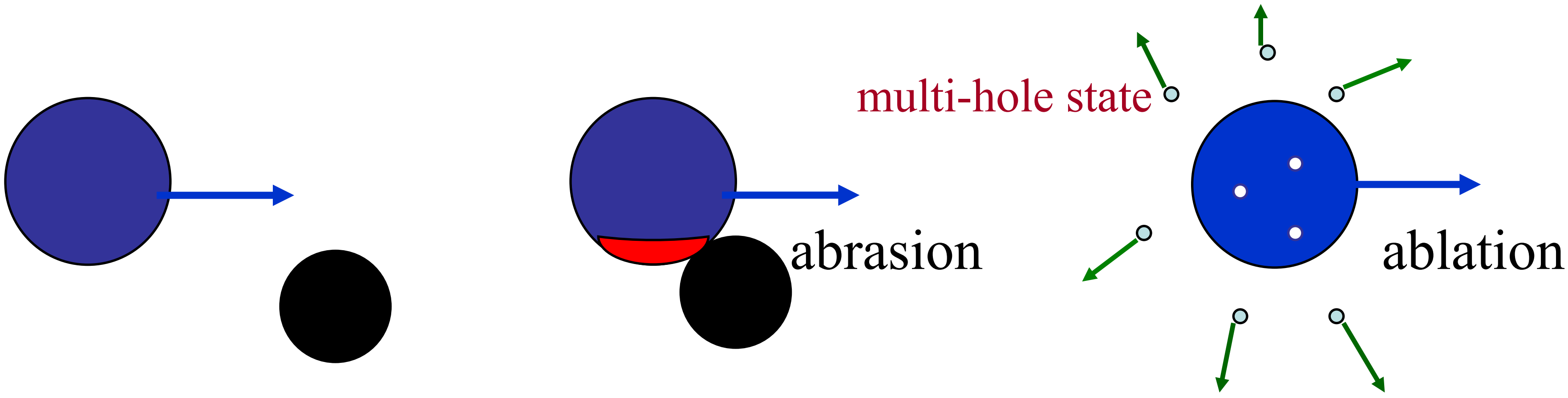

Ablation competes with fission (238U beam)

Survival probability against fission (production cross section)

depends on level density

if $A_{projectile}$-$A_{fragment}$~large (>10)

Statistical abrasion-ablasion model (ABRABLA code)

Excitation energy

~27 MeV/abrated nucleon~

=2 x single particle (holes) energy

Ablated nuclei/abraded nuclei ~2

Fission depends on level density

↓

Good cross sections

A.R. Junghans, M. de Jong, H.-G. Clerc, A.V. Ignatyuk, G.A. Kudyaev, K.-H. Schmidt,

Nucl. Phys. A 629 (1998) 635

^{238}U fragmentation

No fission ....

No shell effects, no collective – – – – – – – –

With shell effects ————————

$$\rho = \frac{\sqrt{\pi}\exp(S)}{12\tilde{a}^{1/4}E^{5/4}}$$

$$S = 2\sqrt{\tilde{a}(E + \delta Uk(E) + \delta Ph(E))}$$

Shell effect + collective — · — · — · —

A.R. Junghans et al., Nucl. Phys. A 629 (1998) 635

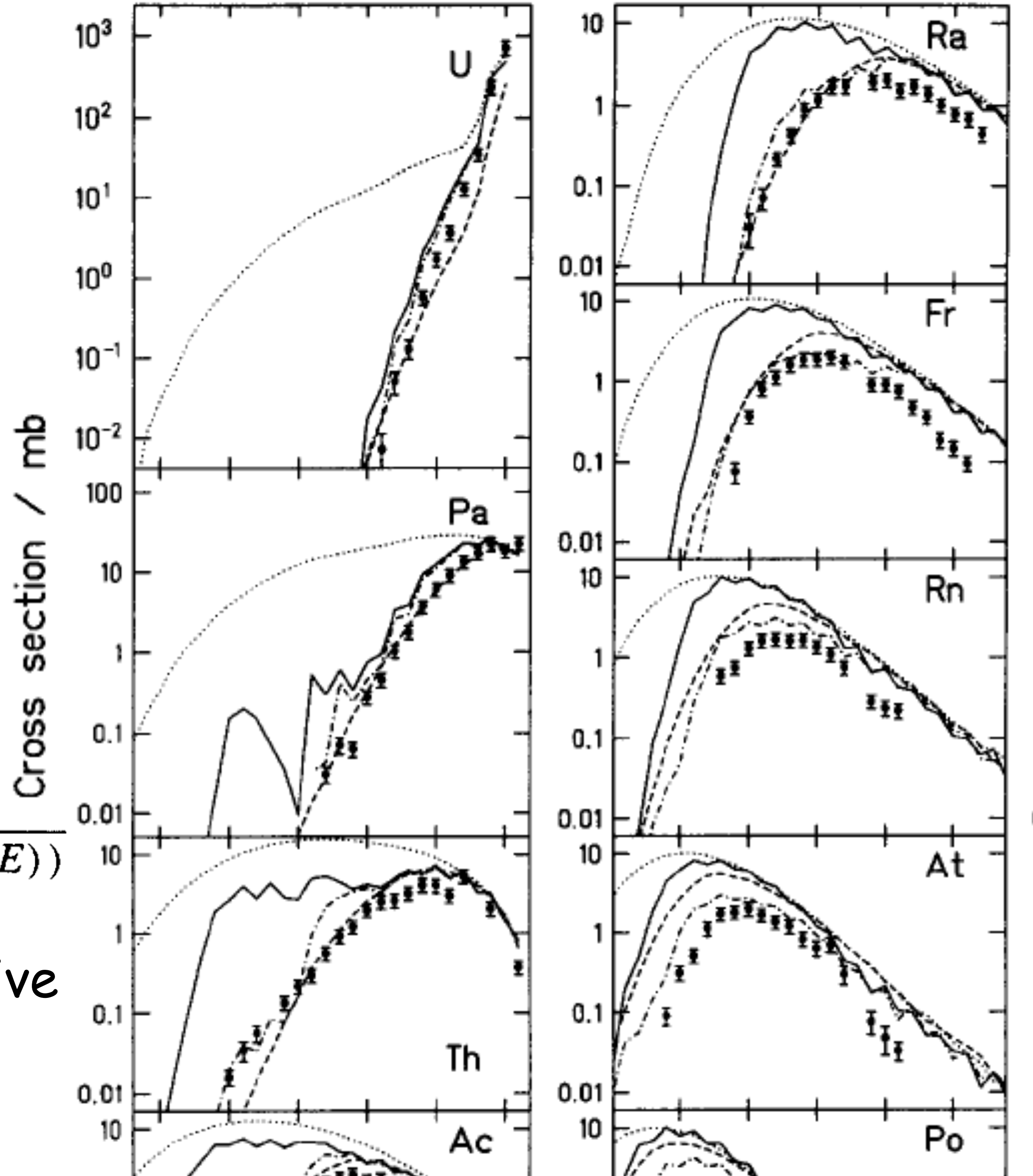

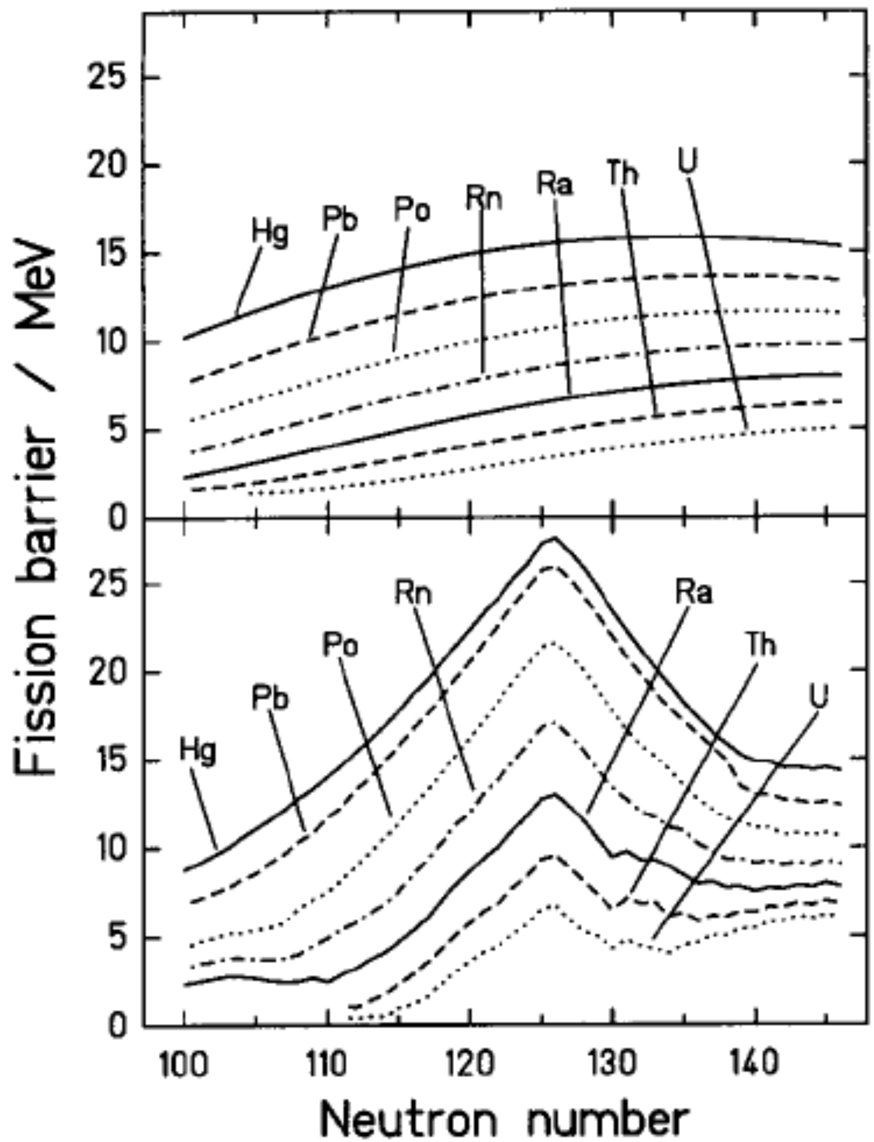

Fig. 2. Fission barriers of nuclei in the region of interest for the present investigation. Upper part: The macroscopic part [37] of the fission barrier at zero angular momentum. Lower part: The curves include the contribution of the ground-state shell effect [38].

Rotational enhancement

$$\rho(E) = K_{\text{coll}}(E)\,\rho_{\text{intr}}(E)$$

Ground-state deformation

Saddle-point def.

Dumping independent on deformation

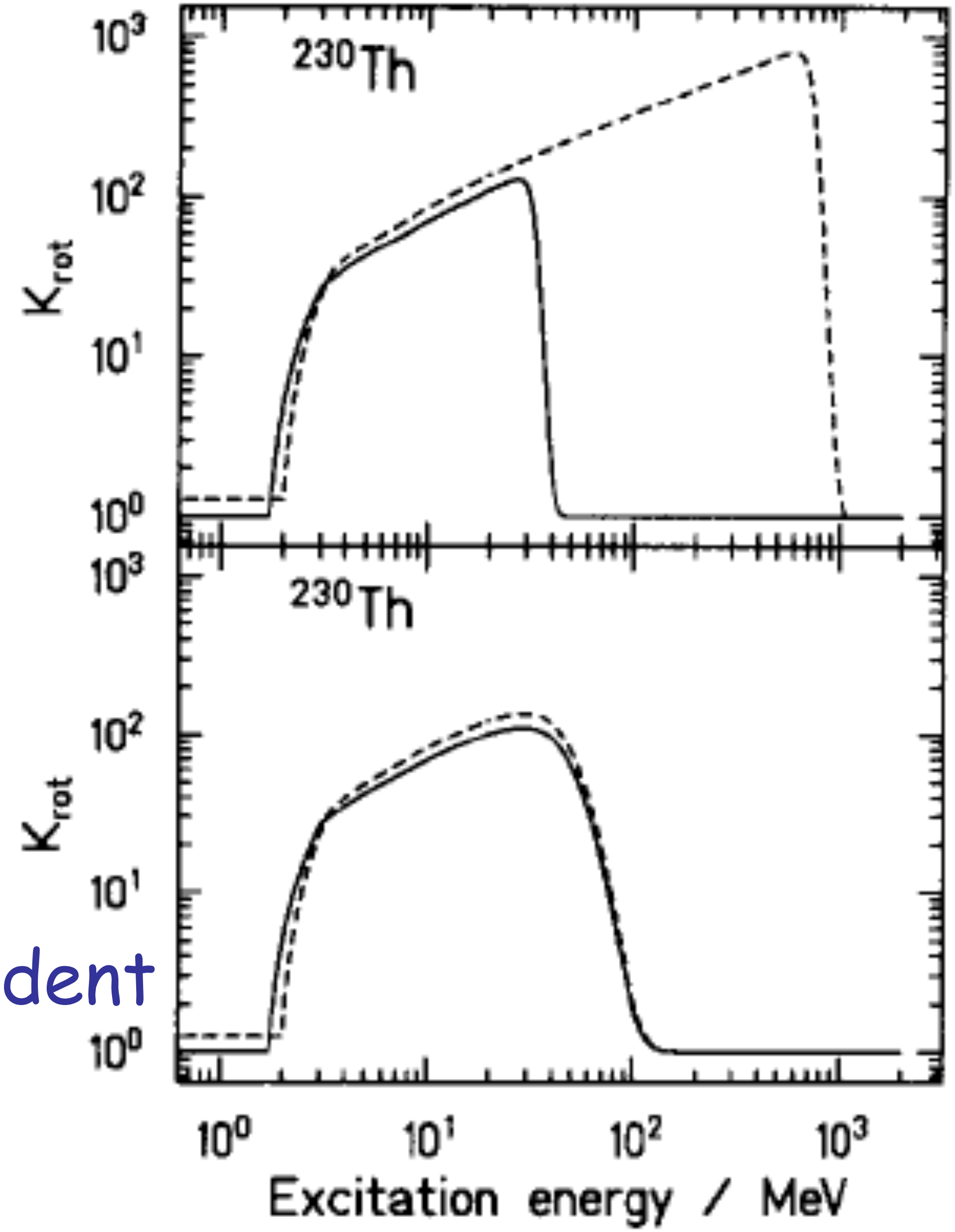

A.R. Junghans et al.,
Nucl. Phys. A 629 (1998) 635

Collective enhancement

rotational

vibrational

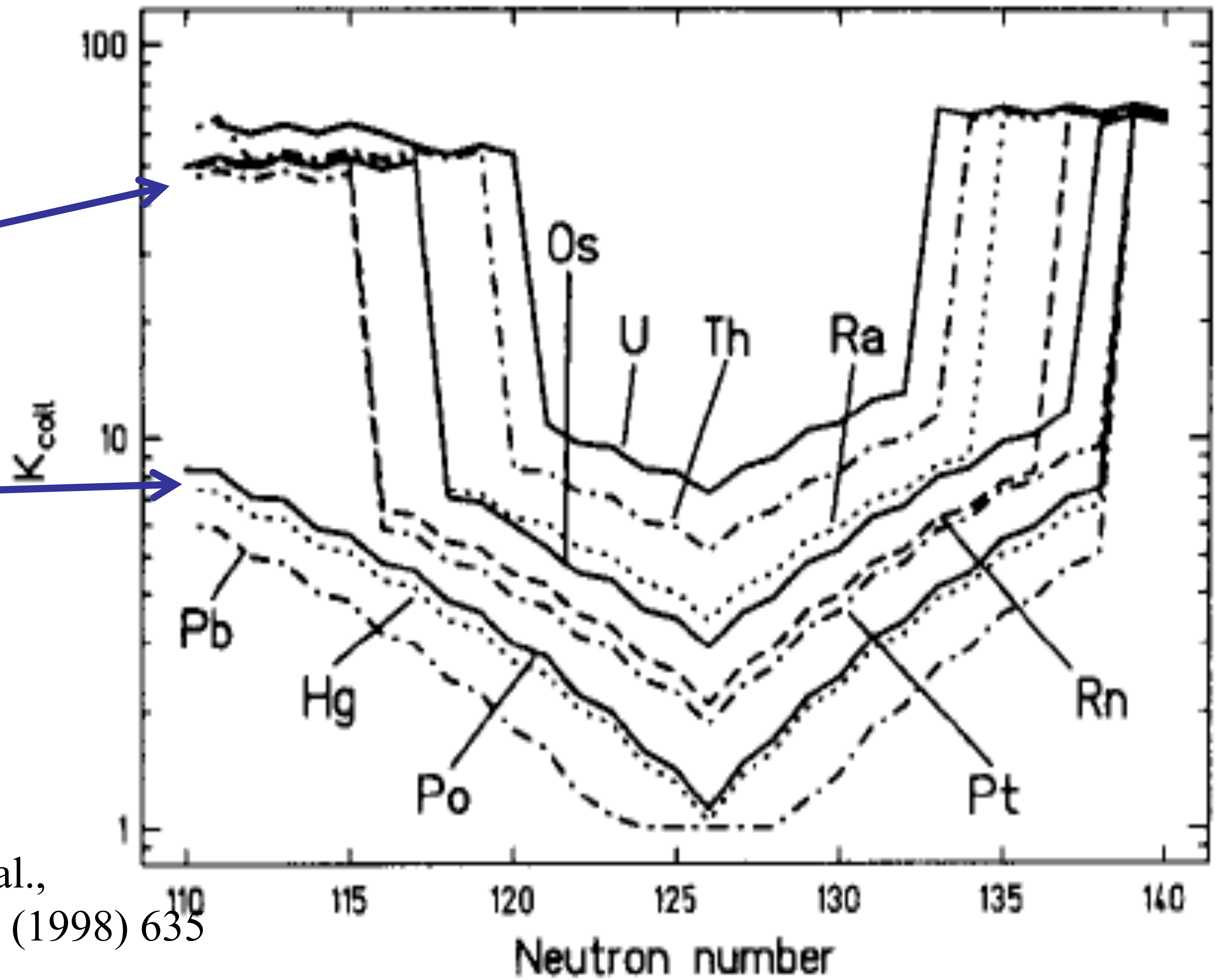

A.R. Junghans et al.,
Nucl. Phys. A 629 (1998) 635

Collective enhancement

Damping dependent on def.

Damping independent on def.

+vibrational enhancement

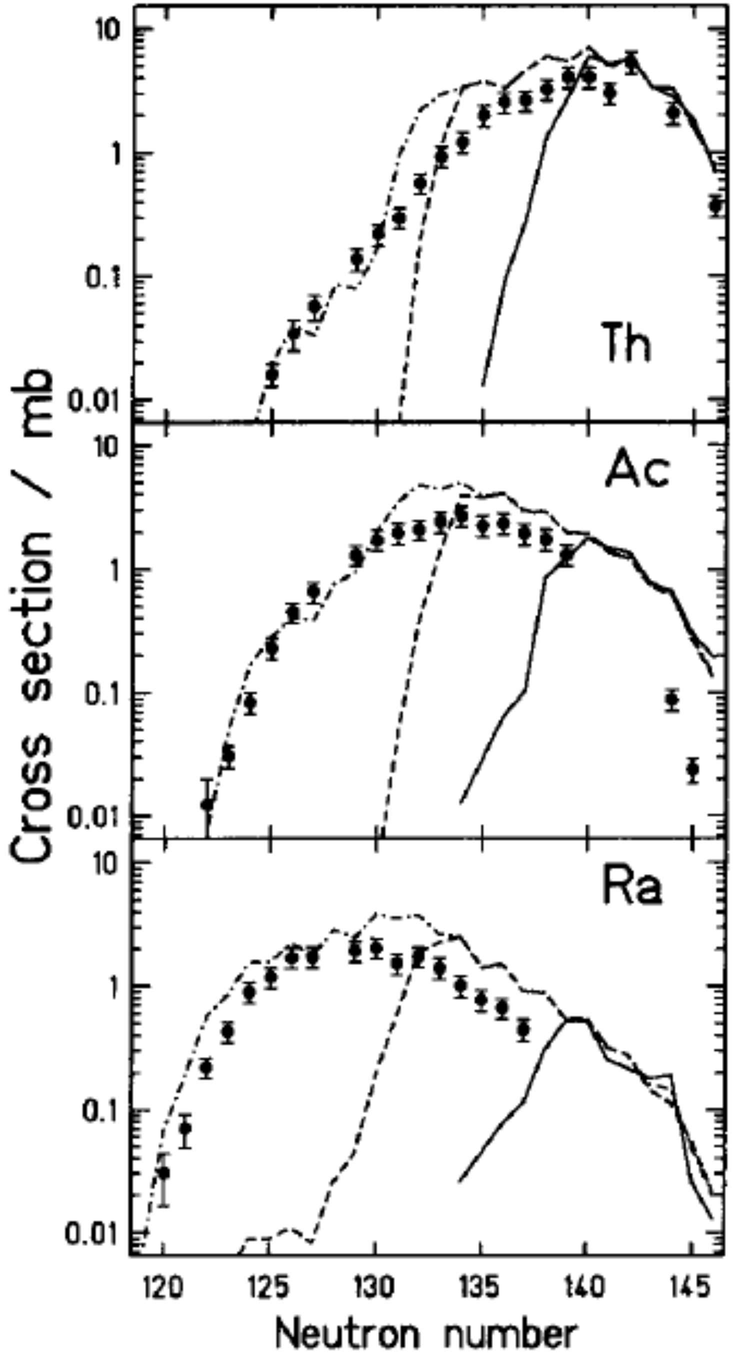

A.R. Junghans et al.,
Nucl. Phys. A 629 (1998) 635

Conclusions from cross section measurements

- No stabilisation against fission near N=126
- Effect of shell stabilisation and collective enhancement on fissility cancels out
- Damping of the collective enhancement in the level density is independent of deformation

A.R. Junghans, M. de Jong, H.-G. Clerc, A.V. Ignatyuk, G.A. Kudyaev, K.-H. Schmidt, Nucl. Phys. A 629 (1998) 635

if $A_{projectile}$-$A_{fragment}$~large (>10)

Statistical abrasion-ablasion model (ABRABLA code)

Angular momentum

from single particle states only

$$\rho_n(U,J) = \frac{2J+1}{2\sigma_n^2}\exp\left(-\frac{J(J+1)}{2\sigma_n^2}\right)\rho_n(U)$$

Spin-cutoff parameter $\sigma_n^2 = 0.234\left(1-\frac{U}{n\epsilon_f}\right)A_p^{2/3}\frac{n(A_p-n)}{A_p-1}$

U –excitation energy from n holes only

Is this good enough?

M. De Jong, A.V. Ignatyuk and K.-H. Schmidt, Nucl. Phys. A 613 (1997) 435

Nuclei	$\overline{U}_1$ [MeV]	$\langle j_z^2 \rangle$
^{48}Ca	9.25	2.08
^{56}Ni	9.61	2.54
^{90}Zr	10.25	3.01
^{120}Sn	10.76	3.38
^{182}W	11.40	4.56
^{208}Pb	10.94	5.50
^{235}U	11.47	5.12

(from simplified shell model)

sics A 613 (1997) 435–444

$$\sqrt{\langle J^2 \rangle} = \sqrt{2}\,\sigma$$

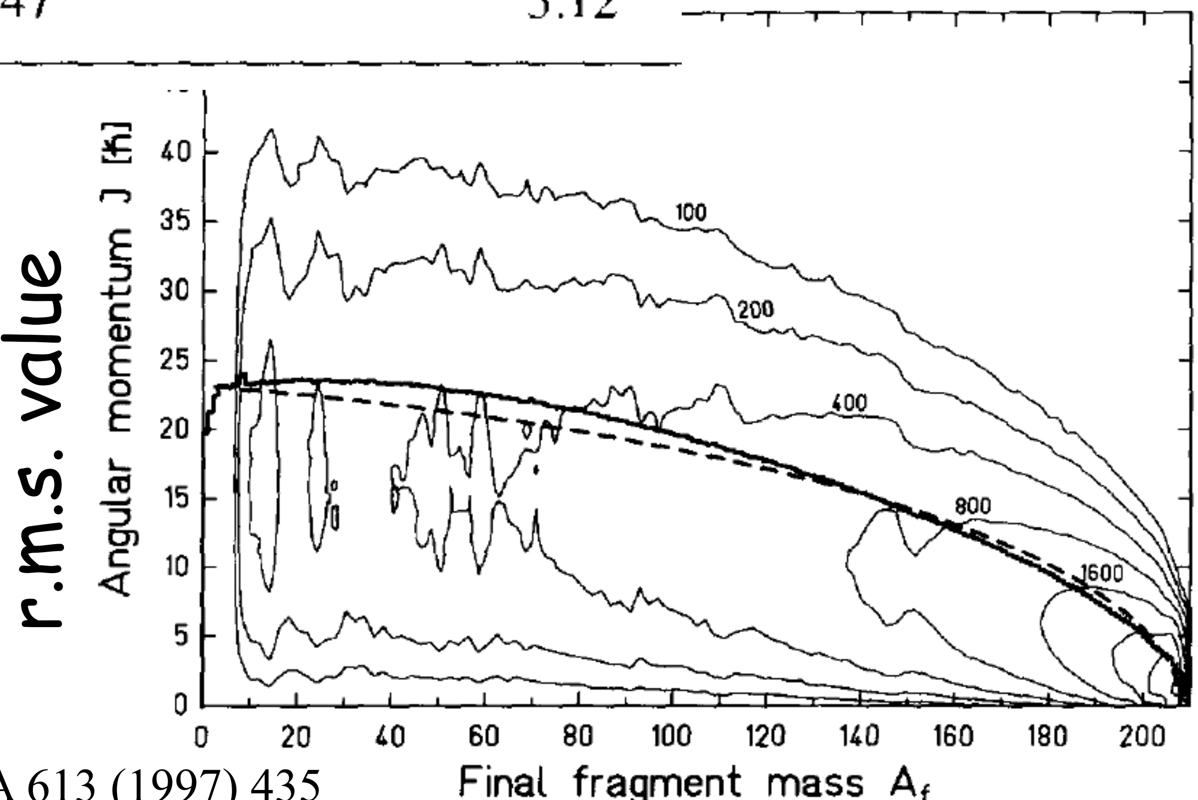

M. De Jong et al., Nucl. Phys. A 613 (1997) 435

In flight fragmentation (and fission): separation and identification

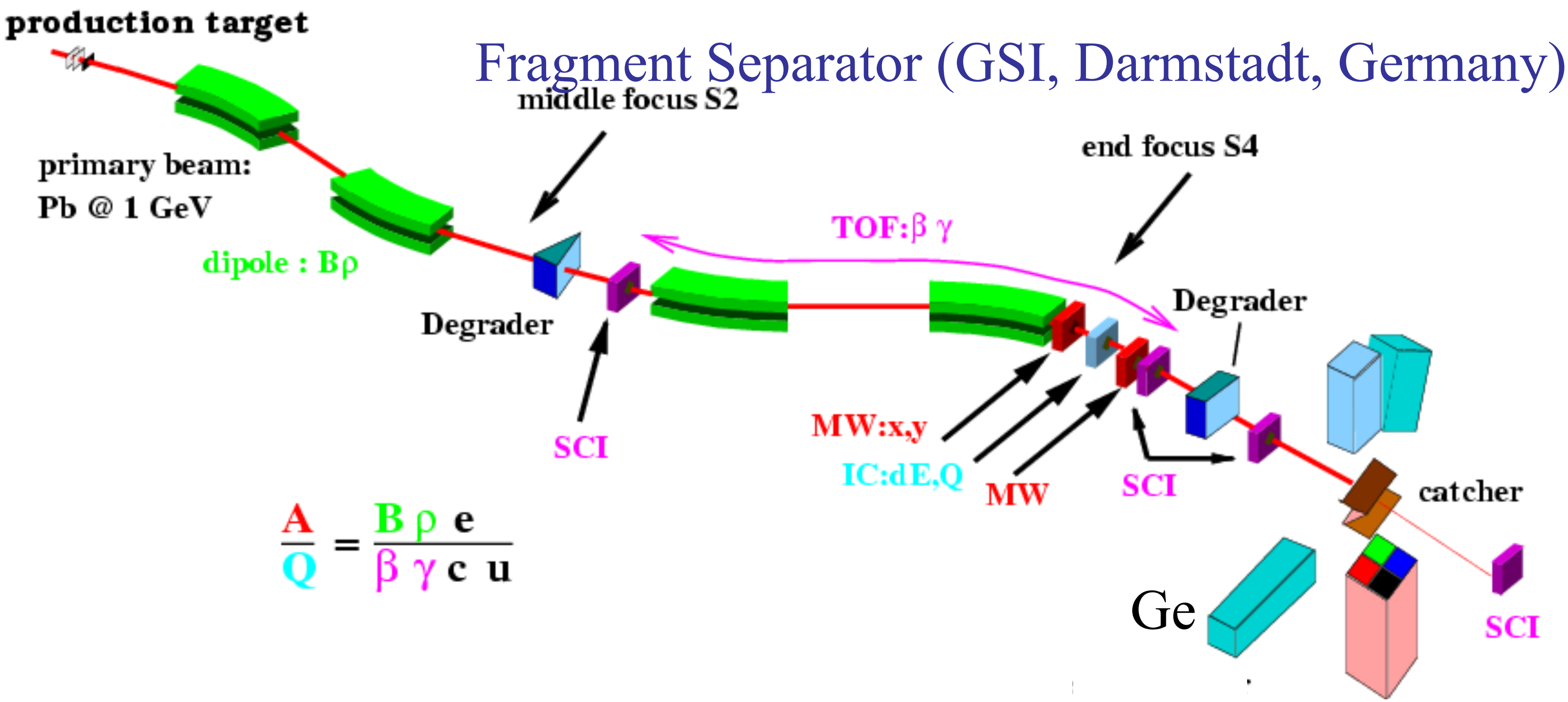

$$\frac{A}{Q} = \frac{B\rho\, e}{\beta\gamma\, c\, u}$$

Relativistic energy fragmentation: => heavy ions

Isomeric decay spectroscopy:

- gamma decay correlated with the fragment
- ***very sensitive***

Stopped Rising Array @ GSI: 15 x 7 element CLUSTERs

ε_γ =11% at 1.3 MeV, 20% at 550 keV, 35% at 100 keV

flight time ~300ns

stopped beam setup

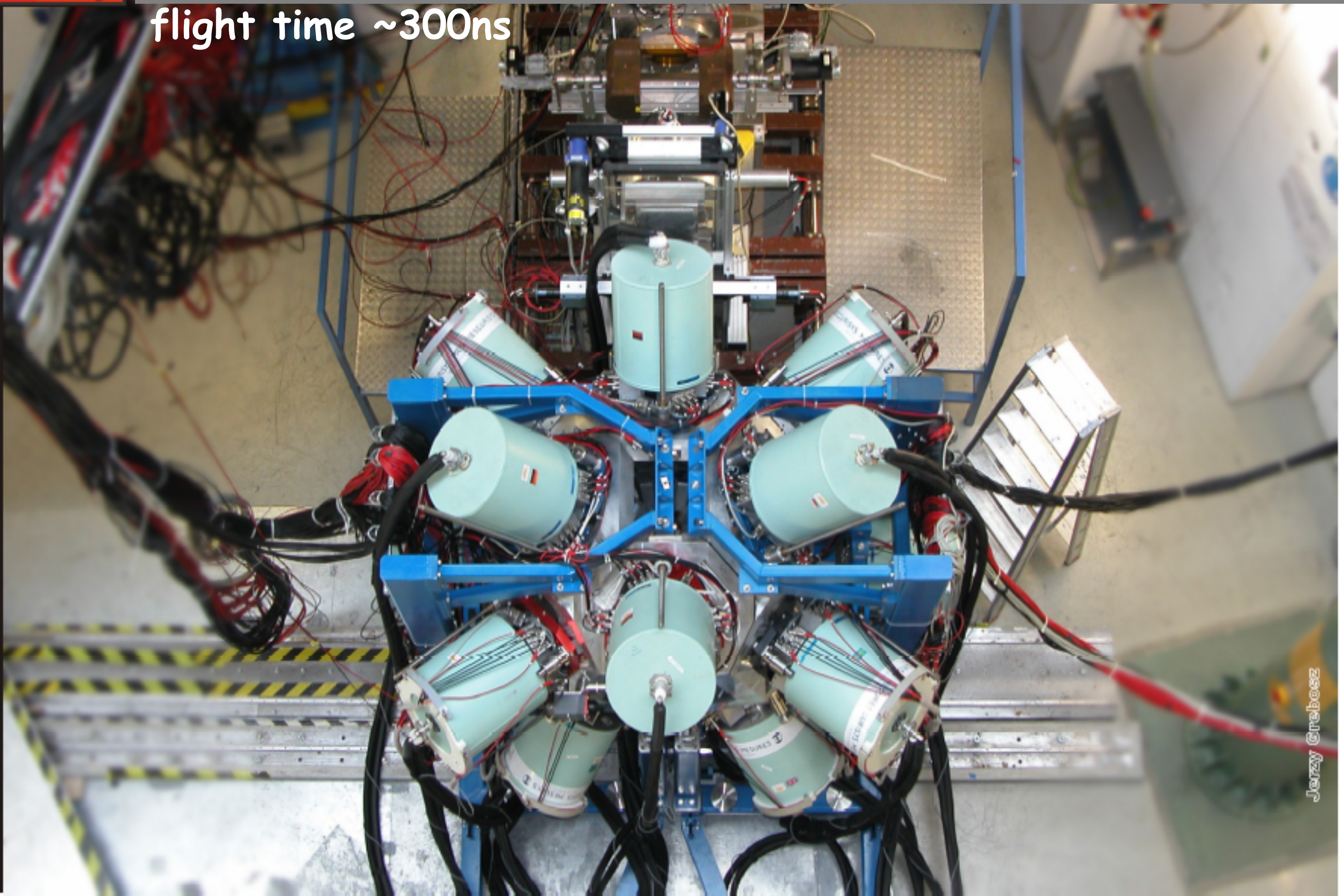

Highest spin from fragmentation: I=(55/2) isomer in ^{213}Rn

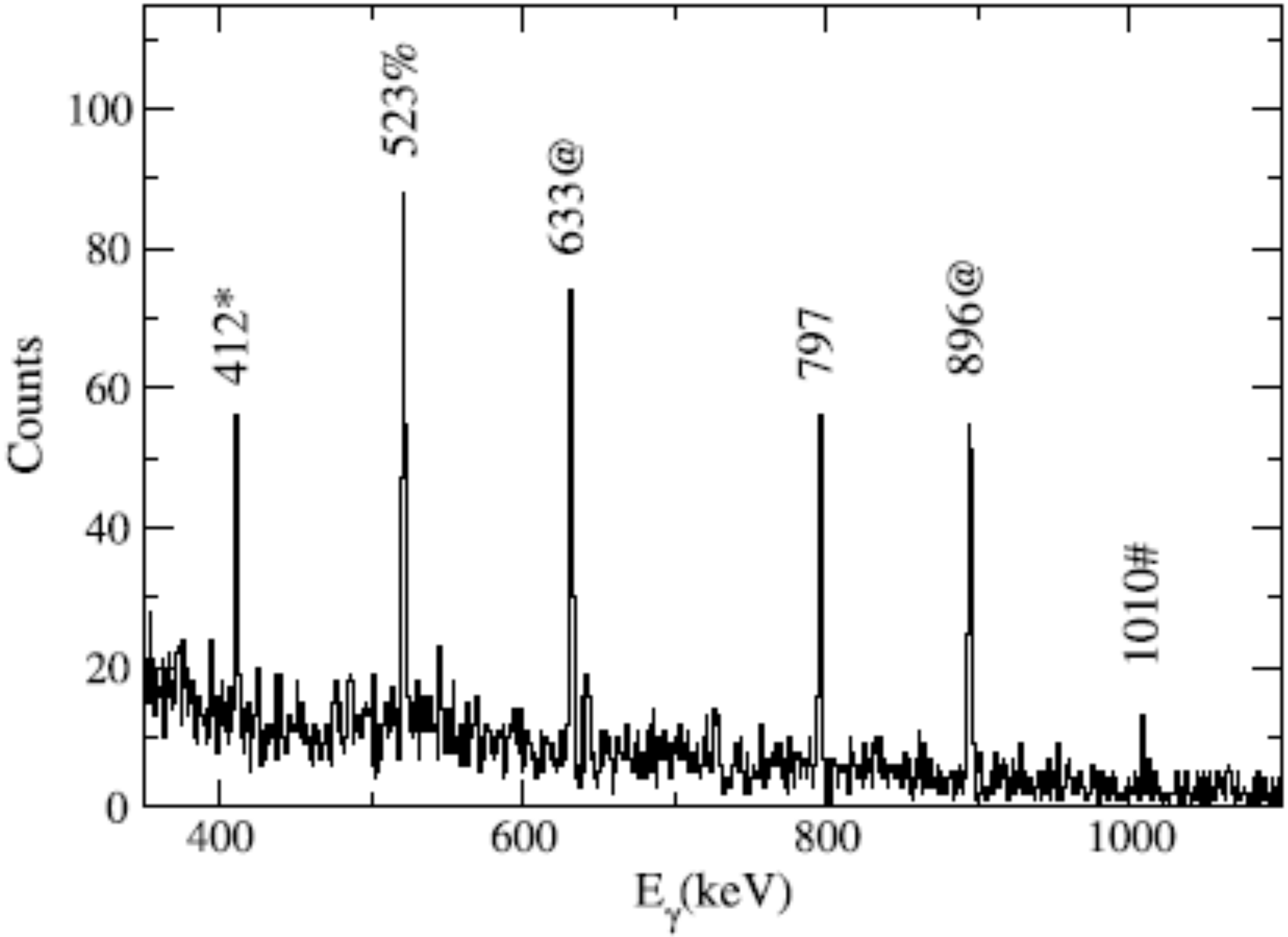

Fig. 1. Gamma-ray energy spectrum obtained in coincidence with ^{213}Rn ions using a time gate of width 1.4 μs starting ~50 ns after the prompt flash. The transitions used to obtain the isomeric ratios for the $(55/2)^+$, $43/2^-$, $31/2^-$ and $25/2^+$ levels are denoted #, *, % and @ respectively.

A.M. Denis Bacelar et al., Phys. Lett. B 723, 302 (2012)

Isomeric ratio

$$R_{\exp} = \frac{N_{isomer}}{N_{total}}$$

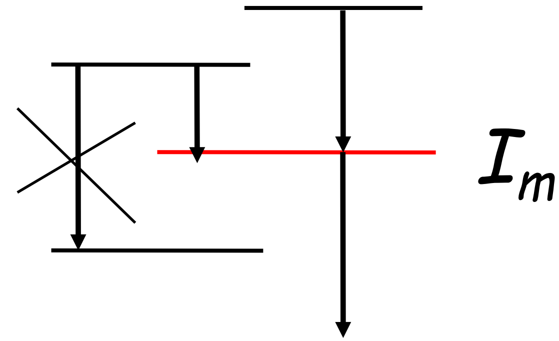

$$\rho_{theo} = \int_{I_m}^{\infty} P(I)\,dI$$

(sharp cut-off approx.)

$$P(I) = \frac{2I+1}{2\sigma_f^2}\exp\left(-\frac{I(I+1)}{2\sigma_f^2}\right)$$

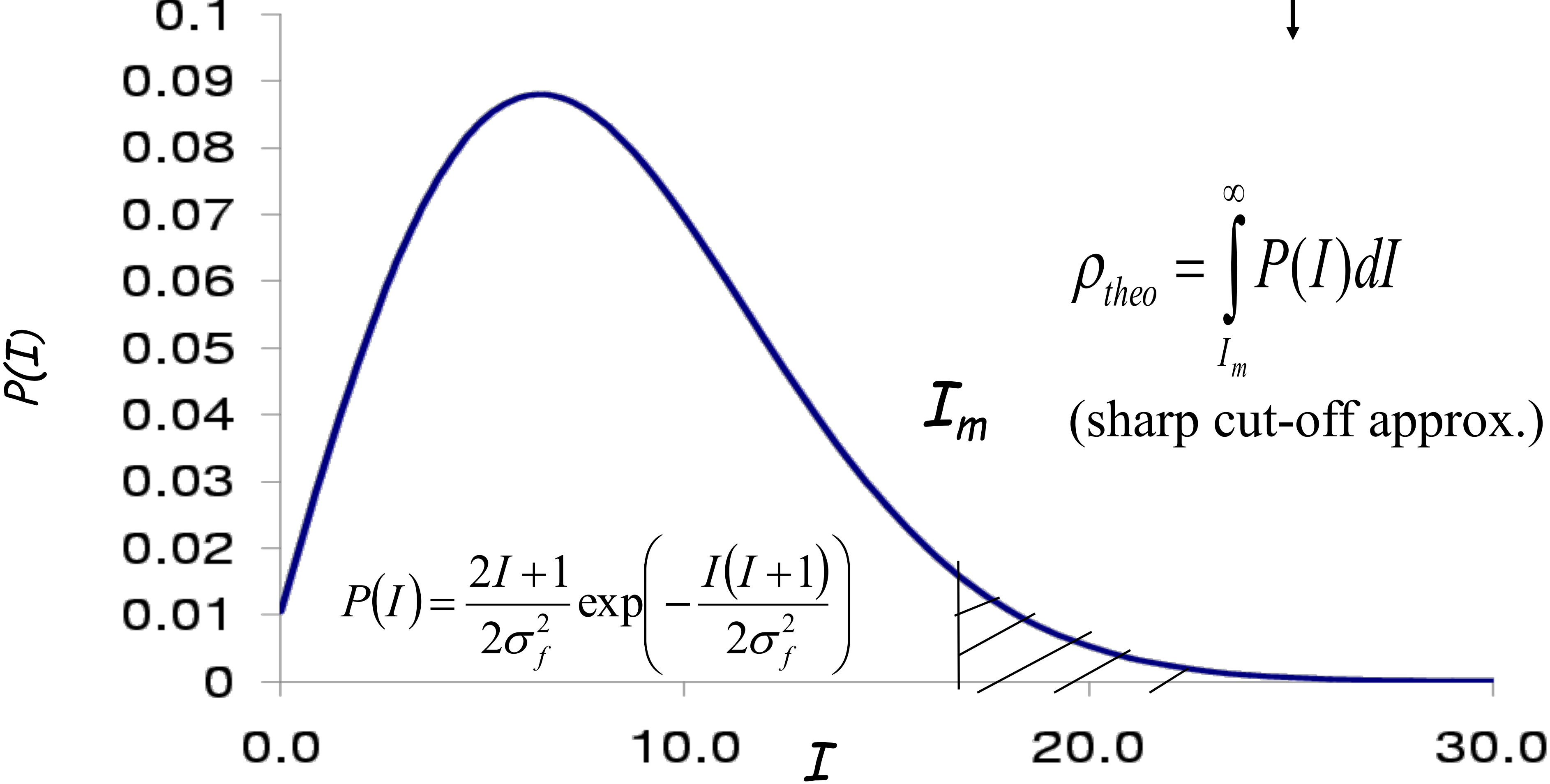

J.-J. Gaimard and K.-H. Schmidt, Nucl. Phys. A 531 (1991) 709

M. De Jong, A.V. Ignatyuk and K.-H. Schmidt, Nucl. Phys. A 613 (1997) 435

Isomeric ratios from ^{208}Pb and ^{238}U fragmentation

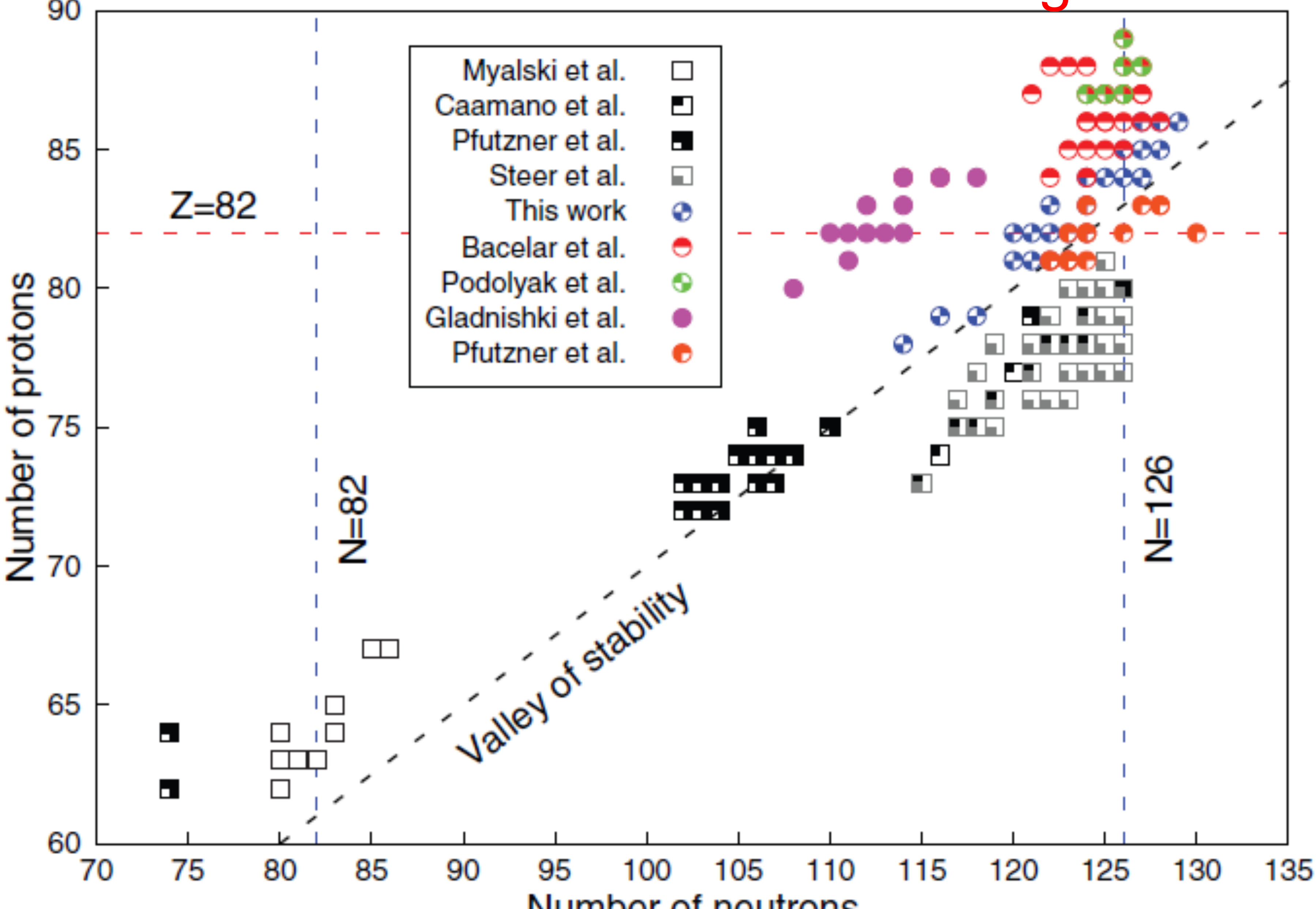

M. Bowry et al., Phys. Rev. C 88, 024611 (2013)

Isomeric ratio vs spin

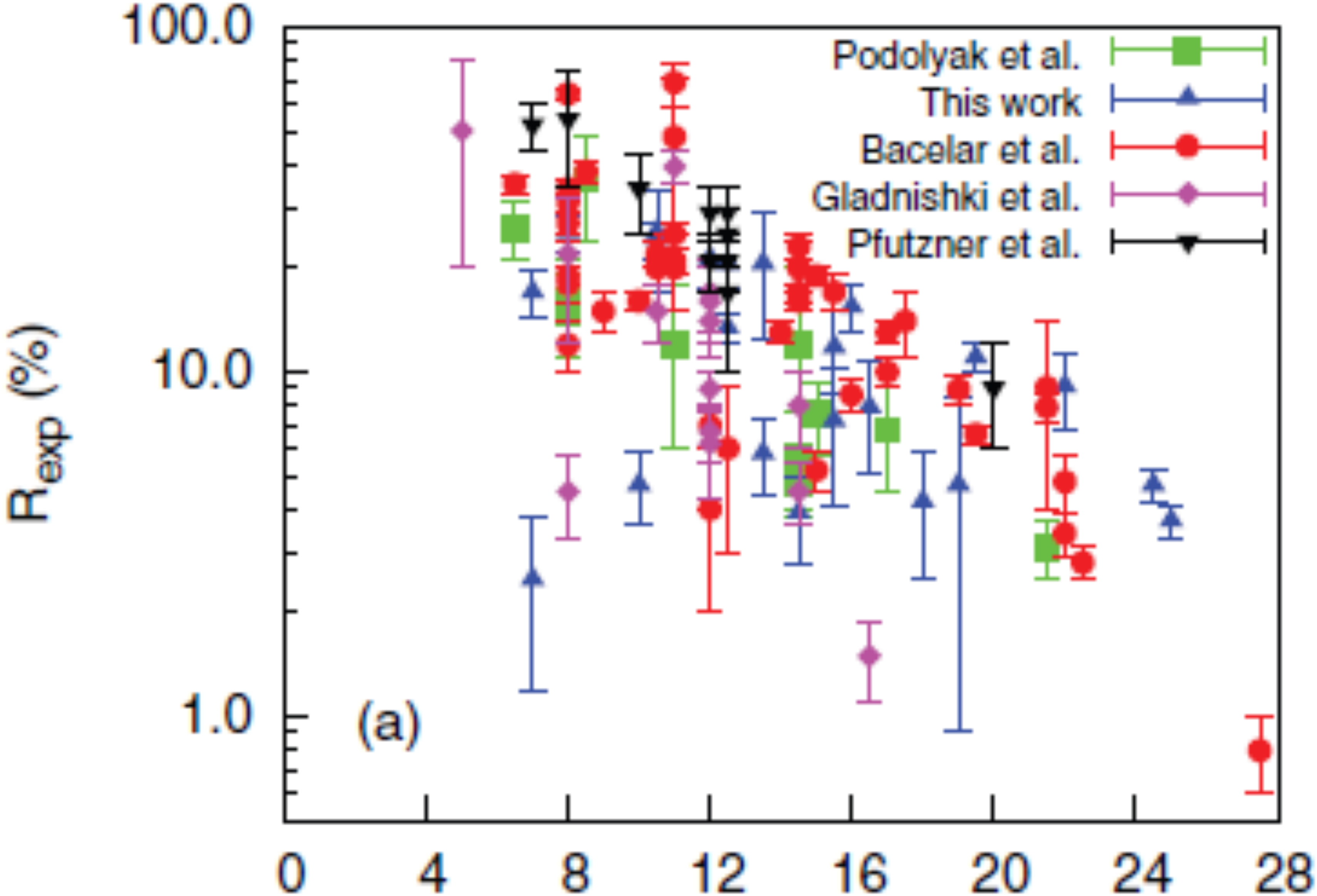

^{238}U beam

M. Bowry et al., Phys. Rev. C 88, 024611 (2013)

Comparison with theory

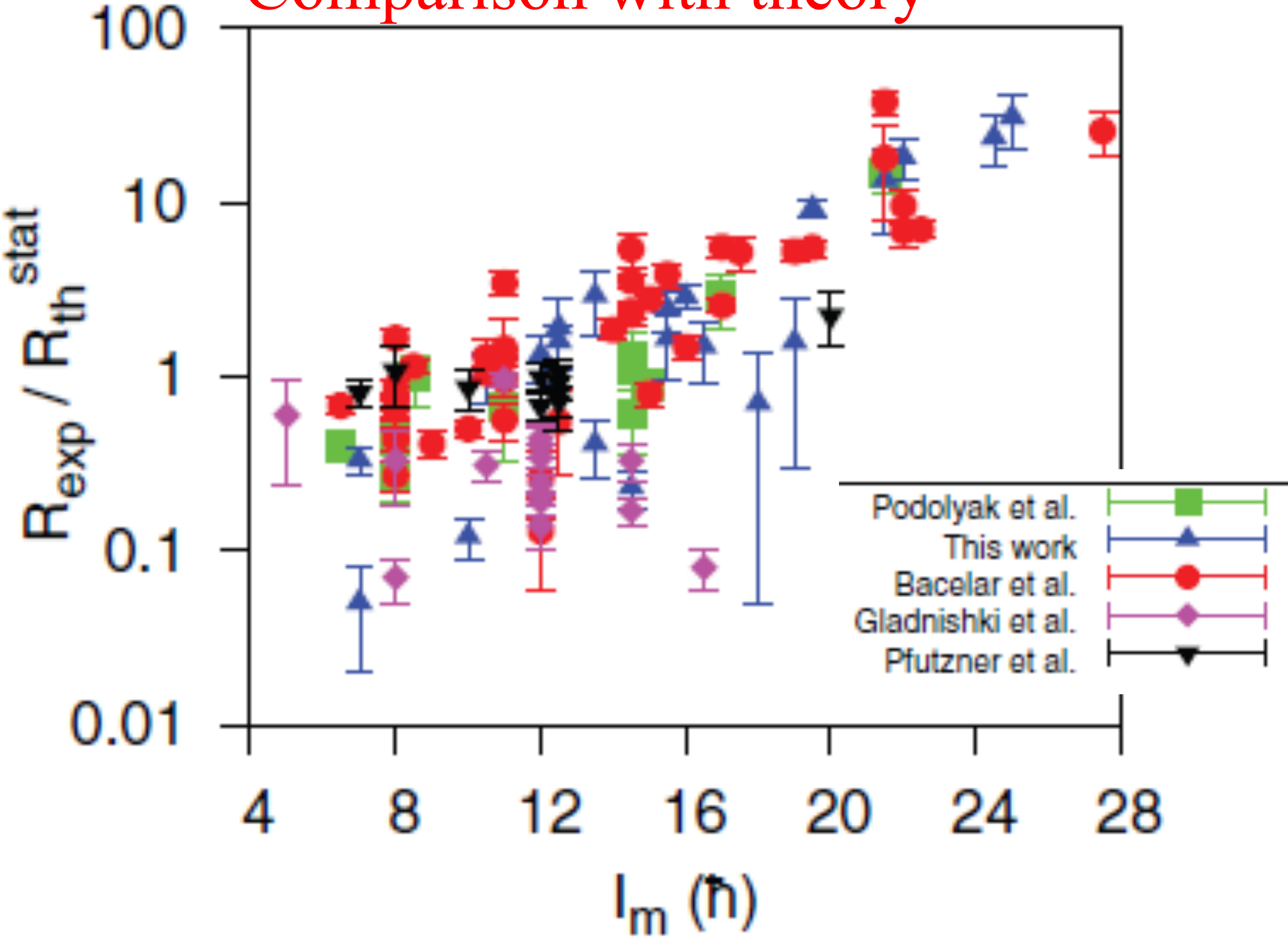

M. Bowry et al., Phys. Rev. C 88, 024611 (2013)

Nuclear structure has to be considered

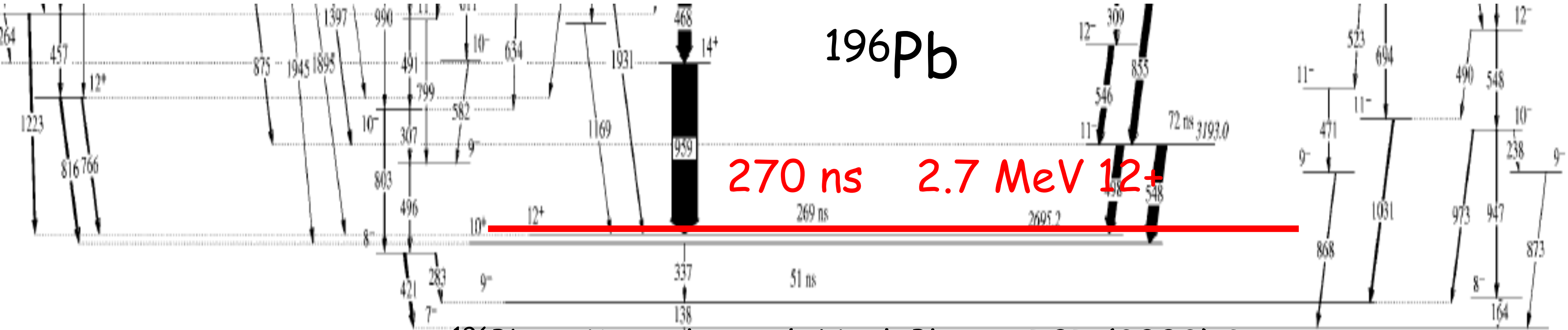

^{196}Pb: A.K.Singh *et al.*, Nucl. Phys. A707 (2002) 3

$^{186}W(^{16}O,6n)$ at 110 MeV; $^{170}Er(^{30}Si,4n)$ at 144 MeV

fusion-evaporation reaction!

$$\varphi = I_{isomer}/(I_{parallel}+I_{isomer}) = I_{isomer} / I_{total}$$

$$\rho_{exp}=R_{exp} / \varphi$$

ρ_{exp} - the probability of populating states with higher spin than the isomer – can be compared with theory!

Without structure considerations

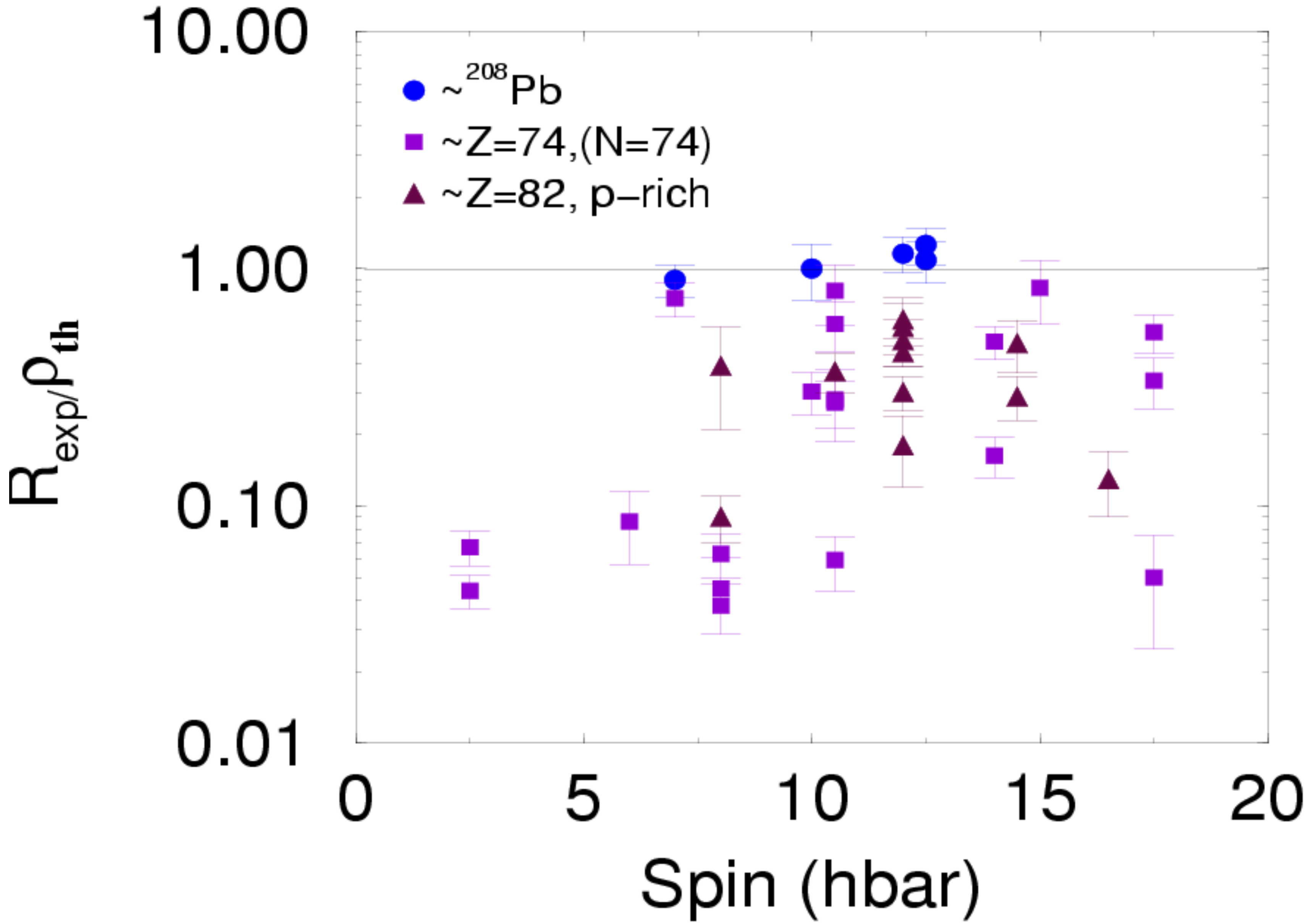

With structure considerations

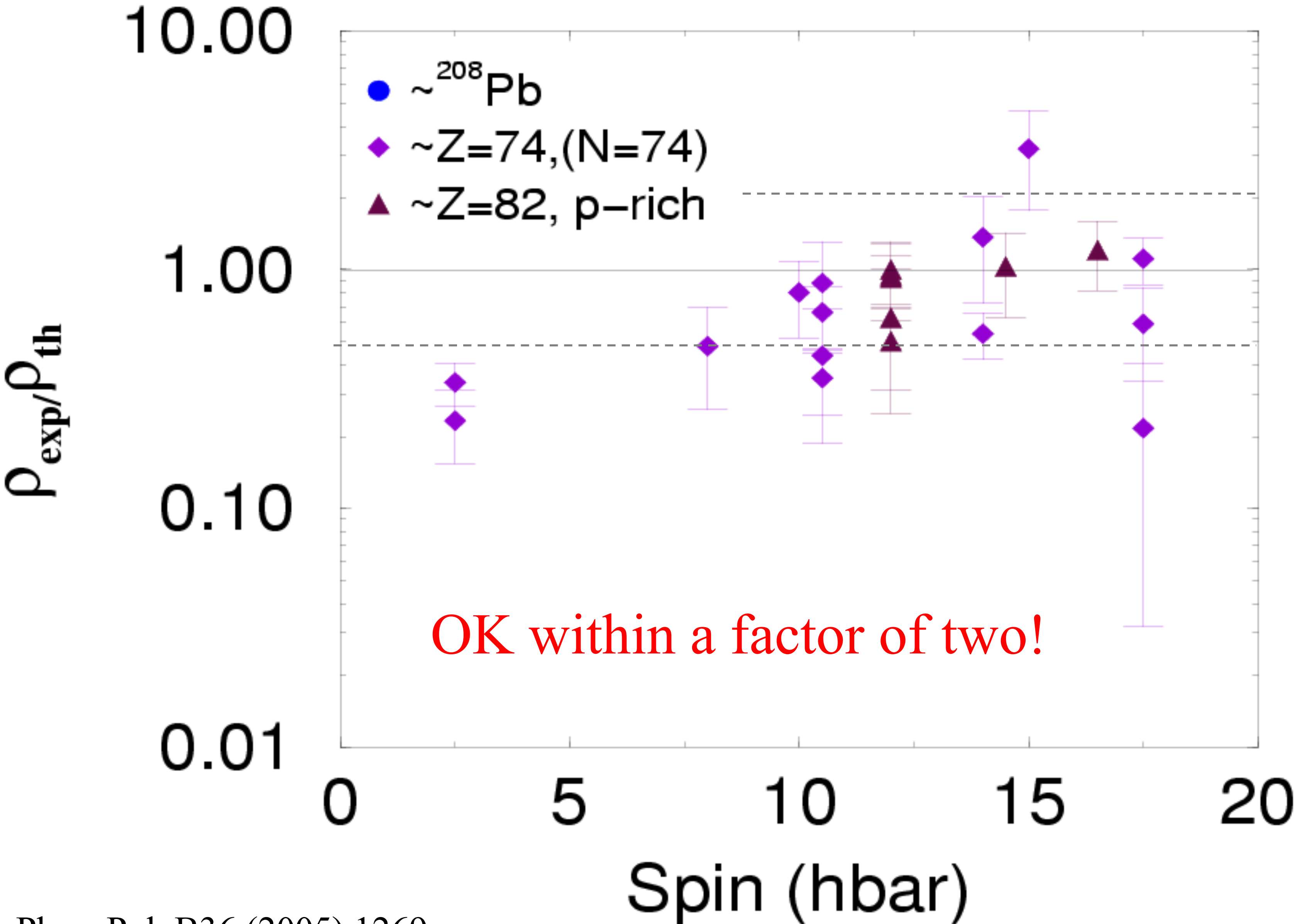

Zs. P. , Acta Phys. Pol. B36 (2005) 1269

Comparison with theory

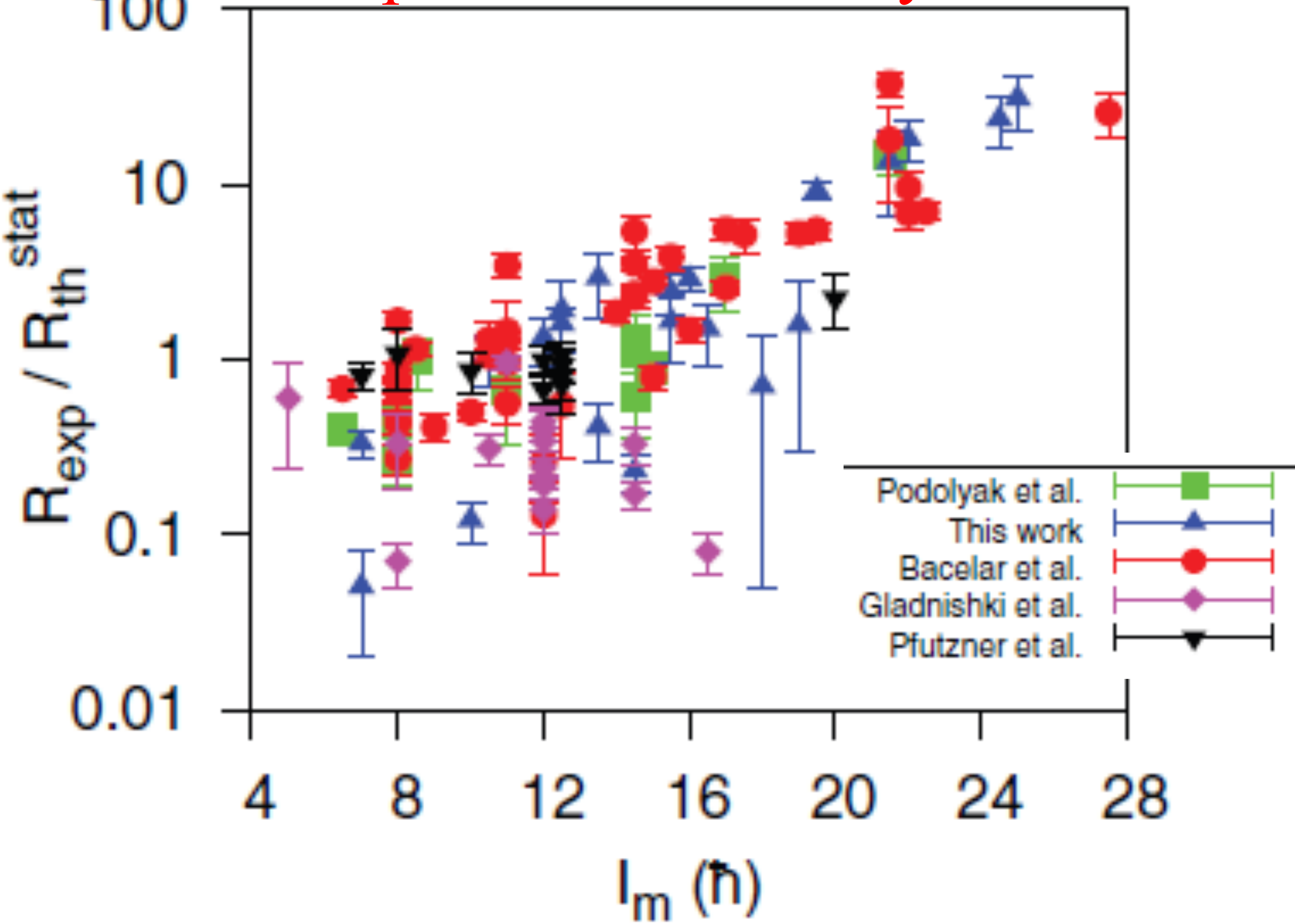

M. Bowry et al., Phys. Rev. C 88, 024611 (2013)

Fragments are slower than projectile: momentum shift (friction)

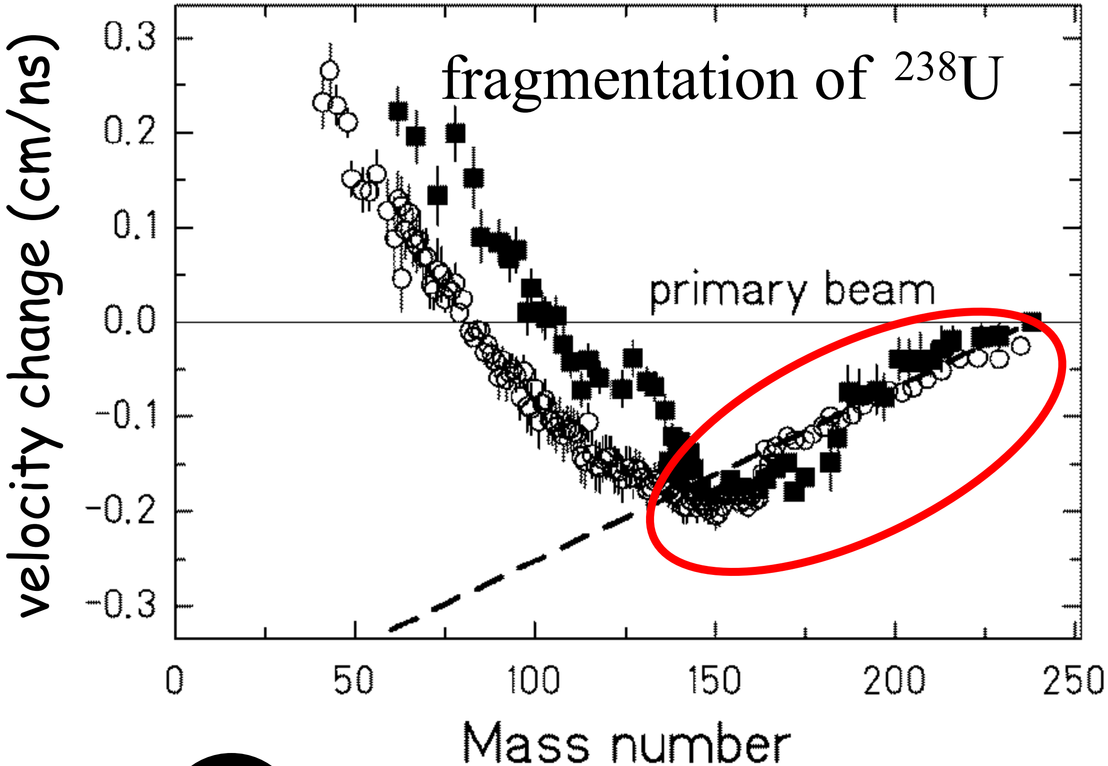

M.V. Ricciardi et al., PRL 90 (2003) 212302

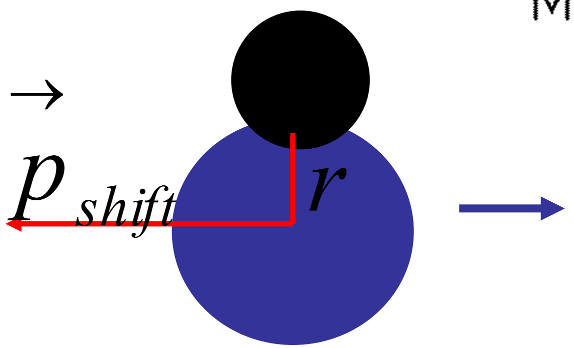

$$\vec{I} = \vec{r} \times \vec{p}_{shift}$$

⇨ angular momentum produced

(collective)

I perpendicular to the beam

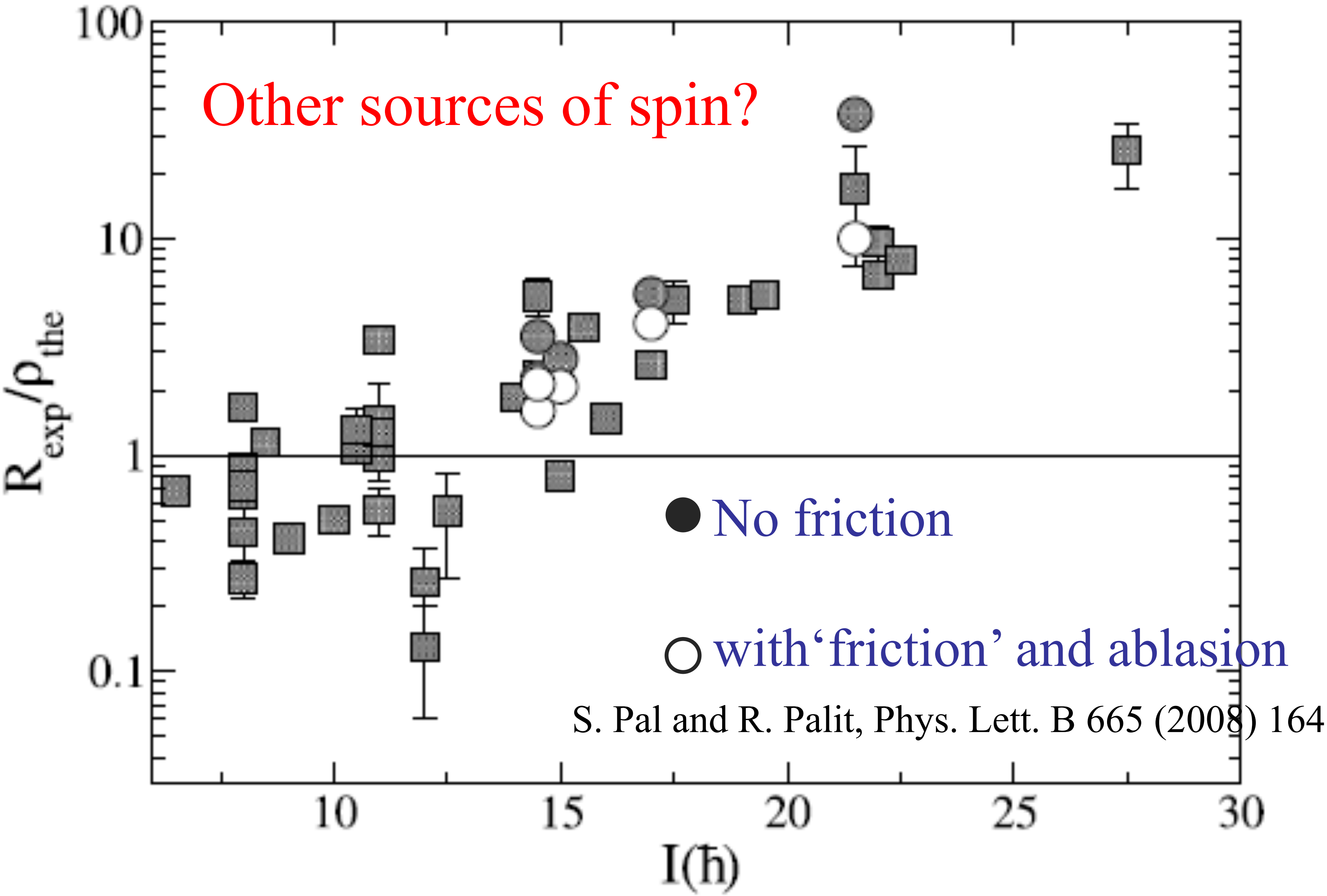

A.M. Denis Bacelar et al., Phys. Lett. B 723, 302 (2012)

Doubled spin-cutoff parameter

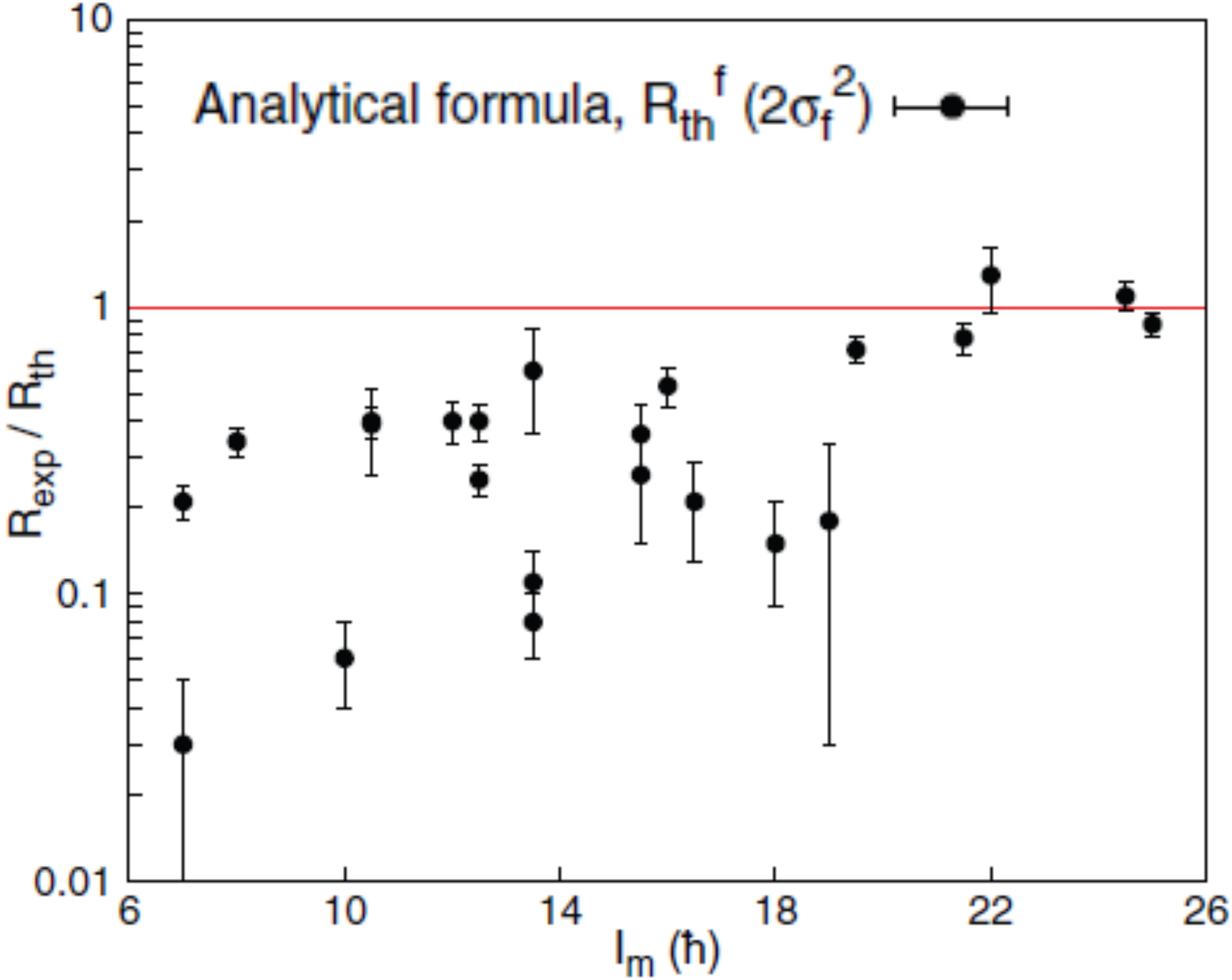

M. Bowry et al., Phys. Rev. C 88, 024611 (2013)

In flight fragmentation (and fission): separation and identification

Fragment Separator (GSI, Darmstadt, Germany)

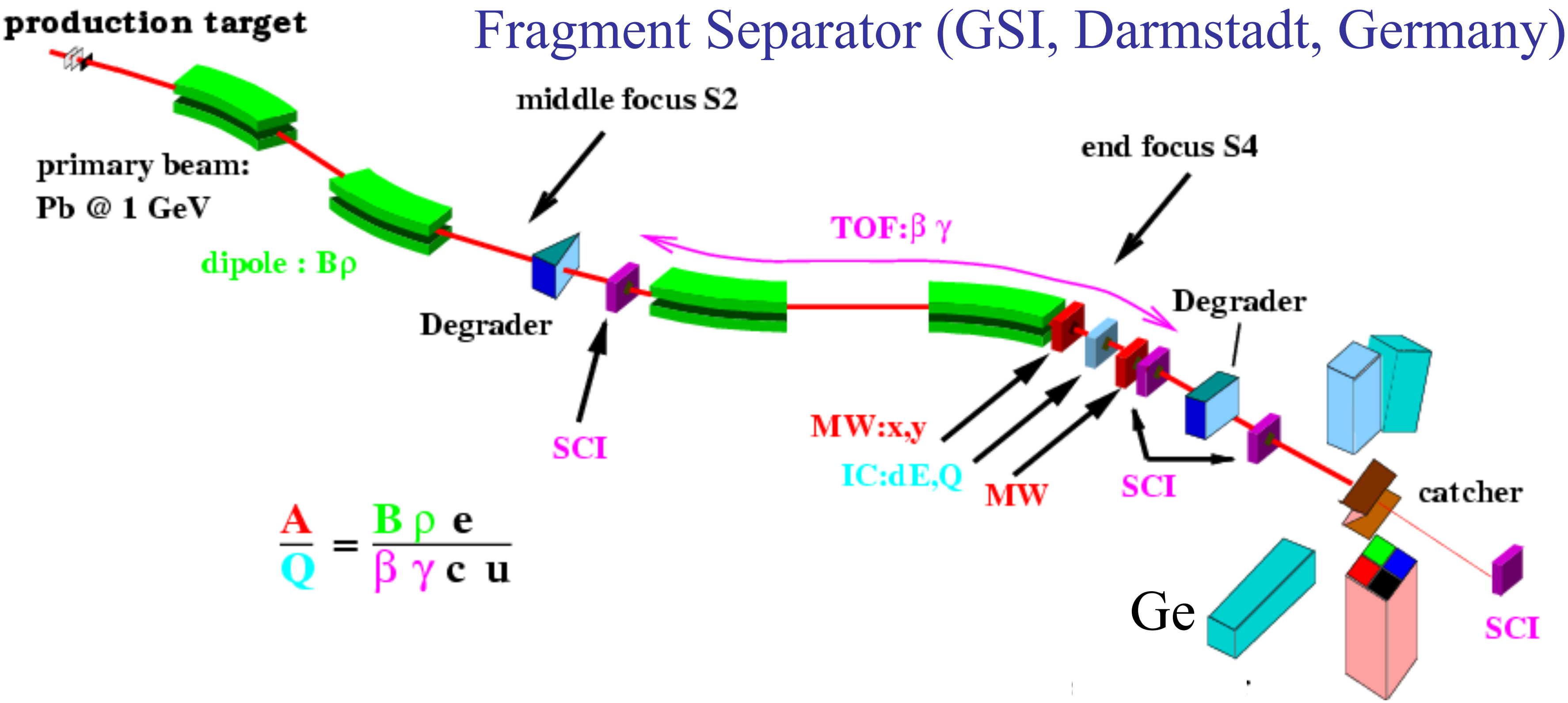

Relativistic energy fragmentation: => heavy ions

Decay (internal and β, α) spectroscopy:

- decay correlated with the fragment
- ***very sensitive*** (ion beams > 1 ion/hour)

Isomeric states (from fragmentation)

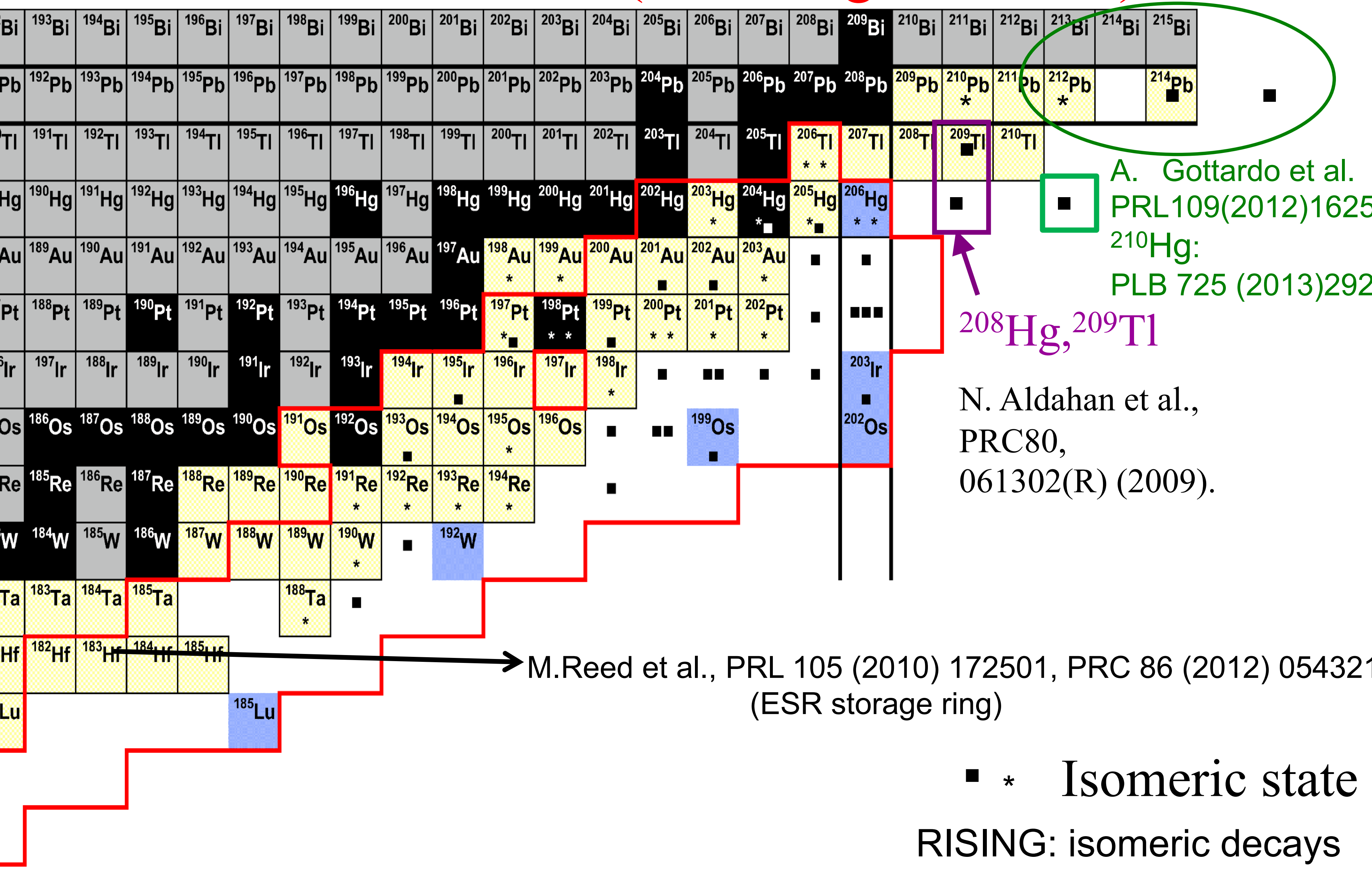

S. Steer et al., Phys. Rev. C 84 (2011) 044313

Identification

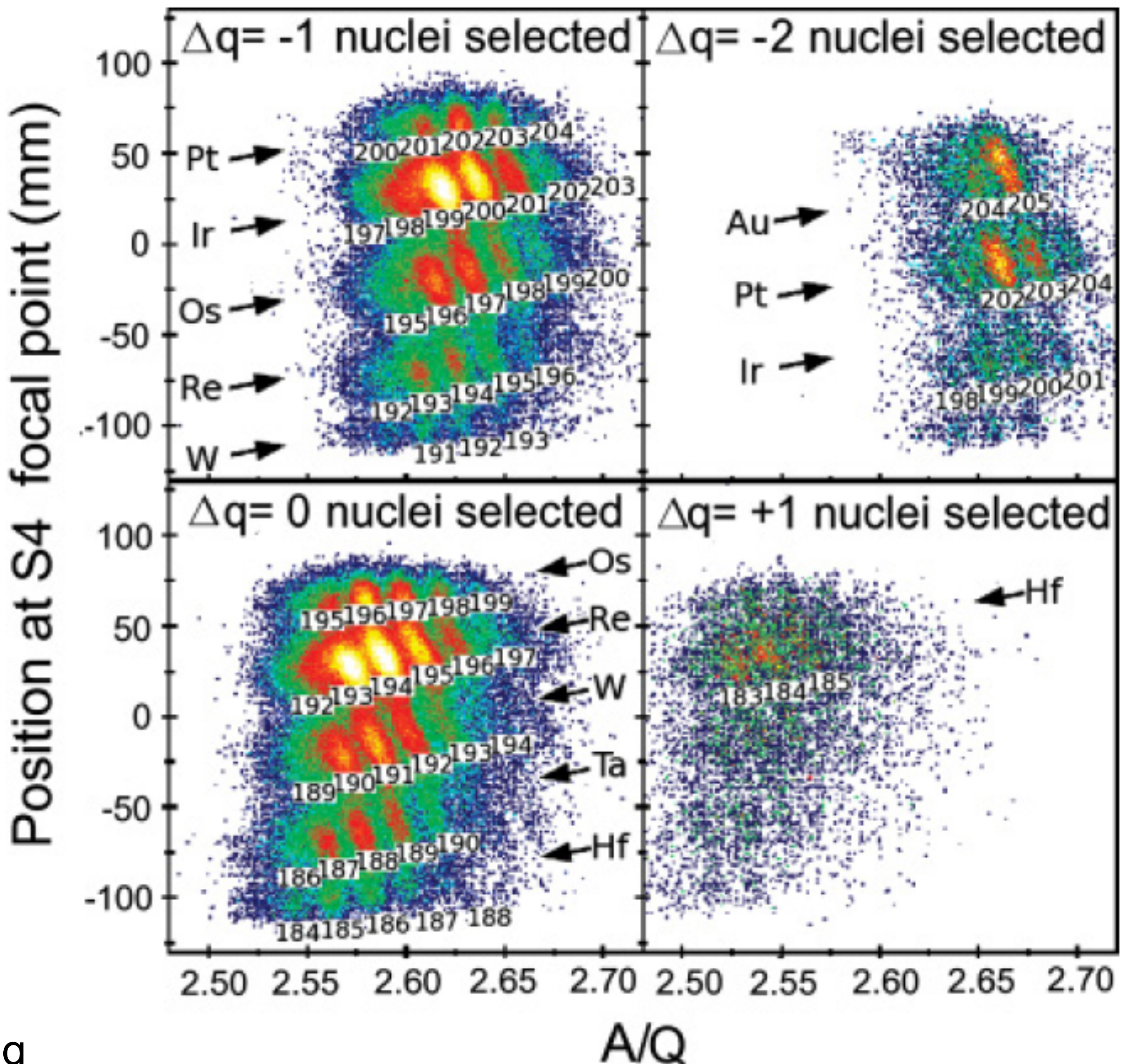

192W setting

Future: several projects

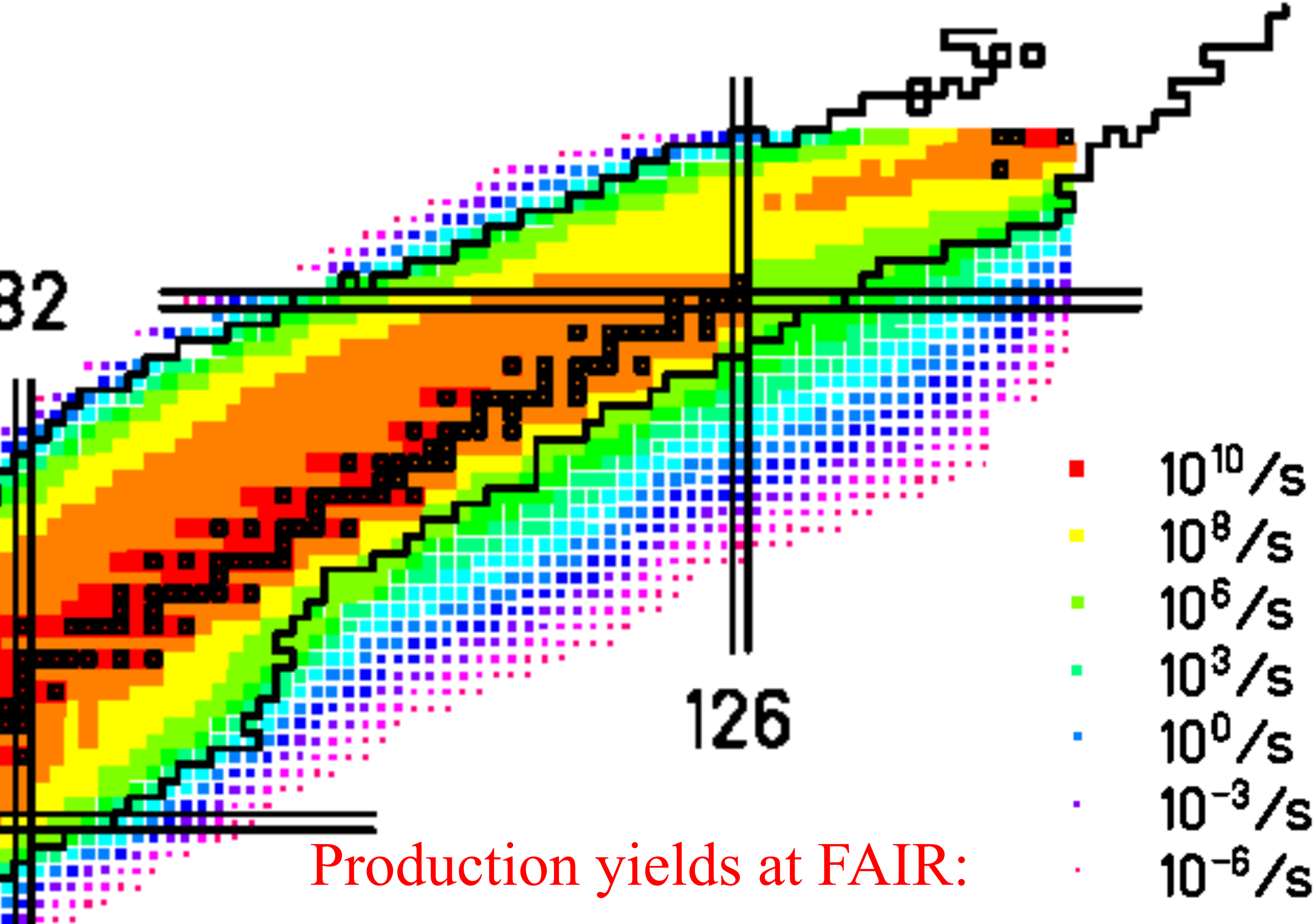

Production yields at FAIR:

Multinucleon transfer reactions: theory

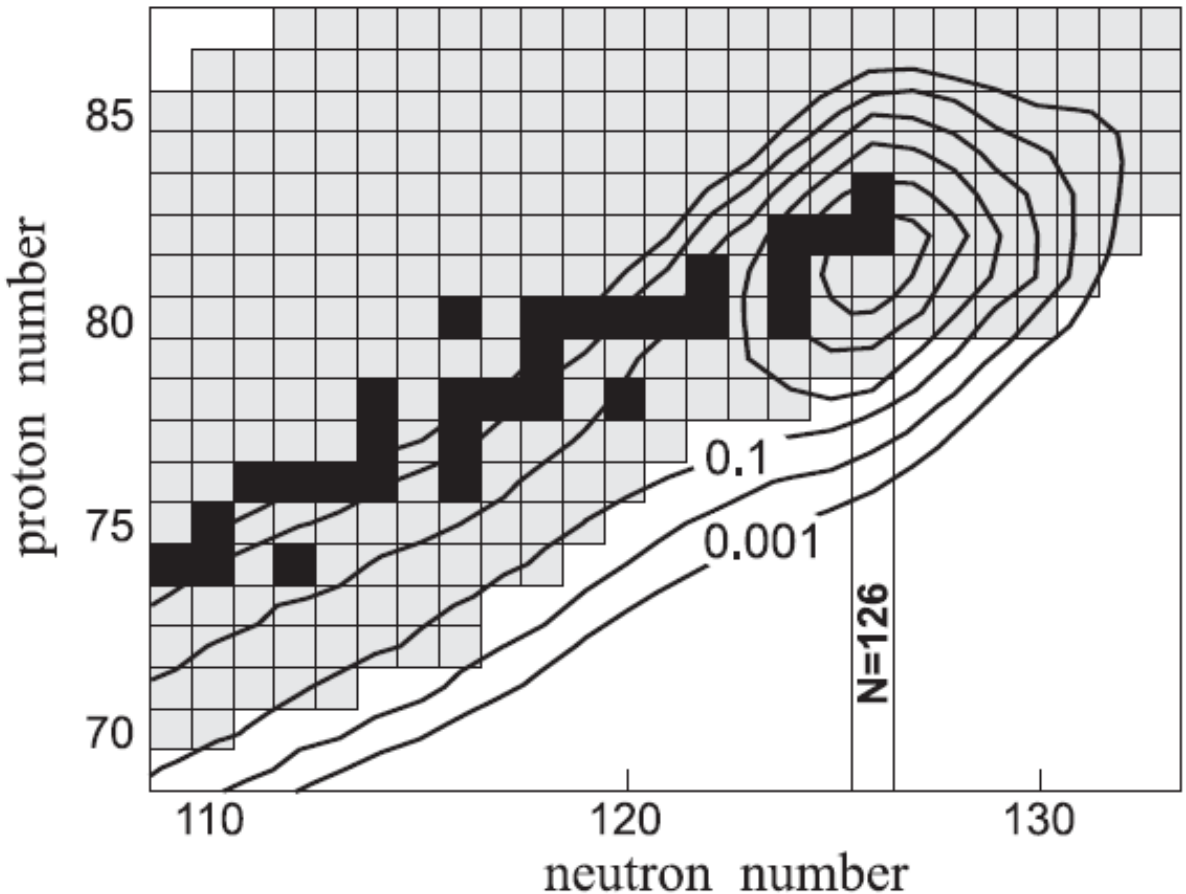

FIG. 4. Landscape of the total cross section $d^2\sigma/dZdN$ (mb, numbers near the curves) for production of heavy fragments in collisions of ^{136}Xe with ^{208}Pb at $E_{c.m.} = 450$ MeV. Contour lines are drawn over 1 order of magnitude.

V. Zagrebaev, W. Greiner, Phys. Rev. Lett. 101, 122701 (2008)

(1) KHH7B interaction: The model space considered consisted of the proton orbitals $d_{5/2}$, $h_{11/2}$, $d_{3/2}$, $s_{1/2}$ below $Z = 82$ and the $h_{9/2}$, $f_{7/2}$, $i_{13/2}$ ones above it, and the neutron orbitals $i_{13/2}$, $p_{3/2}$, $f_{5/2}$, $p_{1/2}$ below $N = 126$ and $g_{9/2}$, $i_{11/2}$, $j_{15/2}$ above. The cross shell two-body interaction matrix elements (TBMEs) are based on the H7B G-matrix [18], while the neutron–proton TBMEs are based on the Kuo–Herling interaction [19] as modified in [20]. These calculations describe accurately valence particle excitations (when no core-breaking is needed). They were used extensively on nuclei below $Z = 82$ along the $N = 126$ line [21–24], as well as for both in the $N > 126$ [25] and $N < 126$ [5,24] regions.

(2) KHM3Y interaction: The model space consisted of the proton orbitals $\mathbf{g_{7/2}}$, $d_{5/2}$, $h_{11/2}$, $d_{3/2}$, $s_{1/2}$ below $Z = 82$ and $h_{9/2}$, $f_{7/2}$, $i_{13/2}$, $\mathbf{f_{5/2}}$, $\mathbf{p_{3/2}}$, $\mathbf{p_{1/2}}$ above it, and the neutron orbitals $i_{13/2}$, $p_{3/2}$, $f_{5/2}$, $p_{1/2}$, $\mathbf{h_{9/2}}$, $\mathbf{f_{7/2}}$ below $N = 126$ and $g_{9/2}$, $i_{11/2}$, $j_{15/2}$, $\mathbf{g_{7/2}}$, $\mathbf{d_{5/2}}$, $\mathbf{d_{3/2}}$, $\mathbf{s_{1/2}}$ above. The additional orbitals, compared to the KHH7B calculations, are shown in bold. The cross-shell, two-body matrix elements are based on the M3Y interaction [26], while the neutron–proton interactions are based on the Kuo–Herling interaction [19] as modified in Ref. [20]. Such calculations gave a good

END

$h^2_{11/2}$ component of the 10+ isomer?

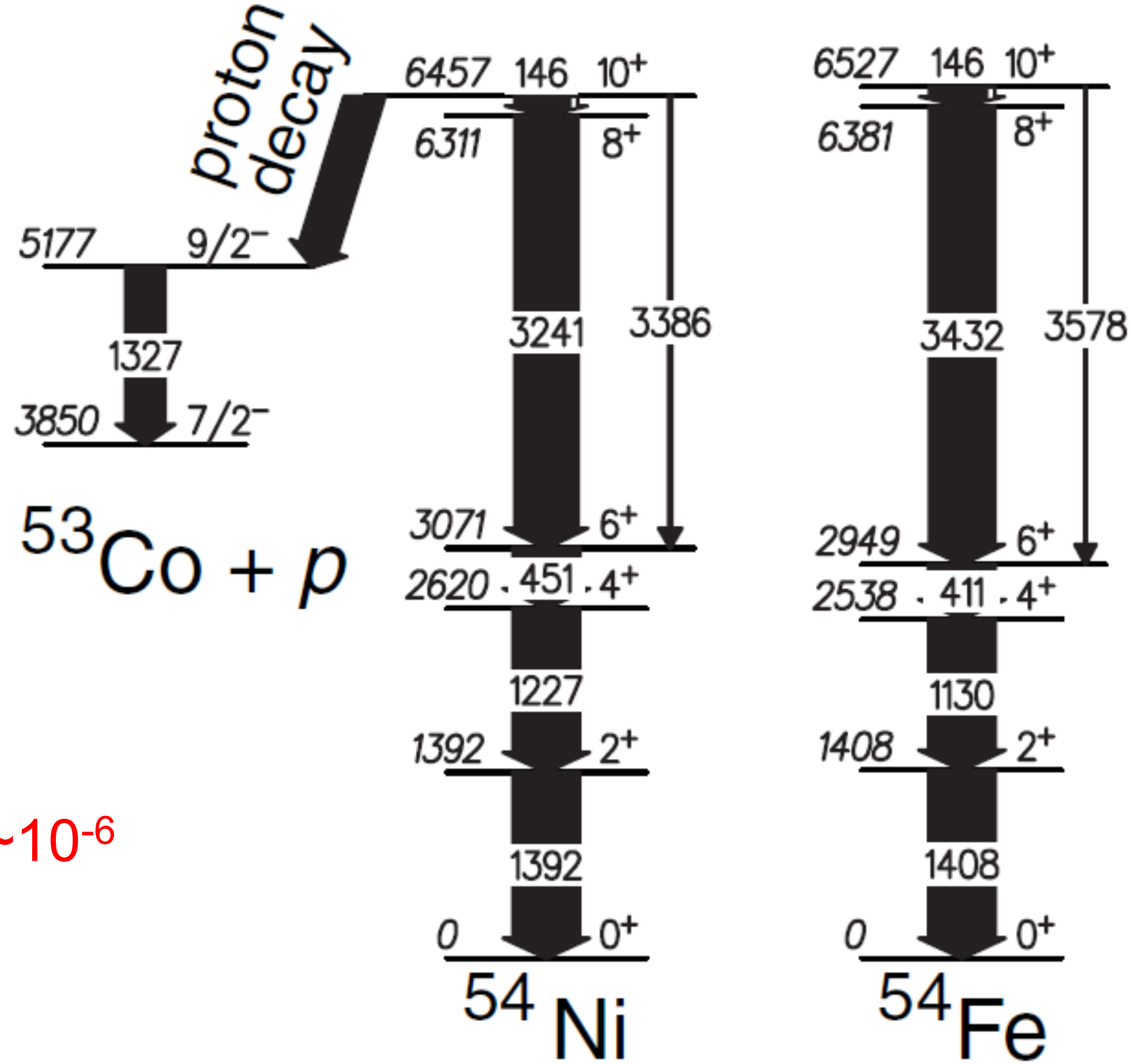

l=5 proton decay

$h^2_{11/2}$ component ~10^{-6}

Very low!

D. Rudolph *et al.,* Phys. Rev. C78, 021301(R) (2008).

Isomeric ratio of the 10^+ isomer

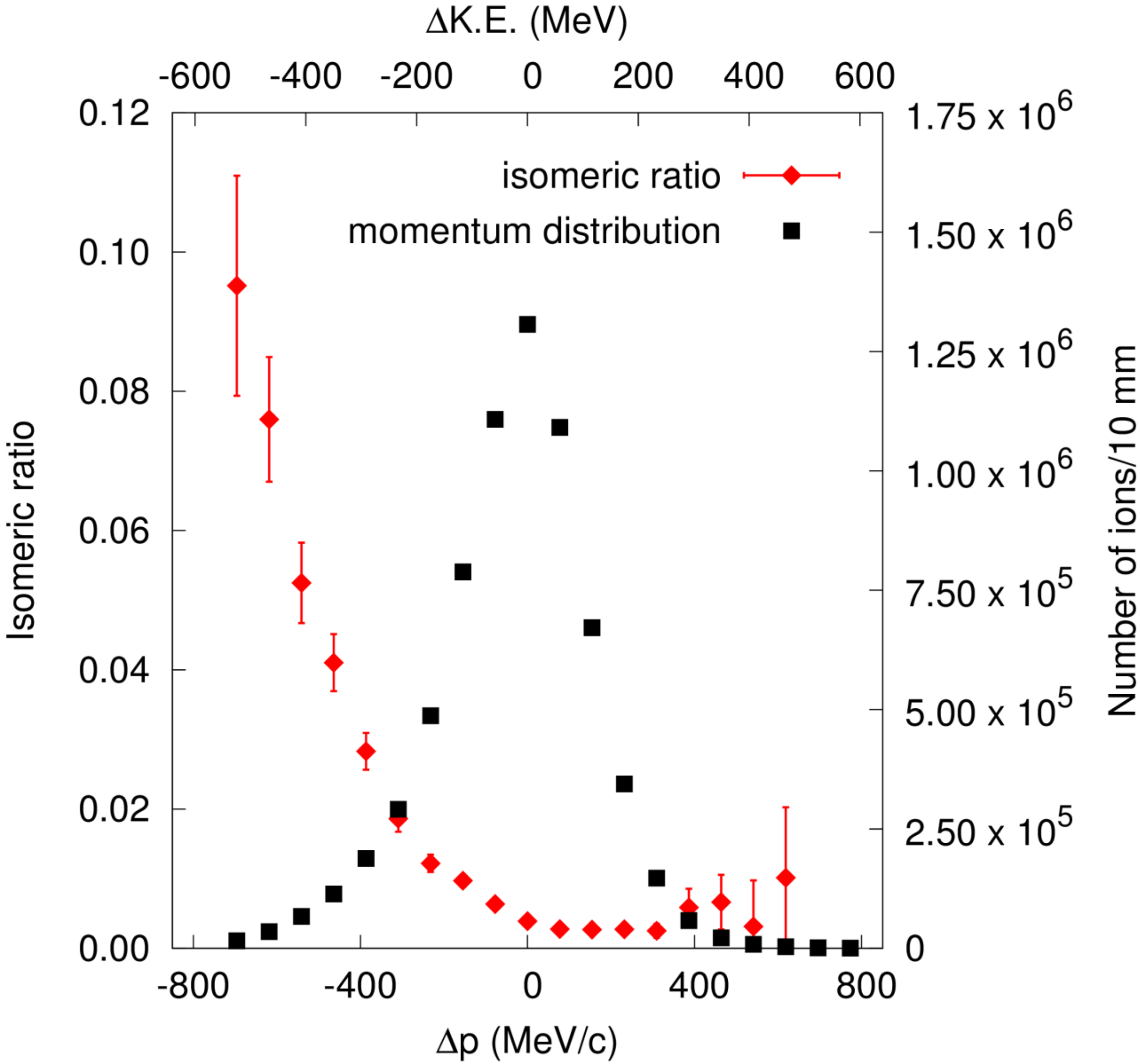

=> the isomer is produced in the low momentum tail

Conclusions

The 10^+ isomer in ^{54}Fe populated from ^{56}Fe at E/A=500 MeV
The 10^+ state is a four particle state
10^+ populated mainly at low momentum

=> It is populated via the Δ resonance

PRL **117,** 222302 (2016) PHYSICAL REVIEW LETTERS week ending 25 NOVEMBER 2016

Role of the Δ Resonance in the Population of a Four-Nucleon State in the ^{56}Fe → ^{54}Fe Reaction at Relativistic Energies

Zs. Podolyák,[1] C. M. Shand,[1] N. Lalović,[2,3] J. Gerl,[3] D. Rudolph,[2] T. Alexander,[1] P. Boutachkov,[3] M. L. Cortés,[3,4] M. Górska,[3] I. Kojouharov,[3] N. Kurz,[3] C. Louchart,[4] E. Merchán,[4] C. Michelagnoli,[5] R. M. Pérez-Vidal,[6] S. Pietri,[3] D. Ralet,[4,3] M. Reese,[4] H. Schaffner,[3] Ch. Stahl,[4] H. Weick,[3] F. Ameil,[3] G. de Angelis,[7] T. Arici,[3,8] R. Carroll,[1] Zs. Dombrádi,[9] A. Gadea,[6] P. Golubev,[2] M. Lettmann,[4] C. Lizarazo,[4,3] D. Mahboub,[10] H. Pai,[4] Z. Patel,[1] N. Pietralla,[4] P. H. Regan,[1] L. G. Sarmiento,[2] O. Wieland,[11] E. Wilson,[1] B. Birkenbach,[12] B. Bruyneel,[13] I. Burrows,[14] L. Charles,[15] E. Clément,[5] F. C. L. Crespi,[16,11] D. M. Cullen,[17] P. Désesquelles,[18] J. Eberth,[12] V. González,[19] T. Habermann,[4,3] L. Harkness-Brennan,[20] H. Hess,[12] D. S. Judson,[20] A. Jungclaus,[21] W. Korten,[13] M. Labiche,[14] A. Maj,[22] D. Mengoni,[23,24] D. R. Napoli,[7] A. Pullia,[16,11] B. Quintana,[25] G. Rainovski,[26] P. Reiter,[12] M. D. Salsac,[13] E. Sanchis,[19] and J. J. Valiente Dóbon[7]

PRESPEC-AGATA campaign

Thanks

Fragmentation of ^{56}Fe on H

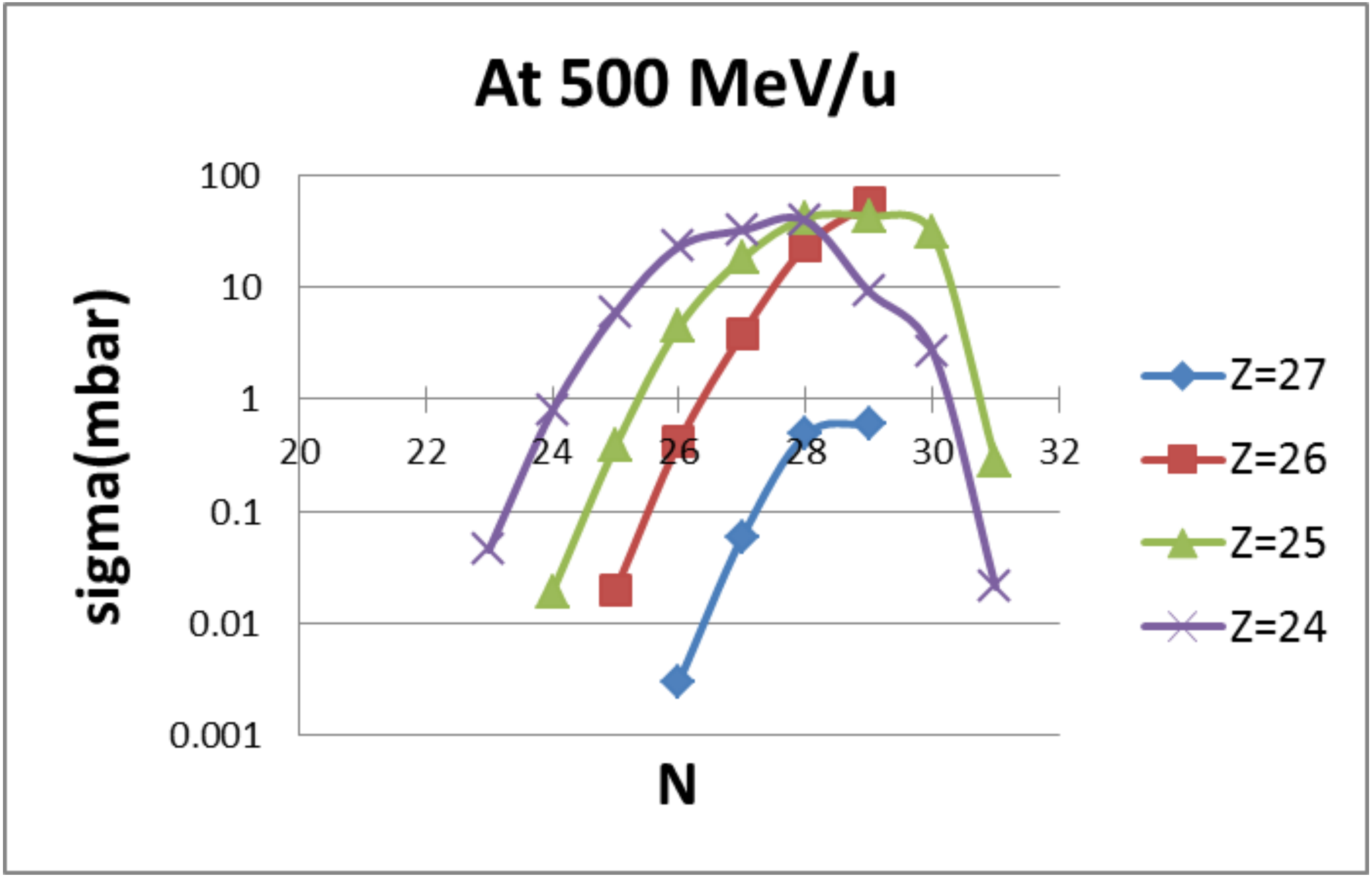

C. Villagrasa-Canton et al., PRC75, 044603 (2007)

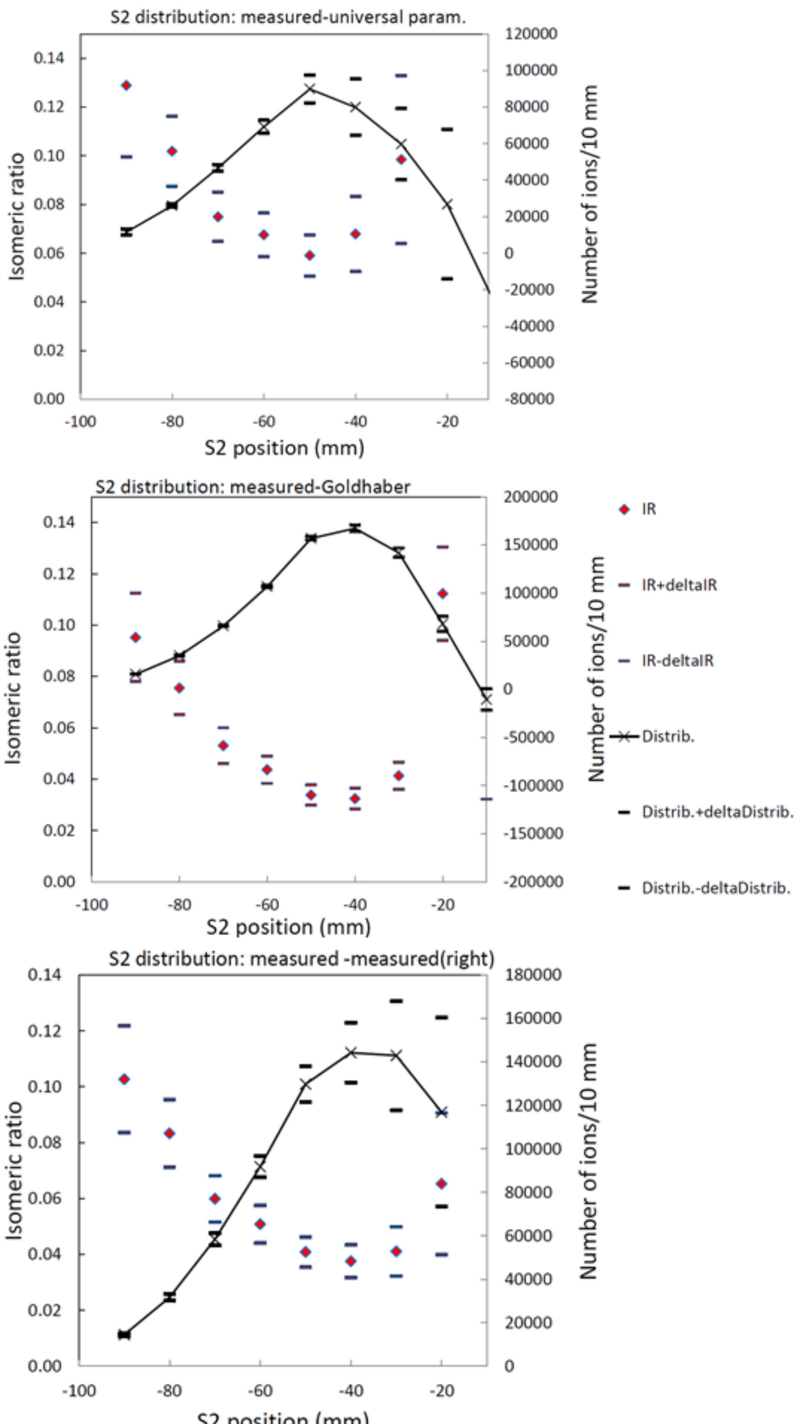
S2 distribution: measured-universal param.
Isomeric ratio
Number of ions/10 mm
S2 position (mm)
S2 distribution: measured-Goldhaber
Isomeric ratio
Number of ions/10 mm
S2 position (mm)
IR
IR+deltaIR
IR-deltaIR
Distrib.
Distrib.+deltaDistrib.
Distrib.-deltaDistrib.
S2 distribution: measured -measured(right)
Isomeric ratio
Number of ions/10 mm
S2 position (mm)

FIRST OBSERVATION OF THE Δ RESONANCE IN RELATIVISTIC HEAVY-ION CHARGE-EXCHANGE REACTIONS

D. Bachelier et al., Phys. Lett. 172, 23 (1986)

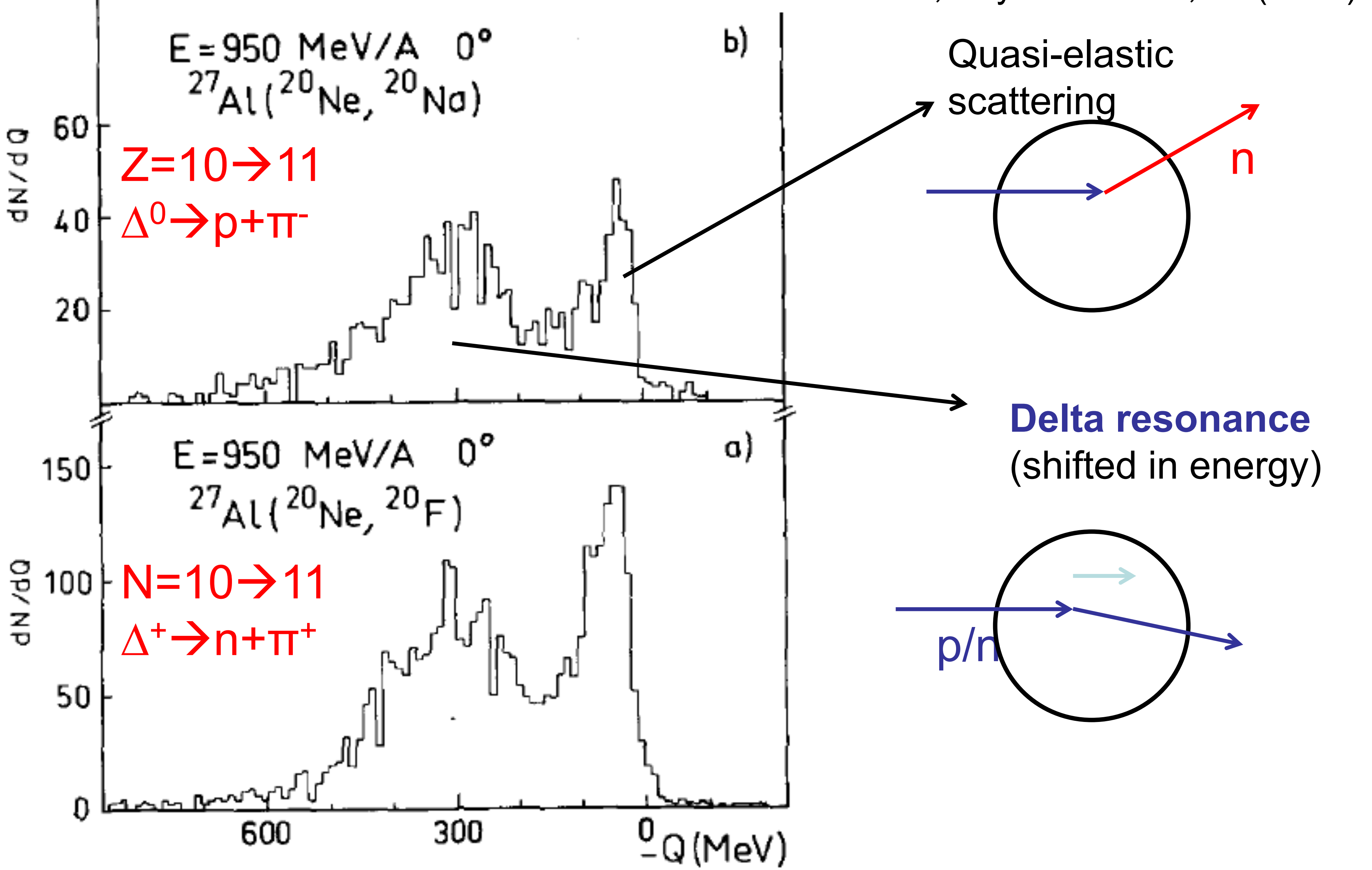

Role of nucleonic resonances in reactions

(but not for individual excited states)

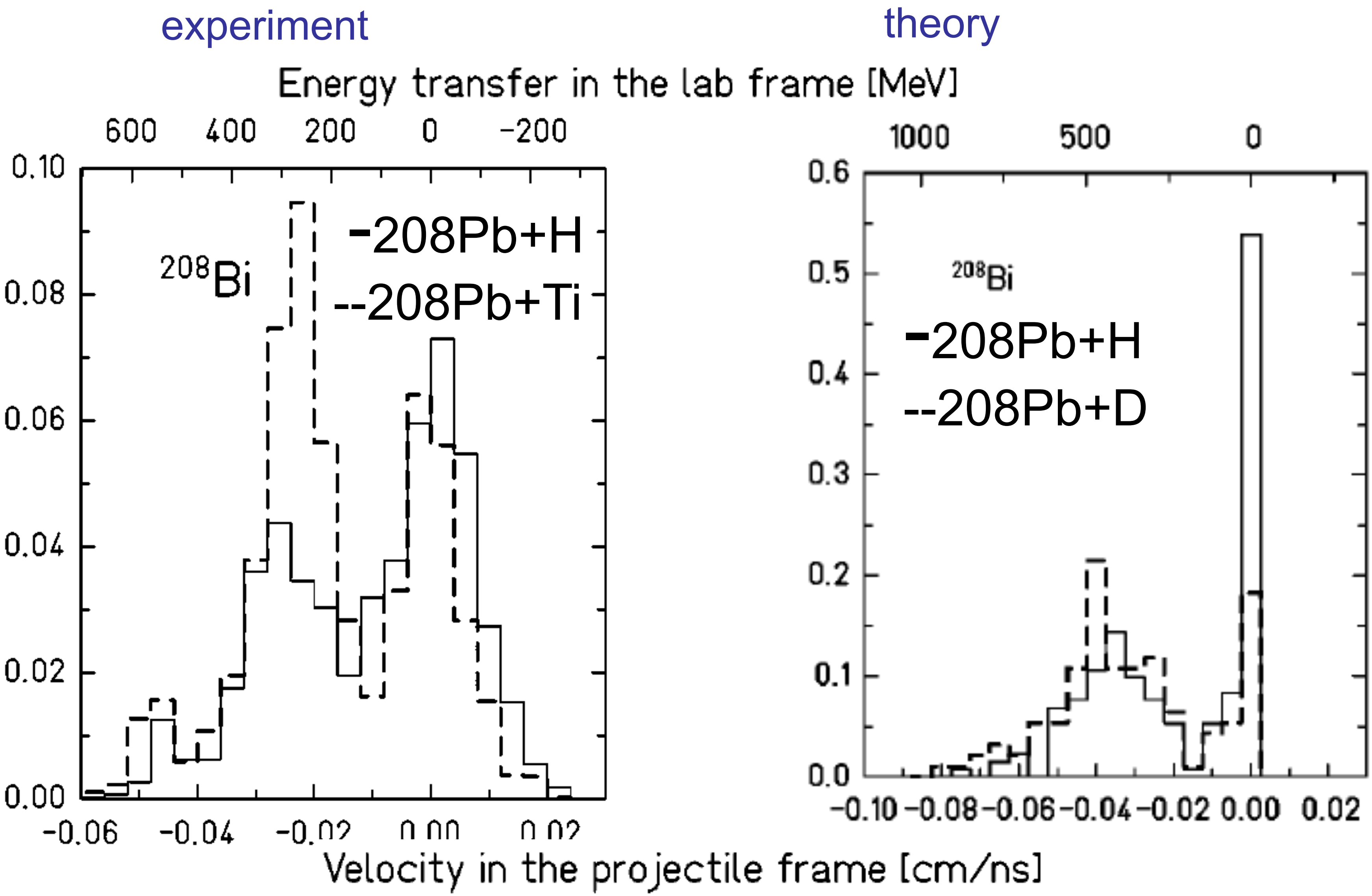

A. Kelic et al., Phys. Rev. C 70, 064608 (2004)

Theory: intranuclear cascade model, e.g. A. Boudard et al., PRC66, 044615 (2002)

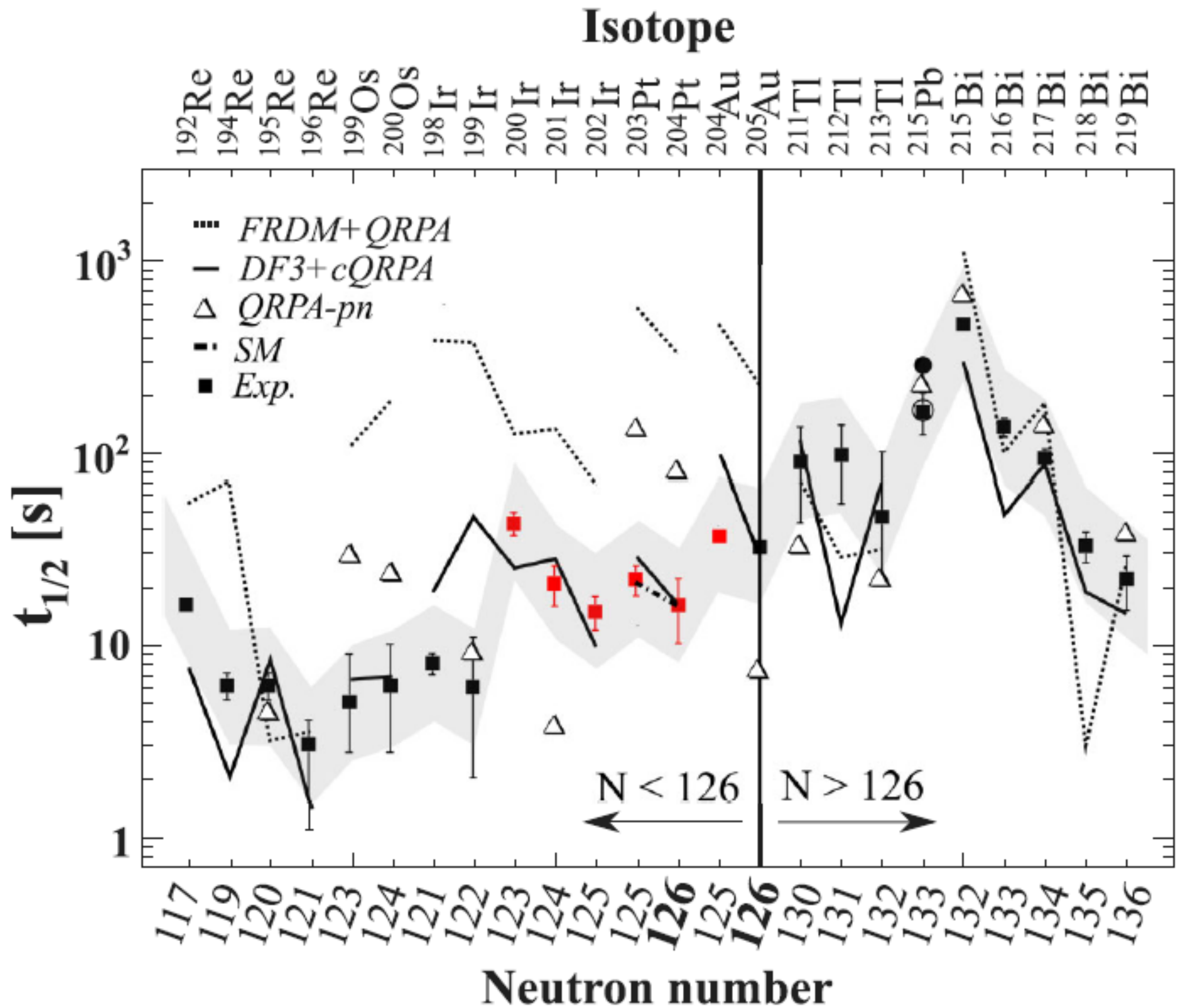

FIG. 3 (color online). Half-life systematics across the $N \sim 126$ shell closure. Results reported in this Letter are shown with red squares. For ^{215}Pb, the FRDM and DF3 predictions are shown with filled and empty circles, respectively. Deviations up to a factor of 2 from the experimental values are indicated with a shaded area. See text for discussion.

A.I. Morales et al., Phys. Rev. Lett. 113, 022702 (2014)

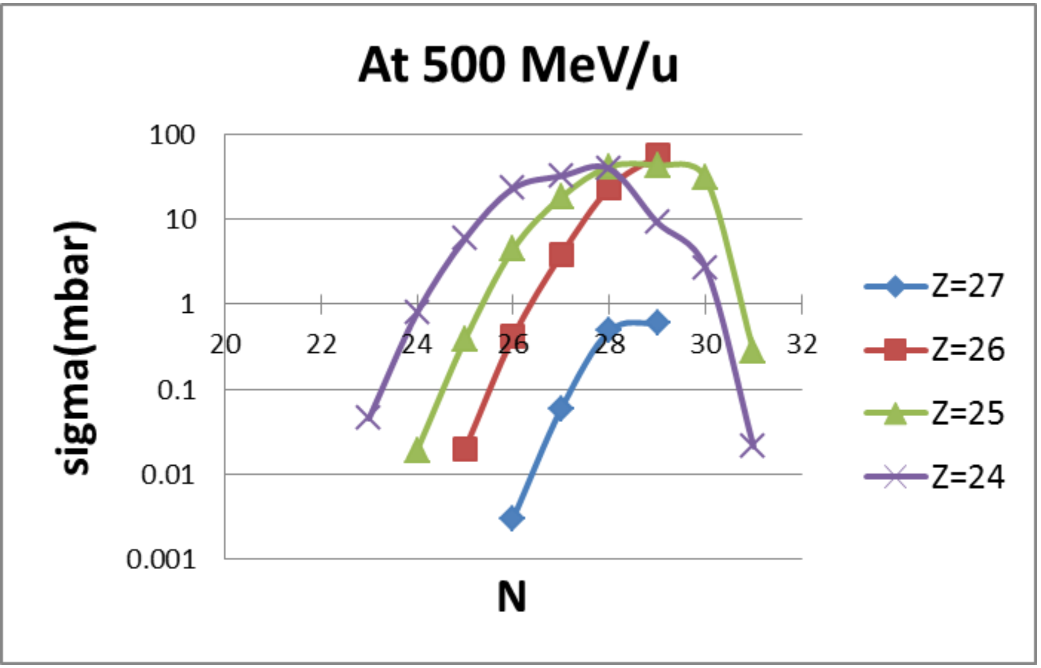

Fragmentation of 56Fe
C. Villagrasa-Canton et al.,
PRC75, 044603 (2007)

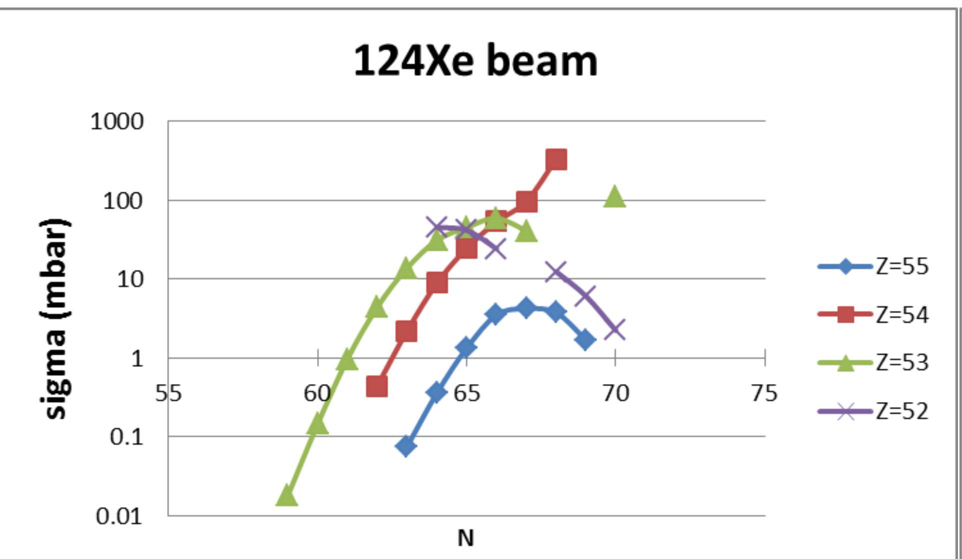

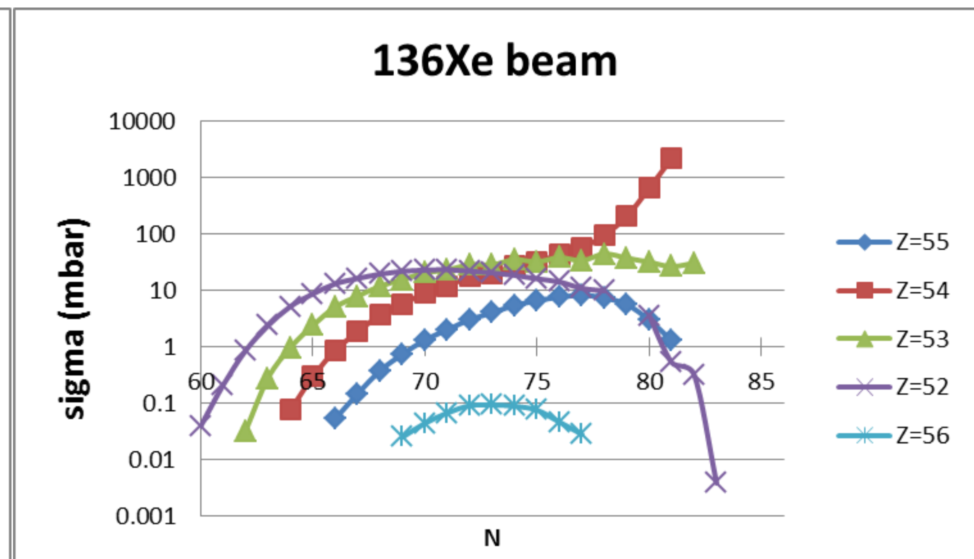

124,136Xe at 1 GeV/u on Pb; D. HENZLOVA et al. PRC78, 44616

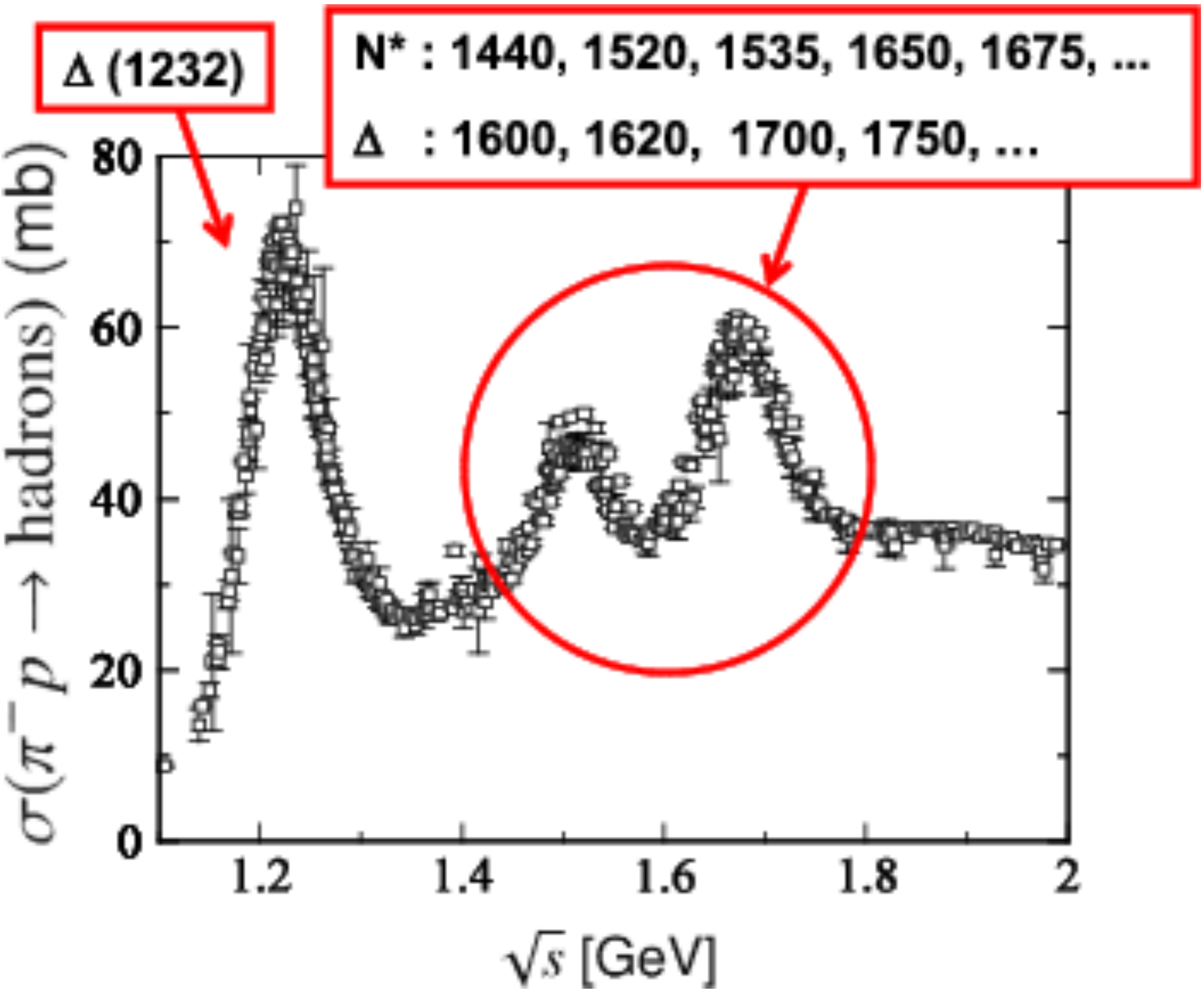

Δ (1232)
N* : 1440, 1520, 1535, 1650, 1675, ...
Δ : 1600, 1620, 1700, 1750, ...
σ(π⁻p → hadrons) (mb)
0
20
40
60
80
1.2
1.4
1.6
1.8
2
√s [GeV]

FIRST OBSERVATION OF THE Δ RESONANCE IN RELATIVISTIC HEAVY-ION CHARGE-EXCHANGE REACTIONS

D. Bachelier et al., Phys. Lett. 172, 23 (1986)

208Pb+H
--208Pb+Ti

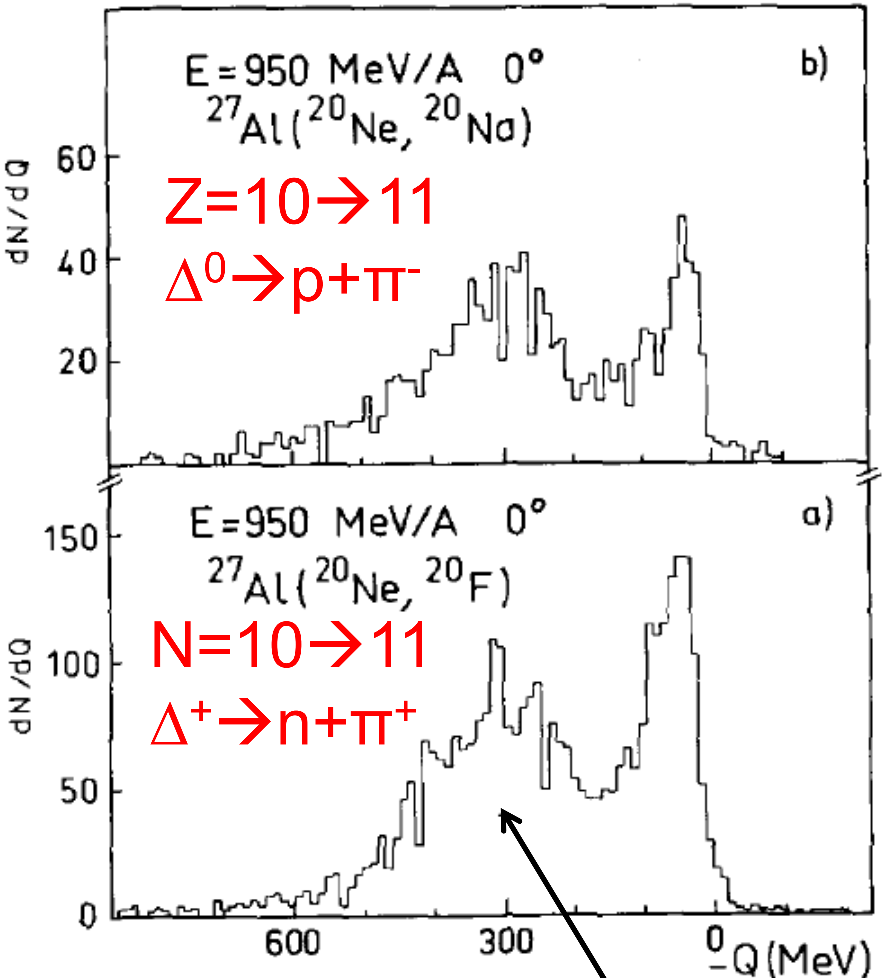

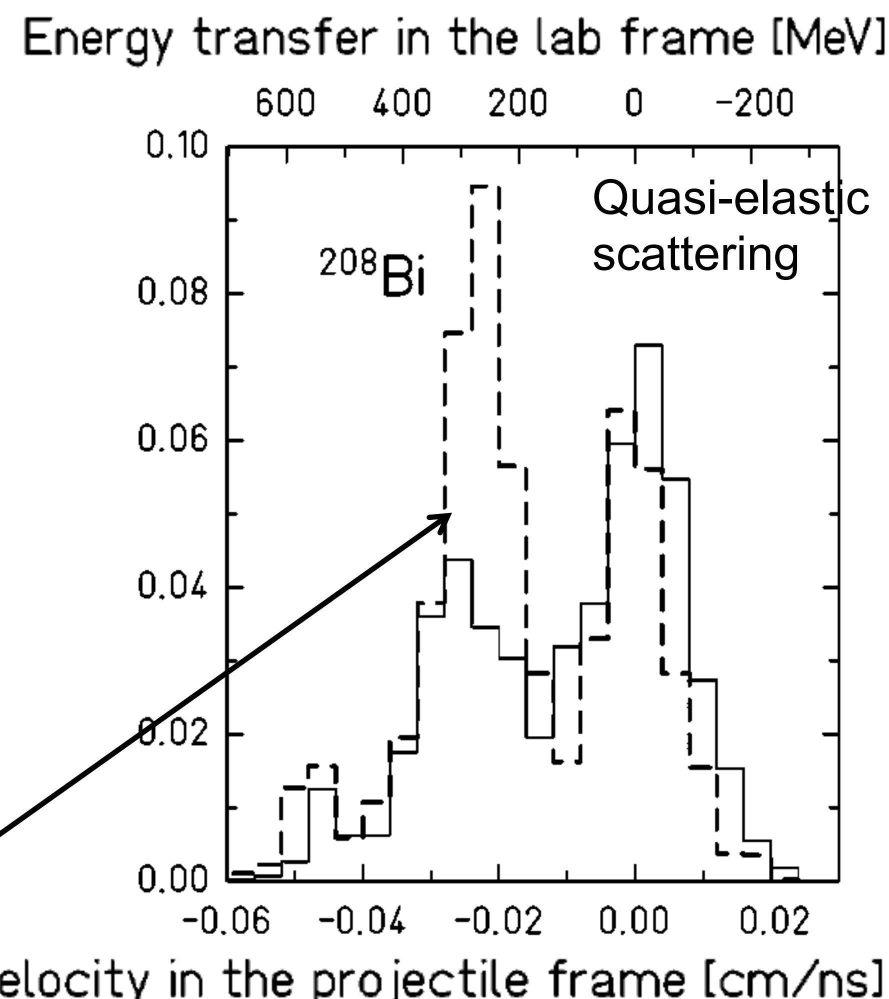

Δ(1232) resonance excitation

A. Kelic et al., Phys. Rev. C 70, 064608 (2004)

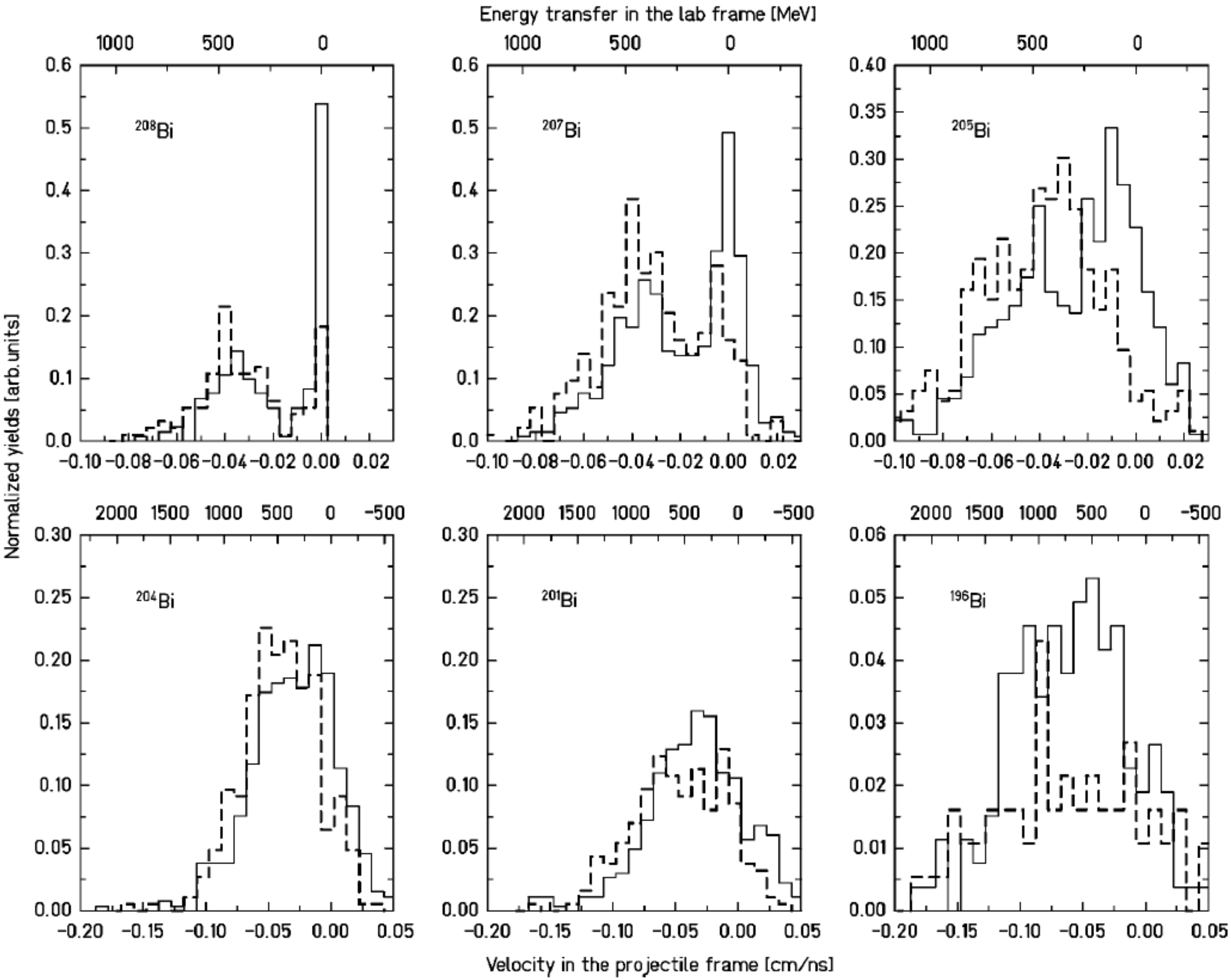

FIG. 12. Calculated velocity distributions of several bismuth isotopes produced in the interaction of 1*A* GeV lead with the proton (full line) and the deuteron (dashed line). The velocity distributions are normalized to the corresponding calculated production cross sections. The calculations were performed with INCL4 +ABLA. The upper x axis shows the energy transfer in the laboratory frame.

A. Kelic et al., Phys. Rev. C 70, 064608 (2004)

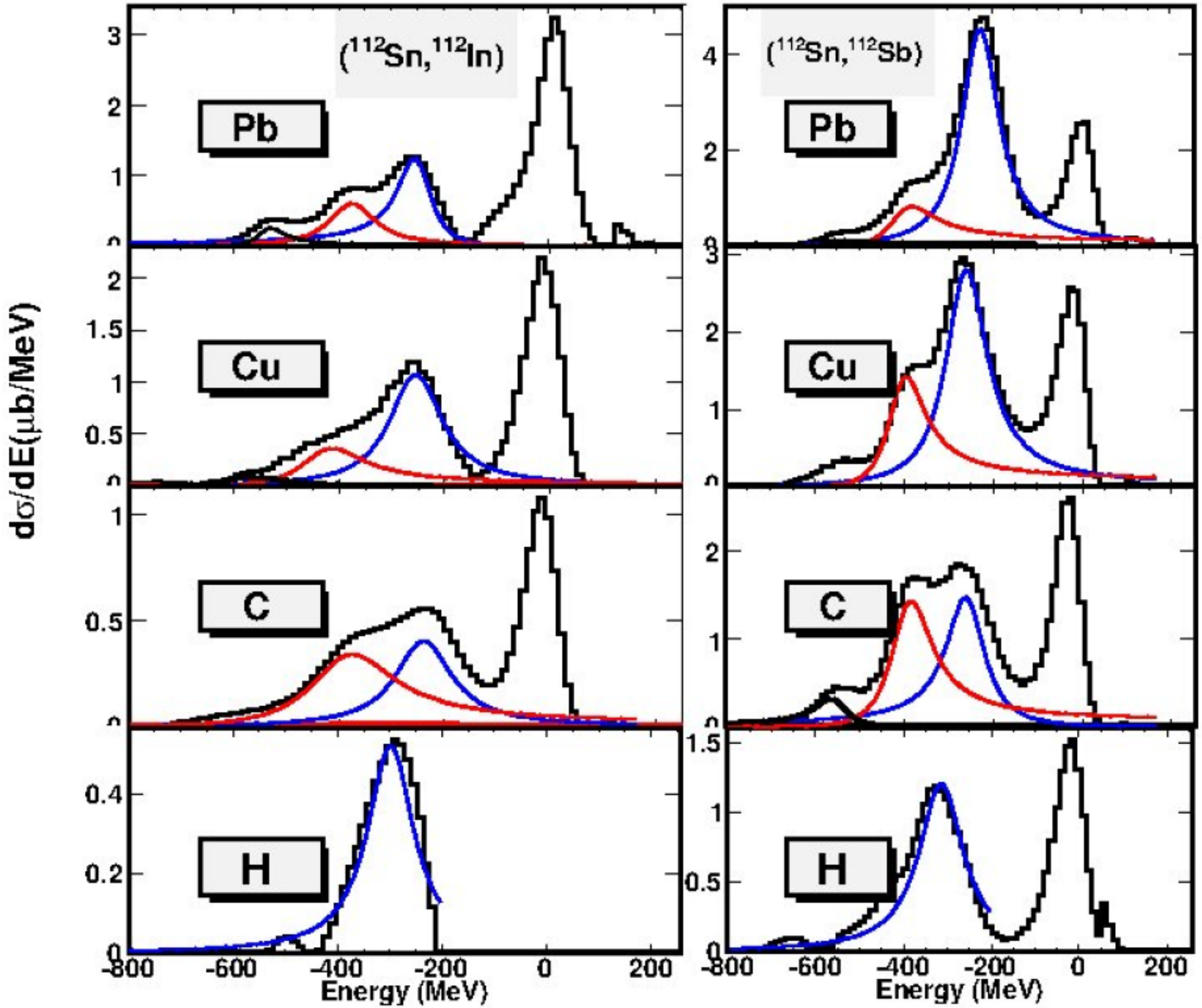

112Sn beam at 1 GeV/u

J. Benlliure et al., JPS Conf. Proc. 6, 020039 (2015)

AGATA detector layout – Status 13-3-2014

6 triplets
3 doublets

22 crystals

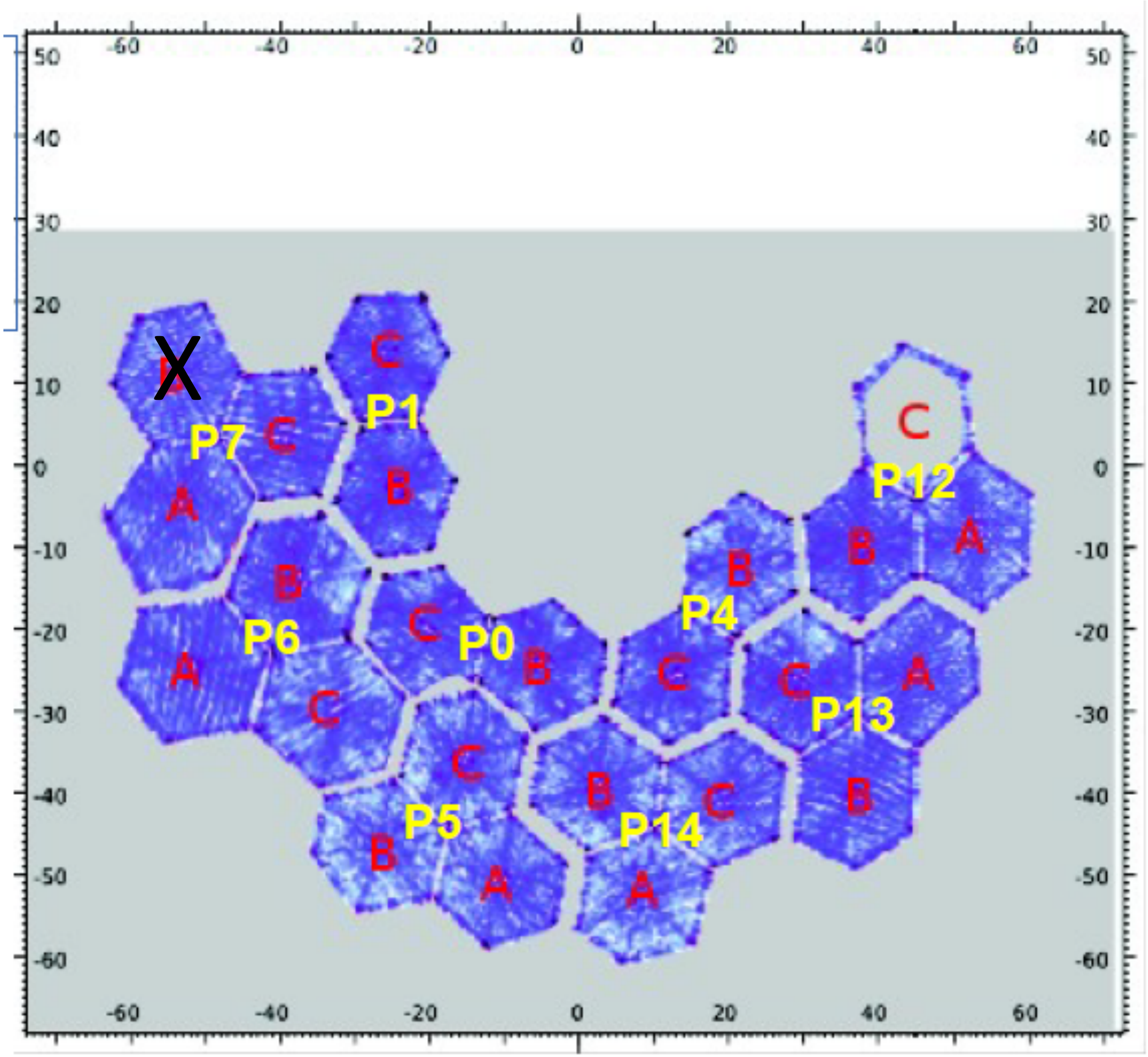

Z →Z+1 processes

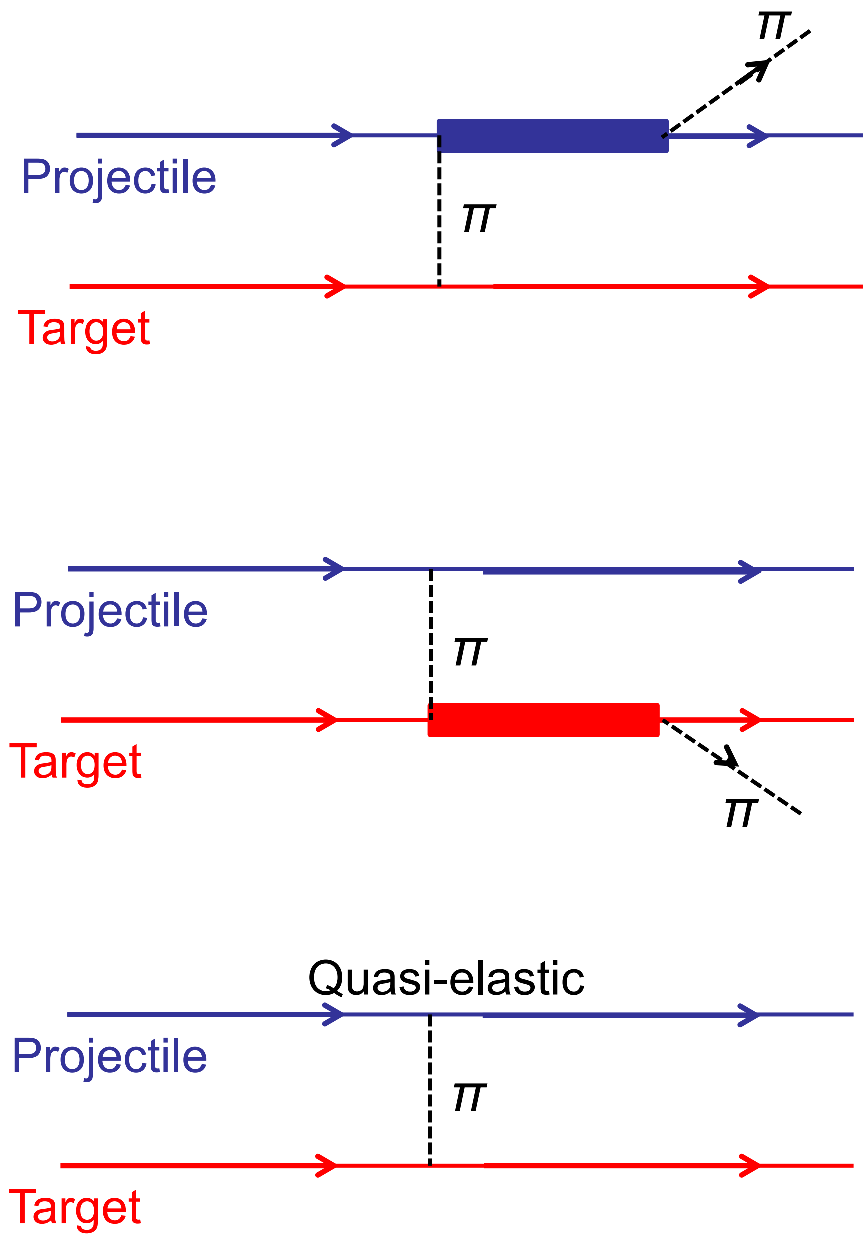

$(^A Z, {}^A(Z+1))$ reaction

Target excitation		Projectile excitation	
$p(n,p)\Delta^0 = p(n,p)n\pi^0$	$[2/3]$	$p(n,\Delta^0)p = p(n,p\pi^-)p$	$[-\sqrt{2}/3]$
$p(n,p)\Delta^0 = p(n,p)p\pi^-$	$[-\sqrt{2}/3]$	$p(n,\Delta^+)n = p(n,p\pi^0)n$	$[-2/3]$
$n(n,p)\Delta^- = n(n,p)n\pi^-$	$[-\sqrt{2}]$	$n(n,\Delta^0)n = n(n,p\pi^-)n$	$[\sqrt{2}/3]$
$p(n,p)P_{11}^0 = p(n,p)n\pi^0$	$[-2]$	$p(n,P_{11}^0)p = p(n,p\pi^-)p$	$[-\sqrt{2}]$
$p(n,p)P_{11}^0 = p(n,p)p\pi^-$	$[2\sqrt{2}]$	$p(n,P_{11}^+)n = p(n,p\pi^0)n$	$[2]$
		$n(n,P_{11}^0)n = n(n,p\pi^-)n$	$[\sqrt{2}]$

$(^A Z, {}^A(Z-1))$ reaction

Target excitation		Projectile excitation	
$p(p,n)\Delta^{++} = p(p,n)p\pi^+$	$[\sqrt{2}]$	$p(p,\Delta^+)p = p(p,n\pi^+)p$	$[-\sqrt{2}/3]$
$n(p,n)\Delta^+ = n(p,n)n\pi^+$	$[\sqrt{2}/3]$	$n(p,\Delta^+)n = n(p,n\pi^+)n$	$[\sqrt{2}/3]$
$n(p,n)\Delta^+ = n(p,n)p\pi^0$	$[-2/3]$	$n(p,\Delta^0)p = n(p,n\pi^0)p$	$[2/3]$
$n(p,n)P_{11}^+ = n(p,n)n\pi^+$	$[-2\sqrt{2}]$	$p(p,P_{11}^+)p = p(p,n\pi^+)p$	$[-\sqrt{2}]$
$n(p,n)P_{11}^+ = n(p,n)p\pi^0$	$[2]$	$n(p,P_{11}^+)n = n(p,n\pi^+)n$	$[\sqrt{2}]$
		$n(p,P_{11}^0)p = n(p,n\pi^0)p$	$[-2]$

I. Vidana et al., EPJ Web of Conferences 107, 10003 (2016)

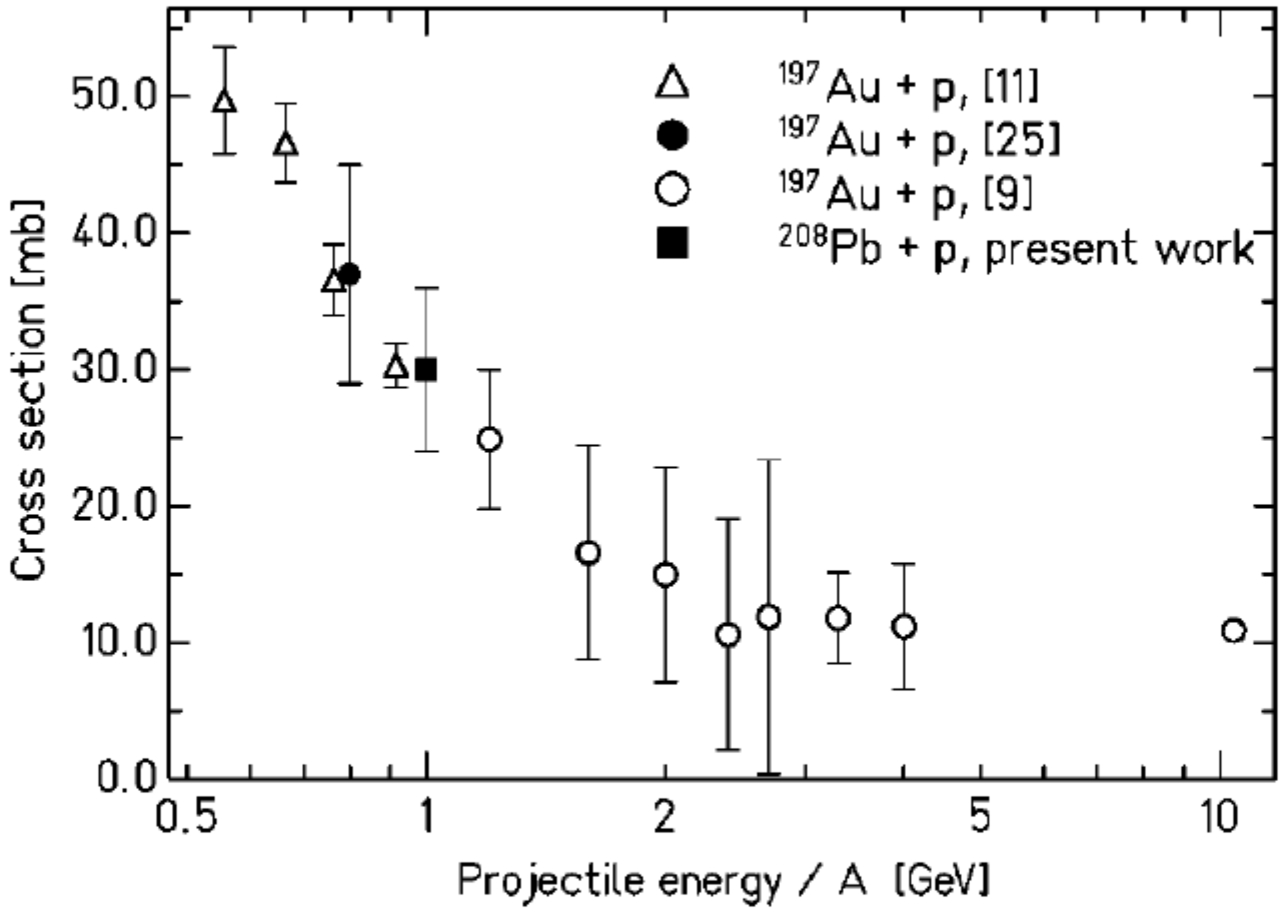

FIG. 8. Total charge-pickup cross section as a function of the projectile energy per nucleon: open triangles, ^{197}Au+^{1}H [11]; full dot, ^{197}Au+^{1}H [25]; full square, ^{208}Pb+^{1}H from the present work; and open dots, ^{197}Au+^{1}H [9]. The data from Refs. [9,11] were extracted from measurements performed with CH_2 and C targets.

Origins of the nuclear shell model

On the "Magic Numbers" in Nuclear Structure

OTTO HAXEL
Max Planck Institut, Göttingen
J. HANS D. JENSEN
Institut f. theor. Physik, Heidelberg
AND
HANS E. SUESS
Inst. f. phys. Chemie, Hamburg
April 18, 1949

A SIMPLE explanation of the "magic numbers" 14, 28, 50, 82, 126 follows at once from the oscillator model of the nucleus,[1] if one assumes that the spin-orbit coupling in the Yukawa field theory of nuclear forces leads to a strong splitting of a term with angular momentum l into two distinct terms $j=l\pm\frac{1}{2}$.

If, as a first approximation, one describes the field potential of the nucleons already present, acting on the last one added, as that due to an isotropic oscillator, then the energy levels are characterized by a single quantum number $r=r_1+r_2+r_3$, where r_1, r_2, r_3 are the quantum numbers of the oscillator in 3 orthogonal directions. Table I, column 2 shows the multiplicity of a term with a given value of r, column 3 the sum of all multiplicities up to and including r. Isotropic anharmonicity of the potential field leads to a splitting of each r-term according to the orbital angular momenta l (l even when r is odd, and vice versa), as in Table I, column 4. Finally, spin-orbit coupling leads to the l-term splitting into $j=l\pm\frac{1}{2}$, columns 5 and 6, whose multiplicities are listed in column 7.

The "magic numbers" (column 8) follow at once on the assumption of a particularly marked splitting of the term with the highest angular momentum, resulting in a "closed shell structure" for each completed r-group, together with the highest j-term of the next succeeding r-group. This classification of states is in good agreement with the spins and magnetic moments of the nuclei with odd mass number, so far as they are known at present. The anharmonic oscillator model seems to us preferable to the potential well model,[2] since the range of the nuclear forces is not notably smaller than the nuclear radius.

A more detailed account will appear in three communications to Naturwissenschaften.[3]

TABLE I. Classification of nuclear states.

1 Oscillator-quantum number r	2 Multiplicity	3 Sum of all multiplicities	4 Orbital momentum l	5 Total angular momentum j	6 l_j-symbol	7 Multiplicities	8 Magic numbers
1	2	2	0	1/2	$s_{1/2}$	2	
2			1	3/2	$p_{3/2}$	4	
	6	8		1/2	$p_{1/2}$	2	
3			2	5/2	$d_{5/2}$	6	14
				3/2	$d_{3/2}$	4	
	12	20	0	1/2	$s_{1/2}$	2	
4			3	7/2	$f_{7/2}$	8	28
				5/2	$f_{5/2}$	6	
			1	3/2	$p_{3/2}$	4	
	20	40		1/2	$p_{1/2}$	2	
5			4	9/2	$g_{9/2}$	10	50
				7/2	$g_{7/2}$	8	
			2	5/2	$d_{5/2}$	6	
				3/2	$d_{3/2}$	4	
	30	70	0	1/2	$s_{1/2}$	2	
6			5	11/2	$h_{11/2}$	12	82
				9/2	$h_{9/2}$	10	
			3	7/2	$f_{7/2}$	8	
				5/2	$f_{5/2}$	6	
			1	3/2	$p_{3/2}$	4	
	42	112		1/2	$p_{1/2}$	2	
7			6	13/2	$i_{13/2}$	14	126
				11/2	$i_{11/2}$	12	
			4	9/2	$g_{9/2}$	10	

[1] See, e.g., H. A. Bethe and R. Bacher, Rev. Mod. Phys. 8, 82 (1937), pars. 32–34.
[2] Which anyhow does not lead to a very different term-sequence compared with that of an anharmonic oscillator, see reference 1.
[3] (a) Haxel, Jensen, and Suess, Naturwiss. (in press). (b) Suess, Haxel, and Jensen, Naturwiss. (in press). (c) Jensen, Suess, and Haxel, Naturwiss. (in press).

Phys. Rev. 75, 1766 (1949)
(also M. Goeppert-Mayer and others)

Example of modern shell model (Zr isotopes)

Proton orbit	Magic number	Neutron orbit
		$1f_{7/2}, 2p_{3/2}$
	82	
		$0h_{11/2}$
$0g_{7/2}, 1d_{5/2,3/2}, 2s_{1/2}$		$0g_{7/2}, 1d_{5/2,3/2}, 2s_{1/2}$
	50	
$0g_{9/2}$		$0g_{9/2}$
$0f_{5/2}, 1p_{3/2,1/2}$		

MCSM

Protons: 28->70
Neutrons: 40->94

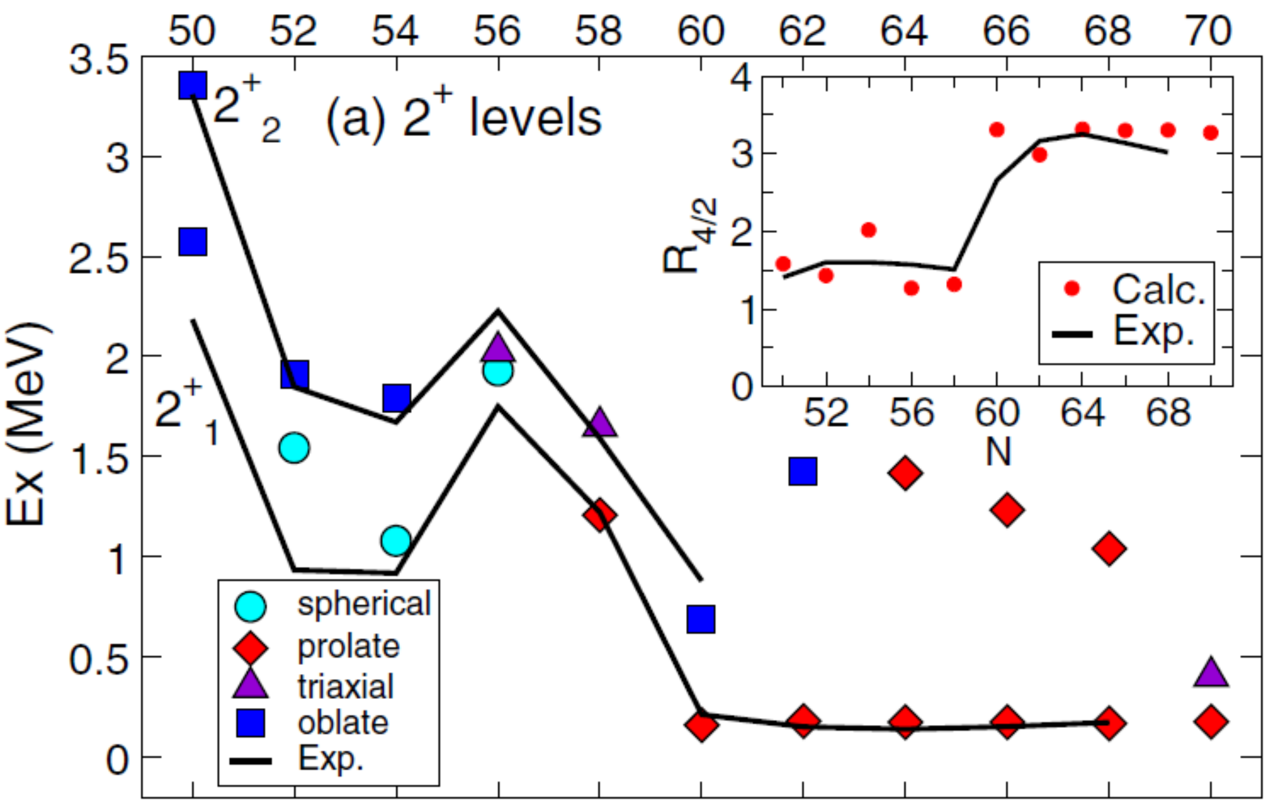

T. Togashi, Y. Tsunoda, T. Otsuka, N. Shimizu, PRL 117, 172502 (2016)

Lifetime measurements

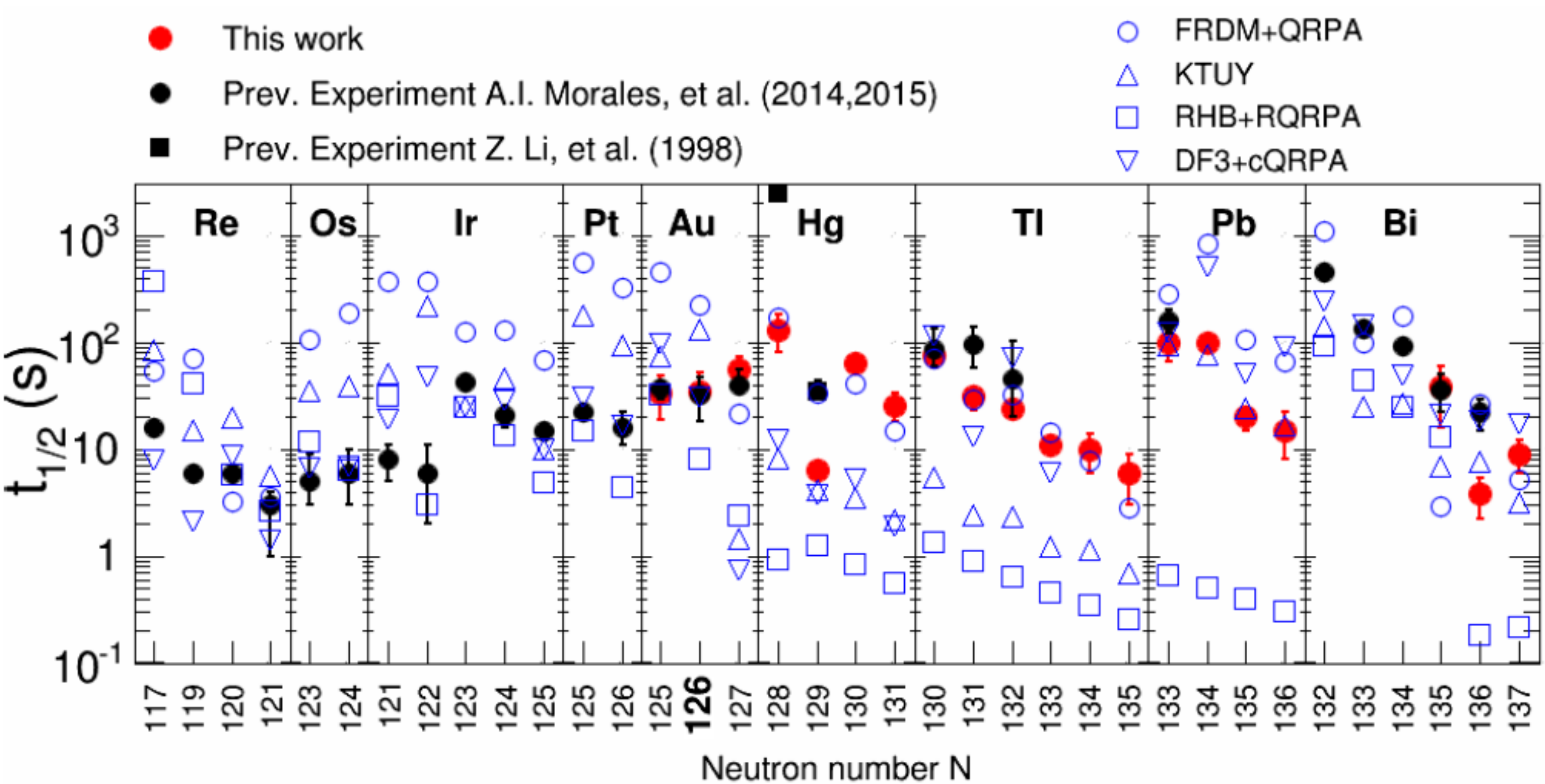

=> For N>126 and Z<82: $t_{1/2}$ (exp) > $t_{1/2}$(theory)

R. Caballero-Folch et al., arXiv:1511.01296

Fragmentation (spallation) reactions at relativistic energies

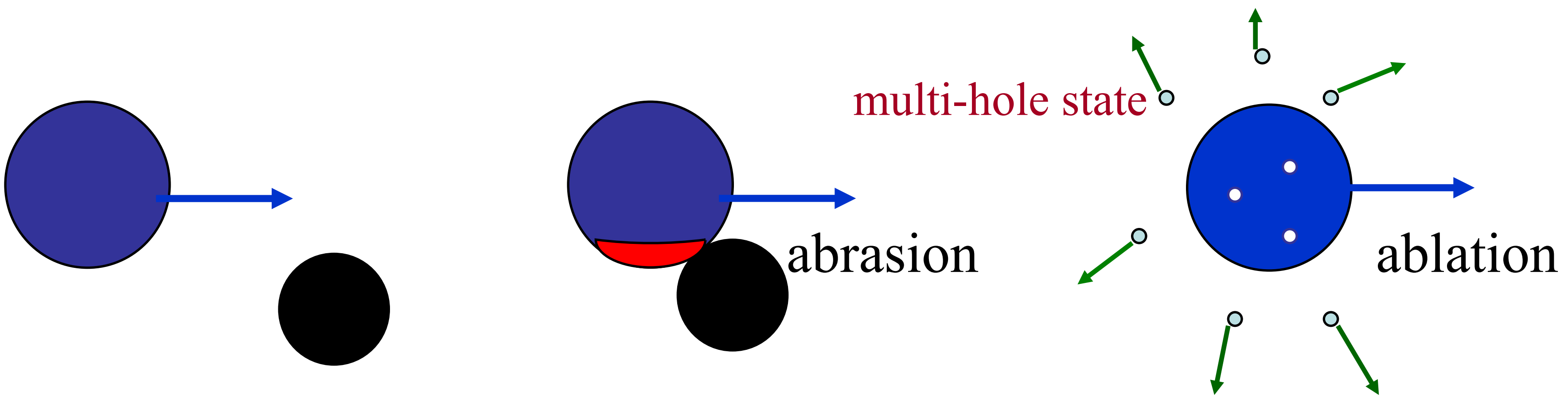

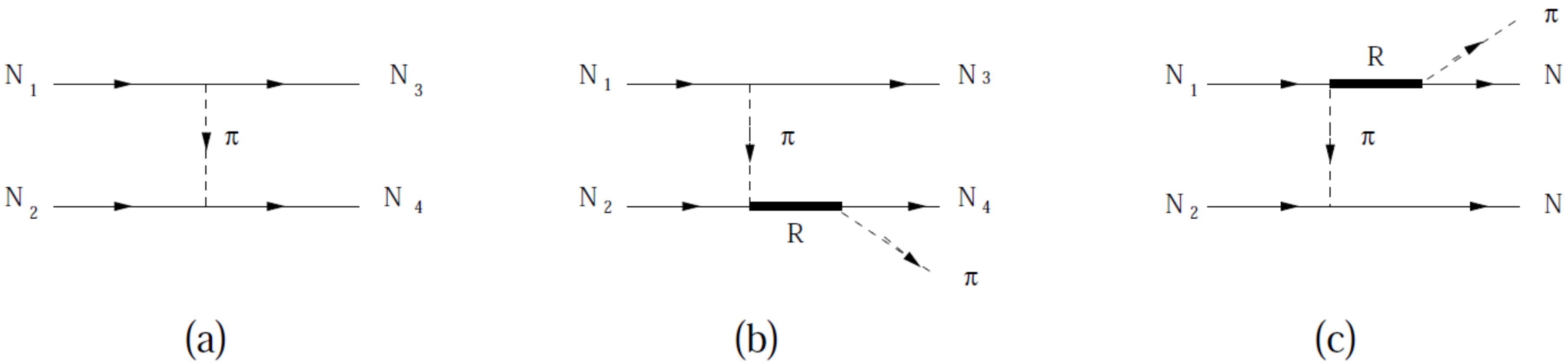

Figure 1. Quasi-elastic (a) and inelastic (b and c) elementary processes contributing to the $({}^{A}Z, {}^{A}(Z \pm 1))$ reaction considered in this model. The resonance R can be either a $\Delta(1232)$ or a $N^*(1440)$.

EPJ Web of Conferences **107**, 10003 (2016)
DOI: 10.1051/epjconf/201610710003

I. Vidana et al., EPJ Web of Conference

Excitation of Δ and N^* resonances in isobaric charge-exchange reactions of heavy nuclei

I. Vidaña[1,a], J. Benlliure[2], H. Geissel[3], H. Lenske[4], C. Scheidenberger[3], and J. Vargas[2]

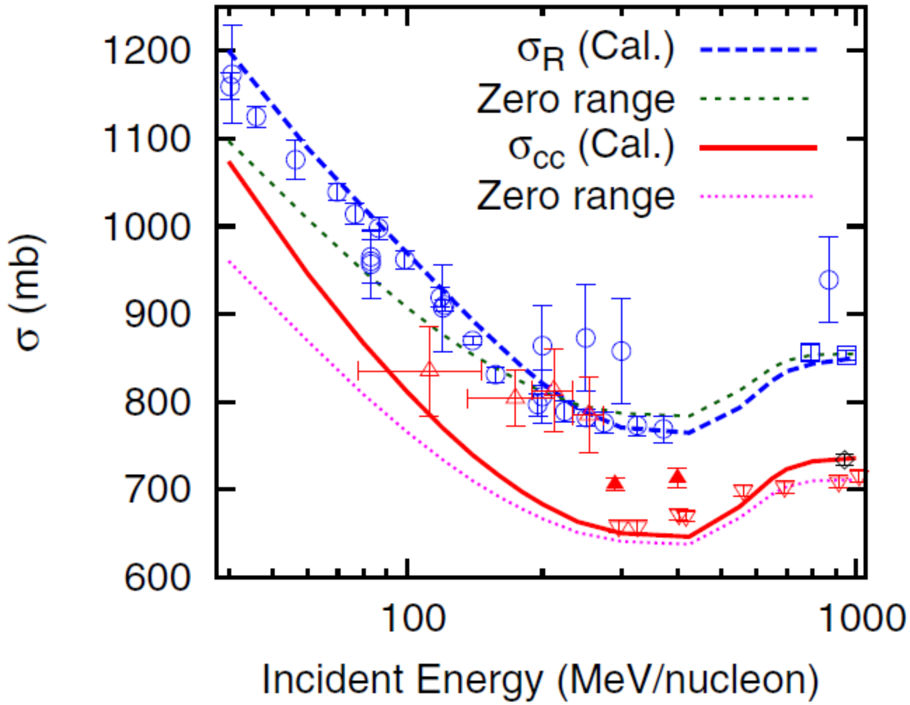

FIG. 1. Total reaction (or interaction) and charge-changing cross sections of ^{12}C on a ^{12}C target as a function of incident energy. Calculations are performed with the HO densities that give $r_p = r_n = 2.326$ fm. Results with the zero-range profile functions are also drawn for comparison. References for the experimental data on σ_R (open circle) and σ_I (open rectangle) are quoted in Ref. [24]. The σ_{cc} data are taken from Ref. [8] for diamond, Ref. [25] for inverted triangle, Ref. [26] for closed triangle, and Ref. [27] for open triangle.

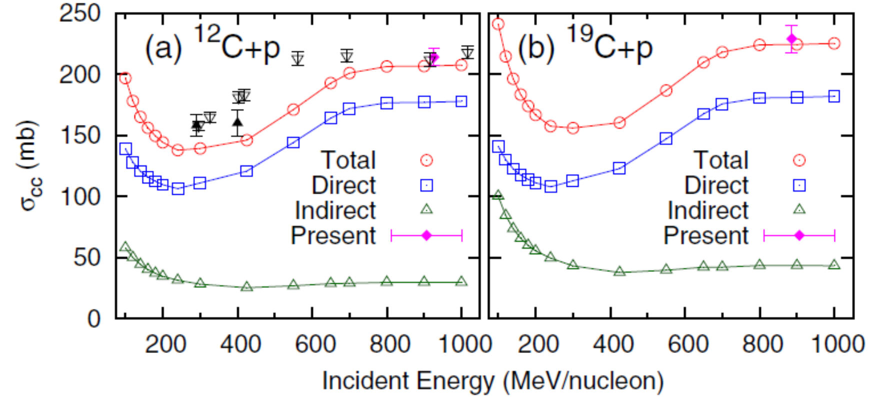

FIG. 3. Energy dependence of charge-changing cross sections of (a) ^{12}C and (b) ^{19}C on a proton target. The data are taken from Ref. [25] for open inverted triangles and from Ref. [26] for closed triangles.

PHYSICAL REVIEW C **94**, 011602(R) (2016)

Parameter-free calculation of charge-changing cross sections at high energy

Y. Suzuki,[1,2] W. Horiuchi,[3] S. Terashima,[4] R. Kanungo,[5] F. Ameil,[6] J. Atkinson,[7] Y. Ayyad,[7] D. Cortina-Gil,[8] I. Dillmann,[6]

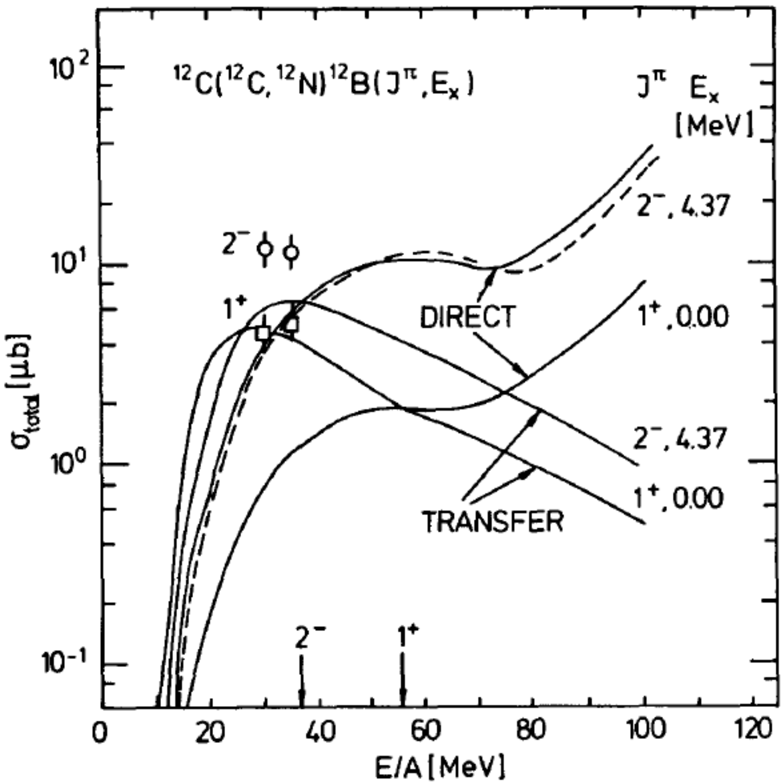

Fig.6: One-step direct and two-step transfer charge exchange cross sections for $^{12}C(^{12}C,^{12}N)^{12}B$ as a function of incident energy per nucleon. For $^{12}B(2^-)$ also the central-plus-tensor direct result (dashed) is shown.

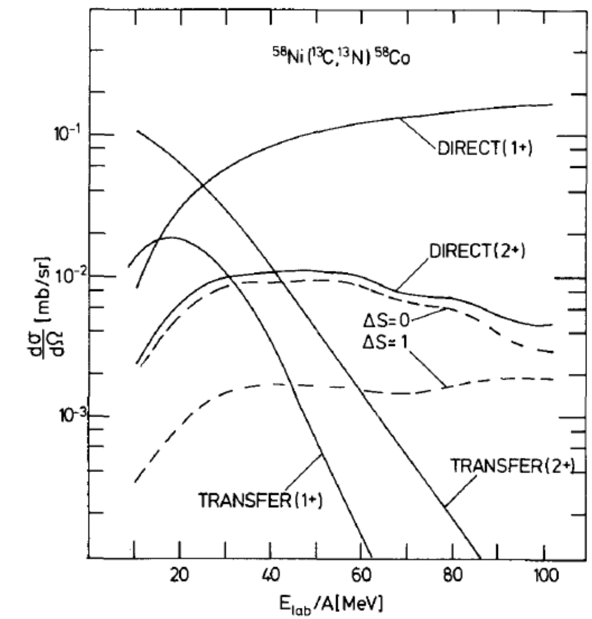

Fig.7: One-step direct and two-step transfer charge exchange cross sections for $^{58}Ni(^{13}C,^{13}N)^{58}Co$ as a function of incident energy per nucleon. Results for $^{58}Co(2^+,g.s.)$ and $^{58}Co(1^+,1.86MeV)$ are shown. For the ground state reaction the non-spinflip ΔS=0 and spinflip ΔS=1 partial cross sections are displayed.

Nuclear Physics A482 (1988) 343c–356c
North-Holland, Amsterdam

THEORY OF HEAVY ION CHARGE EXCHANGE SCATTERING AT LOW AND INTERMEDIATE ENERGIES

H. LENSKE *

^{207,208}Hg beams from molten-lead target at ISOLDE

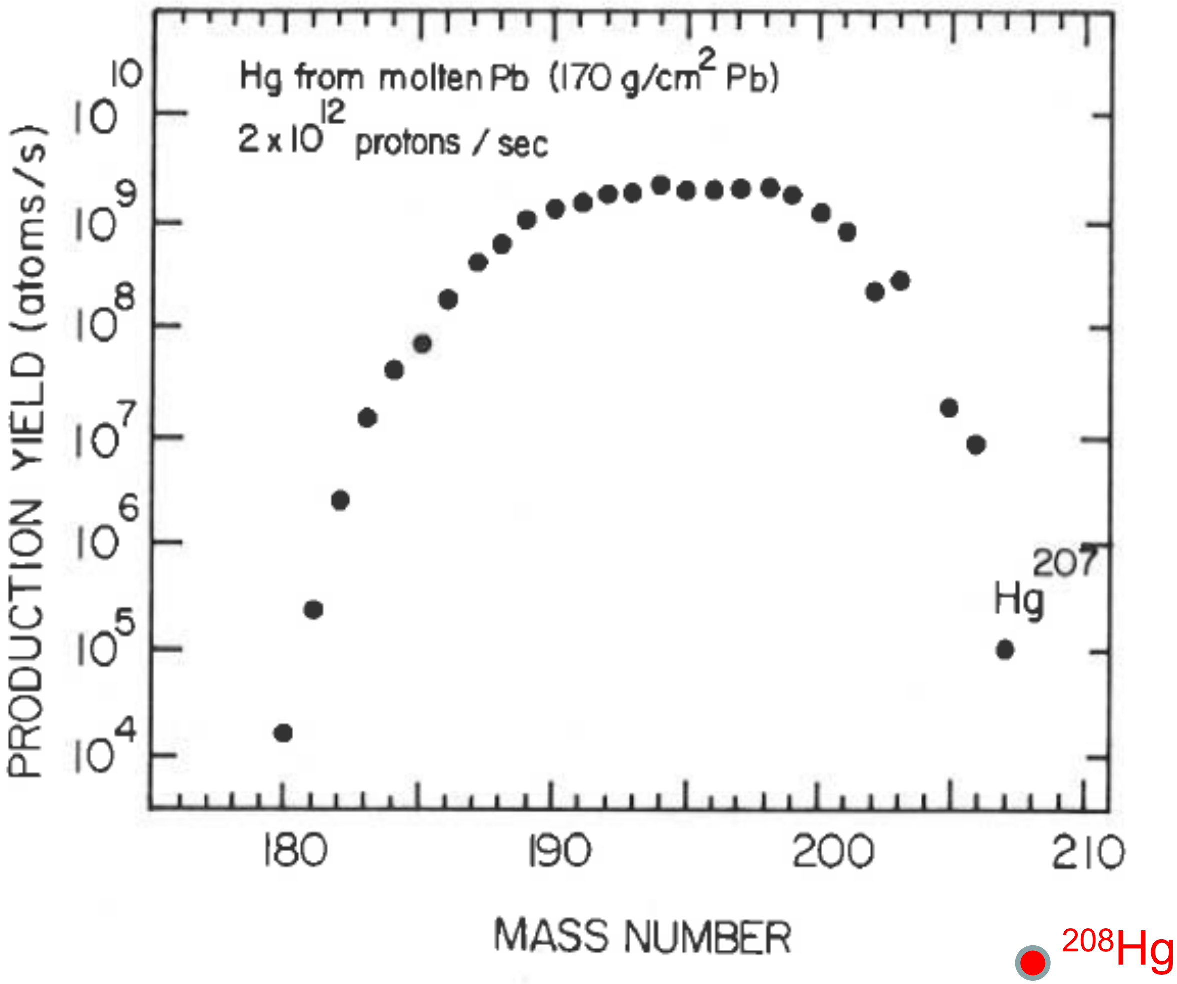

Fig. 1 Production yield in the ISOLDE facility of the mercury isotopes, including ^{206}Hg and ^{207}Hg.

$^{208}Pb(n,2p)^{207}Hg_{127}$?
or/and
$^{208}Pb(,\pi^+ p)^{207}Hg_{127}$?
($p \rightarrow \Delta^+ \rightarrow n + \pi^+$)

$^{208}Pb(t,3p)^{208}Hg_{128}$?
or/and
$^{208}Pb(\alpha,4p)^{208}Hg_{128}$?
or/and
$^{208}Pb(n,\pi^+ p)^{208}Hg_{128}$?
or/and
$^{208}Pb(,\pi^+ \pi^+)^{208}Hg_{128}$?

B. Jonson, O.B. Nielsen, J. Zylicz, CERN-81-09 (1981)
(Proc. Int. Conf. Nuclei far from stability, Helsingor, Denmark. Vol.2 p.640 (1981))

International Conference on Nuclear Data for Science and Technology 2007
DOI: 10.1051/ndata:07762

Volatile elements production rates in a proton-irradiated molten lead-bismuth target

at ISOLDE

Y. Tall[1,a], S. Cormon[1], M. Fallot[1], Y. Foucher[1], A. Guertin[1], T. Kirchner[1], L. Zanini[2], M. Andersson[2], K. Berg[2,3], H. Frånberg[2,3], F. Gröschel[2], E. Manfrin[2], W. Wagner[2], M. Wohlmuther[2], P. Everaerts[3], U. Köster[3,4], H. Ravn[3], E. Noah Messomo[3], C. Jost[5], and Y. Kojima[6]

Interestingly also significant yields of $^{204-210}$At isotopes were observed. At isotopes are produced either by (p, $\pi^- x$n) charge exchange reactions on ^{209}Bi or by secondary reactions involving ^{3}He and ^{4}He. Despite the non-release of

alpha, ^{3}He and pions. These light particles play a major role in the production of astatine isotopes [11]. The dominating direct reactions are ^{209}Bi(p,$\pi^- x$n)$^{210-x}$At. However, for a thick target as used in this experiment, secondary reactions must be taken into account:

$n \to \Delta^0 \to p + \pi^-$

- ^{209}Bi(^{3}He,xn)$^{212-x}$At induced by spallation-produced ^{3}He,
- ^{209}Bi(^{4}He,xn)$^{213-x}$At induced by spallation-produced ^{4}He.

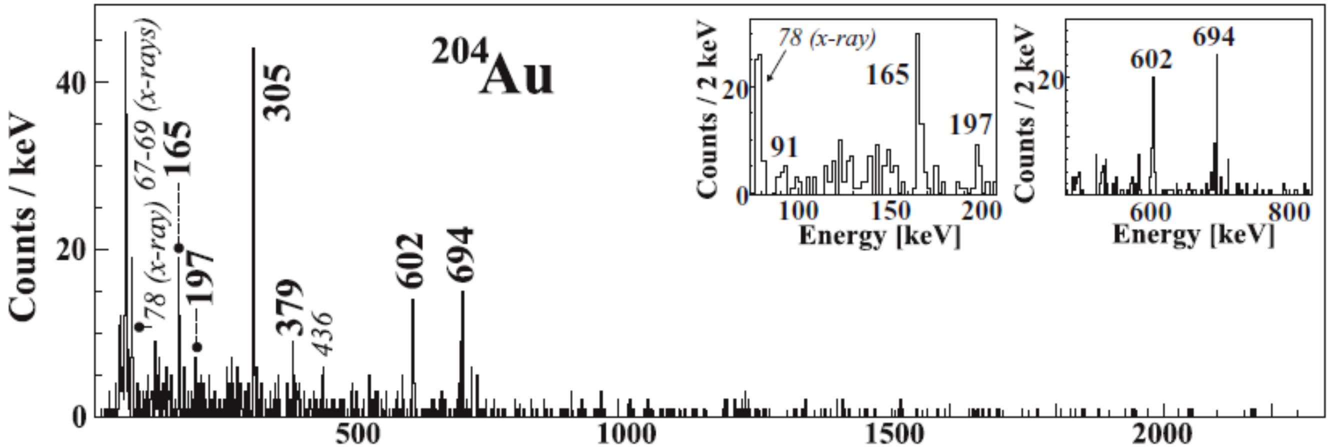

Energy spectrum from

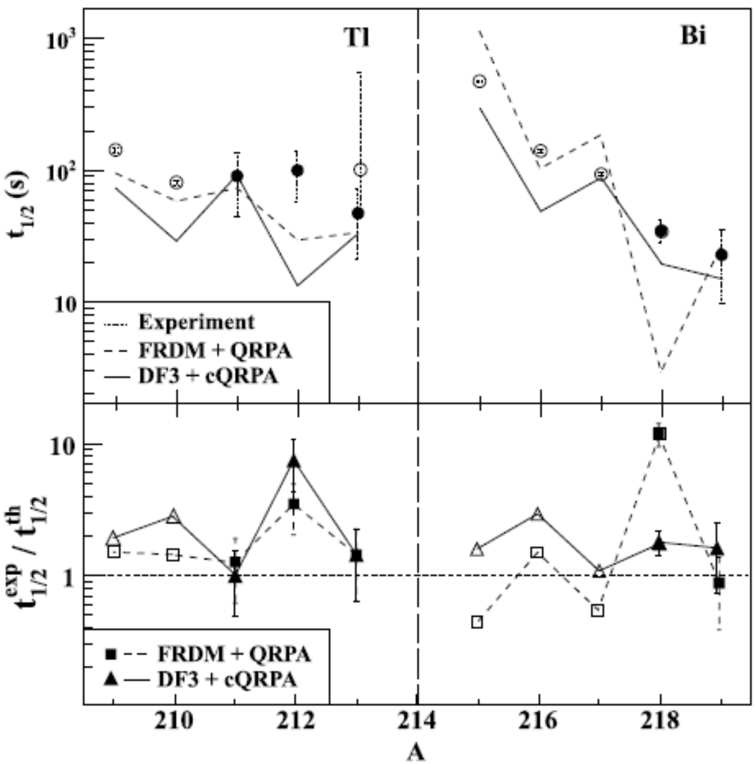

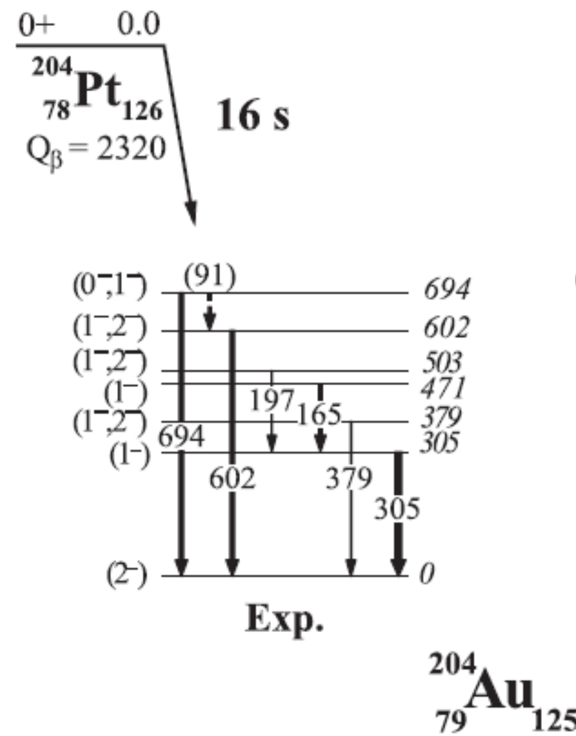

A.I. Morales et al., Phys. Rev. C 88, 014319 (2013)

G. Benzoni et al., Phys. Lett. B 715, 293 (2012)

=> Importance of first-forbidden beta decay

Shell model space

Allowed GT:
νh9/2 -> π h11/2

First-forbidden:
νp1/2->πd3/2
νi13/2 -> π h11/2

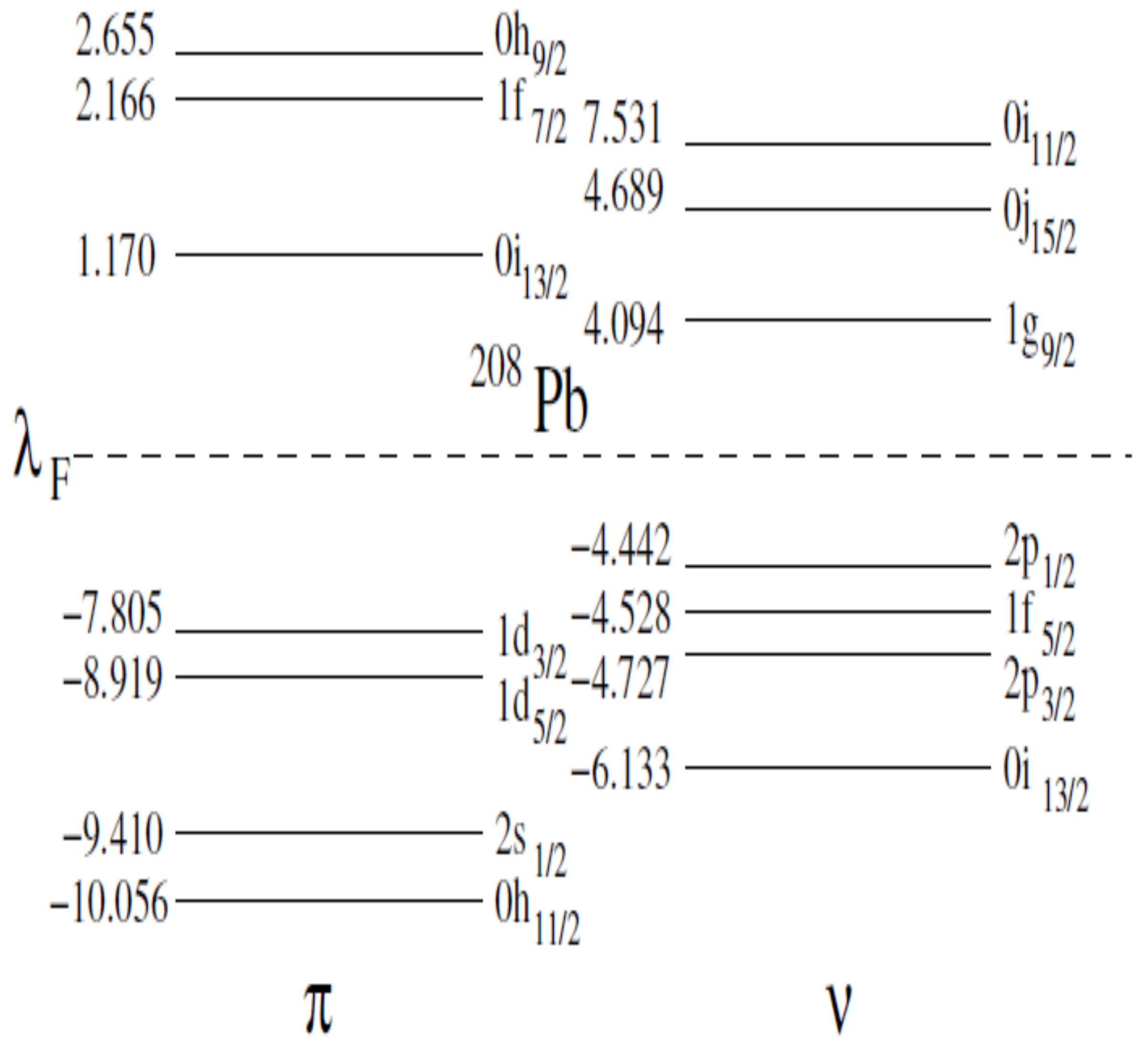

^{208}Pb+^{208}Pb deep-inelastic reaction (thick target experiment)

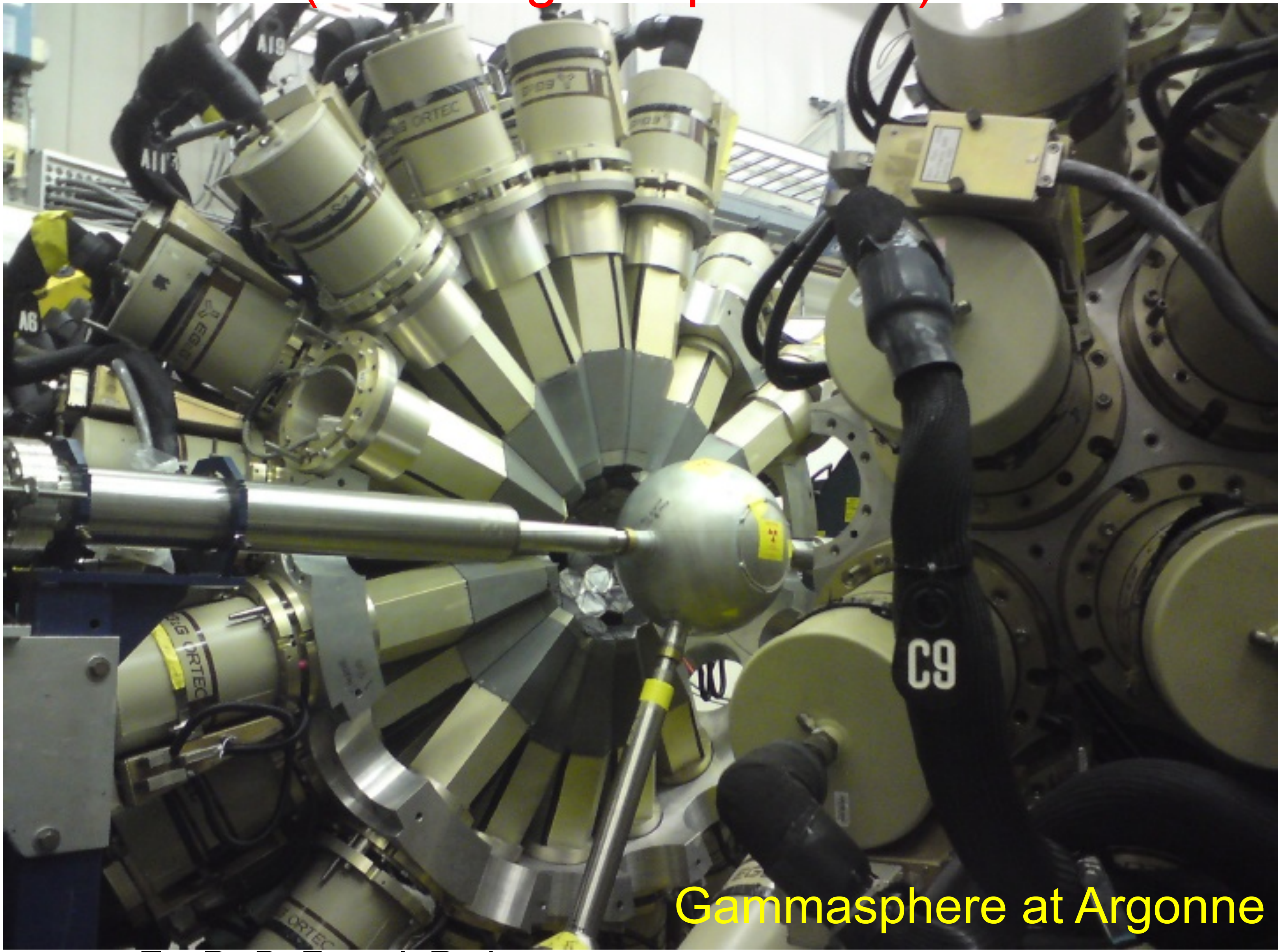

Spokespersons: Zs. P., B. Fornal. R. Janssens

Collective octupole phonons around 208Pb

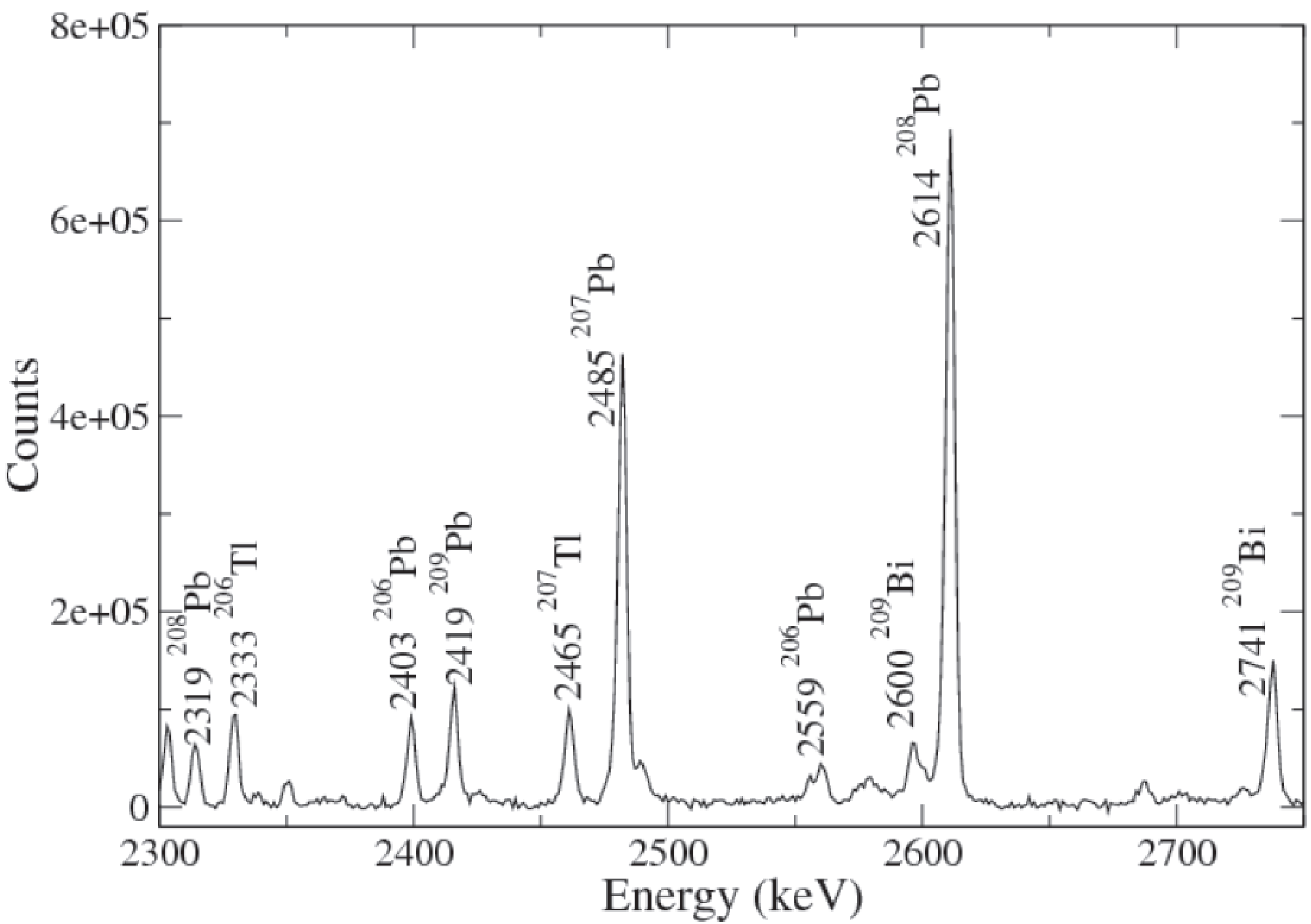

Spin-parities from: decay pattern, intensity balance, angular correlations, angular distributions

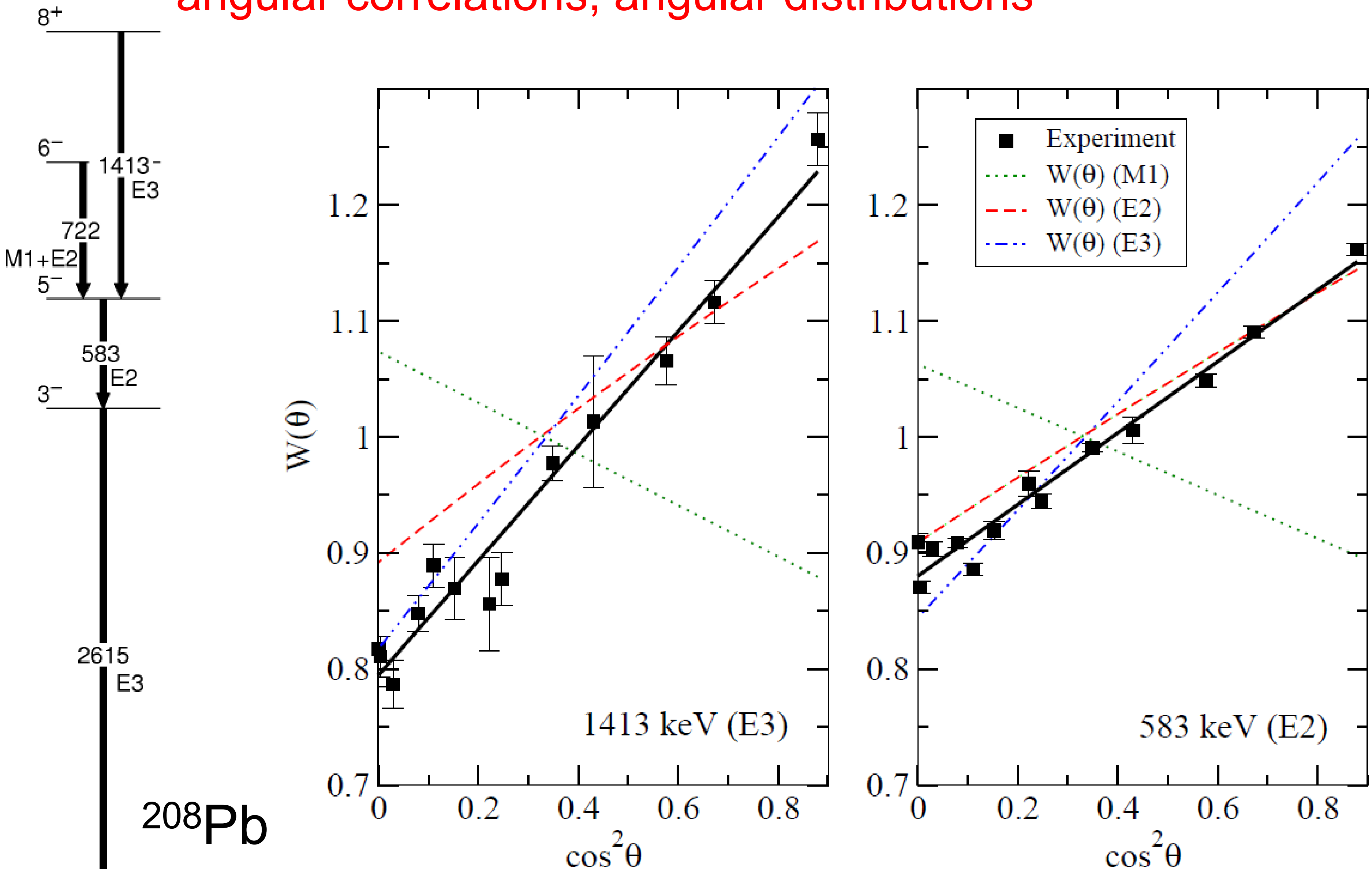

FIGURE 6.9: Angular correlations between the 2614 keV E3 transition and the 1413

^{207}Tl
(Z=81, N=126)

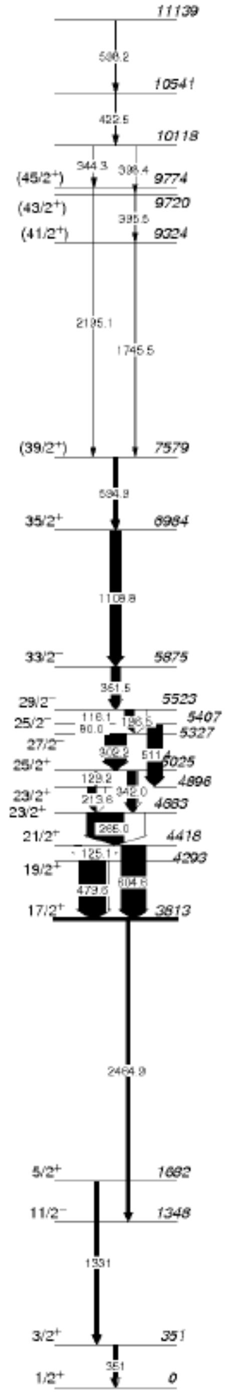

Five-particle states
(uncertain)

Three-particle states
All breaking the
neutron-core

Octupole state

$\pi h^{-1}_{11/2}$

Single particle states

E. Wilson et al., to be published

^{207}Pb

Three-particle states

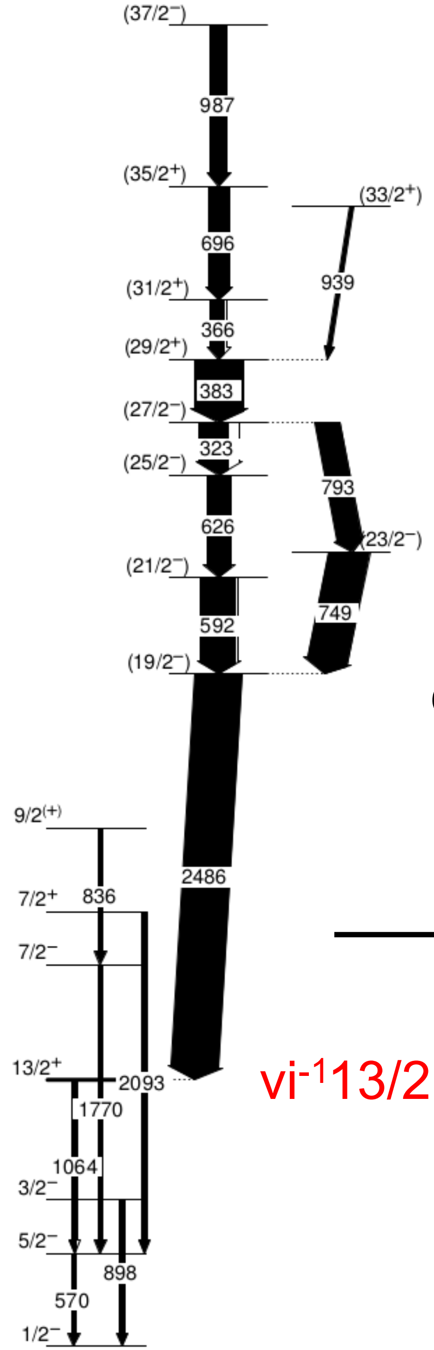

Octupole state

E3 from ang. distrib.

vi^{-1}13/2

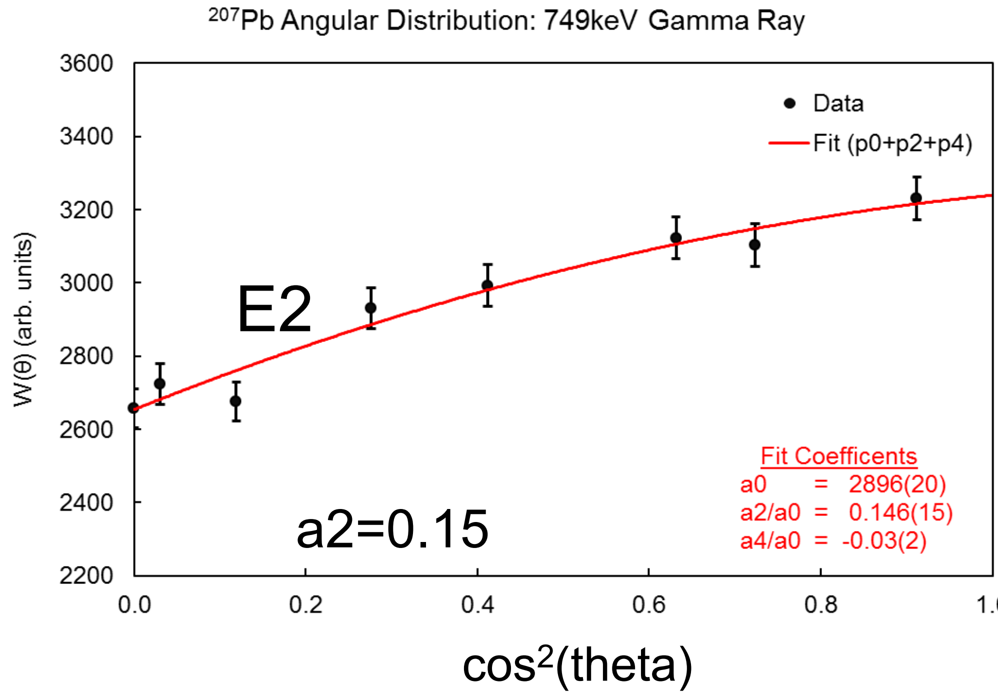

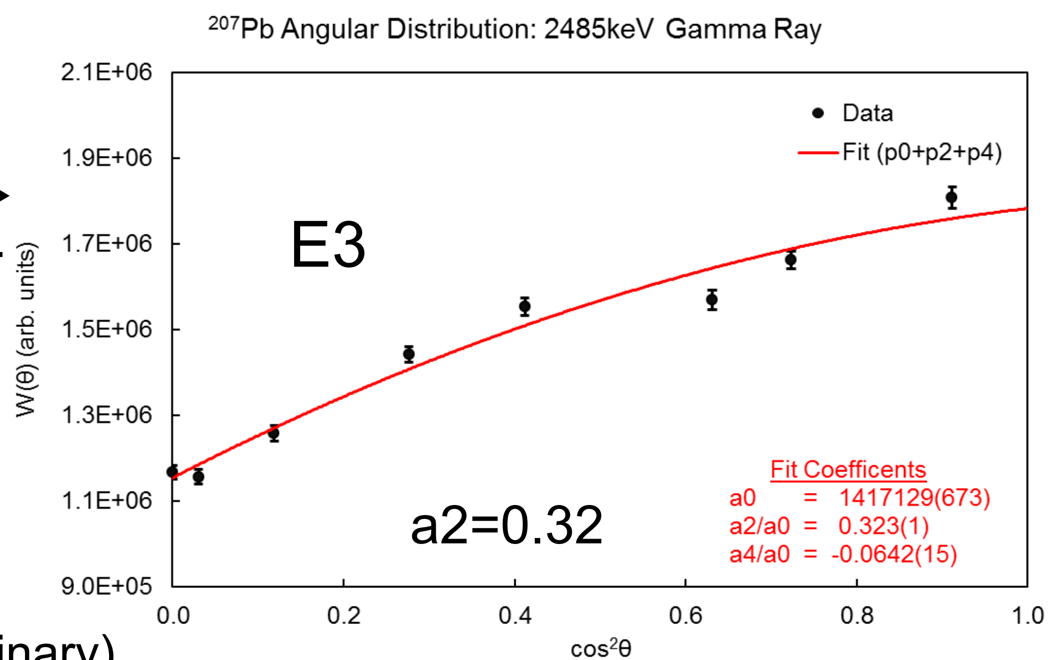

C. Shand et al. (preliminary)

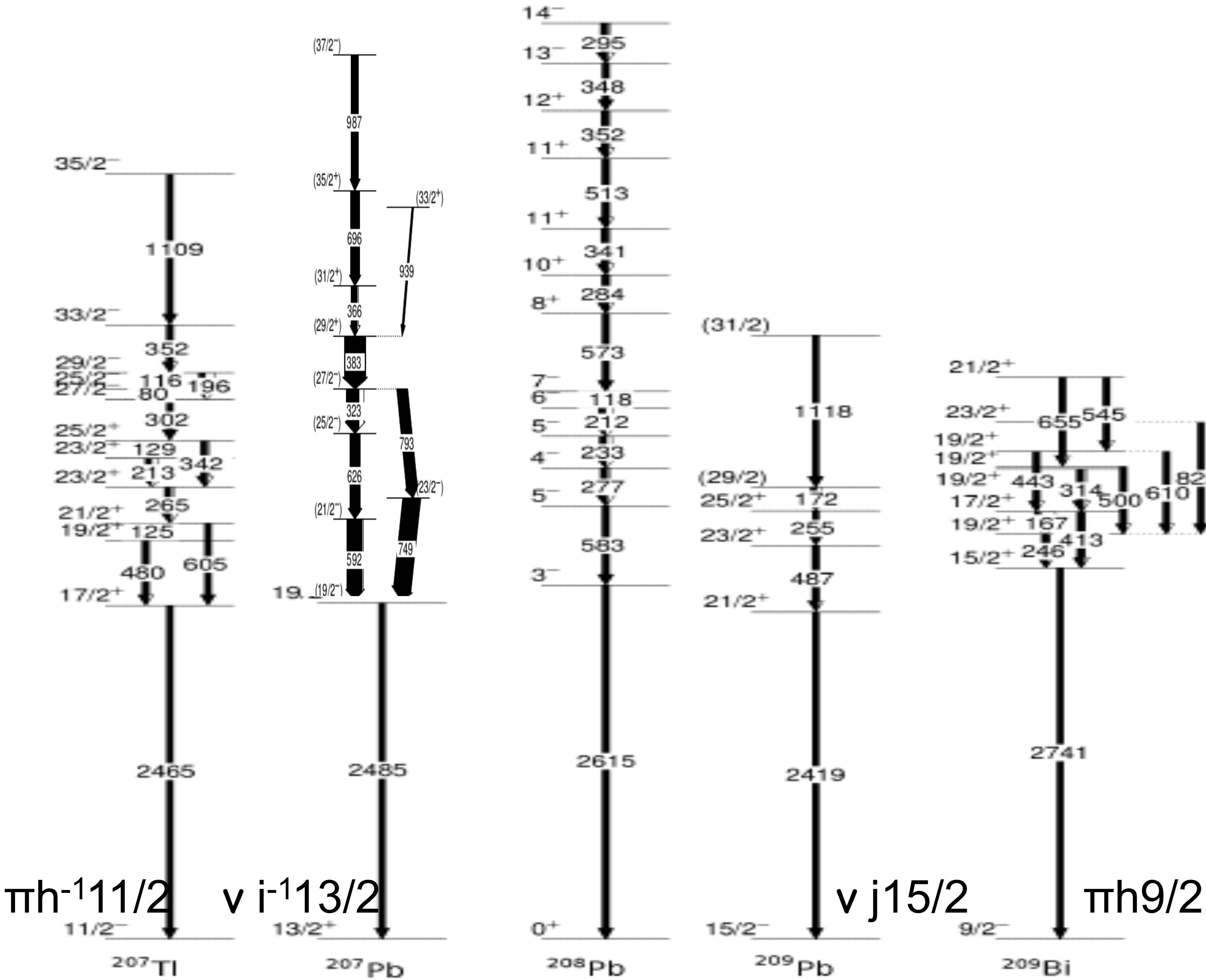

πh-1 11/2
ν i-1 13/2
ν j15/2
πh9/2
207Tl
207Pb
208Pb
209Pb
209Bi
35/2−
33/2−
29/2−
25/2−
27/2−
25/2+
23/2+
21/2+
19/2+
17/2+
11/2−
1109
352
116
196
80
302
129
213
342
265
125
480
605
2465
(37/2−)
(35/2+)
(33/2+)
(31/2+)
(29/2+)
(27/2−)
(25/2−)
(23/2−)
(21/2−)
(19/2−)
13/2+
987
696
939
366
383
323
793
626
592
749
2485
14−
13−
12+
11+
10+
8+
7−
6−
5−
4−
3−
0+
295
348
352
513
341
284
573
118
212
233
277
583
2615
(31/2)
(29/2)
15/2−
1118
172
255
487
2419
21/2+
19/2+
17/2+
15/2+
9/2−
655
545
443
314
500
610
825
167
413
246
2741

$^{208}Tl_{127}$: proton-neutron interaction

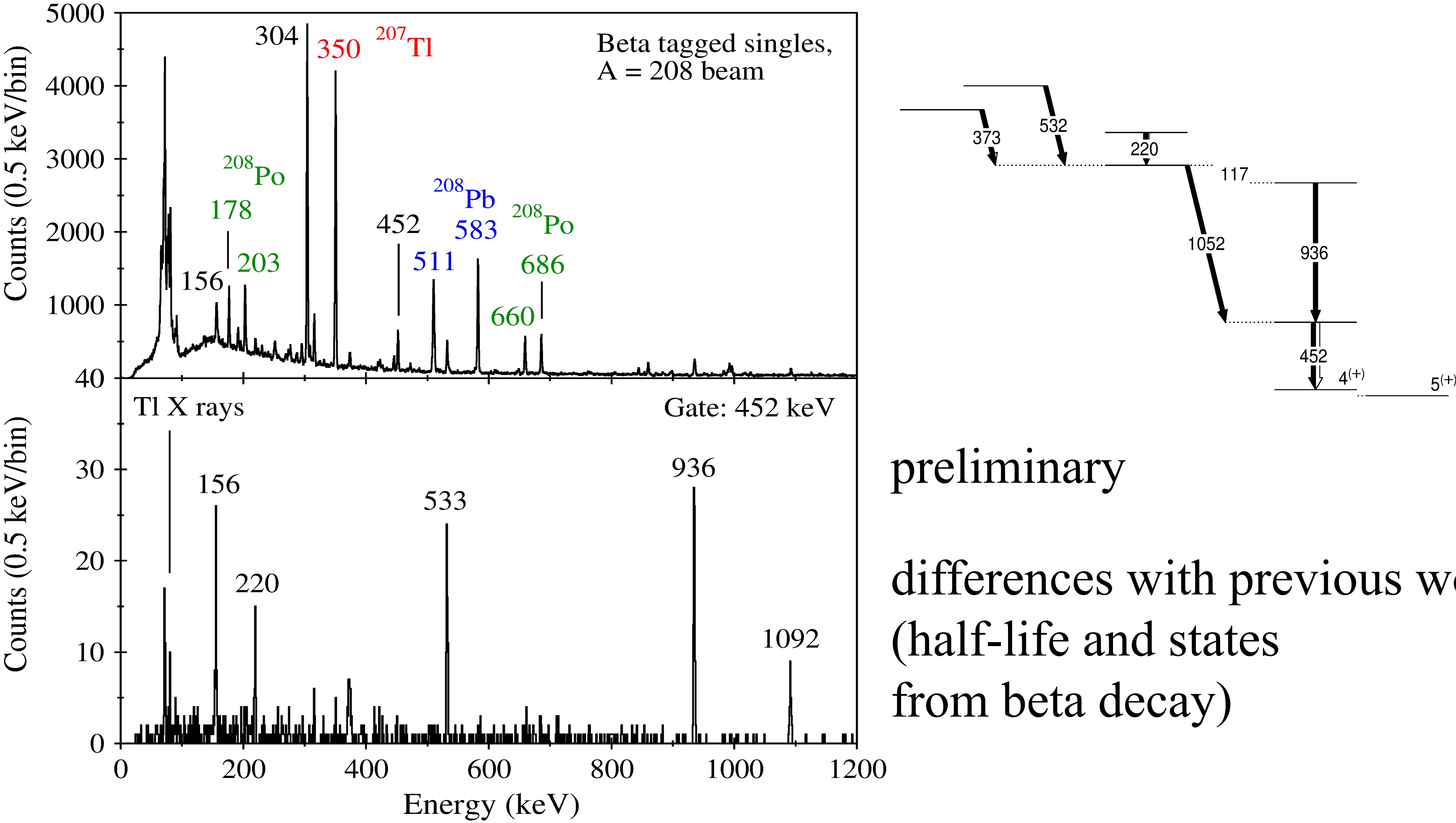

preliminary

differences with previous work (half-life and states from beta decay)

How was ^{208}Hg produced in p+Pb?

ISOLDE exp. 2014, 2016

R. Carroll et al., to be published

^{207,208}Hg beams at ISOLDE

Hg yields from molten Pb targets at ISOLDE

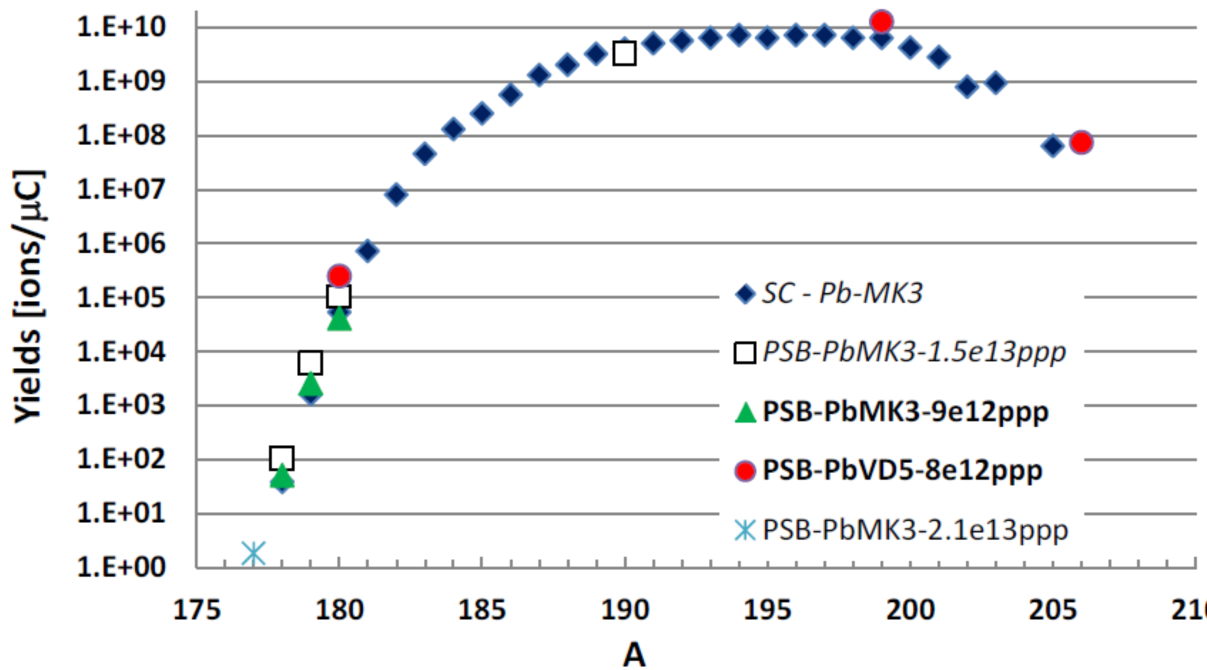

T. Stora, EURISOL town meeting, Oct. 2012

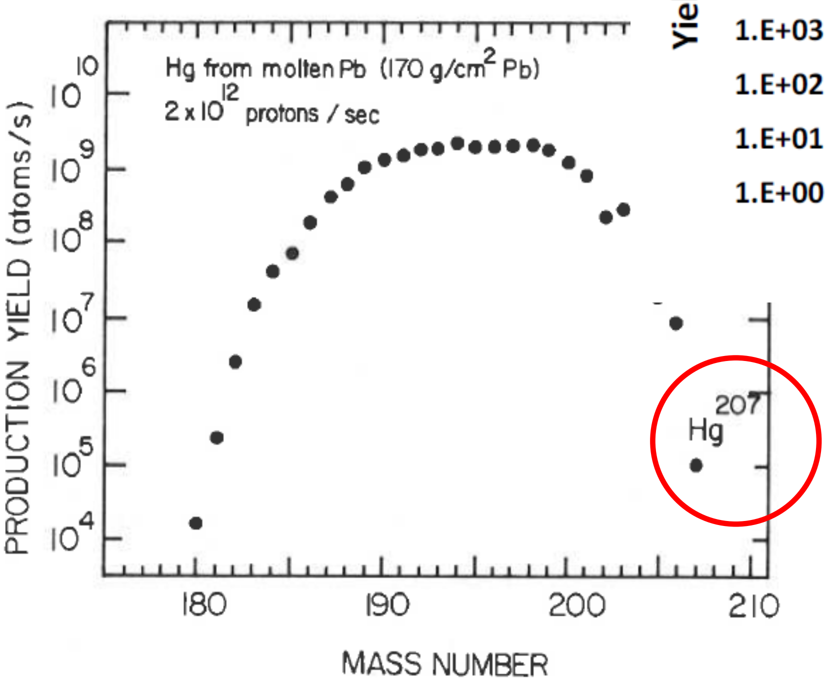

Fig. 1 Production yield in the ISOLDE facility of the mercury isotopes, including ^{206}Hg and ^{207}Hg.

B. Jonson, O.B. Nielsen, J. Zylicz, CERN-81-09 (1981)
(Proc. Int. Conf. Nuclei far from stability, Helsingor, Denmark. Vol.2 p.640 (1981))

^{208}Hg from ^{208}Pb target?

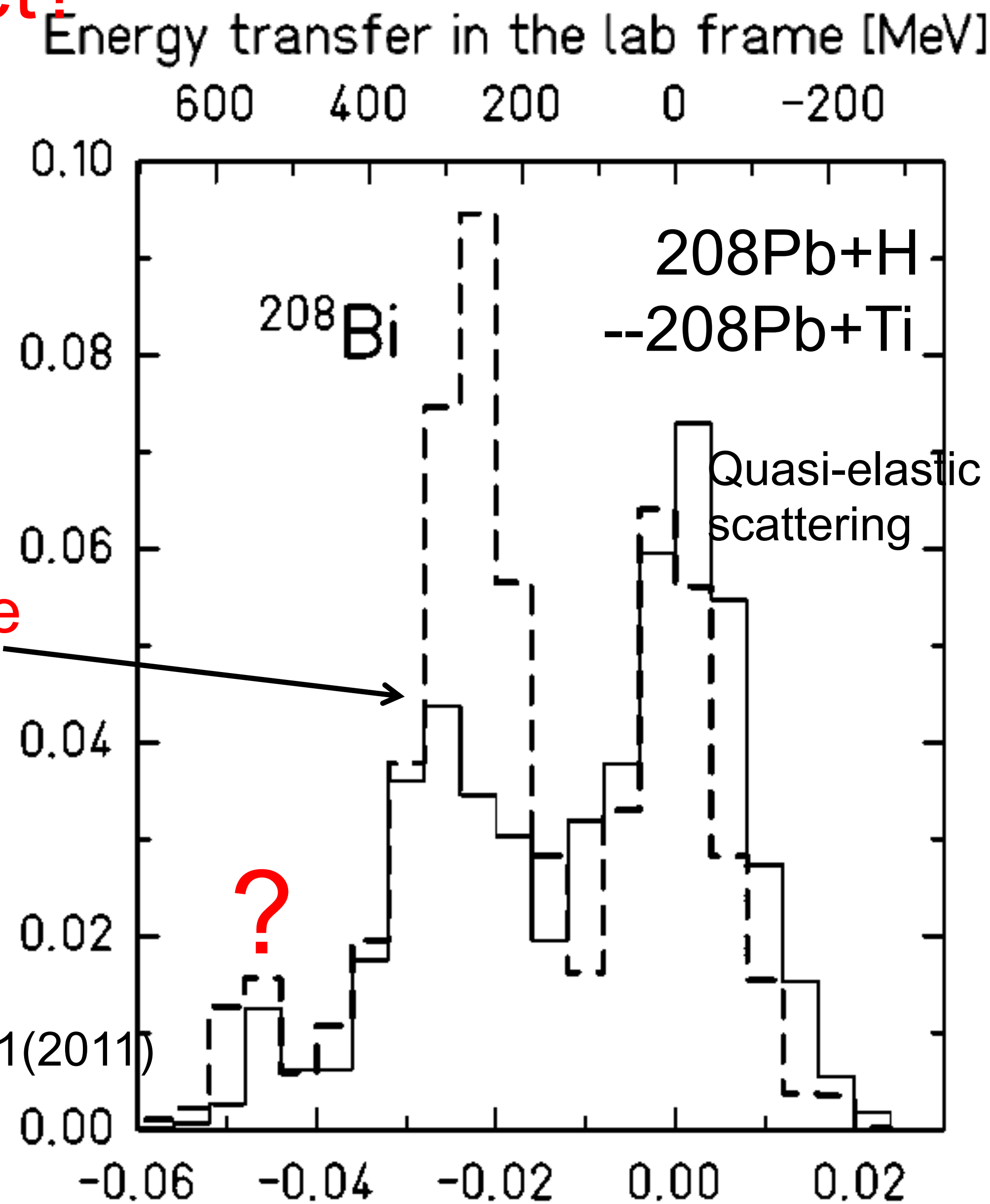

A. Kelic et al., Phys. Rev. C 70, 064608 (2004)

207Hg cross section measured in 208Pb+9Be (from Δ resonance)
A. Morales et al., Phys. Rev. C 84, 011601(2011)

^{206}Hg
(Z=80, N=126)

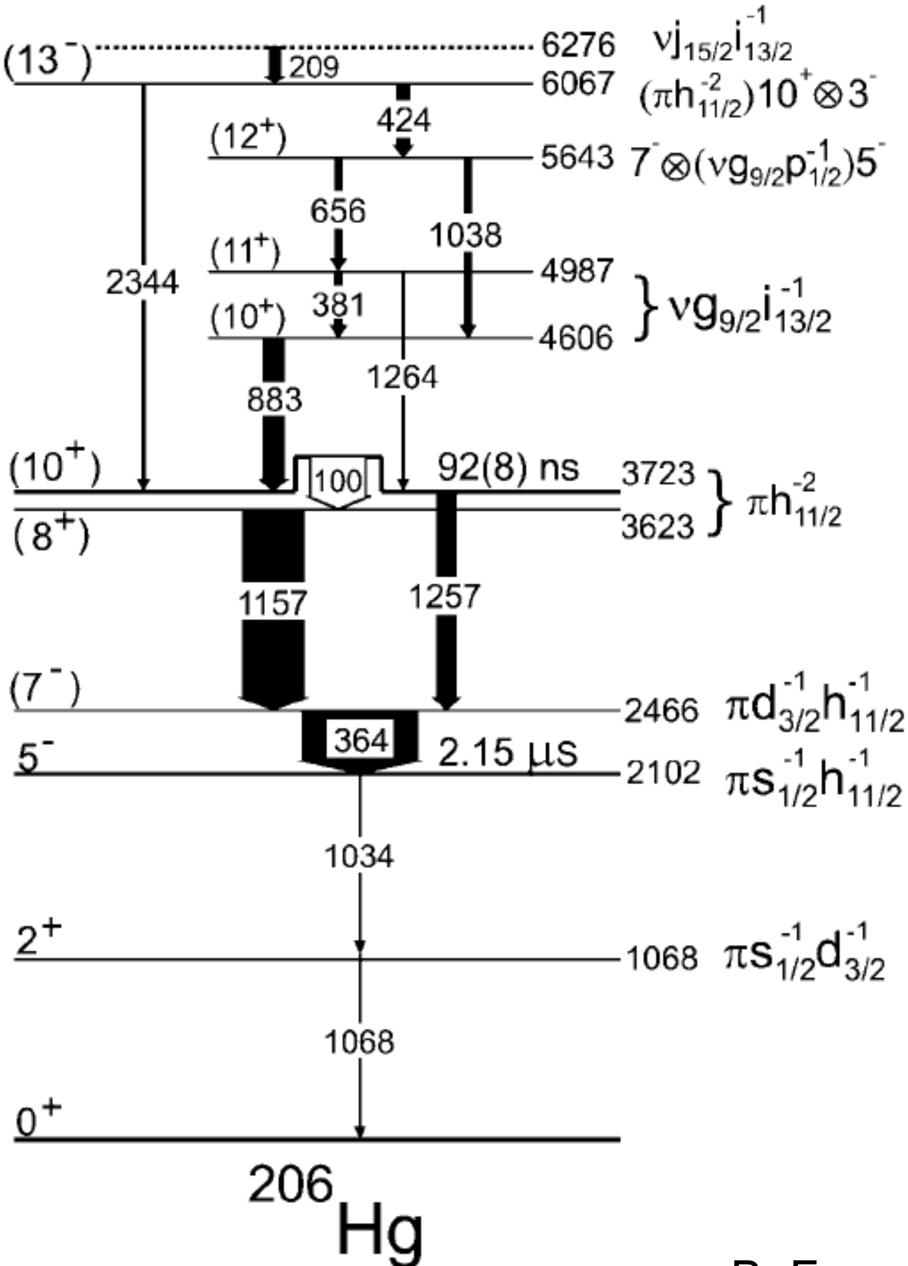

Core breaking states

Two-proton hole states

B. Fornal et al., Phys. Rev. Lett. 87, 212501 (2001)

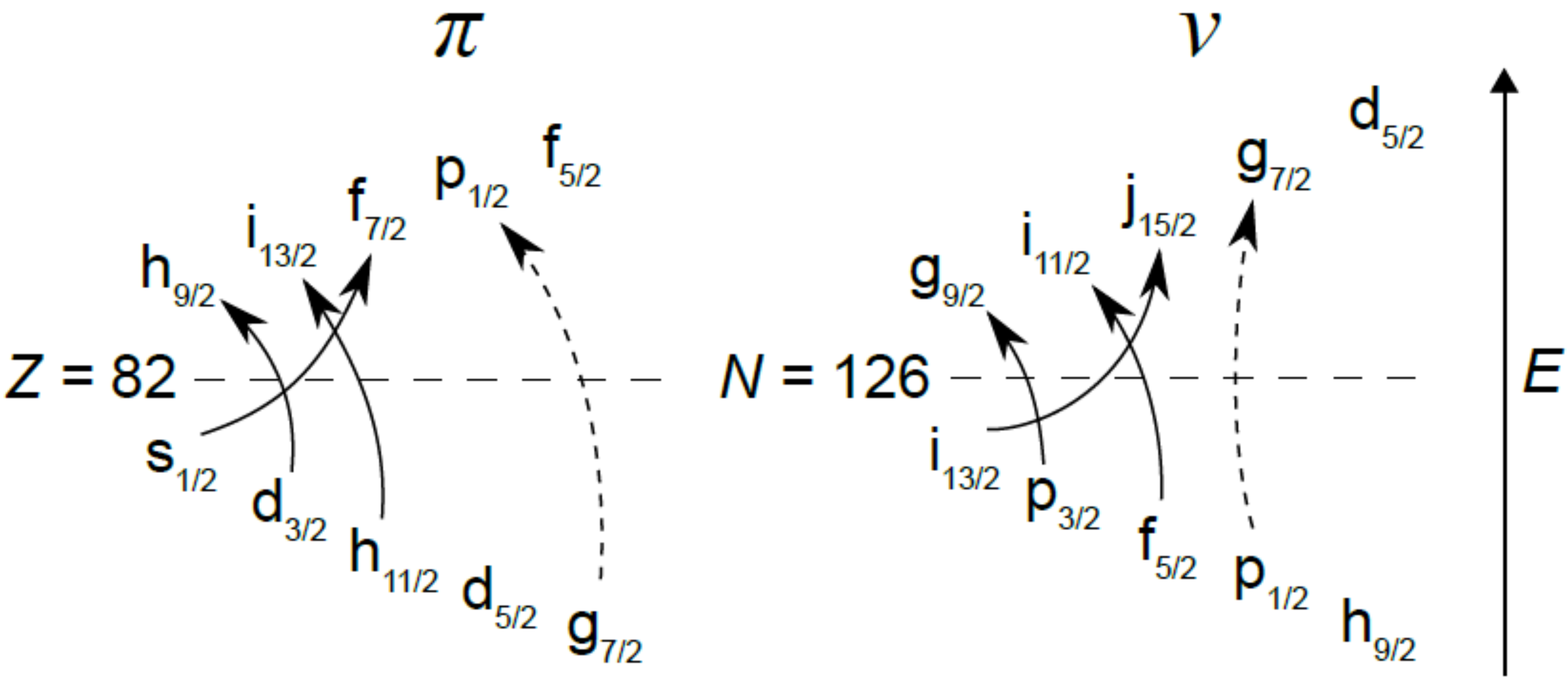

$$\Delta l = \Delta j = 3$$

SlowRI prospects

Mass known:≈2000 → ≈3000 1.5 X

Opt. Spectroscopy ≈600 → >1200 2 X

Expands Knowledge

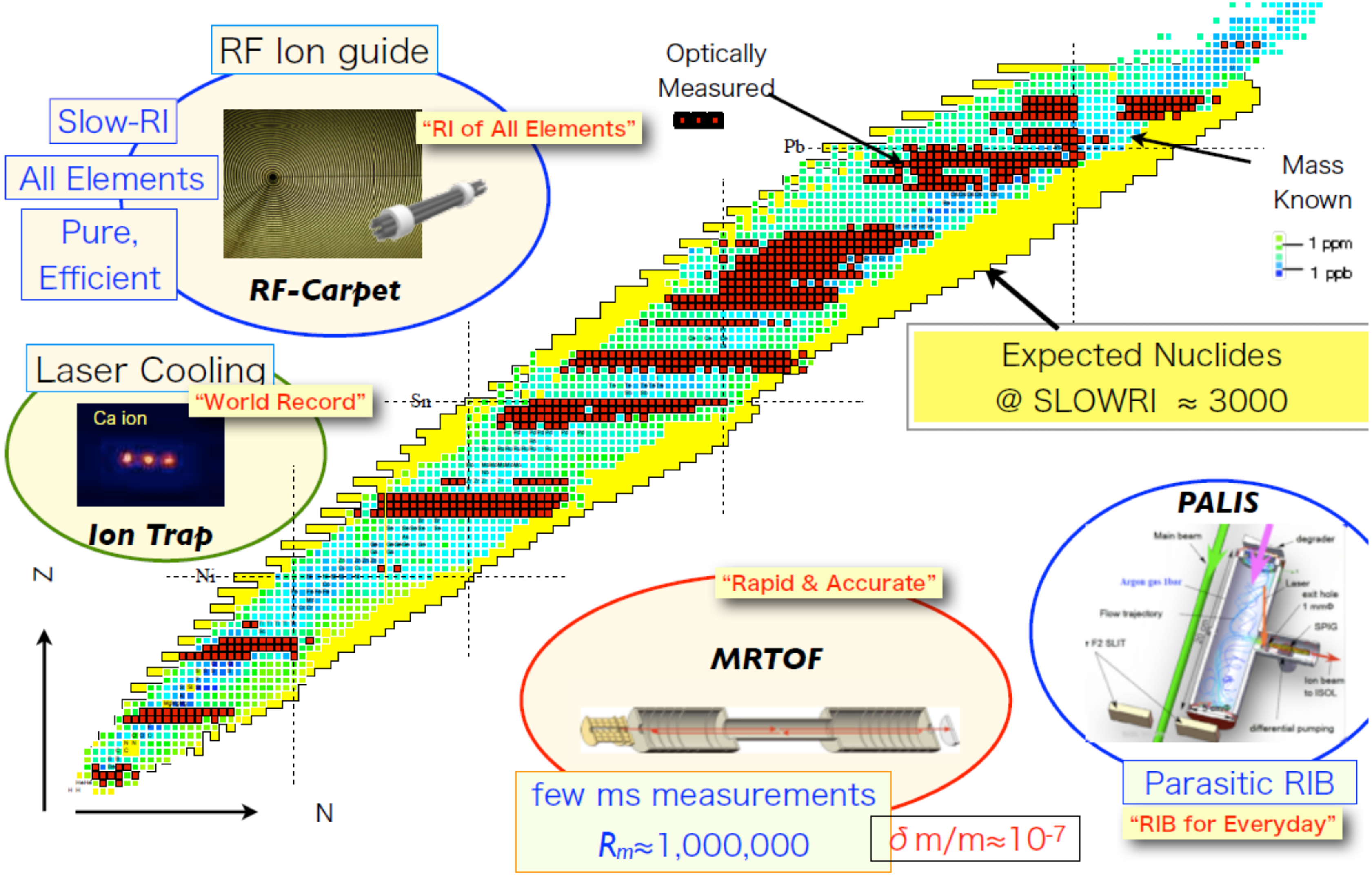

Fist beams in 2015

M. Wada et al., RIKEN Accel. Prog. Rep. 47 (2014) 203

M. Wada, RIKEN

Conclusions

-recently large amount of new experimental info
on neutron-rich nuclei around ^{208}Pb

-along Z=82 experimental information till ^{216}Pb (N=134)

-along N=126 experimental info till ^{203}Ir (Z=77)

-so far it was easy; but now more dedicated setups needed

-shell model needs to be sharpened to improve predictive power

-consistent structure and beta decay calculations needed

Shell model space

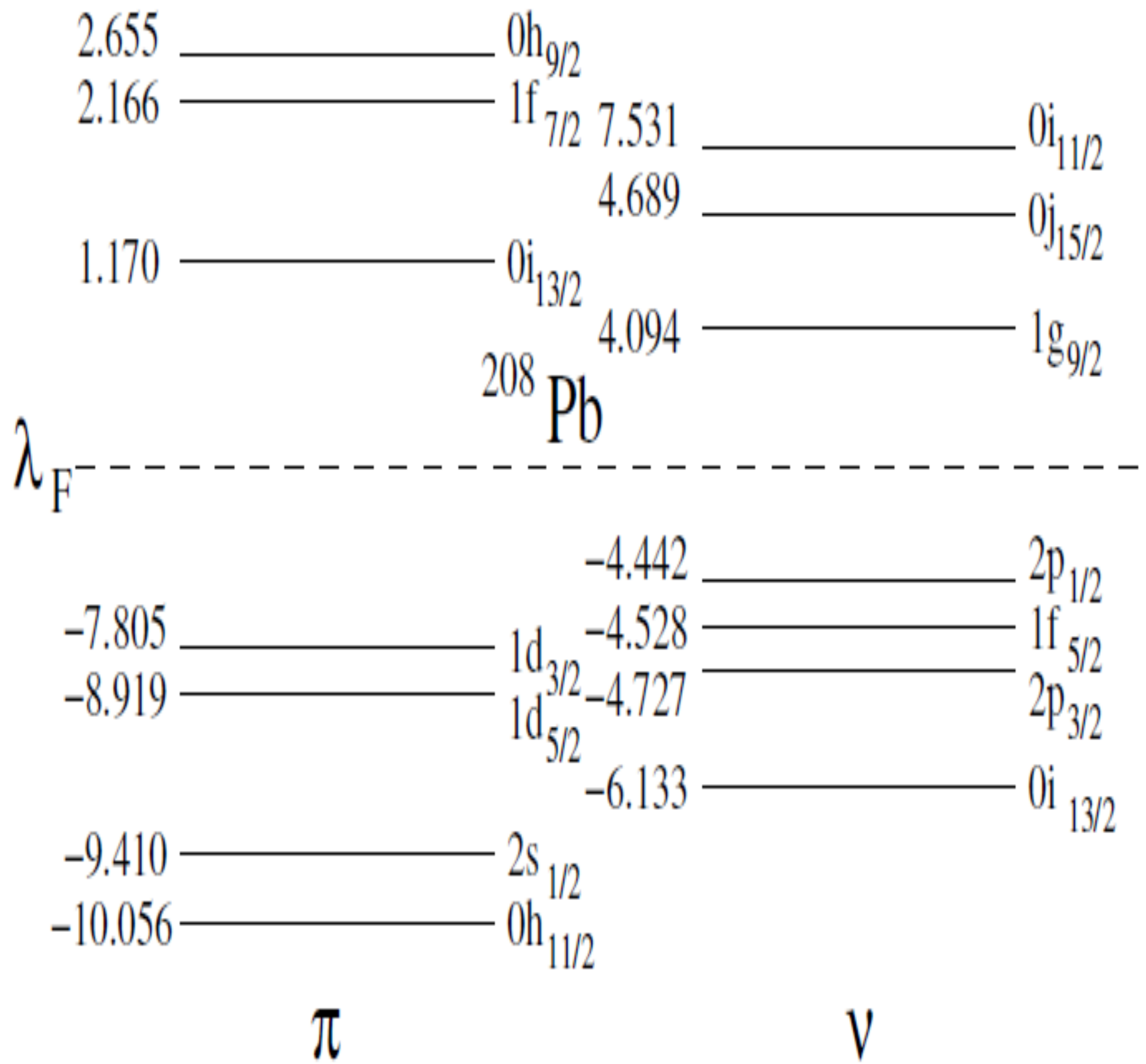

Kuo-Herling interaction

Calculations: H. Grawe

^{208}Pb states

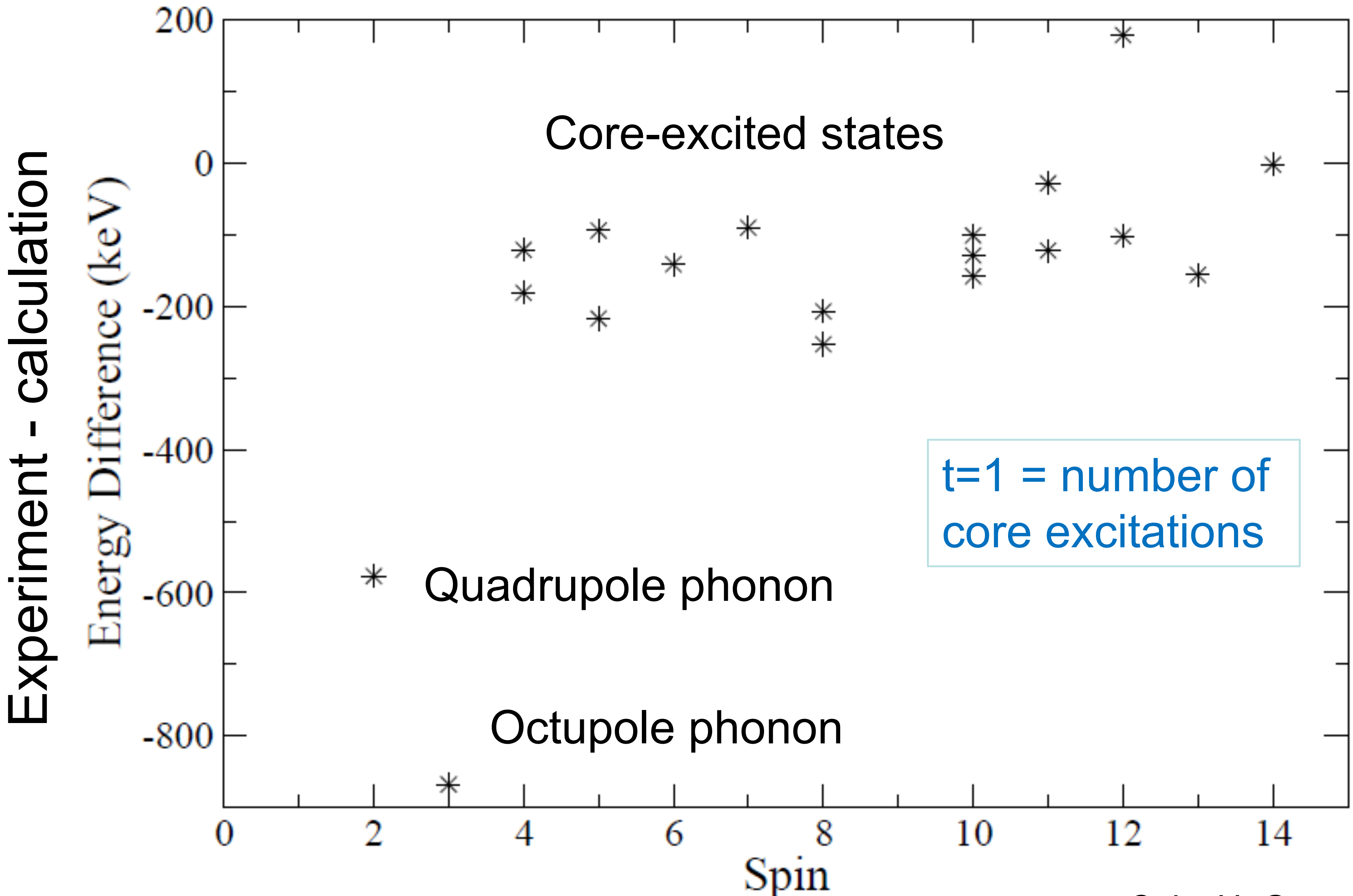

Calc. H. Grawe

=> Good description of 208Pb (Kuo-Herling interaction)

^{207}Tl states

Yrast states populated in ^{208}Pb+^{208}Pb at Gammasphere

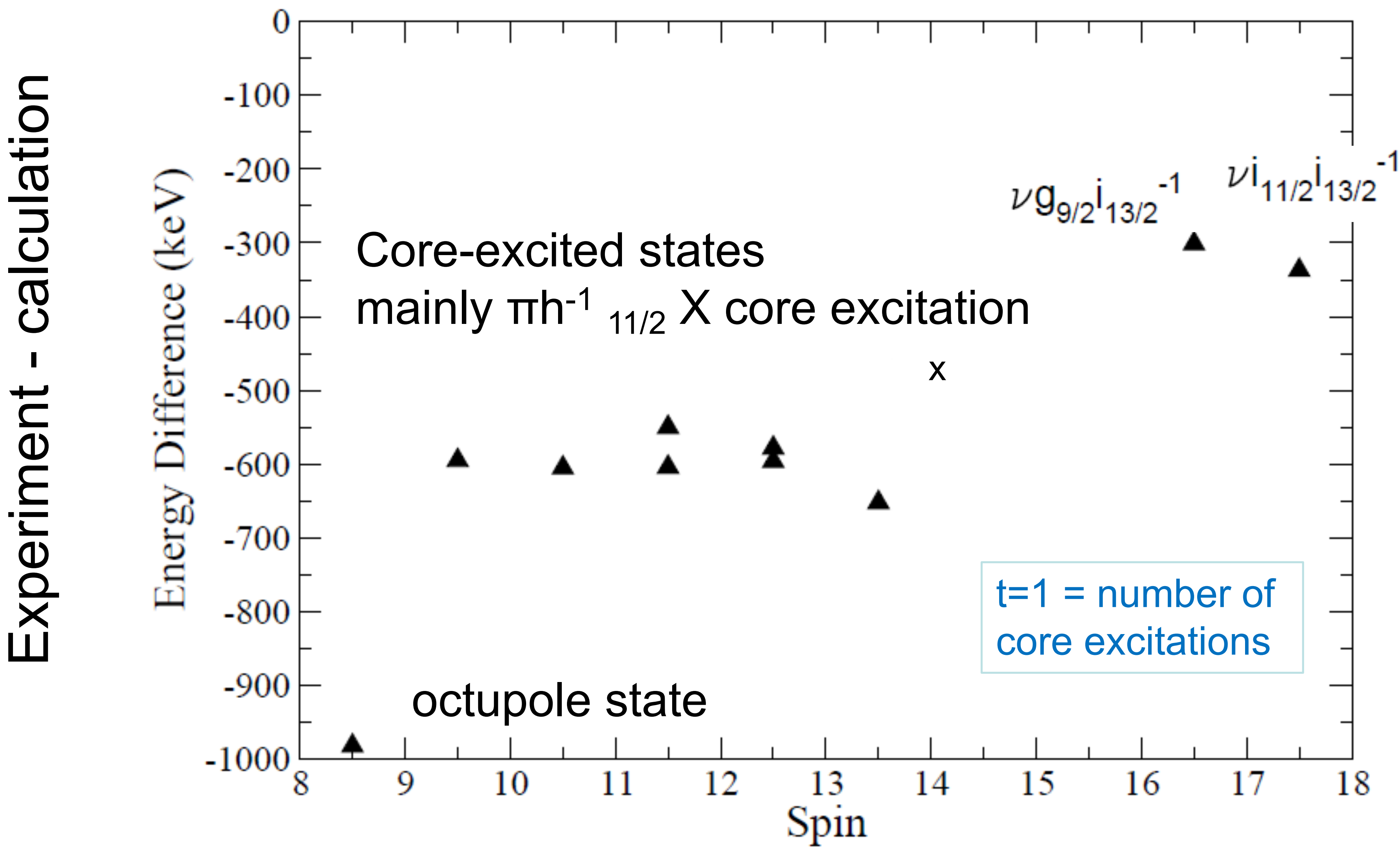

=> Shift of ~600 keV

Shell model: H. Grawe

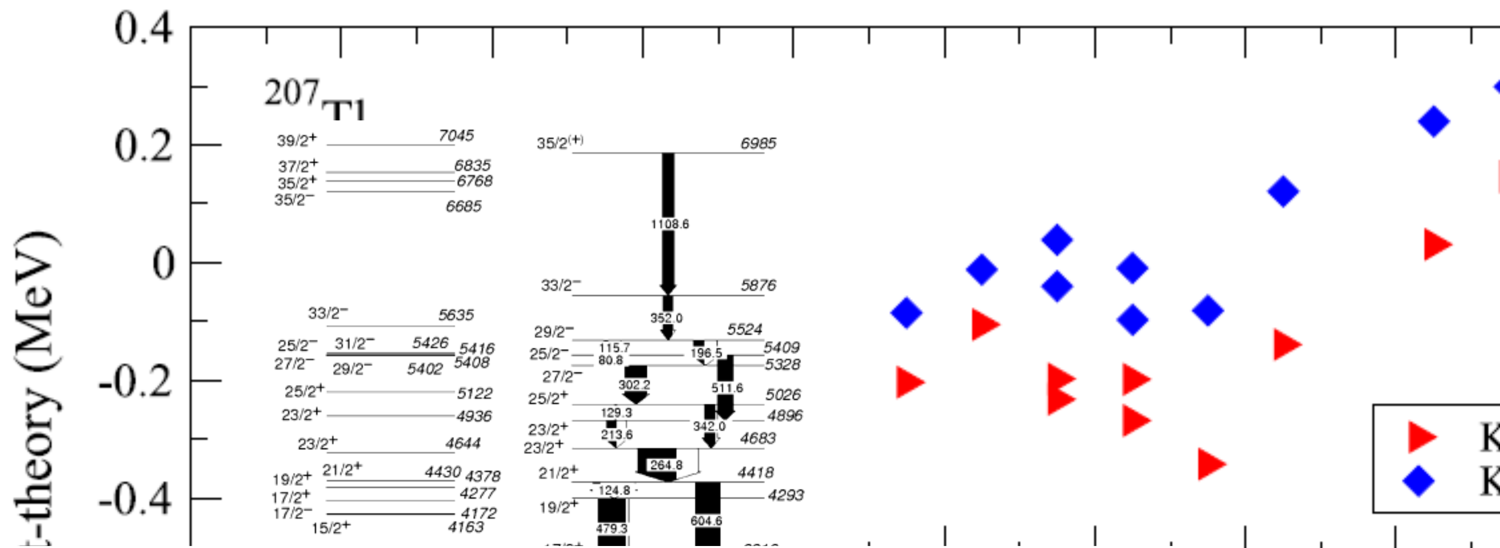

from the breaking of the $N = 126$ neutron core. While the shell-model calculations correctly predict the ordering of these states, their energies are compressed at high spins. It is concluded that this compression is an intrinsic feature of shell-model calculations using two-body matrix elements developed for the description of two-body states, and that multiple core excitations need to be considered in order to accurately calculate the energy spacings of the predominantly three-quasiparticle states.

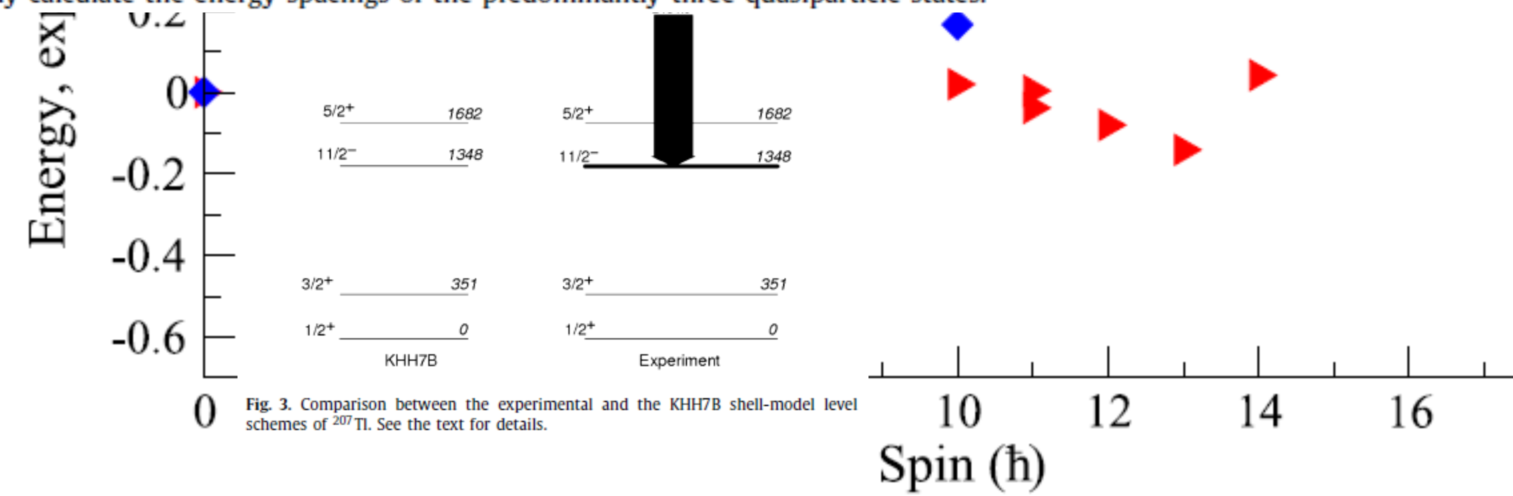

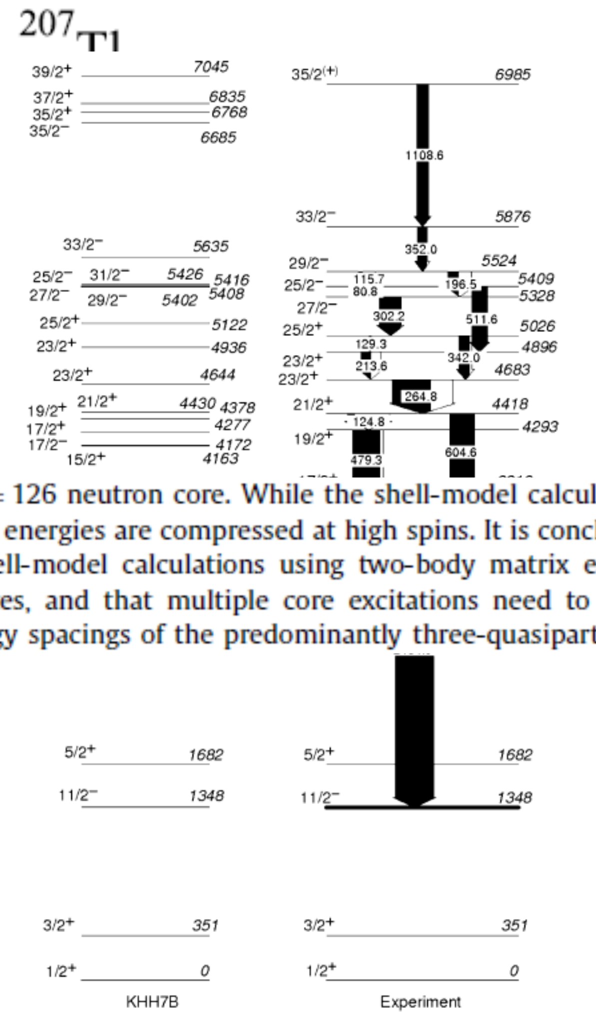

Fig. 3. Comparison between the experimental and the KHH7B shell-model level schemes of ^{207}Tl. See the text for details.

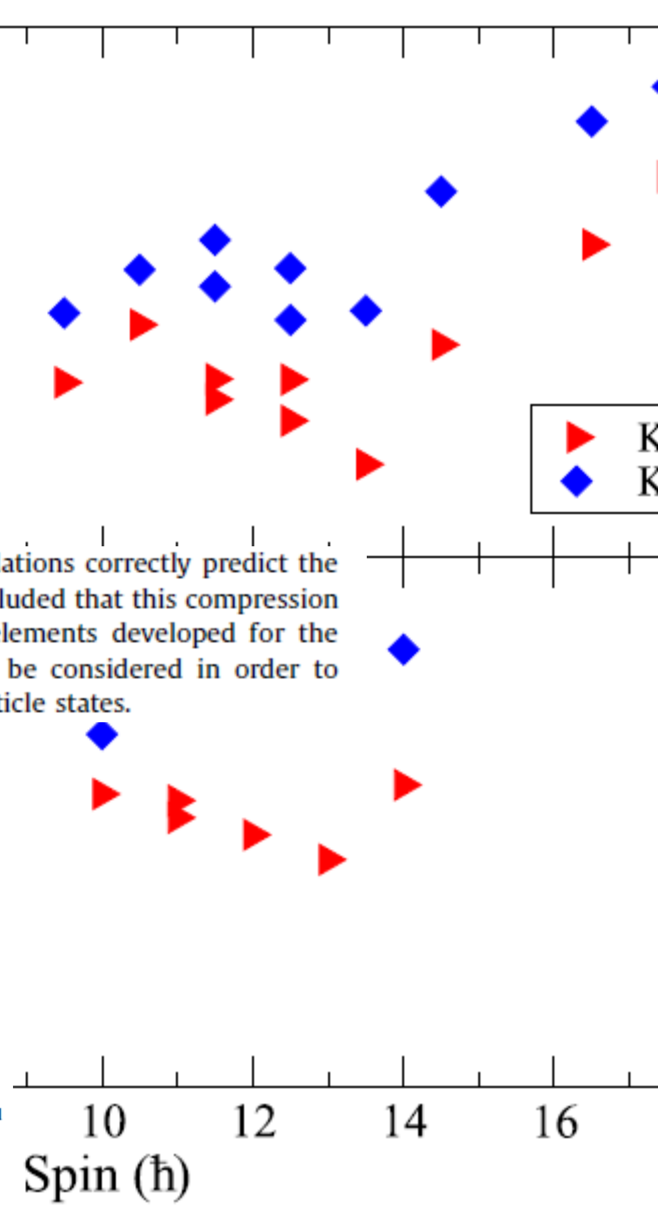

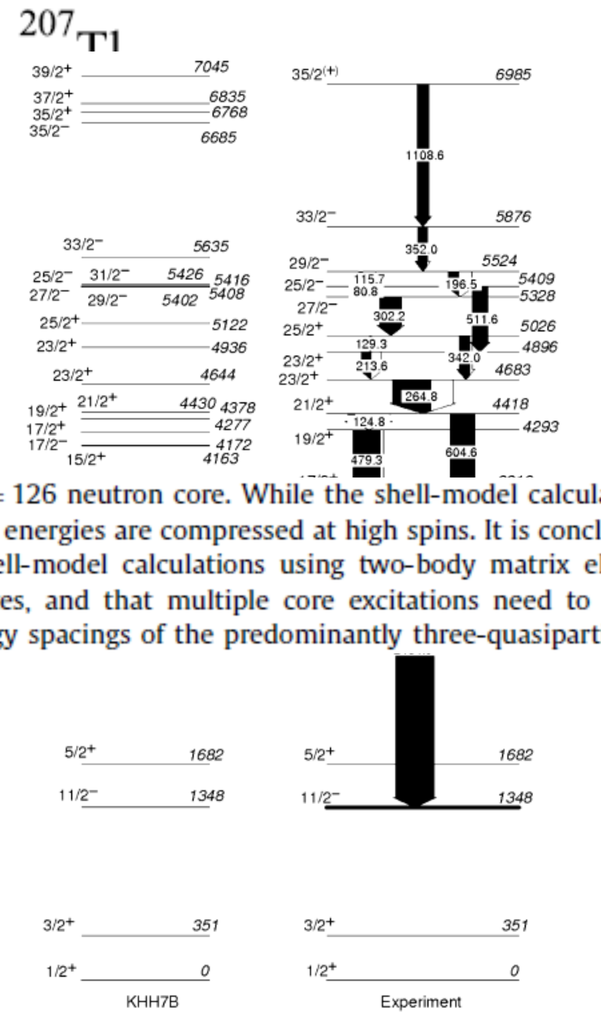

from the breaking of the $N = 126$ neutron core. While the shell-model calculations correctly predict the ordering of these states, their energies are compressed at high spins. It is concluded that this compression is an intrinsic feature of shell-model calculations using two-body matrix elements developed for the description of two-body states, and that multiple core excitations need to be considered in order to accurately calculate the energy spacings of the predominantly three-quasiparticle states.

Fig. 3. Comparison between the experimental and the KHH7B shell-model level schemes of ^{207}Tl. See the text for details.

^{207}Pb; comparison with shell model

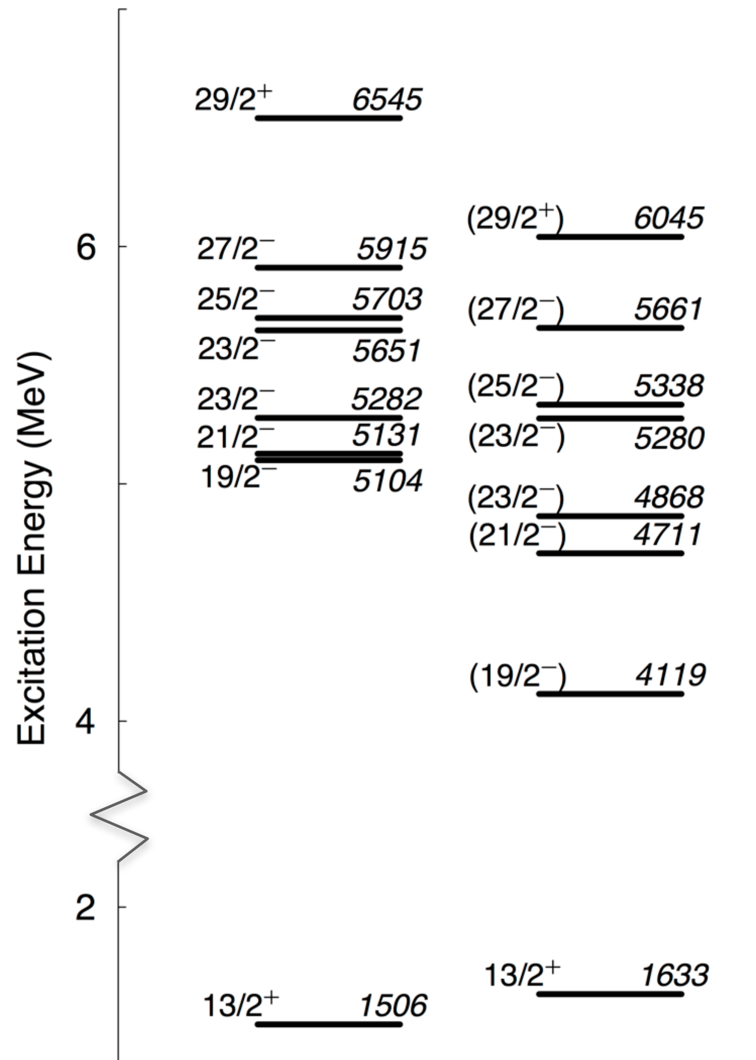

Shell Model

Experiment

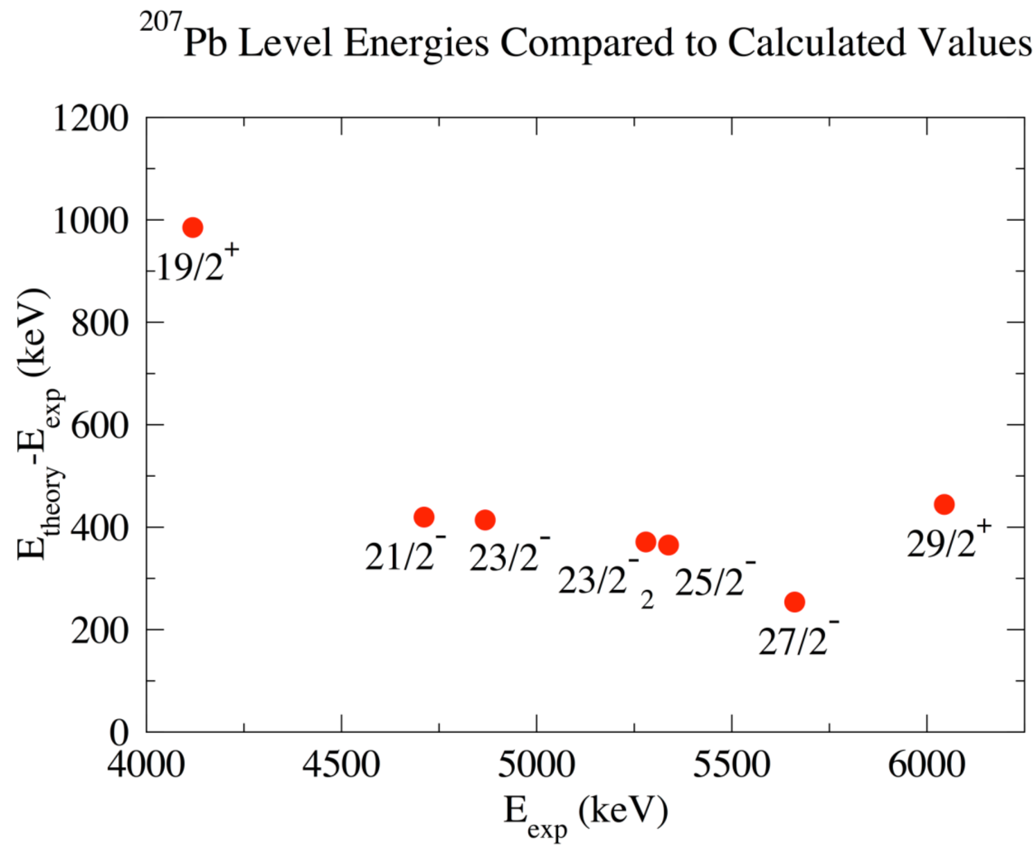

^{98}Cd case

Increasing number of core excitations

more core-excitations
⇒better theoretical description

^{98}Cd is easier for theory,
as below Z=N=50 only g9/2

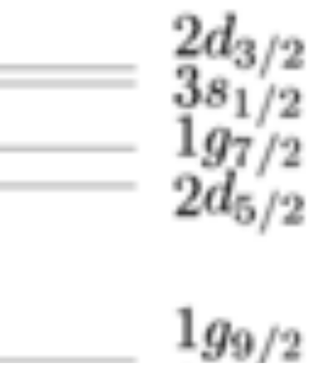

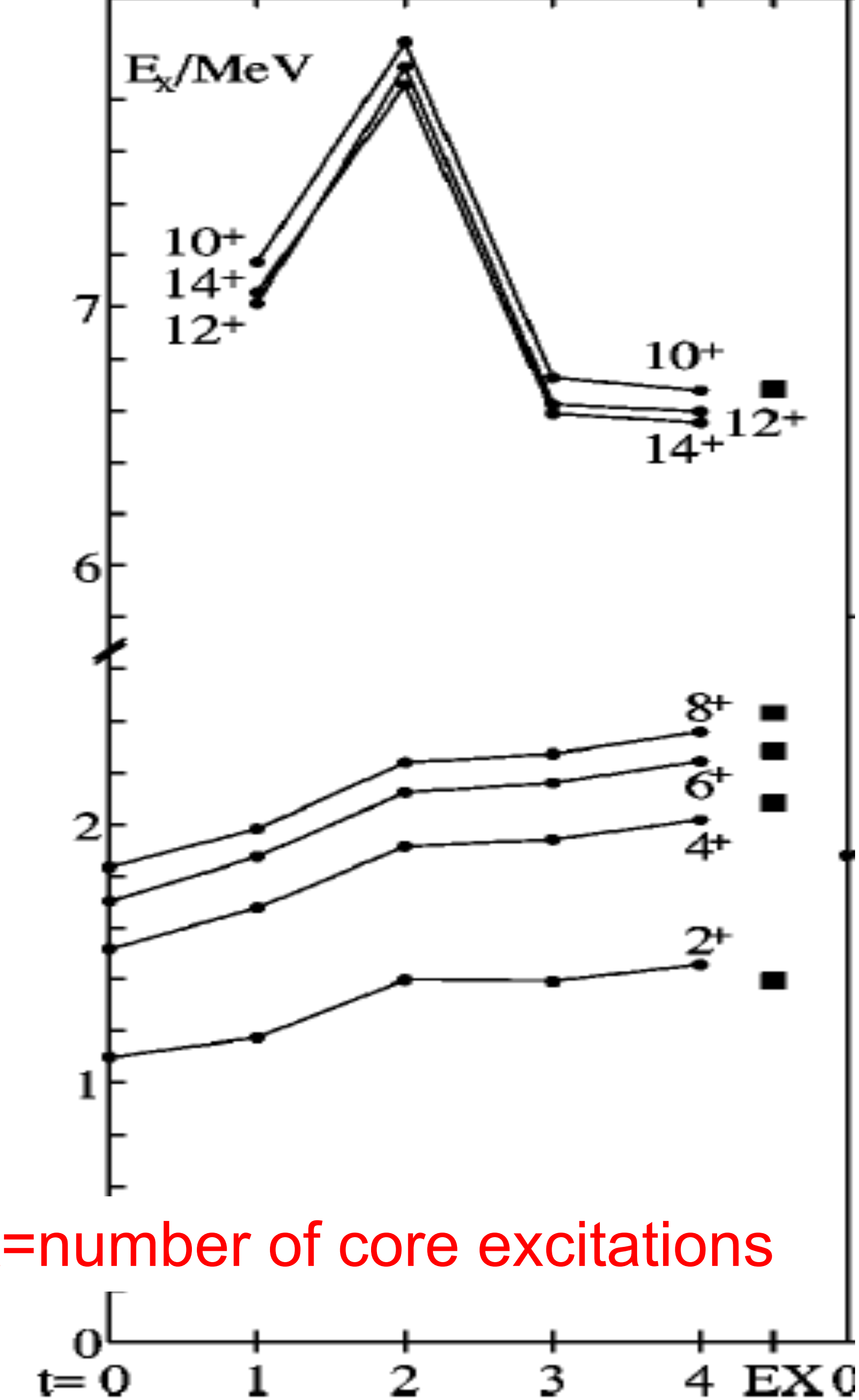

t=number of core excitations

A. Blazhev et al., Phys. Rev. C 69, 064304 (2004)
calculations by E. Caurier, F. Nowacki

What about low-spin core excited states in ^{207}Tl?

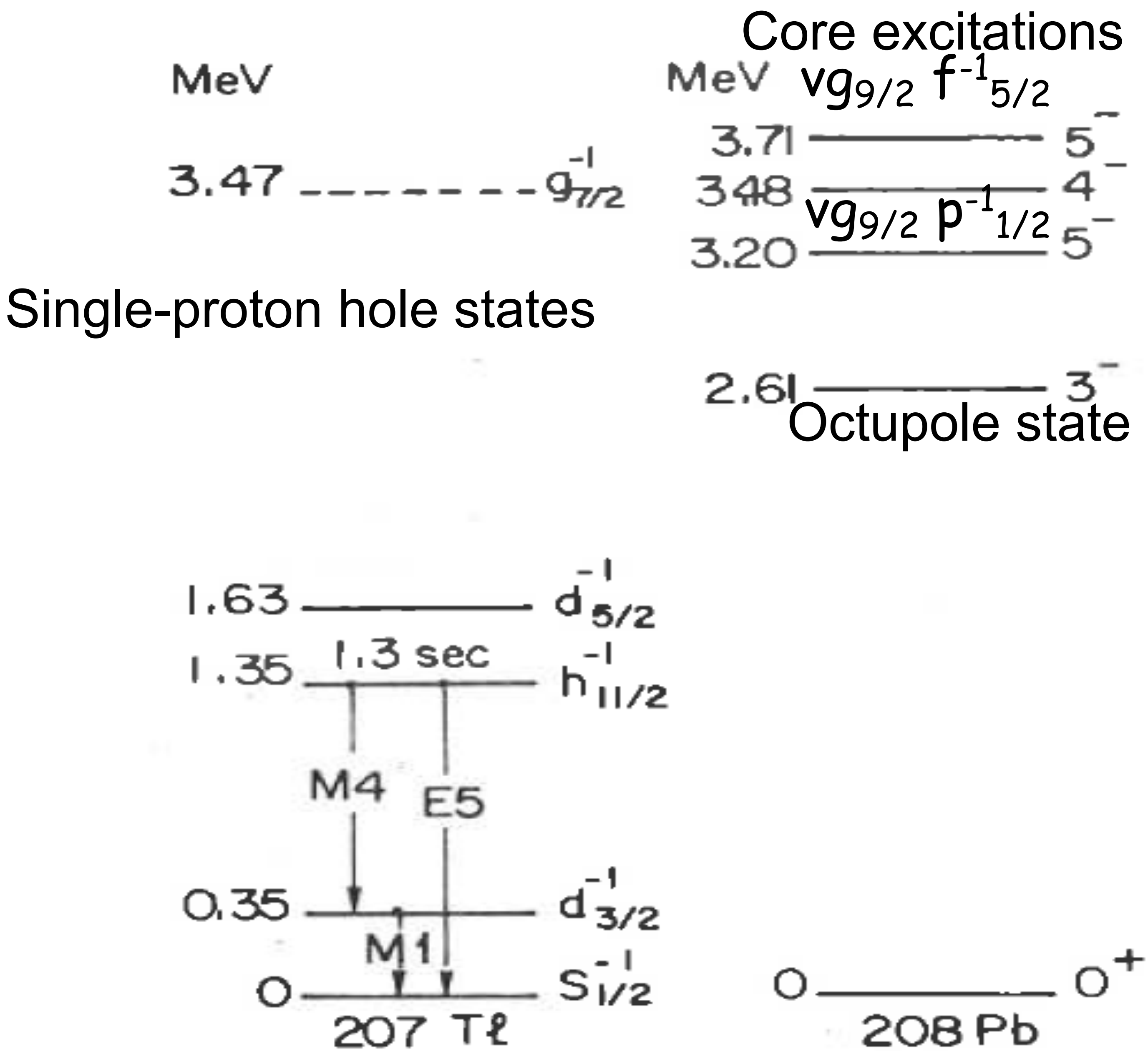

Former experiment

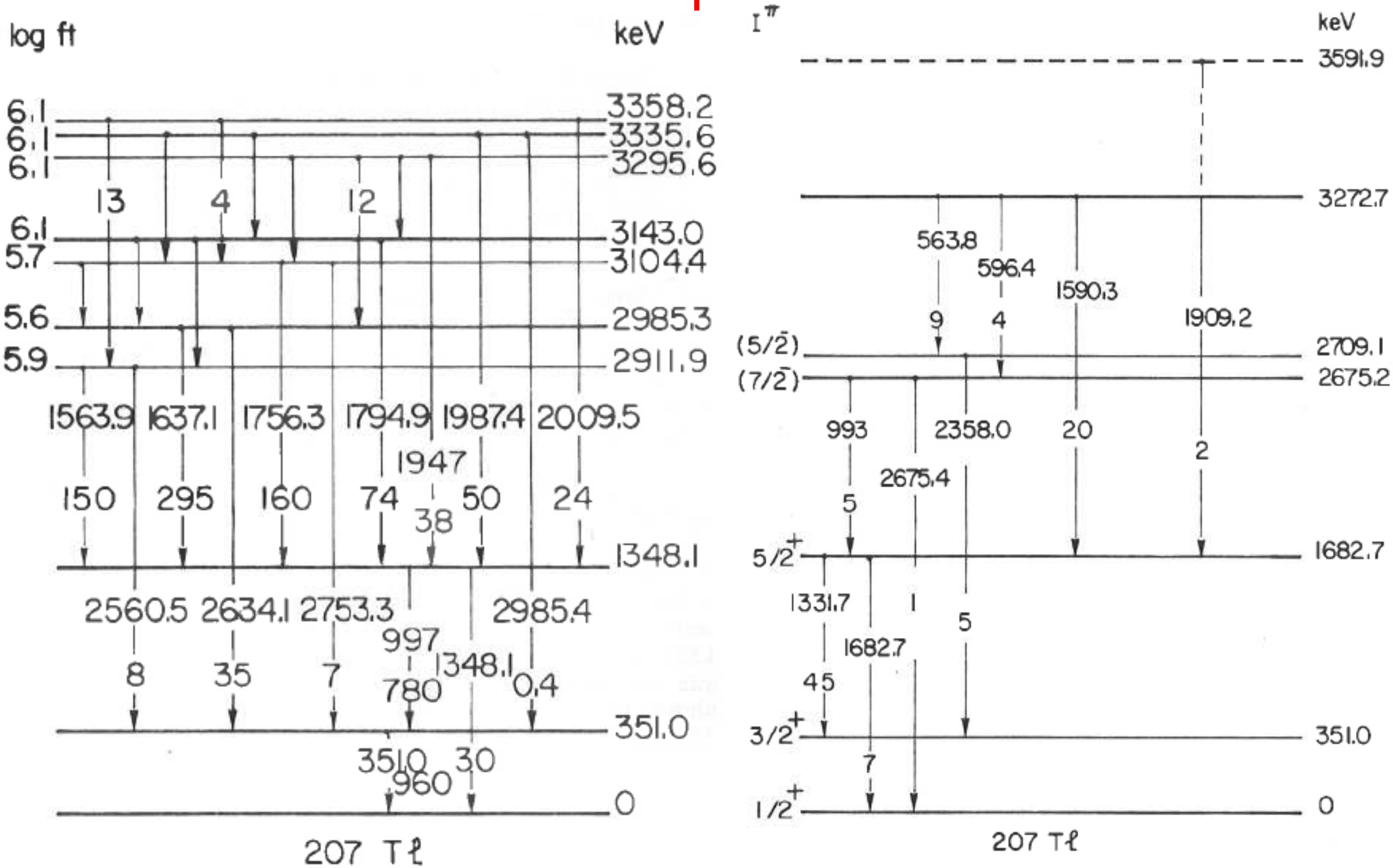

B. Jonson, O.B. Nielsen, J. Zylicz, CERN-81-09 (1981)
(Proc. Int. Conf. Nuclei far from stability, Helsingor, Denmark. Vol.2 p.640 (1981))

Beyond N=126 and Z<82: what do we know?

208Pb Core	**209Pb** lot	**210Pb** lot	**211Pb** lot	**212Pb** 8+ isomer	**213Pb** From beta	**214Pb** 8+ isomer	**215Pb**	**216Pb** 8+ isomer
207Tl lot	208Tl From beta/α	209Tl 17/2+ isomer	210Tl From α	211Tl				
206Hg Yrast till (13-)		208Hg 8+ isomer		210Hg 8+ isomer				
205Au yrast								
204Pt yrast								
203Ir yrast								

Excited states

Production of exotic nuclei (new isotopes)

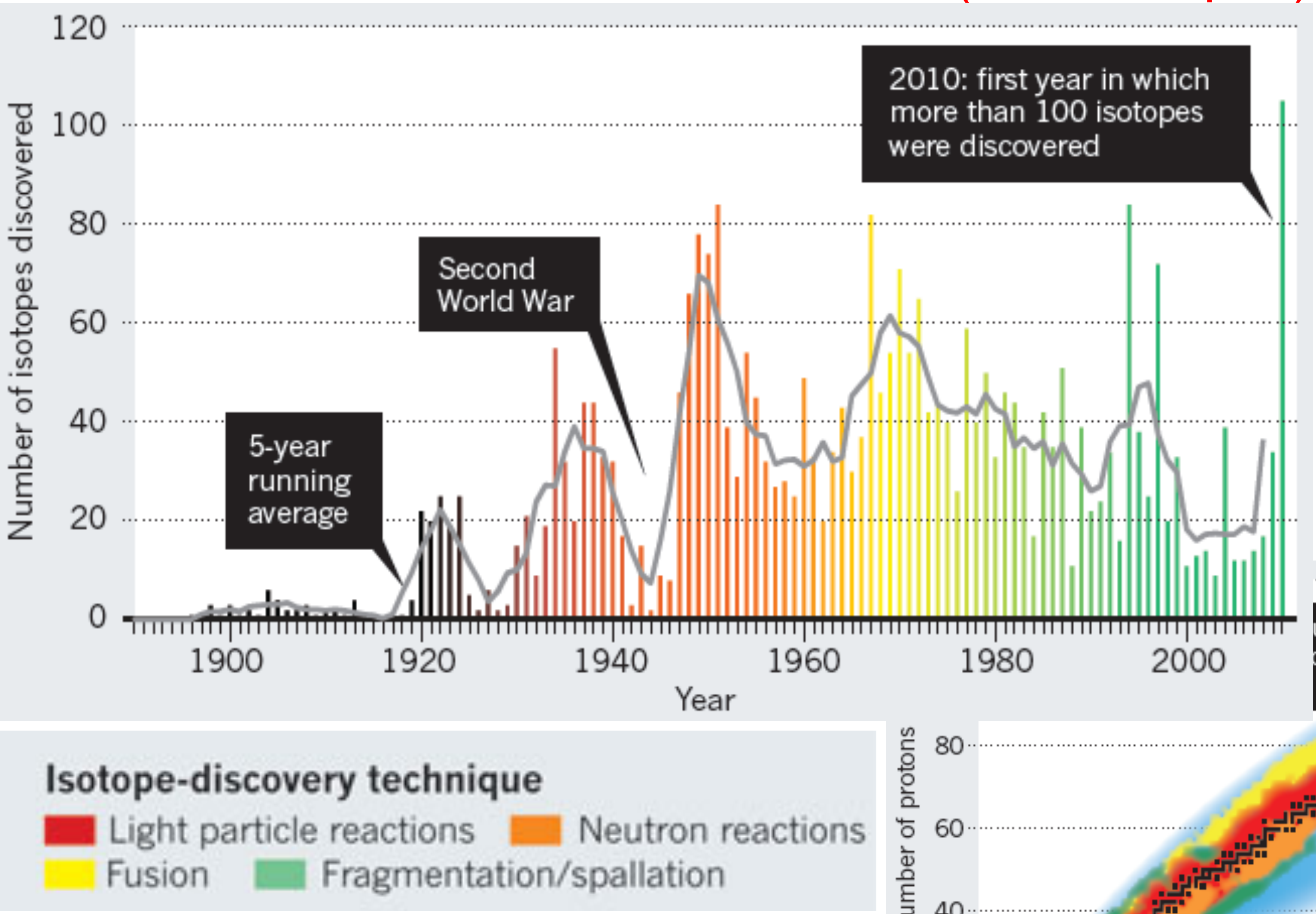

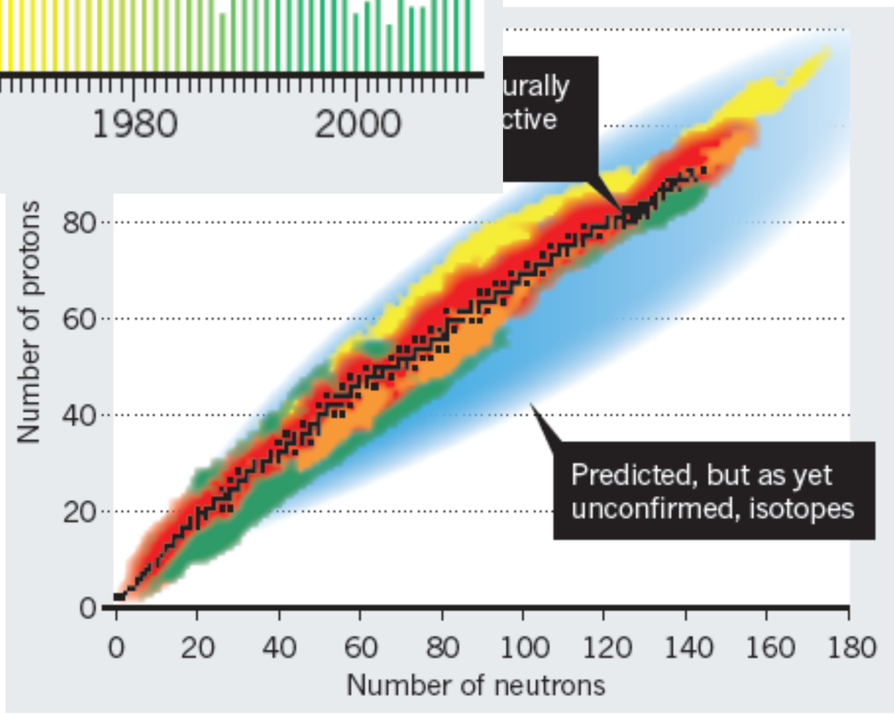

M. Thoennessen, B.M. Sherril, Nature 473 (2011) 25

In flight fragmentation (and fission): separation and identification

Fragment Separator (GSI, Darmstadt, Germany)

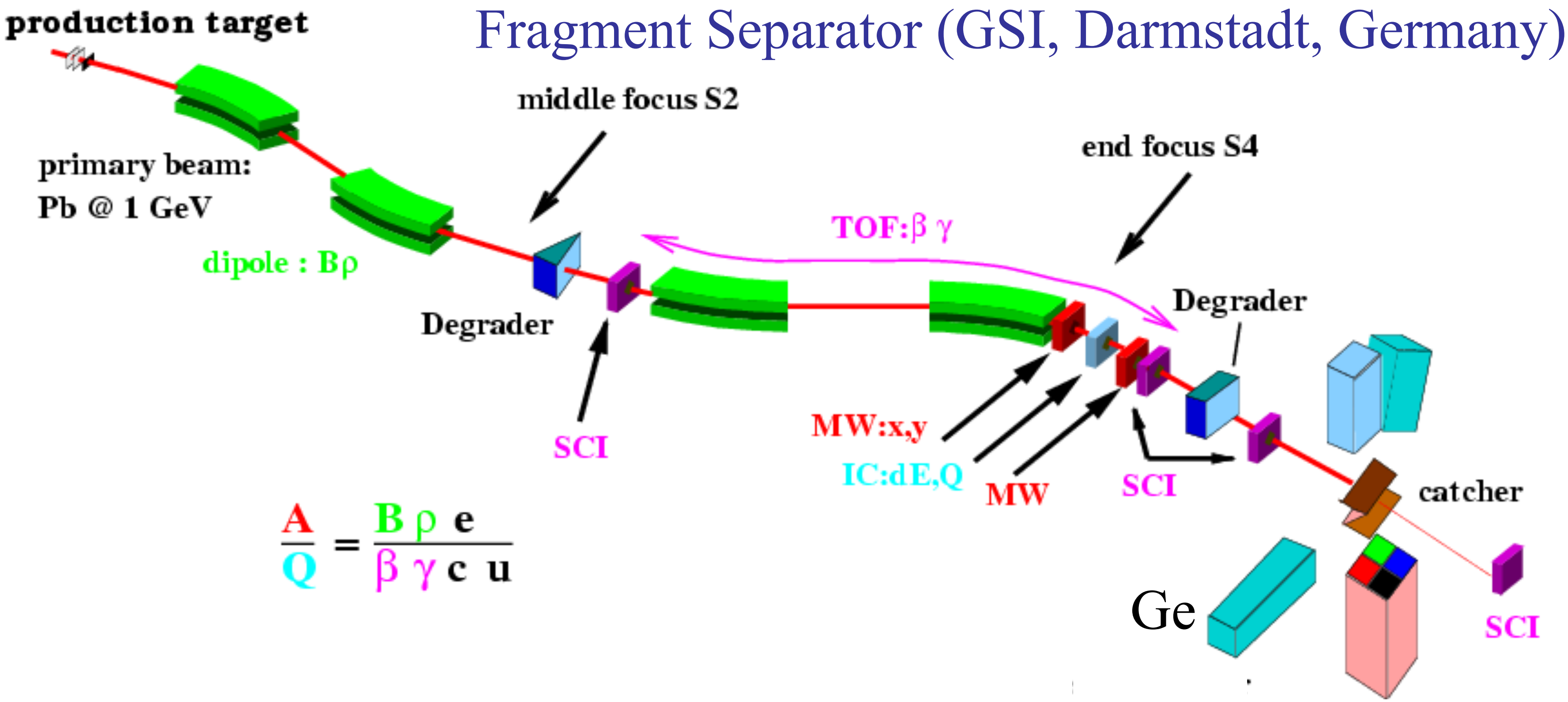

$$\frac{A}{Q} = \frac{B\rho\, e}{\beta\gamma c\, u}$$

Relativistic energy fragmentation: => heavy ions

Decay (internal and β, α) spectroscopy:

- decay correlated with the fragment
- ***very sensitive*** (ion beams > 1 ion/hour)

Identification

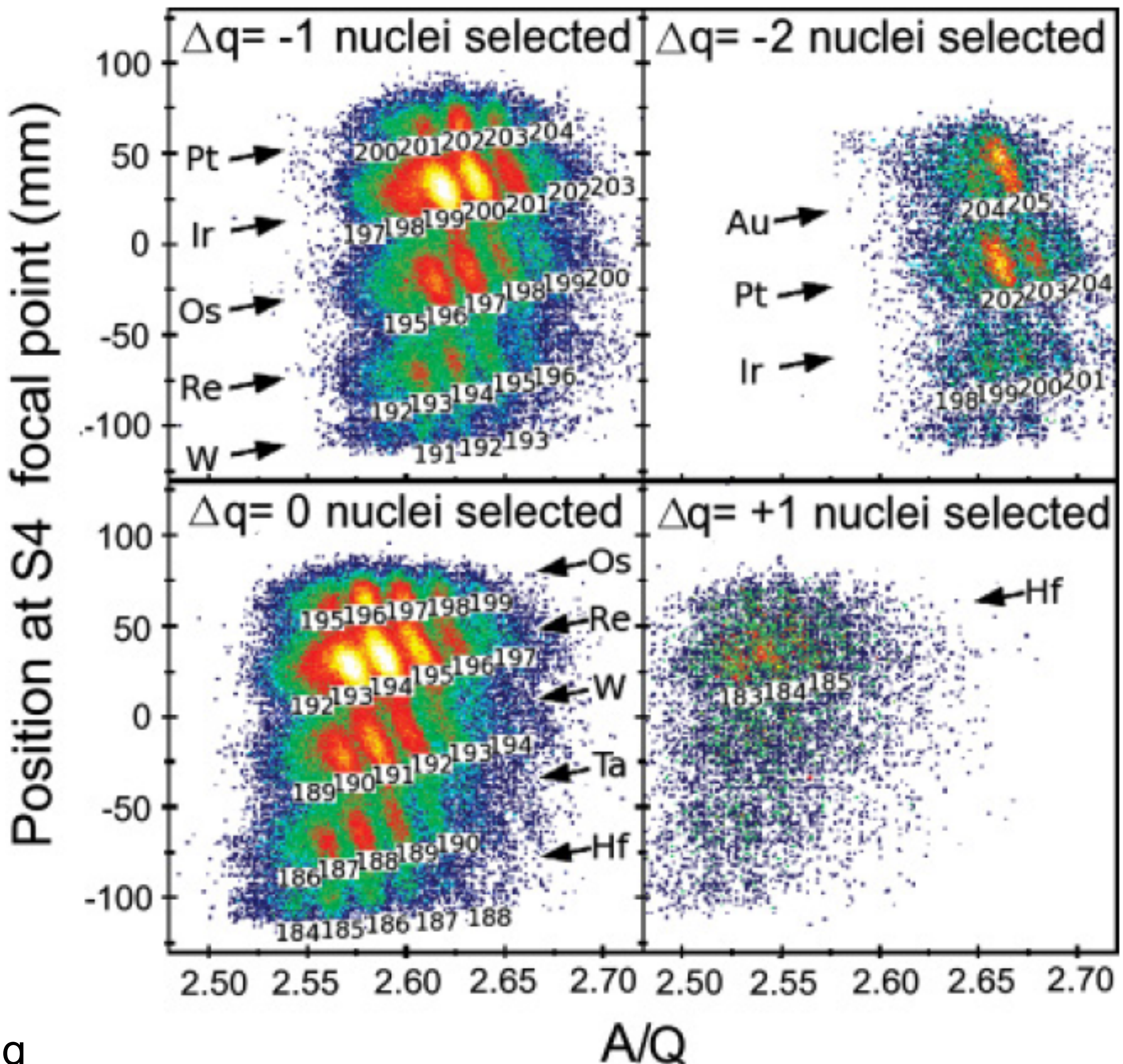

192W setting

RIKEN and heavy nuclei

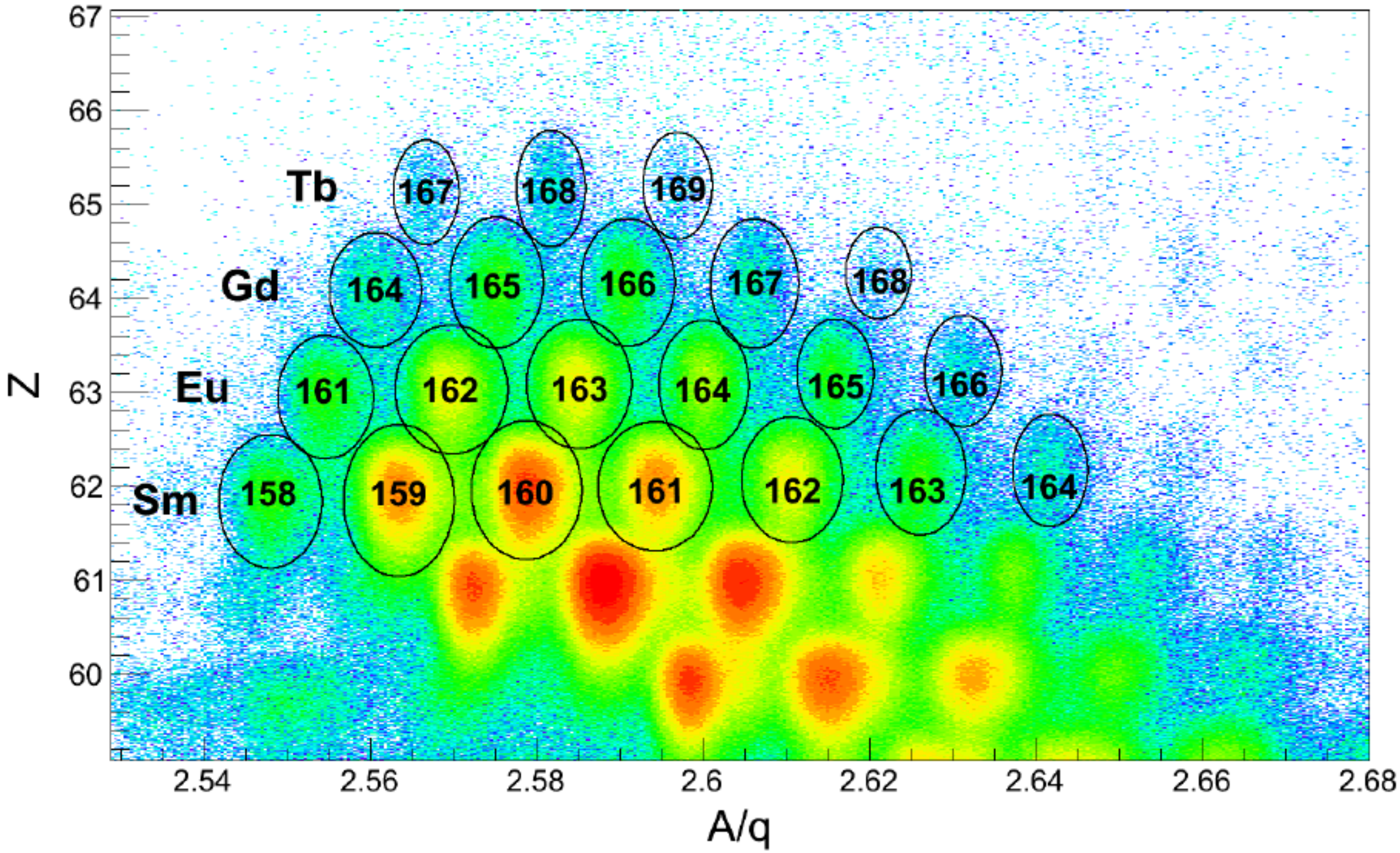

Figure 5.1: Particle identification plot for the isomer setting of the experiment. Nuclei of interest are circled.

Z. Patel, PhD thesis, Univ. of Surrey, 2015

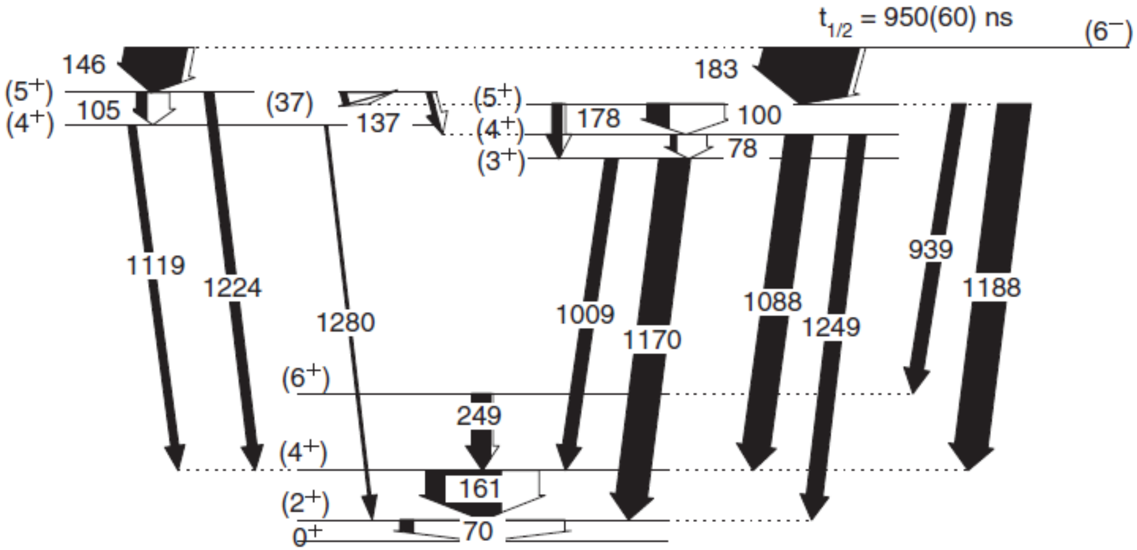

^{166}Gd

Higher mass end of fission

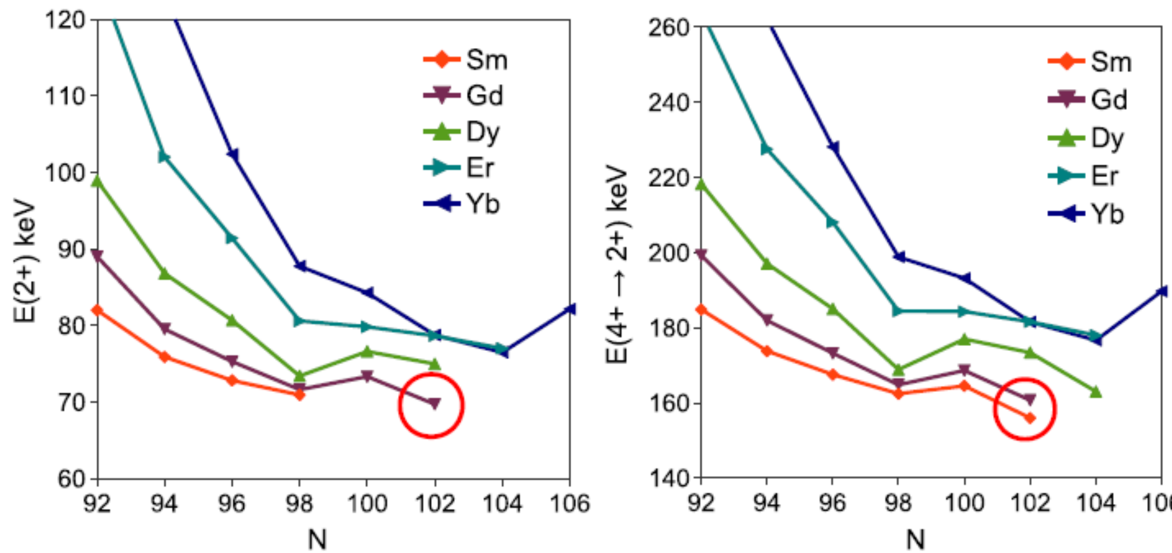

FIG. 4 (color online). Systematics of $E(2^+)$ and $E(4^+ \rightarrow 2^+)$ for Sm, Gd, Dy, Er, and Yb isotopes. All data points from [26] and this work.

New: 166Gd, 164Sm

Z. Patel et al., Phys. Rev. Lett. 113, 262502 (2014)

Heaviest isomer in RIKEN: ^{174}Er (Z=68)

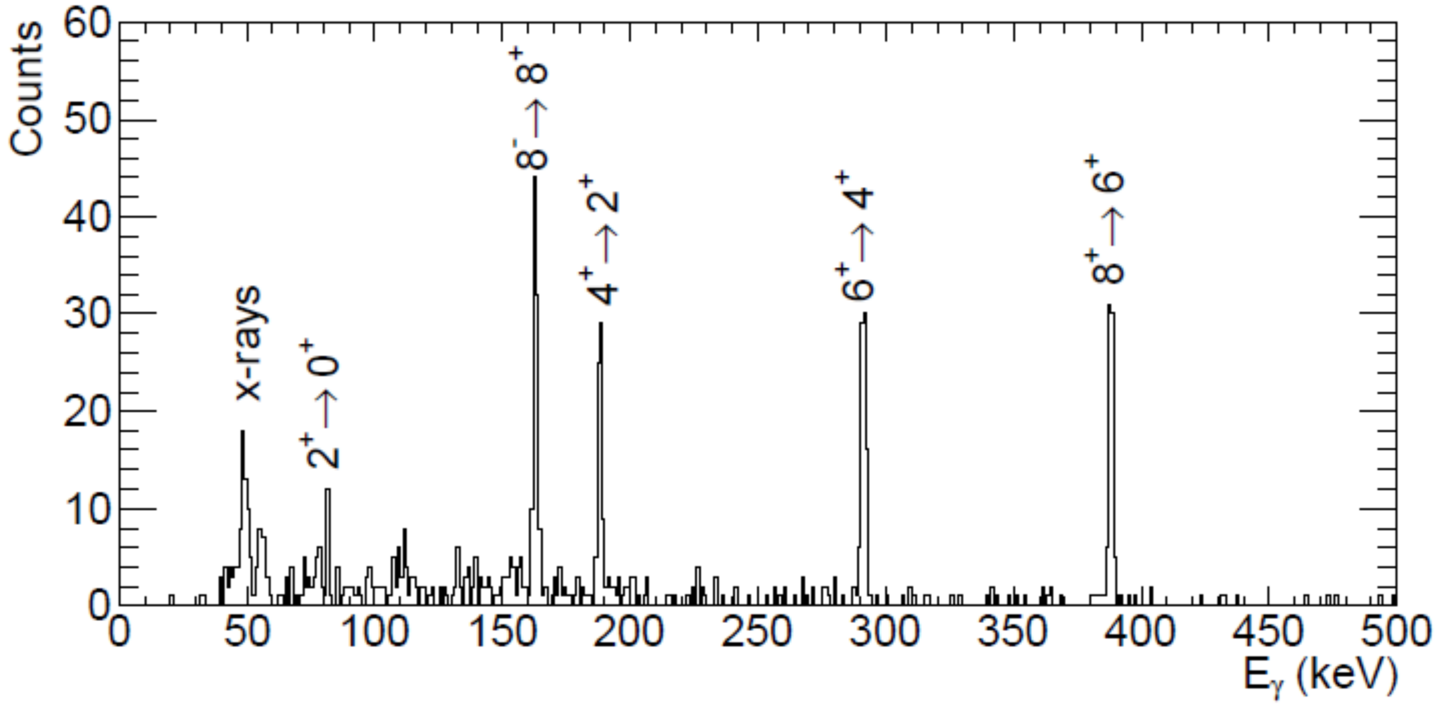

Fig. 2. Combined $\gamma\gamma$-coincidence spectrum gated on the decays from the 8^- isomer in ^{174}Er.

P.-A. Soderstrom et al., RIKEN Accel. Prog. Rep 48 (2015), in print

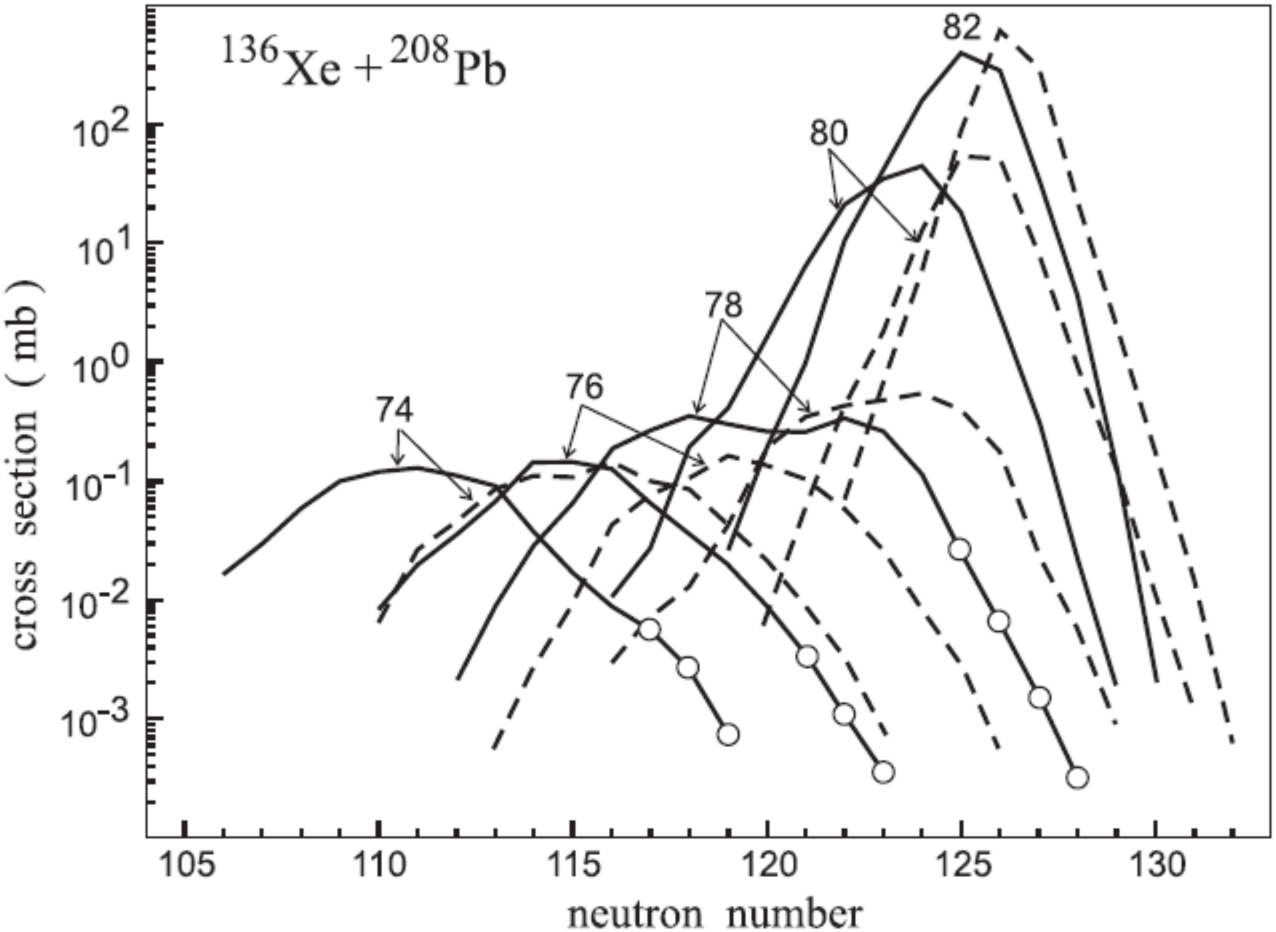

FIG. 5. Cross sections for production of heavy neutron-rich nuclei in collisions of ^{136}Xe with ^{208}Pb at $E_{c.m.} = 450$ MeV. Dashed curves show the yield of primary fragments, whereas the solid ones correspond to survival nuclei. Open circles indicate unknown isotopes.

V. Zagrebaev, W. Greiner, Phys. Rev. Lett. 101, 122701 (2008)

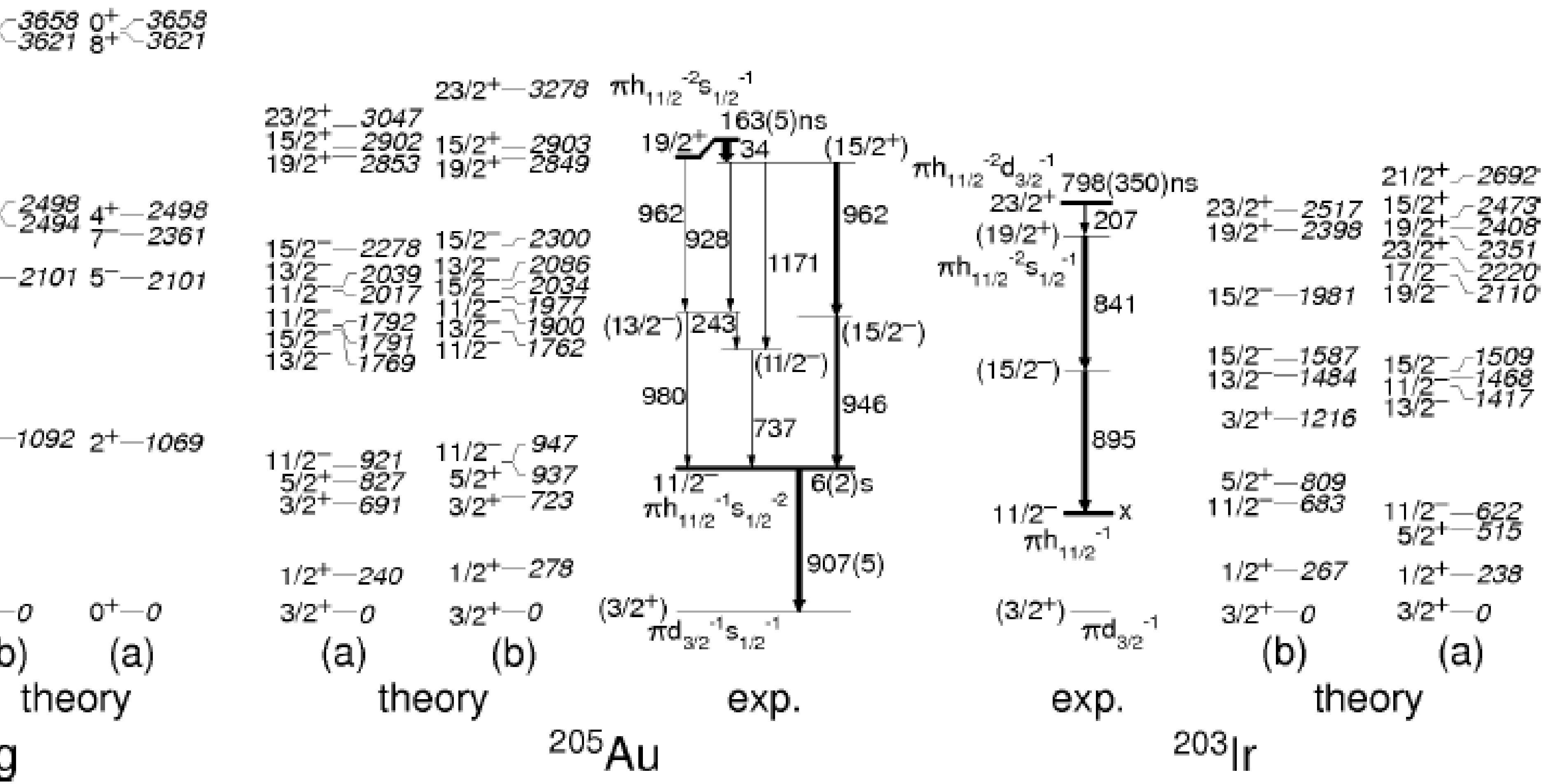

206Hg: B. Fornal et al., PRL 87, 212501 (2001)
204Pt: S.J. Steer et al., PRC 78, 061302 (2008)
205Au: Zs. Podolyák et al, PL B 672, 116 (2009)

Transition strengths in N=126 nuclei

Nucleus	Transition	B(EL) (W.u.) exp.	SM	SM_{mod}
^{206}Hg	$B(E3:10^+ \rightarrow 7^-)$	0.25(3)	0.17	0.21
^{204}Pt	$B(E3:10^+ \rightarrow 7^-)$	0.19(3)	0.21	0.22
203Ir	B(E2:23/2+->19/2+)	0.02(1)[b)]	3.58	0.013
^{206}Hg	$B(E3:5-^+ \rightarrow 2^+)$	0.18(2)	1.17	0.91
^{204}Pt	$B(E3:5-^+ \rightarrow 2^+)$	0.039(5)	0.713	0.612
^{206}Hg	$B(E2:10^+ \rightarrow 8^+)$	0.94(15)	0.87	0.87
^{204}Pt	$B(E2:10^+ \rightarrow 8^+)$	0.80(8)	2.64	1.22
^{205}Au	$B(E2:19/2^+ \rightarrow 15/2^+)$	1.2(2)	3.1	1.7
^{204}Pt	$B(E2:7-^+ \rightarrow 5^-)$	0.017+ →0.0034[a)]	1.21	0.0037

Effective charges: 1.5e for E2 and 2.0e for E3 (to reproduce 206Hg)

[a)] Assuming a transition energy between 10→78 keV.

⇒ Good description of N=126 nuclei
after small modifications of TBMEs

Fragmentation: ^{238}U or ^{208}Pb?

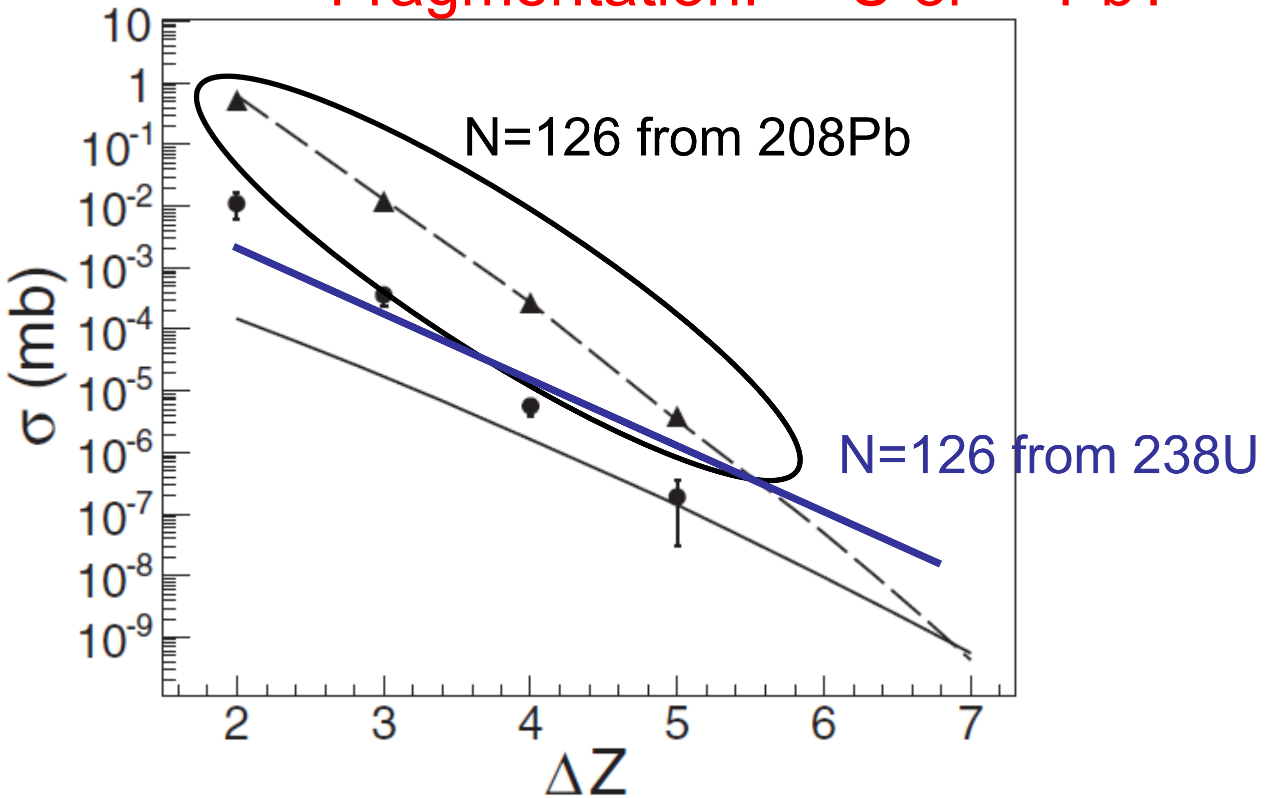

For N=126:

Below 203Ir: 238U

Above 203Ir: 208Pb

FIG. 3. Production cross sections of charge-exchange $N = 127$ isotones (dots, this work) and $N = 126$ fragmentation residues (triangles, from Ref. [10]) as a function of the number of protons removed from the projectile ^{208}Pb. The lines represent fragmentation cross sections of $N = 127$ (solid line) and $N = 126$ (dashed line) isotones obtained with the COFRA [30] code for reactions induced by ^{238}U and ^{208}Pb projectiles, respectively.

A.I. Morales et al., Phys. Rev. C84, 011601 (R) (2011)

Beyond N=126 and Z<82: what do we know?

208Pb Core	**209Pb** Yrast + ~3	**210Pb** Yrast + ~4	**211Pb** From beta	**212Pb** 8+ isomer	**213Pb** From beta
207Tl Up to~35/2	208Tl From beta/α	209Tl 17/2+is omer	210Tl g.s. (5+)	211Tl	
206Hg Yrast till (13-)		208Hg 8+ isomer		210Hg 8+ isomer	
205Au yrast					
204Pt yrast					
203Ir yrast					

Beyond N=126

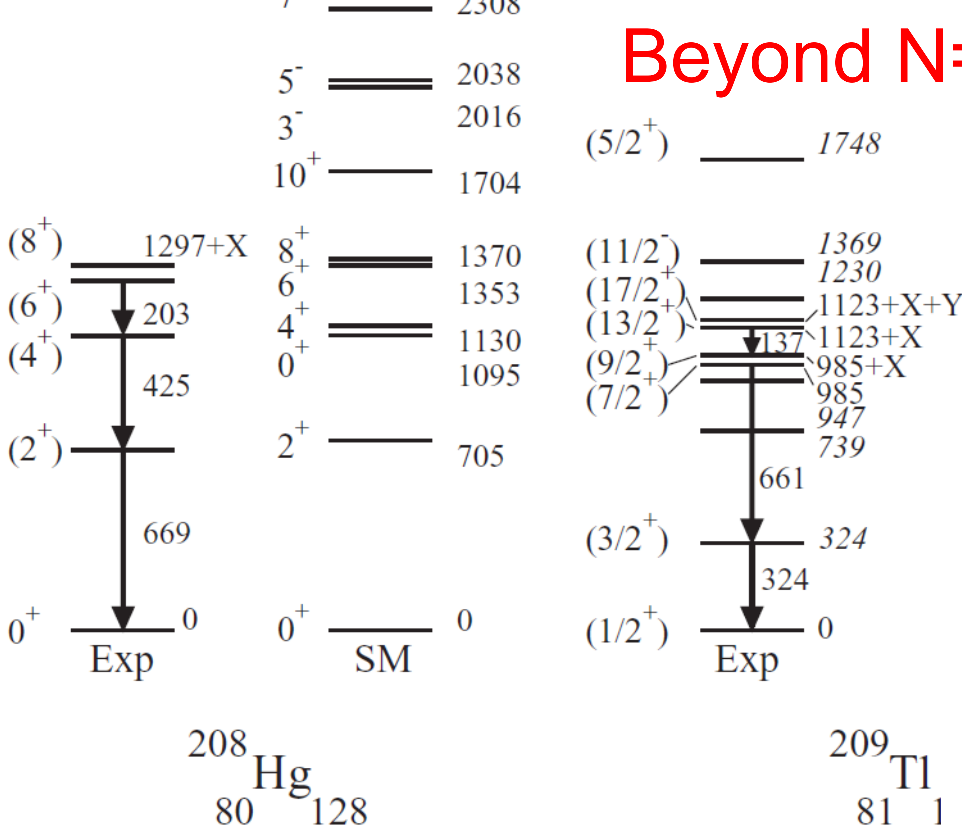

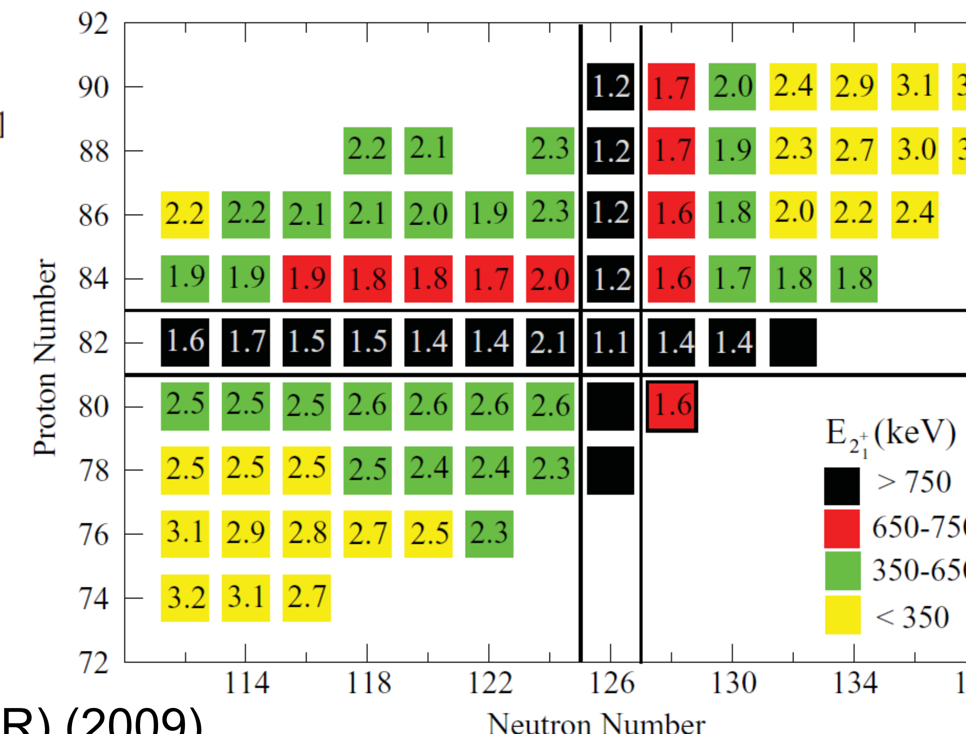

N. Al-Dahan et al., Phys. Rev. C80, 061302(R) (2009)

^{210}Hg (N=130)

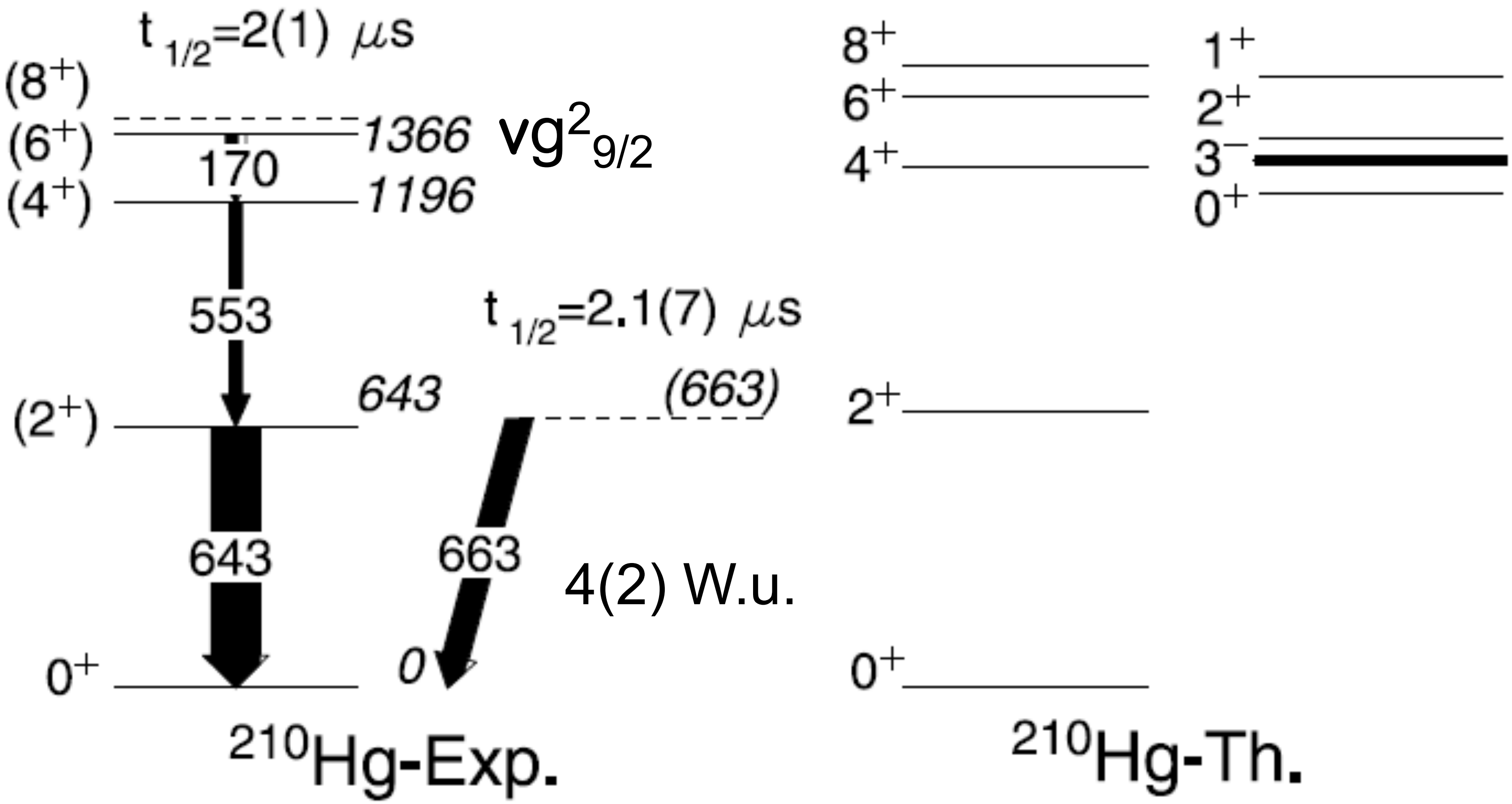

A. Gottardo et al., Phys. Lett. B 725, 292 (2013)

^{207,208}Hg beams at ISOLDE

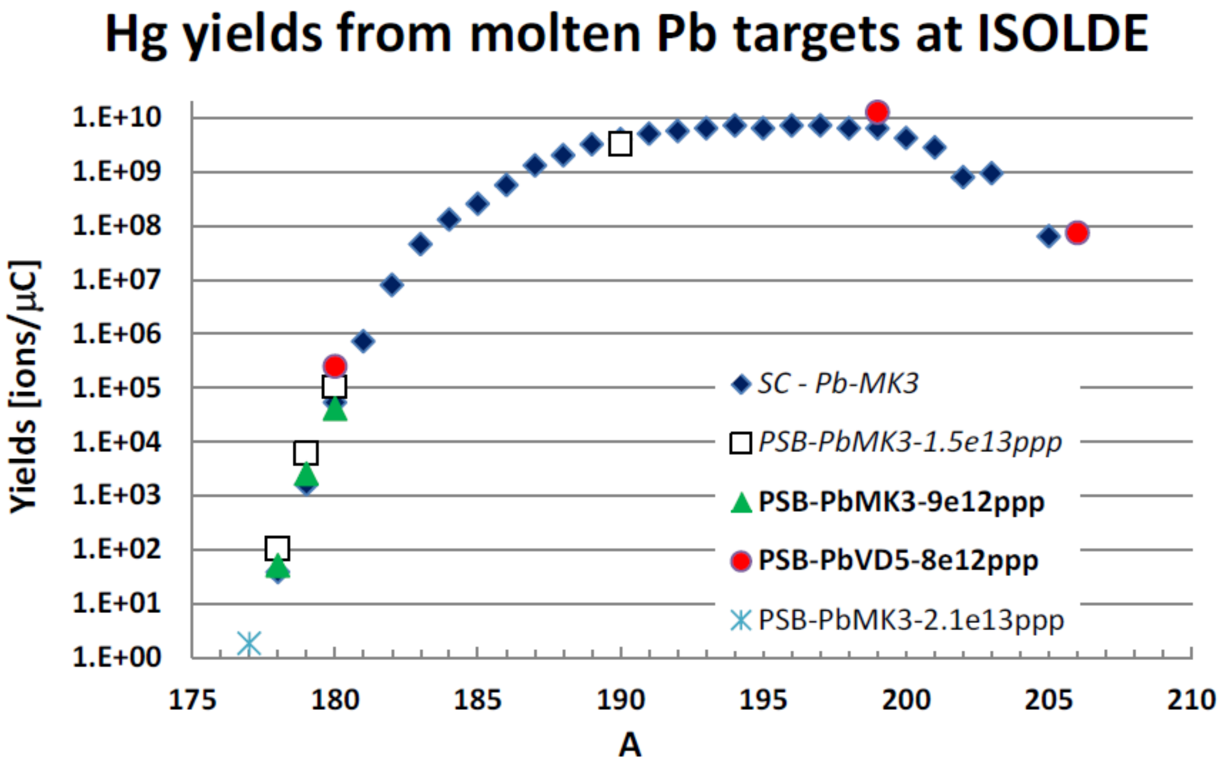

T. Stora, EURISOL town meeting, Oct. 2012

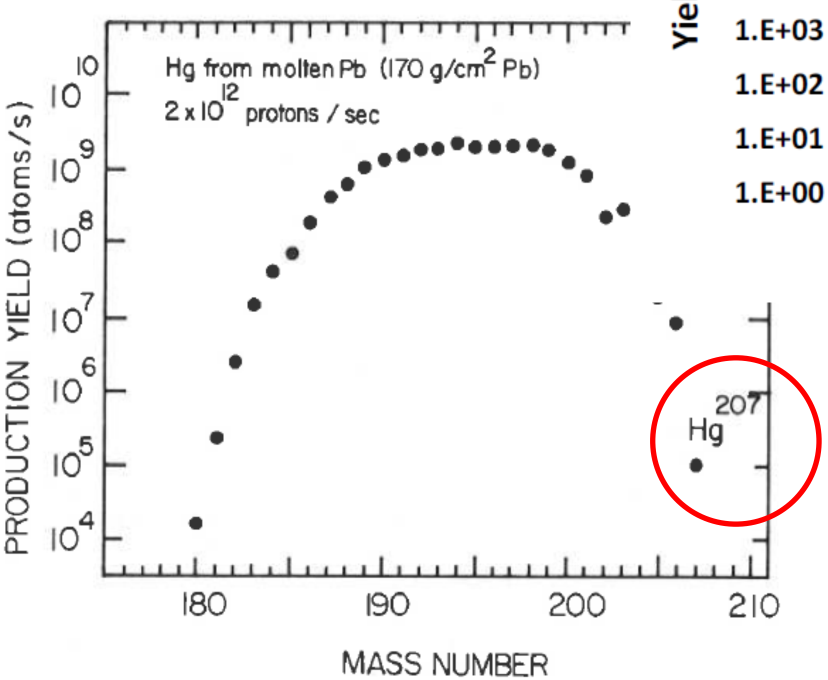

Fig. 1 Production yield in the ISOLDE facility of the mercury isotopes, including ^{206}Hg and ^{207}Hg.

B. Jonson, O.B. Nielsen, J. Zylicz, CERN-81-09 (1981)
(Proc. Int. Conf. Nuclei far from stability, Helsingor, Denmark. Vol.2 p.640 (1981))

Lifetime measurements

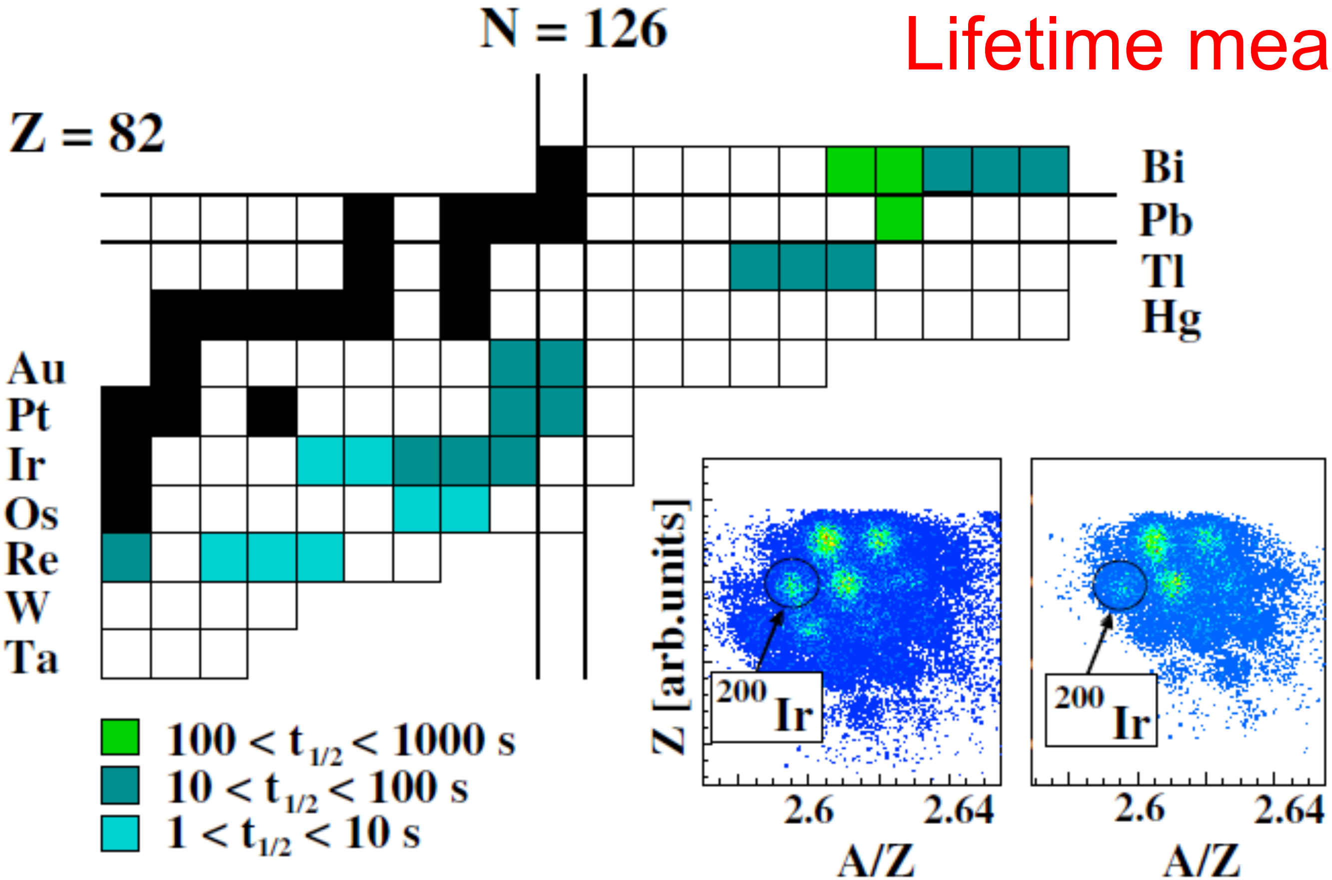

FIG. 1 (color online). Neutron-rich $N \sim 126$ region analyzed during the stopped beam RISING campaign. Measured half-lives are shown in color scale. Inset: Identification plots for Z as a function of A/Z at the final focal plane of the separator (left) and in the active stopper (right).

A.I. Morales et al., Phys. Rev. Lett. 113, 022702 (2014)

Production of exotic nuclei (new isotopes)

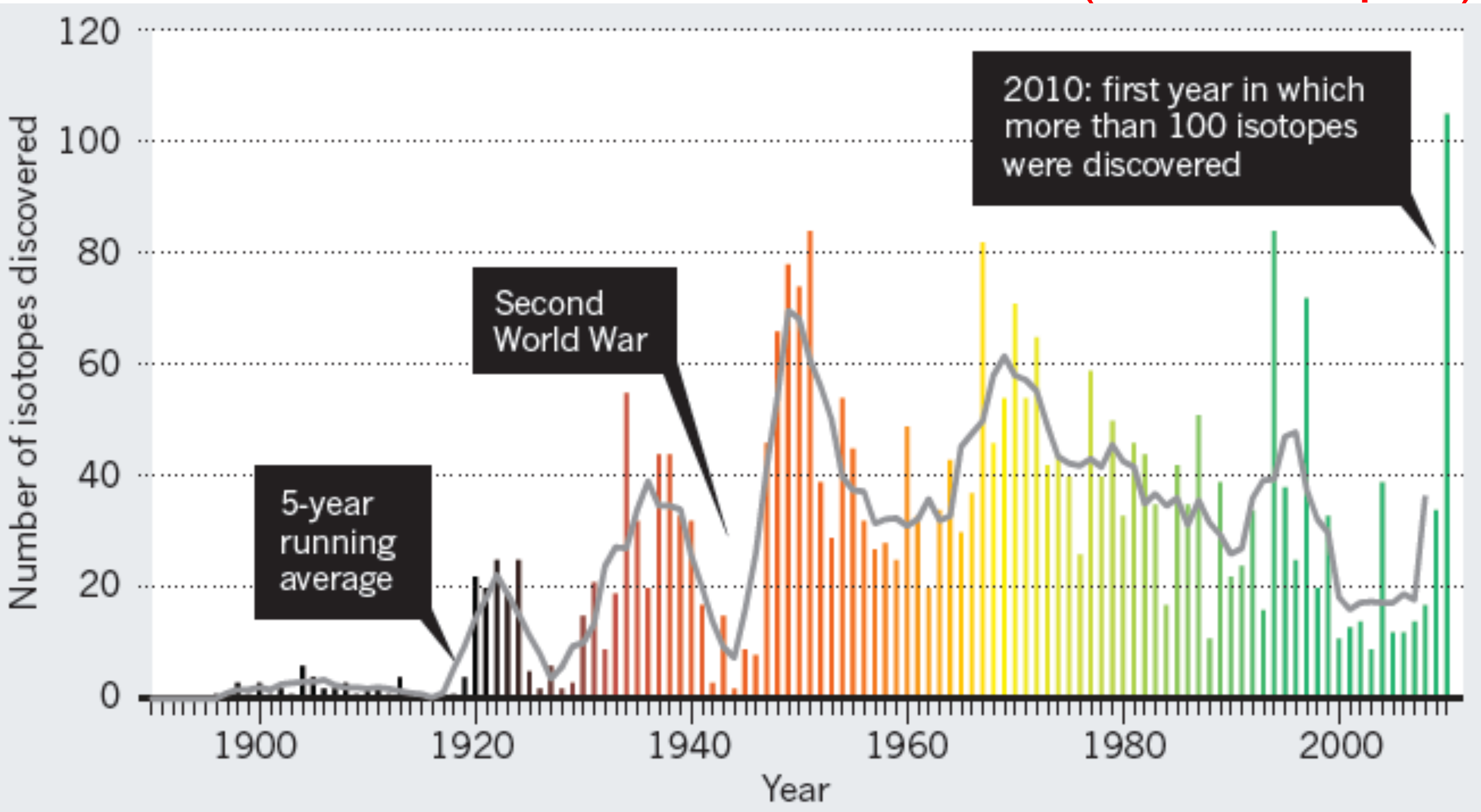

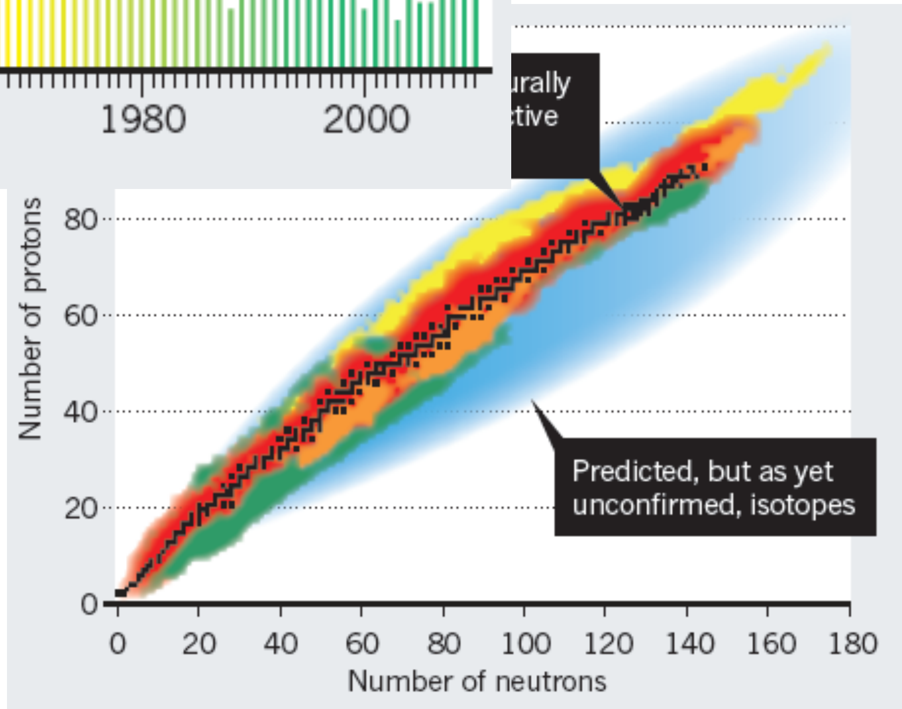

M. Thoennessen, B.M. Sherril, Nature 473 (2011) 25

Along Z=82: neutron-rich lead isotopes

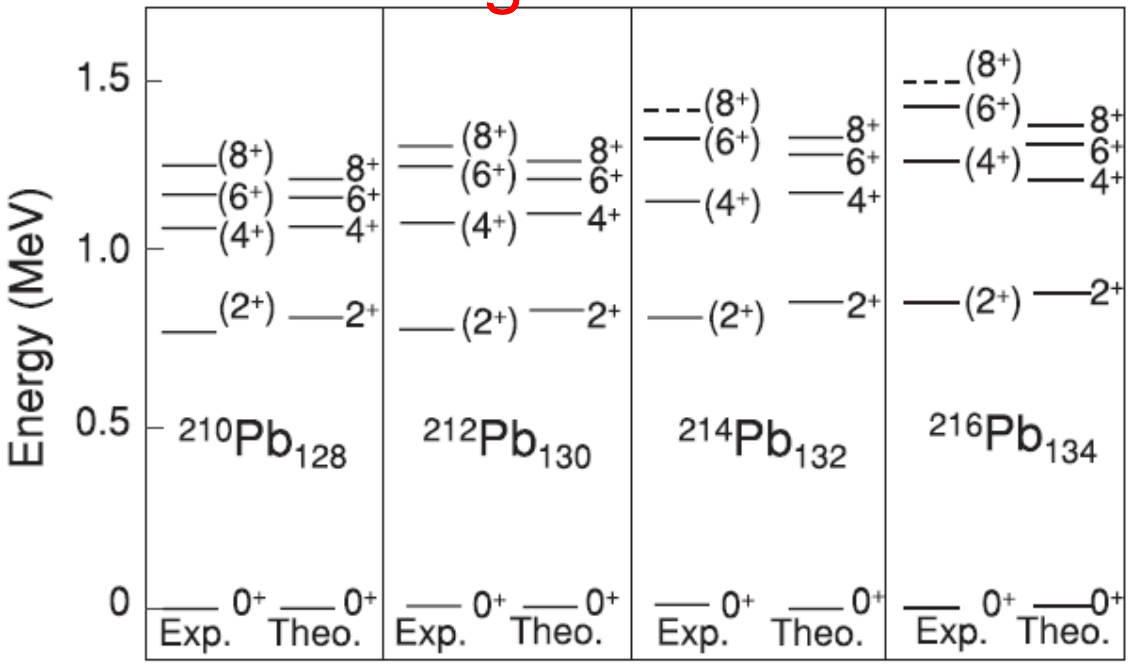

$\nu g^2_{9/2}$ 8^+ isomers

Kuo-Herling interaction

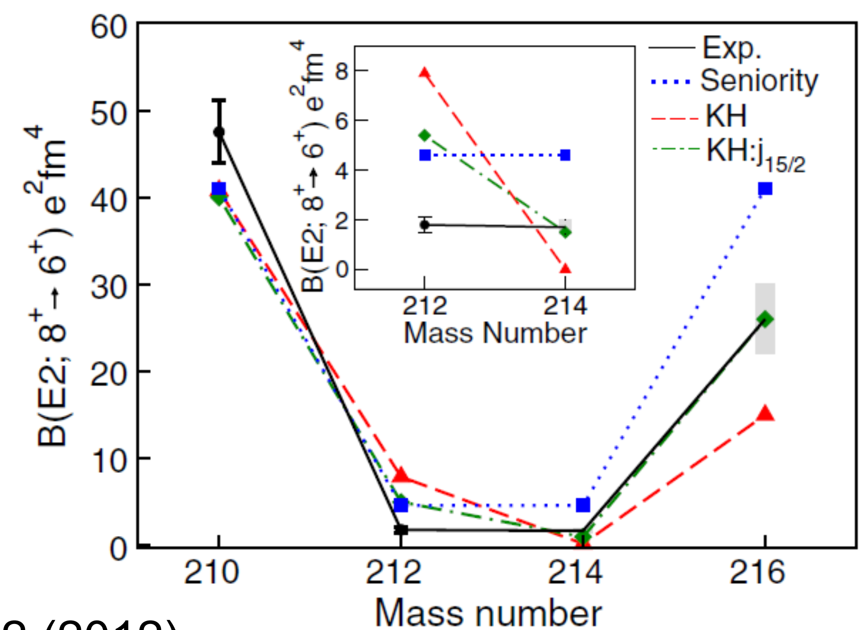

Transition strength explained by considering
effective three-body forces

A. Gottardo et al., Phys. Rev. Lett. 109, 162502 (2012)

Along N=126: $^{203}Ir_{126}$

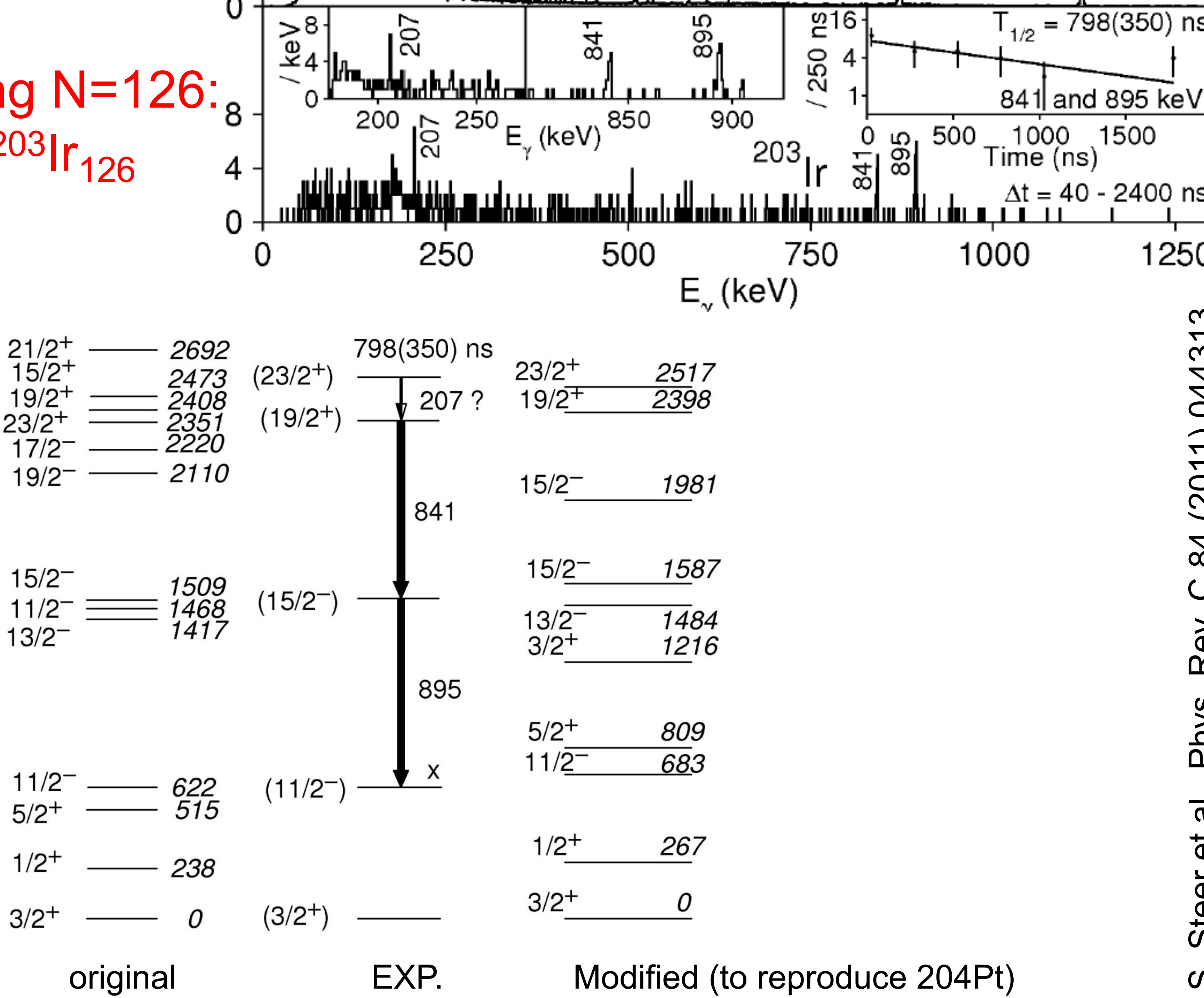

S. Steer et al., Phys. Rev. C 84 (2011) 044313

Beyond N=126 (N=128)

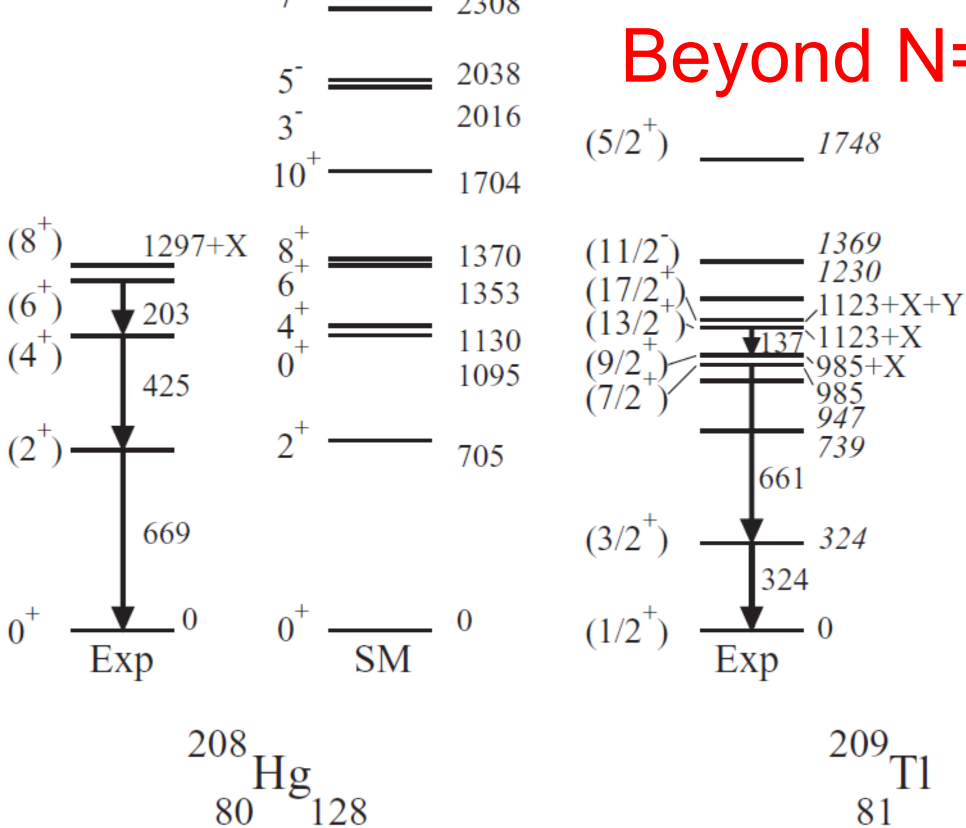

$\nu g^2_{9/2}$ and $\nu g^2_{9/2}\,\pi s_{1/2}$

and isomers

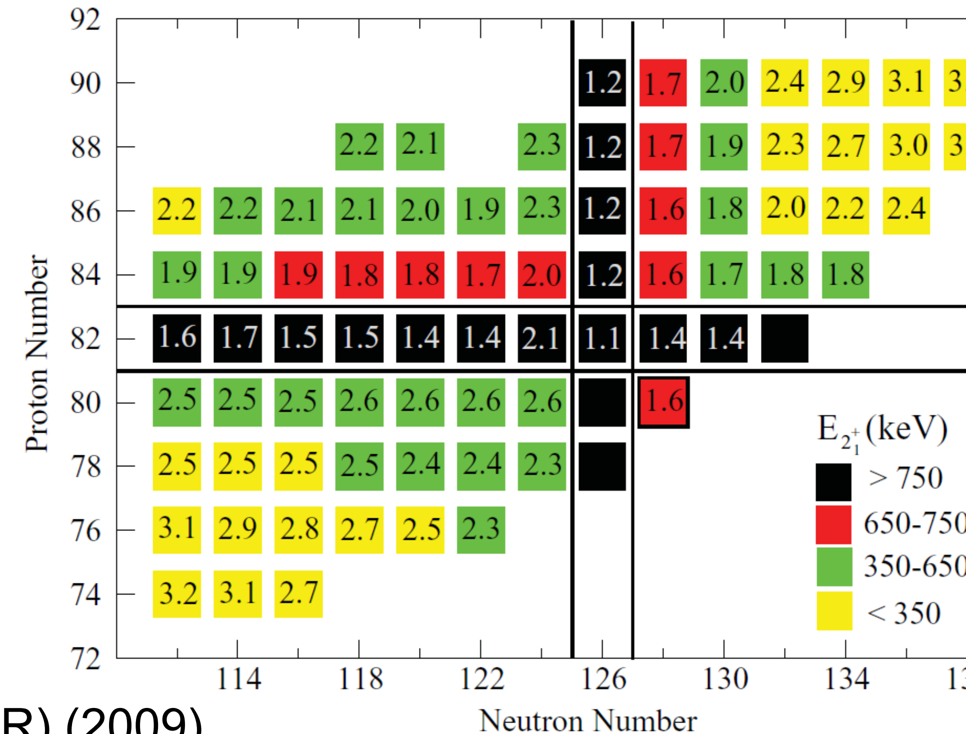

N. Al-Dahan et al., Phys. Rev. C80, 061302(R) (2009)

^{210}Hg (N=130)

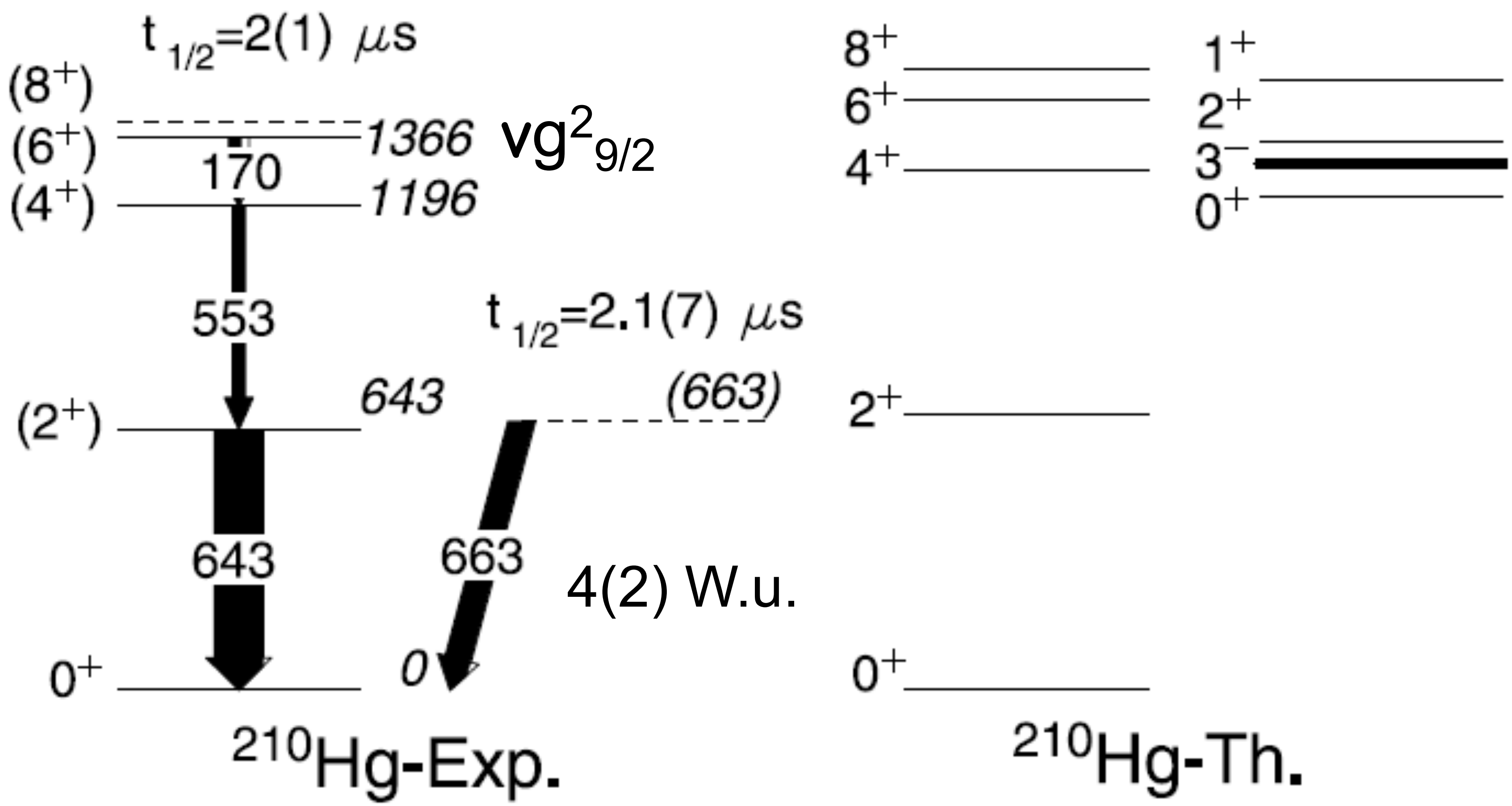

A. Gottardo et al., Phys. Lett. B 725, 292 (2013)

ESR at GSI

Mass of long-lived isomers

4 particles with different m/q

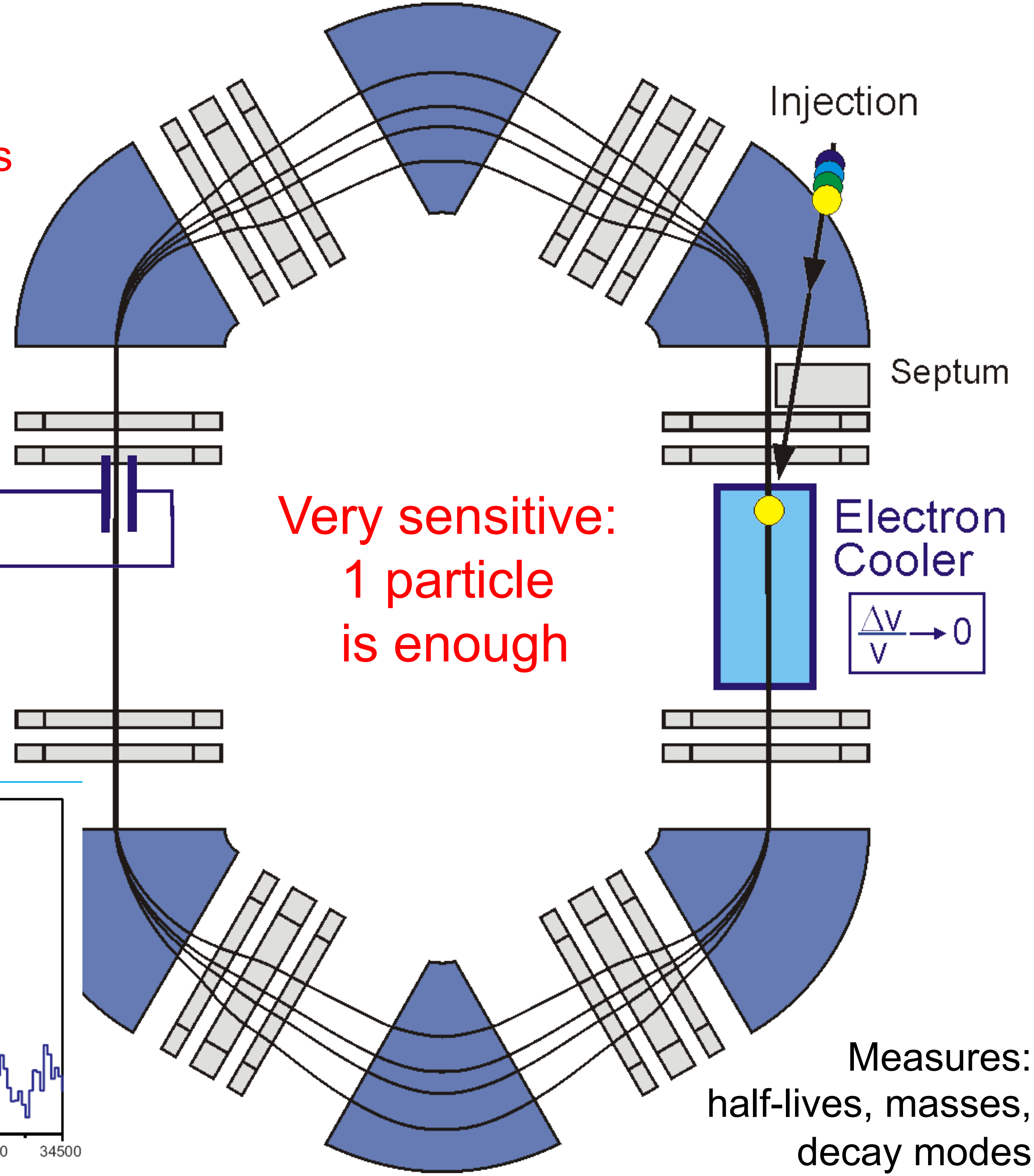

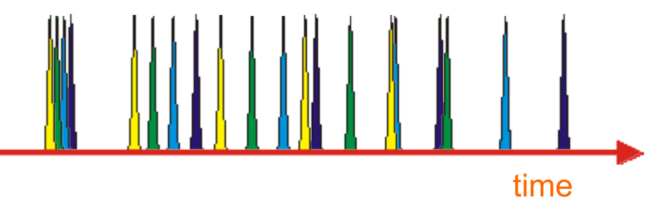

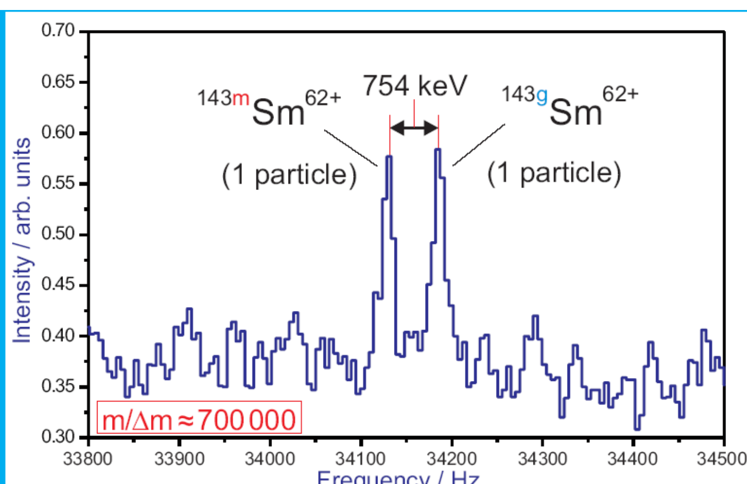

Rare RI ring at RIKEN

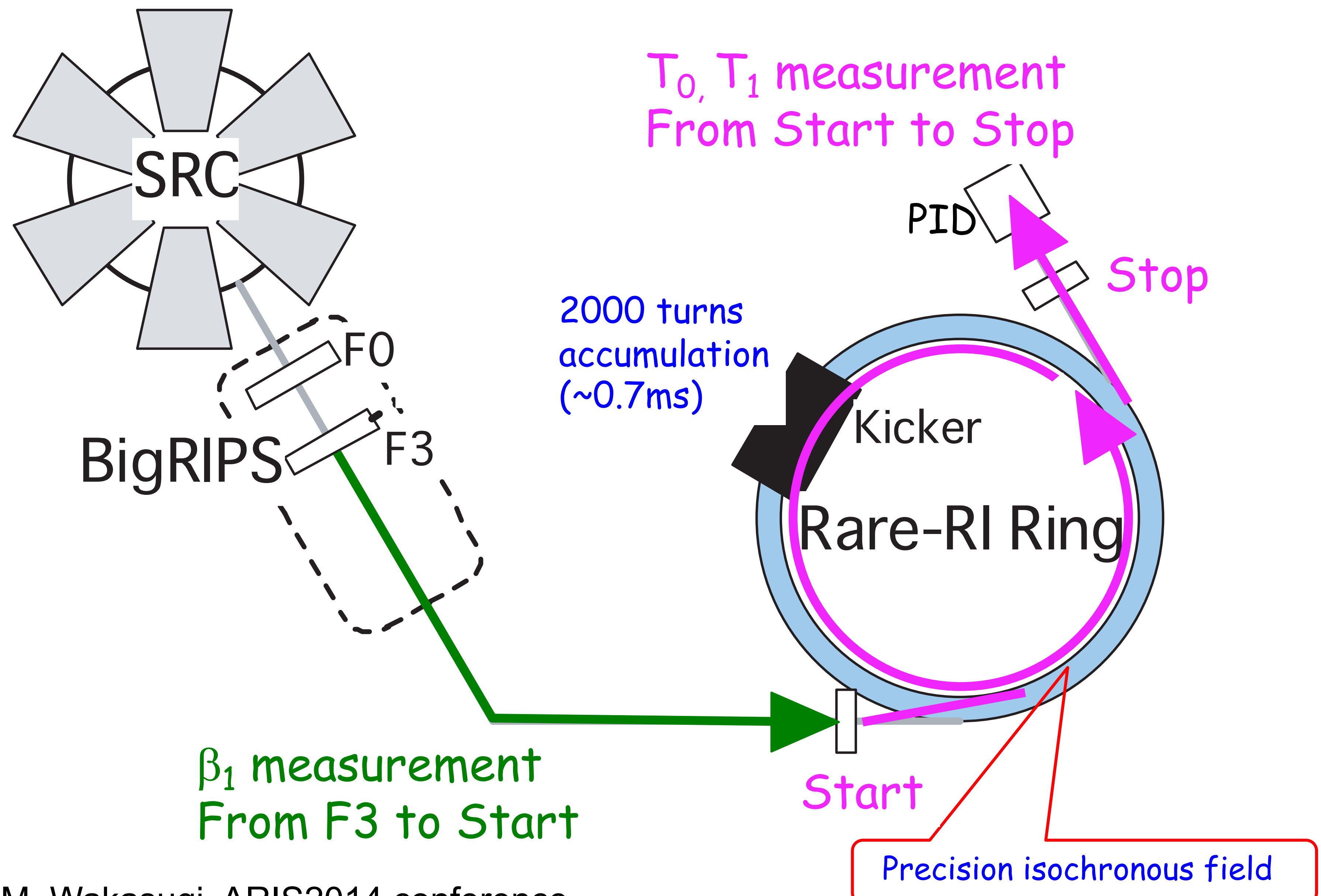

M. Wakasugi, ARIS2014 conference

Commissioning in 2015

SlowRI project: Slow Radioactive Ions at RIKEN

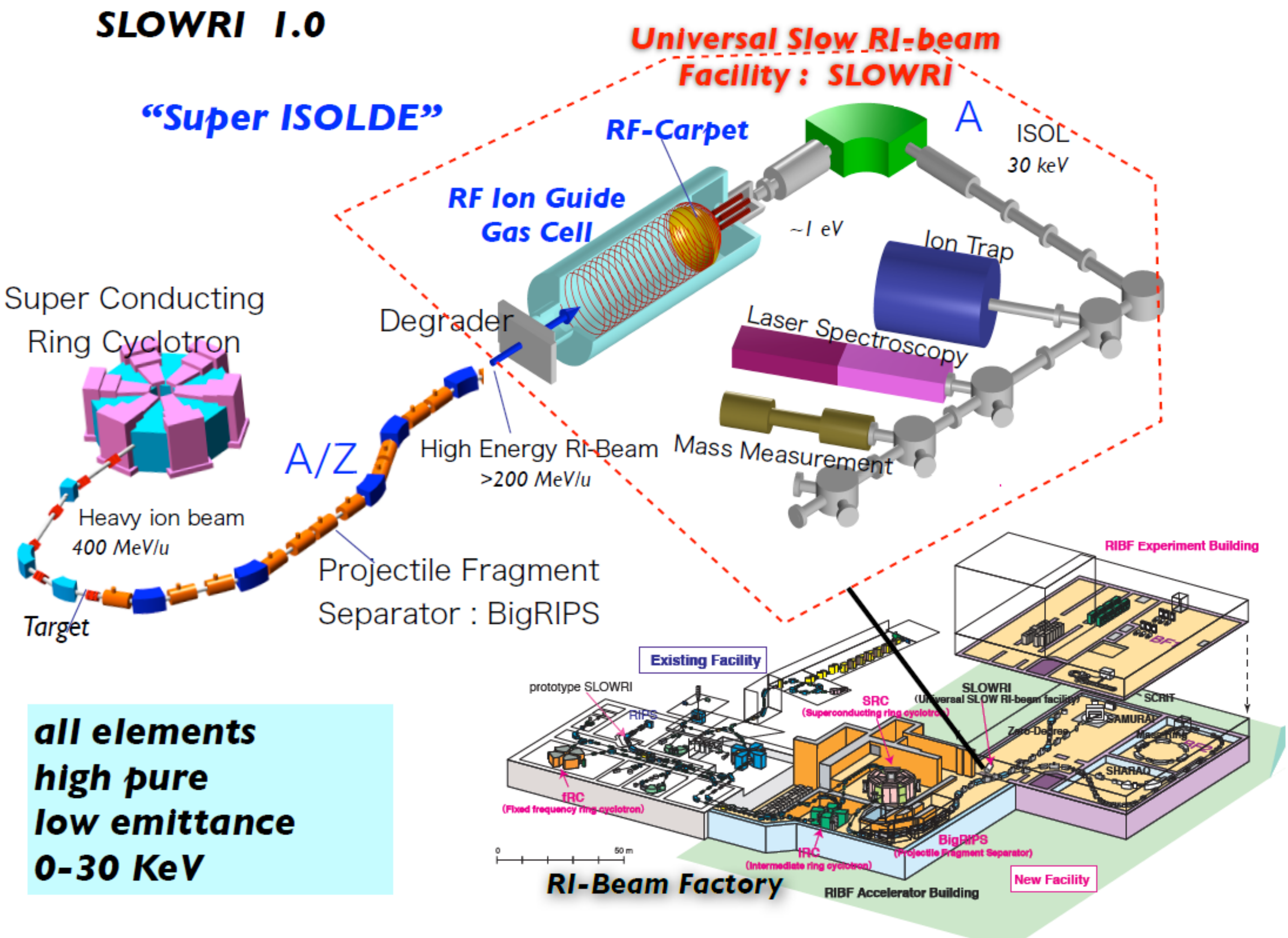

all elements
high pure
low emittance
0-30 KeV

M. Wada et al., Hyperfine Int. 199, 269 (2011)

Multinucleon transfer reactions: experiment

=> Theory generally very good, but …

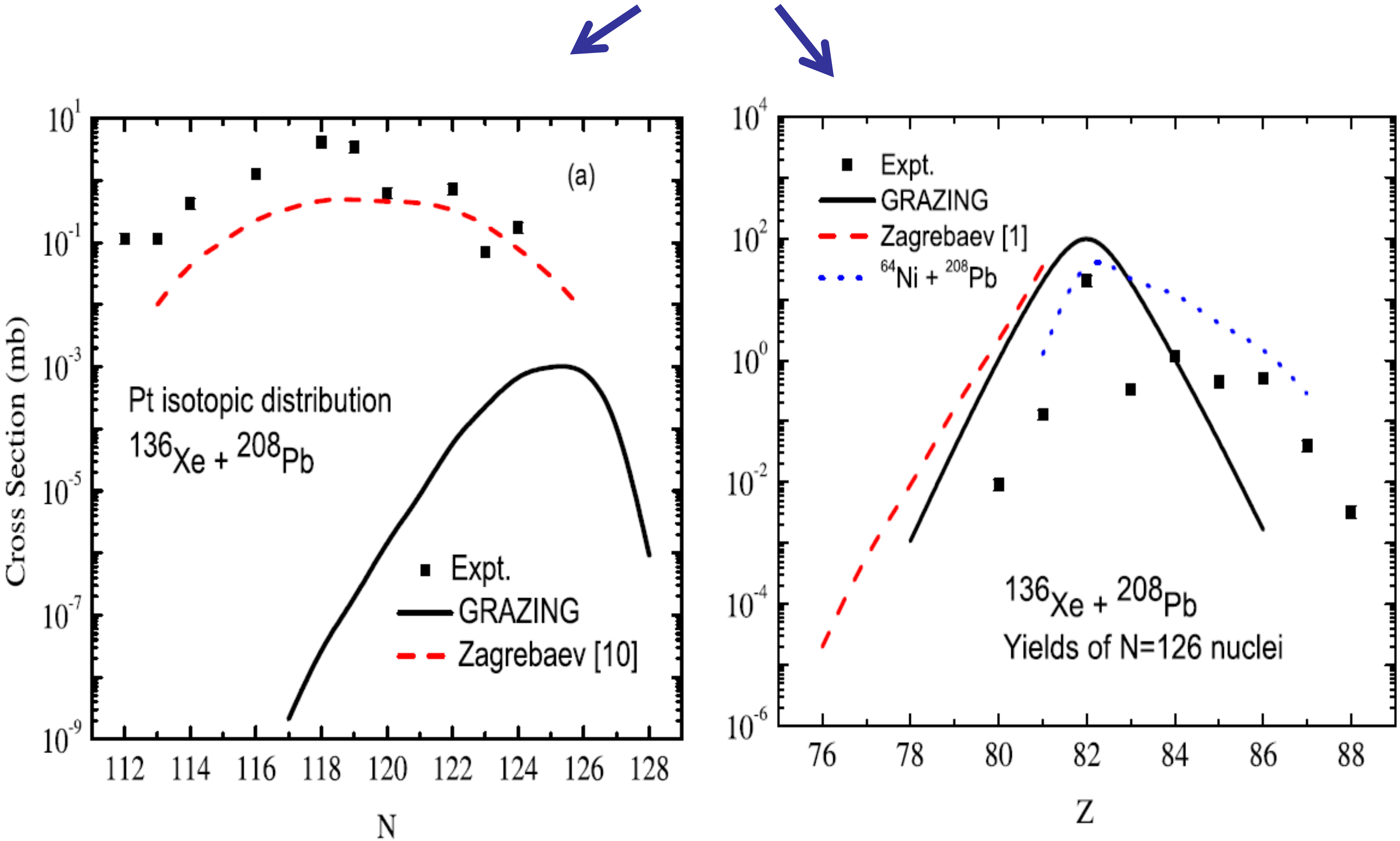

J.S. Barrett et al., Phys. Rev. C91, 064615 (2015)

Future: e.g. KEK Isotope Separation System (KISS)

Z, A identification, clean

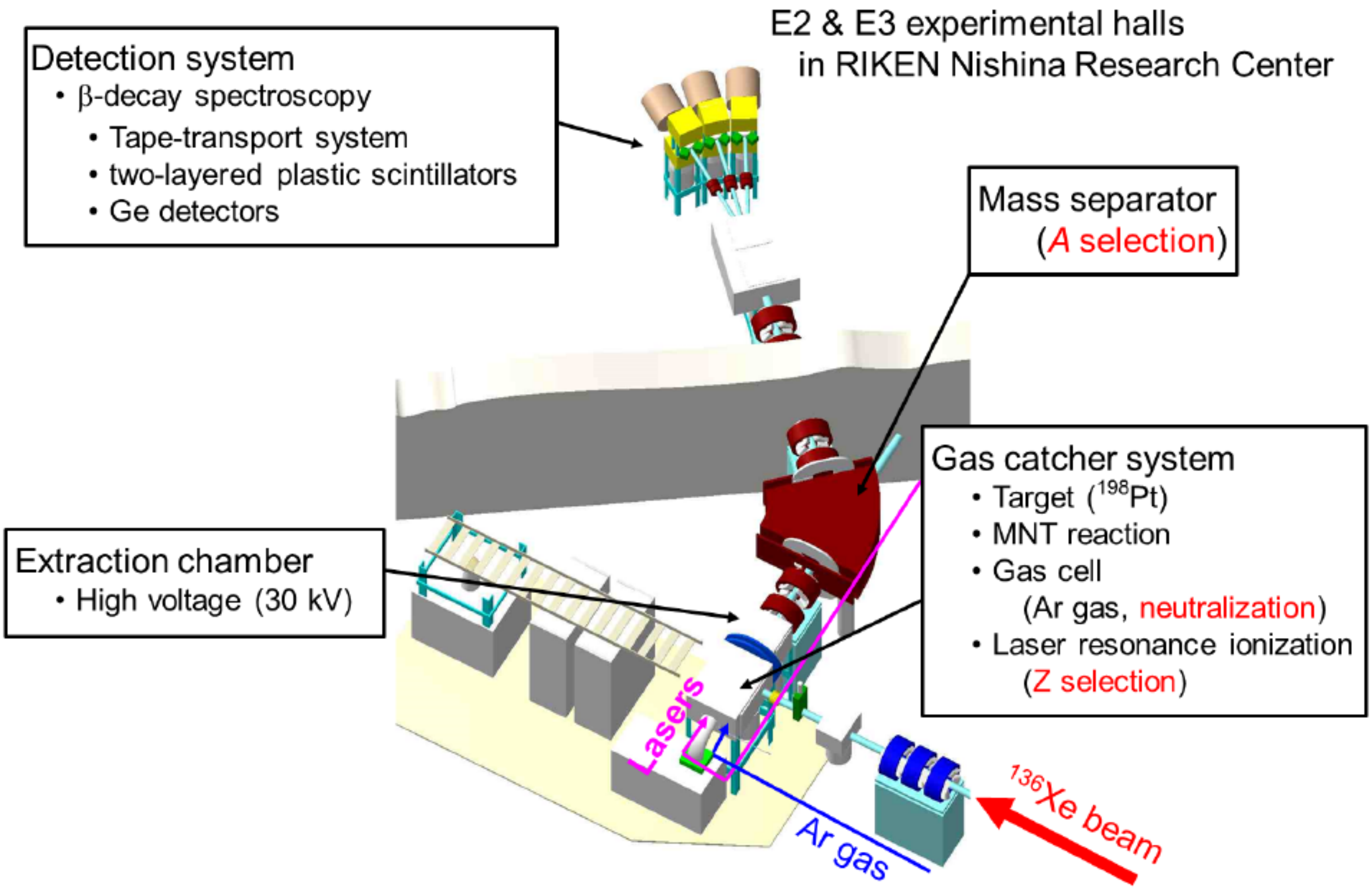

Y.X. Watanabe et al., Nucl. Instrum. Meth. B 317, 752 (2013)

Impact of the first-forbidden β decay on the A~195 r-process peak

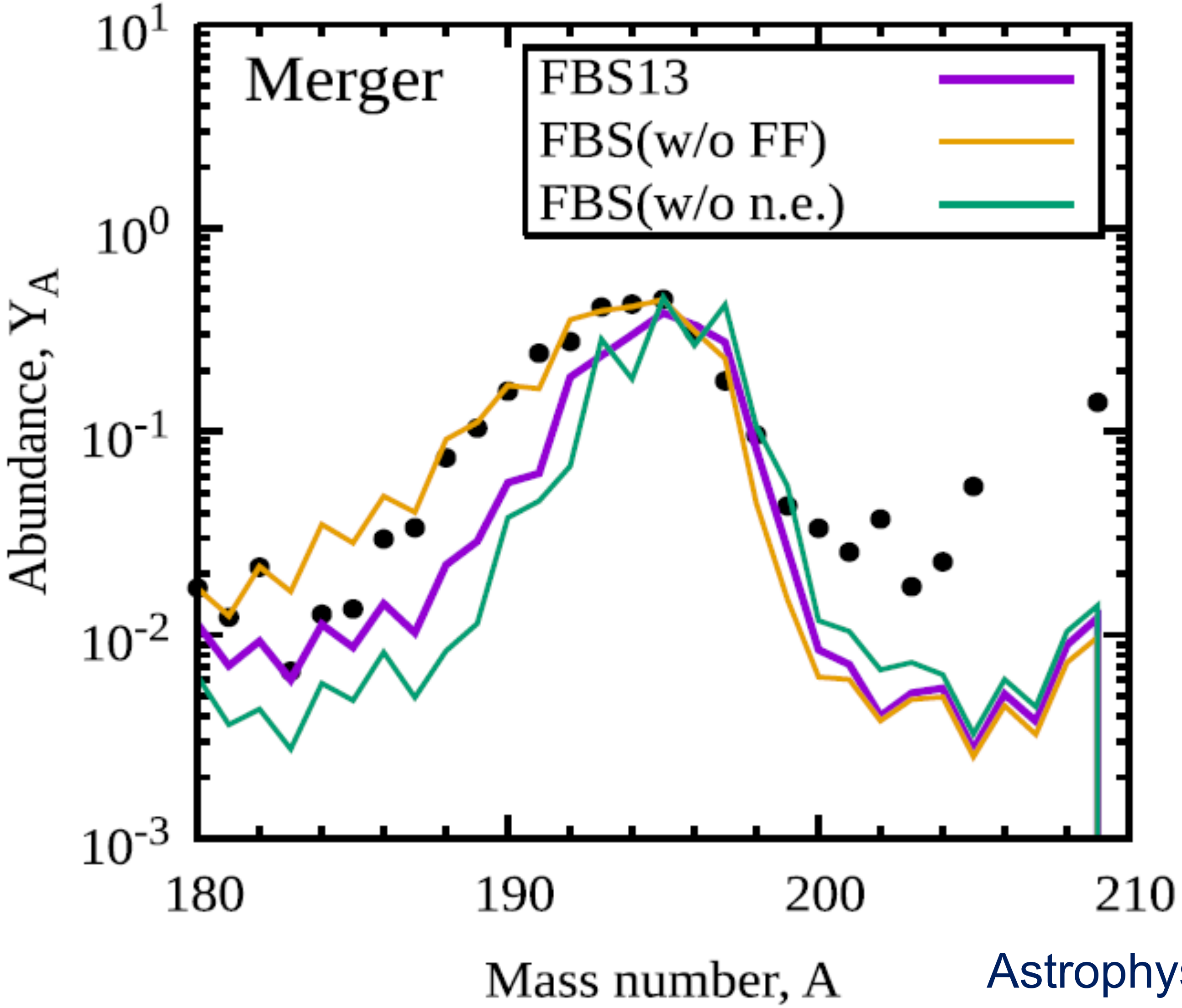

Astrophysical scenario:
Neutron-star merger

N. Nishimura, , Zs. Podolyák, D.-L. Fang, T. Suzuki, Phys. Lett. B 756 (2016) 273

Future: e.g. KEK Isotope Separation System (KISS)

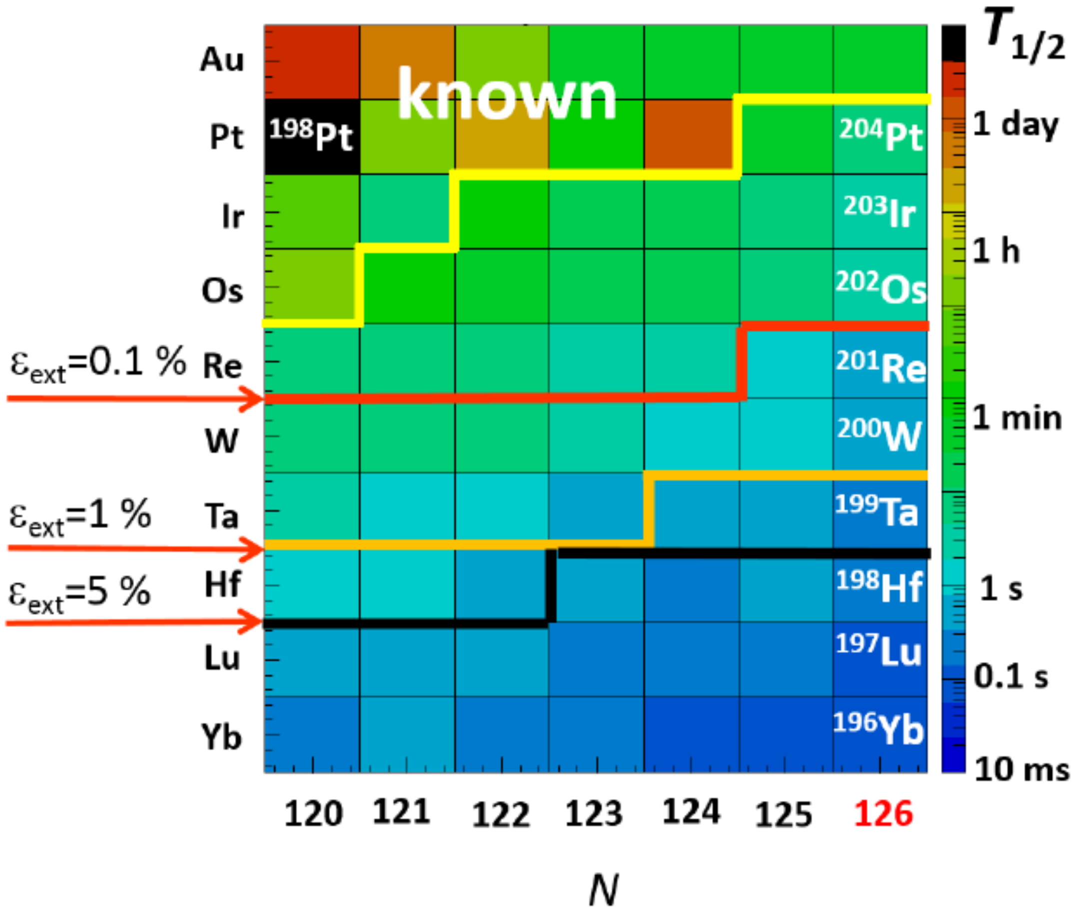

Being tested
E_ext so far 0.2%

$^{136}Xe+^{198}Pt$

Figure 10: Accessible region for lifetime measurement on nuclear chart using the ^{136}Xe beam with the intensity of 10 pnA for different extraction efficiency. The color codes indicate the calculated half lifetime by the KUTY model [9].

Y.X. Watanabe et al., Nucl. Instrum. Meth. B 317, 752 (2013)

In flight fragmentation: separation and identification

Fragment Separator (GSI, Darmstadt, Germany)

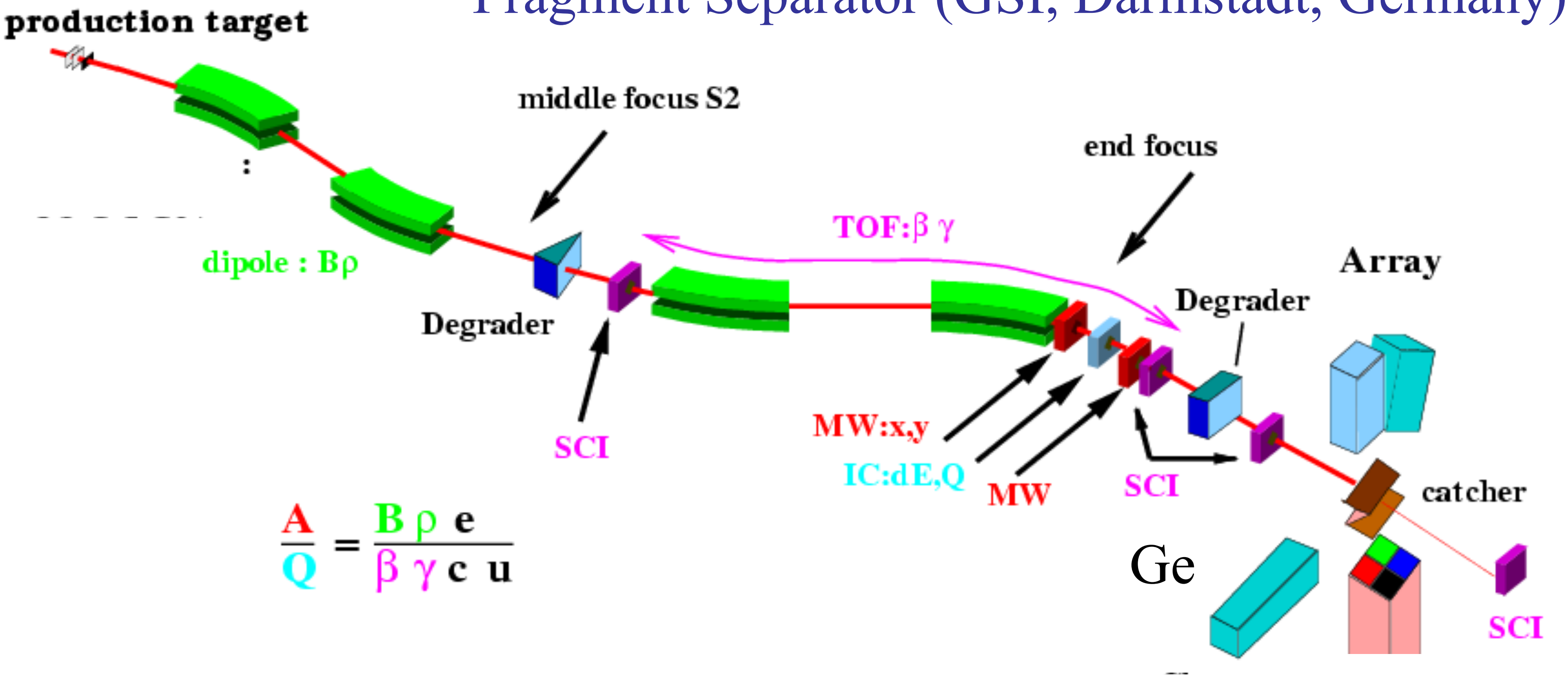

$$\frac{A}{Q} = \frac{B\rho\ e}{\beta\gamma\ c\ u}$$

^{56}Fe beam at E/A=500 MeV.

^{54}Fe secondary beam stopped.

Isomeric decays detected with AGATA array.

γ-ray spectroscopy at GSI

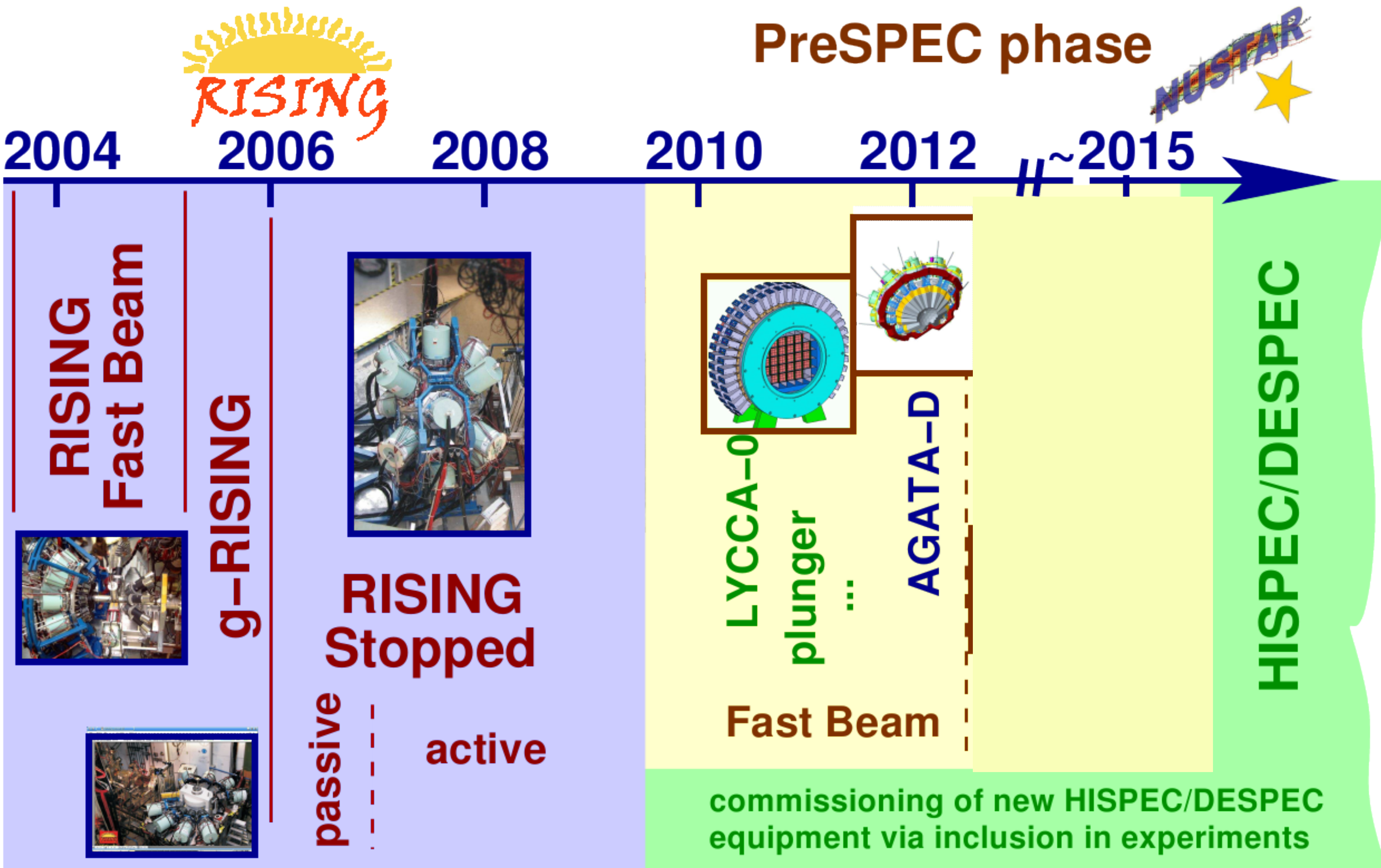

AGATA 2012-2014

AGATA+HECTOR+LYCCA

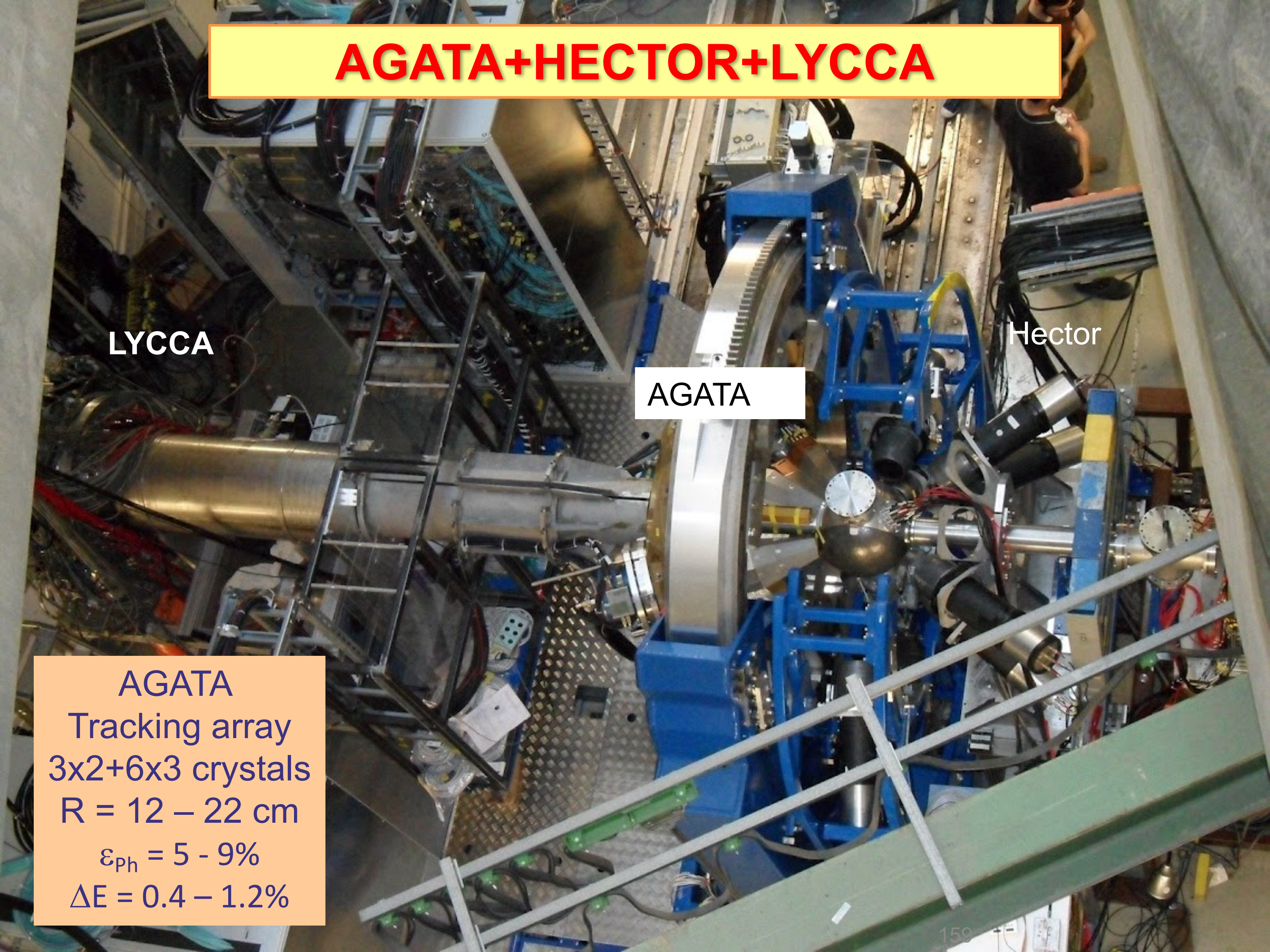

AGATA
Tracking array
3x2+6x3 crystals
R = 12 – 22 cm
ε_{Ph} = 5 - 9%
ΔE = 0.4 – 1.2%

AGATA demonstrator at GSI (Germany) ~20 crystals